Exploring inherent bacterial strains for potential application in biosurfactant production and crude oil biodegradation

A Thesis submitted

in Fulfillments of the Requirements

for the degree of

DOCTOR OF PHILOSOPHY

by

Swati Sharma

166106008

Under the supervision of

Dr. Lalit Mohan Pandey

February 2022

Department of Biosciences and Bioengineering

Indian Institute of Technology Guwahati

Guwahati 781039, Assam, INDIA

DECLARATION

I, hereby declare that the research carried out in the thesis entitled "**Exploring inherent bacterial strains for potential application in biosurfactant production and crude oil biodegradation**," submitted by me to the *Indian Institute of Technology Guwahati*, for the award of the Doctor of Philosophy, is a bonafide work carried out by me under the supervision of Dr. Lalit M. Pandey. The content of this thesis, in full or in parts, has not been submitted to any other University or Institute for the award of any degree or diploma. I also wish to state that nothing in this report amounts to plagiarism to the best of my knowledge and understanding.

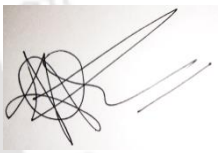

Swati Sharma

Department of Biosciences and Bioengineering,

Indian Institute of Technology Guwahati,

Guwahati - 781039, Assam, India.

Date: February 2022

CERTIFICATE

This is to certify that the thesis entitled "**Exploring inherent bacterial strains for potential application in biosurfactant production and crude oil biodegradation**," submitted by **SWATI SHARMA (166106008)**, a Ph.D. student in the *Department of Biosciences and Bioengineering, Indian Institute of Technology Guwahati*, for the award of the degree of Doctor of Philosophy, is a record of an original research work carried out by her under my supervision and guidance. The thesis has fulfilled all requirements as per the Institute's regulations and, in my opinion, has reached the standard needed for submission. The results embodied in this thesis have not been submitted to any other University or Institute to award any degree or diploma.

Supervisor: Dr. Lalit M. Pandey

Department of Biosciences and Bioengineering,

Indian Institute of Technology Guwahati,

Guwahati-781039, Assam, India.

Date: February 2022

ACKNOWLEDGEMENTS

The journey is timeless when we are blessed with the guidance of peers and superiors. My entire Ph.D. days have quite been a journey, and today, finally, I am about to submit my thesis. It all starts with trust and faith; I would like to extend my gratitude to my supervisor Dr. Lalit Mohan Pandey, who strongly believed in my enthusiasm to carry out this research work. I will always be grateful to him for sharpening my analytical skills and enabling me to change the final outlook through his guidance, ideas and suggestions.

I would also like to extend my sincere gratitude to all my committee members, Dr. Soumen Kumar Maiti, Dr. Senthil Shivaprakashan and Dr. Pakshirajan (my chair head) for their valuable comments, suggestions, constructive criticisms and in finally helping me to reach this milestone.

My special acknowledgement to the Department of Biosciences and Bioengineering (BSBE), Indian Institute of technology Guwahati for giving me a wonderful chance to be a part of this prestigious Institute. The faculty members and staffs of BSBE are also acknowledged for their help and support. Also, I am thankful to the Central Instrument Facility (CIF), IIT Guwahati for letting me perform my experiments using the sophisticated instruments.

Next, I would like to thank my seniors Abshar Hasan, Varun Saxena, Poulami Datta, and labmates Rahul Verma, Laipubam Gayatri Sharma, Aquib Jawed, Vivek Singh Yadav, Aman Bharadwaj, and Rushikesh Fopase, with whom I had shared mind-boggling discussions and empathy when going forward was getting tough. Their absolute presence around was a sense of joy, simmering courage through togetherness. Those pretty little moments like the in-between tea breaks to cheer ourselves up and refresh our minds before getting back to track will always bring a smile to my face. They are like the daily vitamins needed in small amounts but surely. I would also like to express my regards to Anurag Mishra, Mehak, Chinmaya, Shalini and Shilpa for their enthusiastic companionship.

Finally, my greatest gratitude goes to my dear parents, whose reflections in me scattered a thousand wisdom and my family members whose belongings in life let me voyage an infinite distance.

Last but not the least, my head bow down to thee, to almighty God who seeks the seekers.

With sincere gratitude

Swati Sharma

ABSTRACT

The universal and pervasive need for oil as an energy source has caused excessive exploitation, escorted with tragic accidental spills and chronic contamination of the marine ecosystem. Biodegradation is an eco-friendly and effective tool for the remediation of hazardous oil; however, the slower degradation rate limits its exploitation for practical purposes. The selection of potential biodegraders is the key to addressing this challenge. The objective of this thesis was to explore such crude oil-degrading bacteria inherent to oil-contaminated sites and improve their biodegradation efficacy by optimizing the culture conditions and nutrient requirements. The entire thesis has been divided into four main sections.

The first section includes exploring the biosurfactant production ability of a newly isolated bacterial strain *Agrobacterium fabrum* SLAJ 731 and enhancing oil biodegradation ability by optimizing bacterial growth conditions using the One factor at a time approach. The synergistic effect of biosurfactant production on the bacterial crude oil biodegradation efficiency was studied. Further unveiling the effect of biosurfactants as a stimulant in crude oil bioremediation was explored in the second part of the thesis. An isolated oil-degrading strain, *Bacillus subtilis* RSL 2, was preliminarily optimized for the maximum oil degradation and biosurfactant production using the Response surface methodology technique. The produced biosurfactant was investigated for its effect on oil biodegradation in two modes (a) prior addition to media followed by microbial inoculation (sequential mode) and (b) simultaneous addition with inoculum. The findings revealed that biosurfactants improved oil mobilization, making it more bioavailable, enhancing oil biodegradation and biosurfactant production. Bioremediation of crude oil contaminated sites is not limited to a single bacterial species and requires a synergistic and coordinated communication among various inherent bacterial species. Thus, a microbial consortium was designed using *A. fabrum* SLAJ 731, *B. subtilis* RSL2, and an exogenous oil-degrader *Pseudomonas aeruginosa* MTCCP7815 in the third section of the thesis. The biodegradation kinetics of single aliphatic (Hexadecane), aromatic (Phenanthrene) and the binary mixture as co-contaminants by axenic cultures of *Agrobacterium fabrum* SLAJ 731, *Bacillus subtilis* RSL2 and *Pseudomonas aeruginosa* P7815 and their consortium was explored. An integrated kinetic model combining first-order exponential decay and the Monod equation well fitted to the biodegradation

results. The maximum degradations of both substrates were observed for the microcosm compared to axenic cultures, indicating the selected strains' synergistic effects.

To further strengthen the crude oil biodegradation efficiency of the studied microbes, immobilization techniques using suitable non-toxic, economical, and eco-friendly carriers are summarized in the thesis's final section. The microbial carriers were hydrophobically tuned to improve the oil adsorption and thus bioavailability towards microbes and simultaneously reduce the biotoxicity of a high concentration of crude oil. The surface hydrophobicity of the biosorbent was improved by forming hydrocarbon-based self-assembled monolayers for enhancing the surface-oil interactions (adsorption). Henceforth, an integrated biodegradation strategy and a faster removal method like adsorption were addressed to overcome the slower bacterial biodegradation rate. The integrated process proposed a kinetic model, which agreed to simultaneous biosorption and biodegradation. The integrated approach was found to synergistically improve the overall remediation of crude oil, which was also correlated with microbial degradative enzymes activity and biosurfactant production. Hence, hydrophobic bio sorbents immobilized potential oil-degrading and biosurfactant producing consortium shall be used to bioremediation of oil-contaminated sites in the foreseeable future.

CONTENTS

LIST OF FIGURES

LIST OF TABLES

ABBREVIATIONS

Acronyms and Nomenclatures

AH	Alkane Hydroxylase
ANOVA	Analysis of Variance
B+C	Biosurfactant + Cells
BBD	Box–Behnken Design
BC	Biosurfactant inoculated 8 h before cells
BCA	Bicinchoninic Acid
BET	Brunauer–Emmett–Teller
BH	Bushnell Haas
BLAST	Basic local alignment search tool
BSA	Bovine Serum Albumin
C12DO	Catechol 1, 2 dioxygenase
C23DO	Catechol 2, 3 dioxygenase
CCD	Central composite design
CFU/mL	Colony forming unit
CHAPS	3-[(3-cholamidopropyl)dimethylammonio]-1- propanesulfonate
CMC	Critical micelle concentration
CSH	Cell surface hydrophobicity
DAPI	4′,6-diamidino-2-phenylindole
DCW	Dry cell weight
DMSO	Dimethyl sulfoxide
E_{24}	Emulsification index after 24 h incubation
eAH	Extracellular Alkane Hydroxylase
EDX	Energy dispersive X-ray spectroscopy
FESEM	Field emission scanning electron microscope

FTIR	Fourier transform infrared spectroscopy
GC-FID	Gas Chromatography - Flame Ionization Detection
GC-MS	Gas chromatography–mass spectrometry
gDNA	Genomic Di-oxy-ribonucleic acid
HEX	Hexadecane
HPLC-UV	High Performance Liquid Chromatography-UV detector
iAH	Intracellular Alkane Hydroxylase
LB	Luria bertani broth
MATH	Microbial Adhesion to Hydrocarbons
MCM	Microcosm
MI	Diiodomethane
NADH	Nicotinamide Adenine Dinucleotide Hydrogen (Hydride)
NCBI	National Centre for Biotechnology Information
NMR	Nuclear magnetic resonance
OD	Optical density
OFAT	One factor at a time
PBD	Plackett–Burman design
PBS	Phosphate buffered saline
PHE	Phenanthrene
PHE+HEX	Binary mixture of hexadecane and phenanthrene in equal ratio
RSM	Response surface methodology
RT	Retention time
SAMs	Self-assembled monolayers
TEOS	Triethoxyoctylsilane
TFA	Trifluoroacetic acid
TGA	Thermal gravimetric analysis
USEPA	U.S. Environmental Protection Agency

ZOI	Zone of inhibition
XRD	X-ray powder diffraction

Symbols

C_e	Equilibrium substrate concentration (mg/L)
C_0	Initial substrate concentration (mg/L)
k_1	First order constant (h^{-1})
k_d	Biodegradation rate (h^{-1})
k_a	Rate of oil adsorption (h^{-1})
k_L	Langmuir constant (L/mg)
k_s	Half saturation constant (L/g)
m/z	Mass to charge ratio
o/w	Oil in water
q_m	maximum oil adsorption capacity (mg/g)
q_e	Adsorption at equilibrium time (mg/g)
q_t	Adsorption at time t (mg/g)
R^2	Correlation coefficient
R_L	Langmuir separation factor
T	Temperature (K)
t	Time
V	Volume of solution (ml)
W	Weight of the adsorbent (mg)
w/o	Water in oil
δ	Chemical shift (ppm) in NMR
θ	Half of the diffraction angle/Bragg angle
rpm	Revolutions per minute

$k_{D\text{-}MCM}$	Microcosm biodegradation rate
$k_{D\text{-}SLAJ}$	*A. fabrum* biodegradation rate
$k_{D\text{-}P7815}$	*P. aeruginosa* biodegradation rate
$k_{D\text{-}RSL2}$	*B. subtilis* biodegradation rate
μ	Specific growth rate
$Y_{x/s}$	Biomass yield
$Y_{P/S}$	Biosurfactant yield
γ_{ij}	Surface energy
γ_i^d	surface energy due to dispersive component of liquid
γ_i^p	surface energy due to polar component of liquid
γ_j^d	surface energy due to dispersive component of solid
γ_j^p	surface energy due to polar component of solid
q_p	Specific productivity

Chapter 1

Introduction

Crude oil is an extensively exploited fossil fuel resource employed throughout the globe for various purposes. Its characteristic high energy content is due to highly complex and chemically active constituents, mainly comprising a long chain of hydrocarbons. However, such composition threatens the environment during accidental transportation or exploration spillage. Petroleum hydrocarbons pose the highest risk among various top priority contaminants due to poor biodegradability and severe toxicity. They impose severe fatality to the biotic system in the vicinity, arousing the need for rapid and intensive remediation measures (Koutinas et al., 2019). Such spilled oil constituents in the ecosystem become detrimental due to their potentially hazardous composition. In recent decades, such spillage and exposure of hazardous oil to the environment have become frequent and massive.

Various poly-aromatic and aliphatic hydrocarbons contribute to a large part of existing recalcitrant contaminants (Sharma et al., 2019). They possess limited solubility and dissolution rate, which is the primary reason for their persistency in the ecosystem. Various remedies that come into action during oil spillage include the use of skimmers and boomers, which are primarily involved in adsorbing and thus restricting the spread of oil. Incineration is another technique involved in the control of oil spillage. However, these physical tools only transform the pollutant from one form to another. Among the chemical remediation techniques, dispersants such as SDS and SDBS are involved in emulsifying the oil films formed into small droplets for penetration of oxygen, light, and improved bioavailability to microbes. However, their long-term usage showed biotoxicity to various marine lifeforms. Hence, these remedies are optimal at the time of occurrence yet cannot be used for long because of secondary pollutant generation. Acknowledging their role at the time of action is essential; however, there is a need to look for alternatives. In this regard, various researchers have diverted towards using biological tools for remediation purposes.

Due to their regular exposure, various microbes actively participate as bio-remediating agents, hence acclimatizing to such persistent and recalcitrant compounds. Microbes such as fungi, yeast, and algae have shown good biodegradability towards various precarious compounds; however, bacteria are the

most active primary bio-remediating agent (Speight, 2018; Ummalyma et al., 2018). These bacteria are rich in catalytic and degrading enzymes responsible for contaminant removal. Apart from biodegradation ability, another class of microbes is known for producing biosurfactants, an effective tool for improving the bioavailability of hazardous wastes. Biosurfactants are involved in emulsifying oil into smaller droplets which are further utilized as a C source for their growth and metabolism. Hence, every contaminated site is crammed with microbes with diverse operations, working synchronously to achieve maximum biodegradation. Even though bioremediation is considered a sustainable and eco-friendly approach, the slow degradation rate and harsh environmental conditions limit the actual applications of this method (Sharma et al., 2019; Sharma et al., 2019).

The lacuna lies in the susceptibility of microbes to the higher concentration of these contaminants, thus restricting their efficiency at the spill site. The issue of substrate toxicity is addressed by adapting the fed-batch mode of operation (Poontawee and Limtong, 2020; Villegas-Méndez et al., 2021). Further, the slower biodegradation rate remains a challenge for researchers for efficient remediation. On the other hand, surface adsorption is a quick process and finishes within a few hours (Gadore and Ahmaruzzaman, 2021; Kumar et al., 2020; Liang et al., 2018; Salah et al., 2014). Hence, the coupling of the slower biodegradation and faster adsorption is expected to improve the overall oil remediation. Different biosorbents like sawdust, husk, biochar and corn cobs have been explored to remove contaminants. Improved microbial community growth and metabolic activities have been reported by various researchers in the case of surface-assisted biodegradation (Dashti et al., 2019).

Additionally, the surface modification of biosorbents is reported to enhance the adsorption capacity by tuning the interfacial interaction (Abdelwahab et al., 2021; Sharma and Pandey, 2021). Overall, microbial bioremediation faces two major drawbacks: susceptibility towards a higher oil concentration and its limited affinity. Hence, we aimed to empower the microbiological remediation by employing strategies such as; (1) tuning the surface hydrophobicity of adsorbents to improve interfacial interaction and (2) integrated adsorbent and biosurfactant treatments with microbiological remediation.

1.1. Objectives

To bridge the lacunas as evaluated in Chapter 2 and to provide deeper insight into the bacterial oil biodegradation activity, the four thesis objectives are as follows:

1. Exploring the crude oil biodegradation and biosurfactant production abilities of isolated *Agrobacterium fabrum* SLAJ731
2. Biosurfactant mediated crude oil biodegradation by isolated *Bacillus subtilis* RSL 2
3. Design of microbial consortium and exploring their hydrocarbon biodegradation ability
4. An integrated strategy of hydrophobic surface-induced biosorption and microbial biodegradation for the enhanced crude oil remediation

1.2. Thesis Outline

The thesis has been organized into seven chapters based on the four above objectives. A chapter-wise thesis outline is as follows:

1.2.1. Chapter 2

This chapter reviews the existing works of literature discussing the need to look into crude oil as a hazard to the ecosystem when spilled. The various remediation techniques and the need for bioremediation as the most sustainable tool for controlling this hazard have been majorly conferred. Screening of hydrocarbon utilizing and biosurfactant producing bacteria and optimizing their culture conditions to achieve the maximum oil biodegradation efficiency has been highlighted.

1.2.2. Chapter 3

This chapter describes the screening of previously isolated *A. fabrum* bacteria from an oil-contaminated site for biosurfactant-producing abilities. Optimization of bacterial culture requirements to improve its growth and biosurfactant production abilities have been elaborated using the One factor at a time technique. Further, the biosurfactant was characterized, and its effect to induce bacterial catabolic enzyme activity and oil biodegradation efficiency were analysed.

1.2.3. Chapter 4

This chapter focuses on another previously isolated *B. subtilis* strain from oil-contaminated sites. Optimization of bacterial growth conditions to improve its biosurfactant production abilities using Response surface methodology was performed. The biosurfactant was characterized, and its effect on wettability, antibacterial and microbial cell surface hydrophobicity were analyzed. Further, its role as a stimulant on bacterial crude oil biodegradation abilities was highlighted.

1.2.4. Chapter 5

This chapter explored the biodegradation ability of indigenous oil-degrading strains *A. fabrum* and *B. subtilis* and an exogenous *P. aeruginosa* bacterial strain for their aliphatic, aromatic hydrocarbon and their mixture when grown as axenic cultures and consortium. The kinetics of biodegradation and decay rates were estimated to imitate their behaviour as a consortium at oil-contaminated sites.

1.2.5. Chapter 6

This chapter endorses physiochemical coupled biological tools as an integrated strategy to overcome their discrete drawbacks and maximize their effectiveness as a whole system. A biosorption coupled bacterial biodegradation model was opted to minimize the biotoxicity, poor bioavailability and affinity of crude oil at high concentration. A biosorbent was chosen, and its hydrophobicity was tuned using octyl self-assembled monolayers. The biosorbent dosage was preliminarily optimized using RSM statistical tool and later inoculated with bacteria to explore their effectiveness in overall oil biodegradation. Later, a kinetic model was deduced to evaluate the overall biosorption coupled biodegradation model. Further, using this integrated strategy, a fed-batch mode was opted to increase the bacterial oil biodegradation ability.

1.2.6. Chapter 7

This chapter summarizes the overall contributions of present research work and provides possible future implications of results in the direction of bioremediation techniques

Chapter 2

Review of literature

This chapter reviews the hazards of crude oil constituents and addresses various remediation techniques explored in the existing literature to control spilled crude oil-based petroleum hydrocarbons contamination. The advantage of bioremediation of crude oil over various physiochemical techniques and the significance of biodegradation and biosurfactant production abilities of inherent bacterial species are emphasized. Optimization of various factors regulating bacterial oil biodegradation and biosurfactant production ability are discussed. The design of microconsortium using potential oil-degraders and biosurfactant producers and their integration with physiochemical techniques to achieve improved remediation efficiency has been highlighted.

2.1. Crude oil origin and characteristics

Geological processing of organic materials buried deep beneath the sediments of oceans and lakes for thousands of years leads to crude oil formation. The lesser density of crude oil causes its upward migration leading it to get trapped within impermeable rocks acting as a crude oil reservoir (Hunt, 1990). The chemical composition of crude oil varies based on the chemical nature of the organic matter and the sediment or reservoir physiological conditions (heat, pressure, age). **Table 2.1** shows the average crude oil composition based on its elemental and compound constituents. The major constituents of crude oil are categorized as saturated hydrocarbons, aromatic hydrocarbons, asphaltenes, and resins (Harayama et al., 1999).

The percentage contribution of these major constituents decides the physical nature of the crude oil, thus differentiating them as light, medium, and heavy crude oil. Light crude oil is abundant in saturated hydrocarbons, making them the least viscous and dense whereas, medium and heavy crude oil comprises a higher proportion of asphaltenes and resins, making them highly viscous and denser. The density of crude oil varies from 0.7-0.8 g/cm^3 for light crude oil, 0.8-0.9 g/cm^3 for medium crude oil, and 0.9-0.95 g/cm^3 for heavy crude oil (National Academies of Sciences, 2016). American Petroleum

Institute (API) has developed an API gravity parameter to determine oil density. It is calculated using **equation 2.1** expressed as,

$$API = \left(\frac{141.5}{Specific\ gravity\ of\ oil}\right) - 131.5 \quad (2.1)$$

Table 2.1. Average elemental and compound composition of crude oil in relative percentages (Demirbas et al., 2015; National Academies of Sciences, 2016)

Elemental compositions		**Compounds composition**				
Overall	**(%)**	**Crude oil types**	**Aliphatic (%)**	**Aromatics (%)**	**Resins (%)**	**Asphaltenes (%)**
C	79.5-87.1	Light	92	8	1	0
H	11.5-14.8	Medium	78	15	6	1
S	0.1-3.5	Heavy	38	29	20	13
N and O	0.1-0.5	Diluted Bitumen	25	22	33	20

The crude oil is categorized as light, medium, heavy and bitumen when API values are ≥ 31.1 °, ≥ 22.3 °, ≥ 10 ° and < 10 °, respectively (Demirbas et al., 2015; Paliukaite et al., 2014). Also, light crude oil exhibits lower viscosity ~ 1 to 5 mPa.s due to lesser components of asphaltenes and resins, whereas medium crude oil and heavy crude oil viscosity range from 10-100 mPa.s 500-500,000 mPa.s, respectively. **Figure 2.1** depicts the variation in the proportion of various components of crude oil (National Academies of Sciences, 2016).

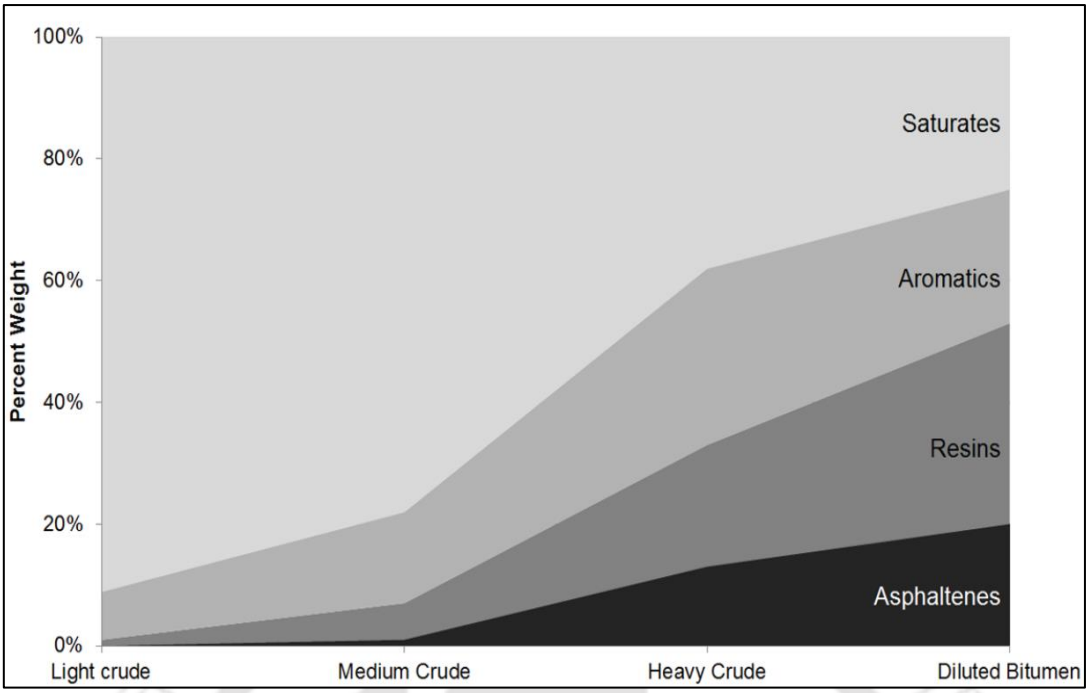

Figure 2.1. Typical classification of crude oil based on variation in the percentage of its constituents Adapted from Ref. (National Academies of Sciences, 2016) with permission from The National Academic Press

2.2. Sources of crude oil contamination and its hazard

Oil is a hydrocarbon-rich naturally occurring resource that becomes a hazard to nature when it gets spilled due to accidental discharges due to collisions of tankers, pipeline breakdown, or leakages during drilling and transportation. The exposure of oil spills to the environment leads to the 'weathering' phenomenon (Davis and Gibbs, 1975). Weathering involves various physical and chemical changes to the crude oil due to environmental factors **(Figure 2.2)**. These changes include different physical processes involving oil spreading onto the water surface, followed by oil dispersions into small oil particles, emulsion formation, adhesion of oil to matter which later leads to oil sedimentation.

Like water, soil also often comes in contact with crude oil due to natural oil seeping or deliberate/ accidental bursting or leaking of pipelines, leading to oil adhesion to soil particles. These physical processes do not affect the chemical structure of the oil. Few of the physiochemical processes such as evaporation and dissolution also led to change in the physical state of oil, yet not affecting its chemical nature (Payne et al., 1991).

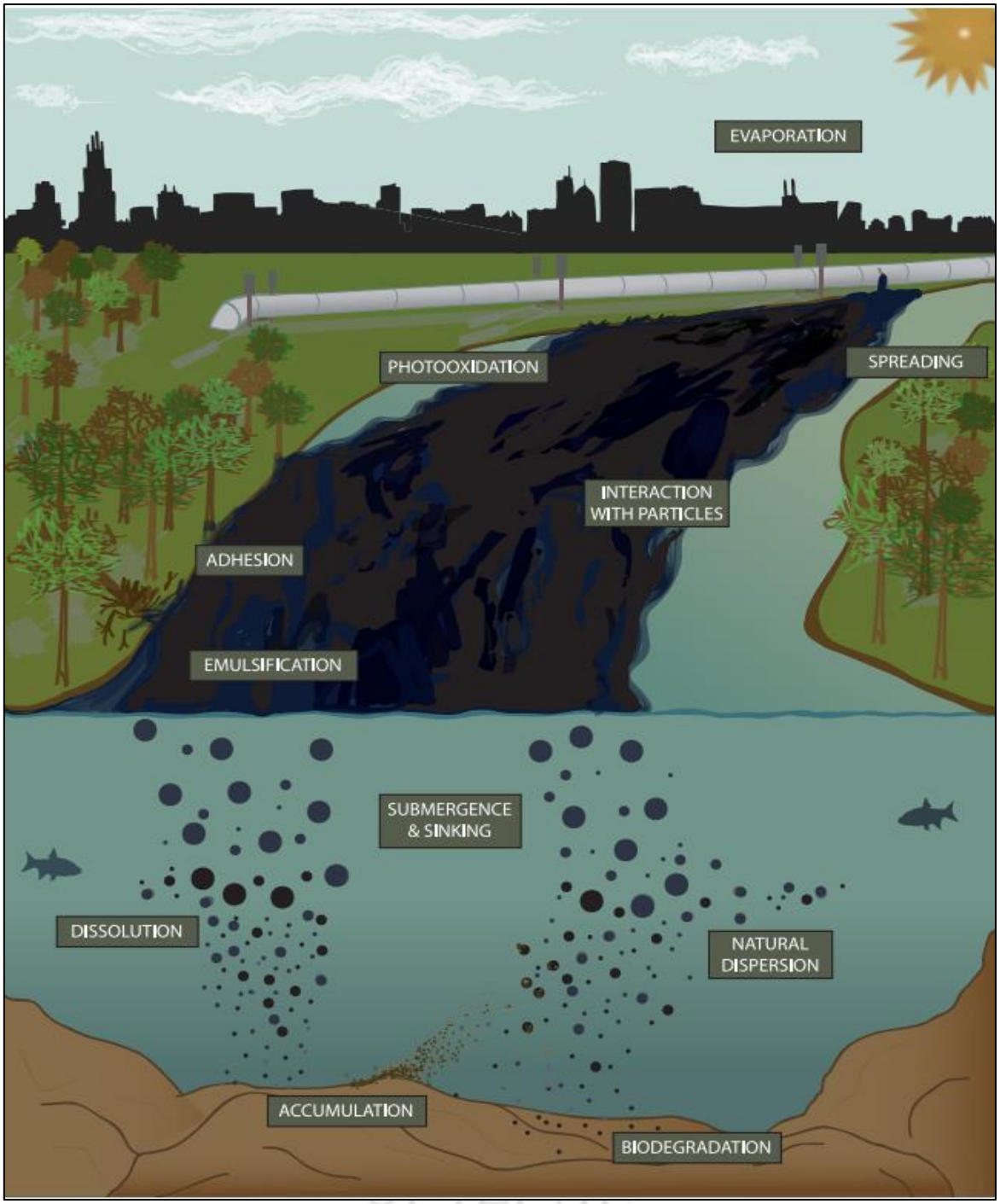

Figure 2.2. Various weathering processes act on the spilled crude oil due to pipeline leakage. Adapted from Ref. (National Academies of Sciences, 2016) with permission from The National Academic Press

On the contrary, photooxidation and biodegradation are major weathering phenomenon that causes the oxidation of oil, thus affecting its chemical composition. It includes reactions involving the formation or cleavage of covalent bonds of hydrocarbons (Bacosa et al., 2015). Among the various components

of crude oil, photooxidation under solar irradiation results in oxygenation of aromatic hydrocarbons more rapidly than others, generating various carboxylic and alcoholic derivatives, which are more persistent, thus increasing the toxicity by many folds. In an *ex-situ* study, photooxidation of crude oil resulted in oxidation of 37 % aromatic hydrocarbons and 14 % aliphatic hydrocarbon, concluding recalcitrant nature of asphaltenes and resins as no significant photooxidation was reported for them (D'Auria et al., 2009).

On the other hand, biodegradation of crude oil involves microbes mediated catalysis of oil either aerobically or anaerobically. Aerobic biodegradation is more prominent and faster than anaerobic biodegradation. However, the process takes from months to years to biodegrade crude oil components (Das and Dash, 2014). Unlike photooxidation, microbial biodegradation acts on individual components based on the microbial catalytic specificity. Few microbes act faster on aliphatic components, whereas others are more active towards cyclic or aromatic hydrocarbons, making the entire process very diverse, which has been further discussed in the next section of the chapter.

The surge for removing these spilled oils from the exposed ecosystem has been comprehensively documented in many reports describing the toxicity of crude oil to humans and other associated flora and fauna (Aguilera et al., 2010; Ahmed and Fakhruddin, 2018; Khan et al., 2018). According to a study, a minimum of 12 km^2 of oil film per ton of oil spilled is formed, which is large enough to prevent the oxygen exchange within the spilled region, destroying the inheriting ecosystem irreversibly (Wang et al., 2019). Studies revealed that crude oil toxicity affects each step of the trophic level commencing from cells to the ultimate ecosystem (Colvin et al., 2020). For example, the cells exposed to hydrocarbons exhibit early apoptosis, phagocytosis, and membrane instability (Hannam et al., 2010). Impaired metabolism of organs and increased mortality rate are also evidenced as ill effects of crude oil toxicity (Laurel et al., 2019). The toxicity also affects the population level, such as slow and impaired larval development and poor viability of offspring (Bender et al., 2021). Further, the ecosystem also exhibits a shift in community behavior due to long-term exposure to crude oil (Murphy et al., 2021). In a study, the ill-effects of crude oil exposure on *Pimephales promelas* and *Catostomus commersonii* eggs and embryos as increased mortality and delayed reproductive growth were reported (Kavanagh et al.,

2013). The toxicity is chronic due to the presence of various carcinogenic and mutagenic components of crude oil

2.3. Current tools for the control of crude oil contamination

The various measures to diminish the crude oil hazards are physical, chemical, and biological methods. Among the physical techniques, 'controlled burning' is the most common, where the spilled oil is burnt; however, the technique only works well when the oil film is thick, and the surface water is calm, limiting the mixing of oil and water. Also, the process led to the release of burnt residues which are still harmful to the affected area (Mullin et al., 2003). A comparative study on toxic effects of *in-situ* burnt oil residues to the initial unweathered oil reported no significant reduction in the toxicity suggesting the *in-situ* burning does not reduce the concentration of toxic components of oil that are already segregated within the water body before burning (Johann et al., 2021).

Another physical technique uses mechanical barriers (booms) to prevent oil spread, followed by hydrophobic adsorbents such as polypropylene skimmers to prevent oil migration (Bhardwaj and Bhaskarwar, 2018). Nevertheless, the non-biodegradable nature of the adsorbents portends the generation of secondary pollutants. Various researches are ongoing in the design of superhydrophobic adsorbents focusing on their high adsorption capacity, reusability and non-toxicity to the ecosystem. Pinto et al. stated the applicability of polyurethane foam with pore size < 500 µm for the oil adsorption capacity of 30 g/g, extending for 300 g/g using repetitive use; however, the foam was non-biodegradable (Pinto et al., 2016). Habibi et al. also explored polyacrylic-coated polyurethane/carbon black/h-boron nitride@Fe_3O_4 sponge for the oil adsorption ability of up to 66,400 times of its weight; however, the sponge cannot be further used after 20 cycles (Habibi and Pourjavadi, 2022). For this, biomass-derived aerogels, foams and sponges have gained various research communities due to their environmental friendliness and economic feasibility. **Table 2.2** summarizes various natural biosorbents explored for oil adsorption in the recent decade.

Table 2.2. List of various reported oil biosorbents and their maximum oil adsorption capacity

S.No.	Biosorbents	Adsorbate	C_0 (g/L)	q_m (mg/g)	Reusability	Ref.
1	Chitosan-based polyacrylamide hydrogel	Crude oil in water	30	2300	NA	(Sokker et al., 2011)
2	Sodium hydroxide and cetyl pyridium chloride modified bagasse	Engine oil in seawater	3.10	80.25	NA	(Pachathu et al., 2016)
3	Sodium hydroxide and cetyl pyridium chloride modified bagasse	Engine oil in wastewater	17.38	192.58	NA	(Pachathu et al., 2016)
4	Acetylated bagasse	Crude oil	47	9100	NA	(Behnood et al., 2016)
5	3-aminopropyltriethoxysilane modified bagasse	Engine oil washing wastewater	10	750	NA	(Guilharduci et al., 2017)
6	Polyacrylonitrile coated bagasse	Diesel oil in artificial seawater	20	8400	6	(Abdelwahab et al., 2017)
7	Macroalga *Enteromorpha intestinalis* biomass	Crude oil in seawater	10	2308	NA	(Boleydei et al., 2018)
8	Fruit shell residue from *Xanthoceras sorbifolia*	Crude oil in water	0.52	75.1	NA	(Liu et al., 2018)
9	Modified *G. applanatum* mushroom	Rapeseed oil	NA	1800-3100	4	(Balzamo et al., 2019),
10	Chitosan biosorbent	Crude oil in saline wastewater	0.09	9	NA	(Vidal et al., 2019)

Aside from restricting the oil migration using oil sorbents, physical measures are often ineffective when the spilled area is huge to contain, or the oil is too viscous, causing clogging of sorbents used (Flaherty and Jordan, 1989). In this case, chemical treatment is applied to disintegrate and reduce oil viscosity. Application of dispersants such as Corexit 9500 and 9527 and Superdispersant-25 (SD-25) have been reported to accelerate the biodegradation of oil as they aid the natural breakdown of oil making into tiny droplets (10-100 micron-sized), thus improving their bioavailability for microbial catabolism

(Techtmann et al., 2017; Zahed et al., 2011). However, lately, various researchers have discouraged using these chemical dispersants, increasing the water's overall polyaromatic hydrocarbons (PAHs) content (Martinović, Kolarević et al. 2015). Ramachandran et al. reported 6- to 1100-fold higher PAH fractions due to dispersants (Ramachandran et al., 2004). Hook et al. also reported similarly increased concentrations of PAHs: Acenaphthylene, Acenaphthene, Fluorene and Phenanthrene by 1.8, 2.4,2.4, and 4.4 folds in the presence of 1:100 oil: dispersant (Slickgone NS) as loading concentration (Hook and Osborn, 2012). Many aquatic toxicology studies reported adverse effects of oil dispersants on marine life, such as reduced feeding rate of *Crassostrea virginia* (Jasperse et al., 2018) bioaccumulation in Bivalves (Durier et al., 2021; Scarlett et al., 2005). At a loading concentration of 10:1 oil: dispersant ratio, the inhibitory concentration (IC_{10}) value 0.07 g/L, which was 4.5 g/L in the absence of dispersants (Hook and Osborn, 2012). The most exploited aquatic dispersant used for oil spill control is Corexit, which has reported lethal concentration (LC_{50}) value in the range of 14-20 ppm for various invertebrates (Wise and Wise, 2011). Thus, the current physical and chemical measures need to be carefully planned before further practicing. **Table 2.3** lists the major merits and demerits of the various crude oil remediation strategies.

Table 2.3. Various crude oil remediation techniques with their merits and demerits (Dave and Ghaly, 2011)

S. No	Type of treatment	Tools	Merits	Demerits
1	Physical treatment	Booms Skimmers Adsorbents	• Highly efficient as the adsorbed oil is converted from liquid phase to semi-solid phase in a short time • Reduces hazard by inhibiting the spreading of oil • Adsorbed oil can be easily recovered and reprocessed prior to reuse • Adsorption capacity is ~ 70 to 100 times of adsorbent weight, and adsorbents can be reused for several cycles • No change in the chemical characteristics of oil	• Only effective in calm weather conditions • Effectiveness reduces during strong winds and currents • Adsorption depends on the thickness of oil spread • Adsorbents are often prone to clogging due to floating water debris • Naturally occurring organic adsorbents are less selective and sink after sometimes, thus making it difficult to recover for repetitive cycles • Natural inorganic sorbents are associated with health risks if inhaled, such as vermiculite and clay • Synthetic sorbents are expensive to manufacture and non-biodegradable after their usage
2	Chemical treatments	Dispersants Solidifiers	• Rapid in the mode of action treating 90 % of oil • Less costly than physical tools • Not dependant on weather conditions • Dilutes thick oil slick into small oil particles, increasing the surface area of oil for microbial degradation	• Oil cannot be recovered after treatment • Dispersant effectiveness depends on the chemical characteristics of sea and oil • Dispersants are a potential hazard to the ecosystem • The chemical agents cannot be reused

3	Thermal	*In-situ* burning	• Rapid in action and highly efficient • Requires no specialized equipment	• Effective in calm weather conditions and freshly spilled oil • May create secondary fires • Ash residues sink and contaminate underground water
4	Biological treatment	Bacteria Fungi Algae Plants	• Restores the ecosystem completely • Environment friendly and economic	• Biodegradation efficiency varies greatly on the bioavailability of oil and nutrients • Spilled sites are always nutrient derived, and the addition of nutrients externally sometimes leads to eutrophication • Asphaltic residues remain unaffected by biodegradation • High initial oil concentration inhibits the biodegradation process and extends the lag phase by 2-4 weeks • Limited biodegradability and relatively longer treatment time required

2.4. Bioremediation of crude oil: a sustainable approach

Crude oil bioremediation uses biological agents to degrade, remove or detoxify contaminants from the oil-contaminated site (soil/water/air). It involves using microbes, plants, metabolic enzymes, or their products to detoxify toxic contaminants (Wolf et al., 2020). Bioremediation has tremendous advantages over conventional physical and chemical methods. No harmful secondary waste generation and renewable resource utilization make the entire process cost-effective and eco-friendly. During the Exxon-Valdez spillage in the Gulf of Alaska (Alaska, U.S.), it was reported that the overall expenditure in shoreline cleaning using bioremediation was lesser than the single-day expense of physiochemical tools deployed for the action (Speight, 2018). Hence, bioremediation has come up as a suitable solution to the widespread environmental contamination.

Microbes contribute to the highest of existing biodegradation in the biosphere. Microbes are equipped with machinery to utilize these hazardous contaminants as substrates for their routine metabolism. Various bacteria such as *Pseudomonas* sp., *Bacillus* sp., *Acinetobacter* sp., *Rhizobium* sp. have been found highly functional in the bioremediation of crude oil. Few bacteria such as *Rhodococcus* sp., *Pseudomonas* sp., *Alcanivorax* sp., *Geobacillus* sp. and *Aeribacillus* sp. are involved in biodegradation of alkane fractions of oil more effectively (Niescher et al., 2006; Park and Park, 2018; Shao and Wang, 2013). Whereas few bacteria such as *Brevibacterium* sp., *Pseudomonas* sp., *Halomonas* sp., *Aeribacillus* sp., are more capable of biodegrading aromatic fractions of the oil (Carolin et al., 2021; Grimm and Harwood, 1999; Monzón et al., 2018; Singh and Tiwary, 2017; Tao et al., 2020). In addition, few bacteria of class *Pseudomonas* spp., *Bacillus* spp., *Stenotrophomonas* spp., *Enterobacter* spp., and *Microbacterium* spp, are capable of metabolizing resins and asphaltenes fractions of oil (Gao et al., 2017; Shahebrahimi et al., 2019; Tavassoli et al., 2012). Similarly, various fungi such as *Rhizopus* sp., *Aspergillus* sp., *Penicillium* sp. and *Fusarium* sp., have come up as promising candidates for this purpose (Chang et al., 2020; Rajendran et al., 2020; Ruiz-Lara et al., 2020; Zegzouti et al., 2020). Apart from these microbes, a few plants, namely, *Eichhornia* sp., *Amaranthus* sp., and *Phragmite*s sp., have also been extremely helpful in remediating the contaminated hydrocarbon ecosystem. The bioremediation study with plant *A. retroflexus* revealed that root inhabiting fungal strains were more capable of bioremediating petroleum-contaminated soil due to the release of certain root exudates that

improved the fungal biodegradation ability (Mohsenzadeh and Rad, 2015). Similarly, a reduction in petroleum hydrocarbon concentration by 74.7 and 82.3 % was obtained in soil planted with *P. australis* and *E. crassipes*, respectively, due to improved rhizobacterial microbial load as plantation acted as biostimulant (Ubogu et al., 2019).

2.4.1. Mechanism of crude oil biodegradation

Biodegradation majorly involves the breakdown of oil mediated by a set of oxidation-reduction, peroxidation, methylation and complexation reactions (Ojuederie and Babalola, 2017; Siracusa, 2019). The main principle intended in this chemical reaction is the catabolism of oil components into smaller carbon units to decrease their toxicity and increase their affinity and permeability to be used as substrate. However, this information is highly generic and varies from species to species. Since most of the microbes involved in bioremediation are inherent to the contamination site and cannot be cultured using existing research tools, the exact process involved is not yet clearly understood. Various lab-scale studies have been performed for the isolation of such inherent microbes from the oil-contaminated site, identifying their behavior and metabolic activity to control the contamination (Chang et al., 2020; Datta et al., 2018; Ibrahim et al., 2020; Ohadi et al., 2017; Schlusselhuber et al., 2018; Thavasi et al., 2011; Vigneshwaran et al., 2018).

Oil biodegradation can be broadly classified as aerobic and anaerobic, depending on a terminal electron acceptor **(Figure 2.3)**. During aerobic biodegradation of hydrocarbons, microbes utilize oxygen as an electron acceptor. The hydrocarbons are oxidized to their alcoholic derivatives with mono/di-oxygenase or hydroxylase enzymes. This oxidation could be terminal, sub-terminal or both. It is followed by the formation of aldehyde/ketone bodies that later are transformed into carboxylic acid isoforms before entering into the fatty acid metabolism via β-oxidation yielding acetyl CoA **(equation 2.2)**.

$$RH \xrightarrow{Alkane\ hydroxylase} R-CH_2OH \xrightarrow{Alcohol\ dehydrogenase} RCHO \xrightarrow{Aldehyde\ dehydrogenase} RCOOH \xrightarrow{acyl\ CoA\ synthetase} RCO-SCoA \xrightarrow{\beta\ oxidation} acetyl\ CoA \quad (2.2)$$

The most explored enzyme in the aerobic biodegradation of aliphatic hydrocarbons is alkane hydroxylase (Alk B). This non-heme membrane-bound enzyme uses oxygen as a terminal electron acceptor to oxidize alkane using rubredoxin as an electron transfer system. It was discovered in hydrocarbon-degrading bacterial plasmid *Pseudomonas putida* GPo1 (Sierra-Garcia and de Oliveira, 2013). The plasmid genome study revealed the presence of OCT plasmid, comprising two operons: (1) alkBFGHJKL and (2) alkST (Shao and Wang, 2013). The first operon codes all the necessary enzymes responsible for alkane hydroxylation, such as the membrane-bound Alk B enzyme and its co-factor Rubredoxin (Alk G). The second operon codes for the enzyme (Rubredoxin reductase, i.e., AlkT and AlkS) responsible for regulating the activity of operon-1 associated enzymes (Marchant et al., 2006). A similar plasmid system has been reported to be active in various other alkane degrading microbes and hence has been opted as a suitable genetic marker for the hydrocarbon utilizing microbes. However, researchers have also identified other analogous genes coding for enzymes such as alkane monooxygenase for long-chain substrates (ladA) and Flavin binding monooxygenase (almA), mostly found in extremophiles (Park and Park, 2018). Similarly, methane monooxygenase (MMO) responsible for oxidation of C1-4 carbon chains, and cytochrome P450 is responsible for catalyzing C5-16 carbon chains.

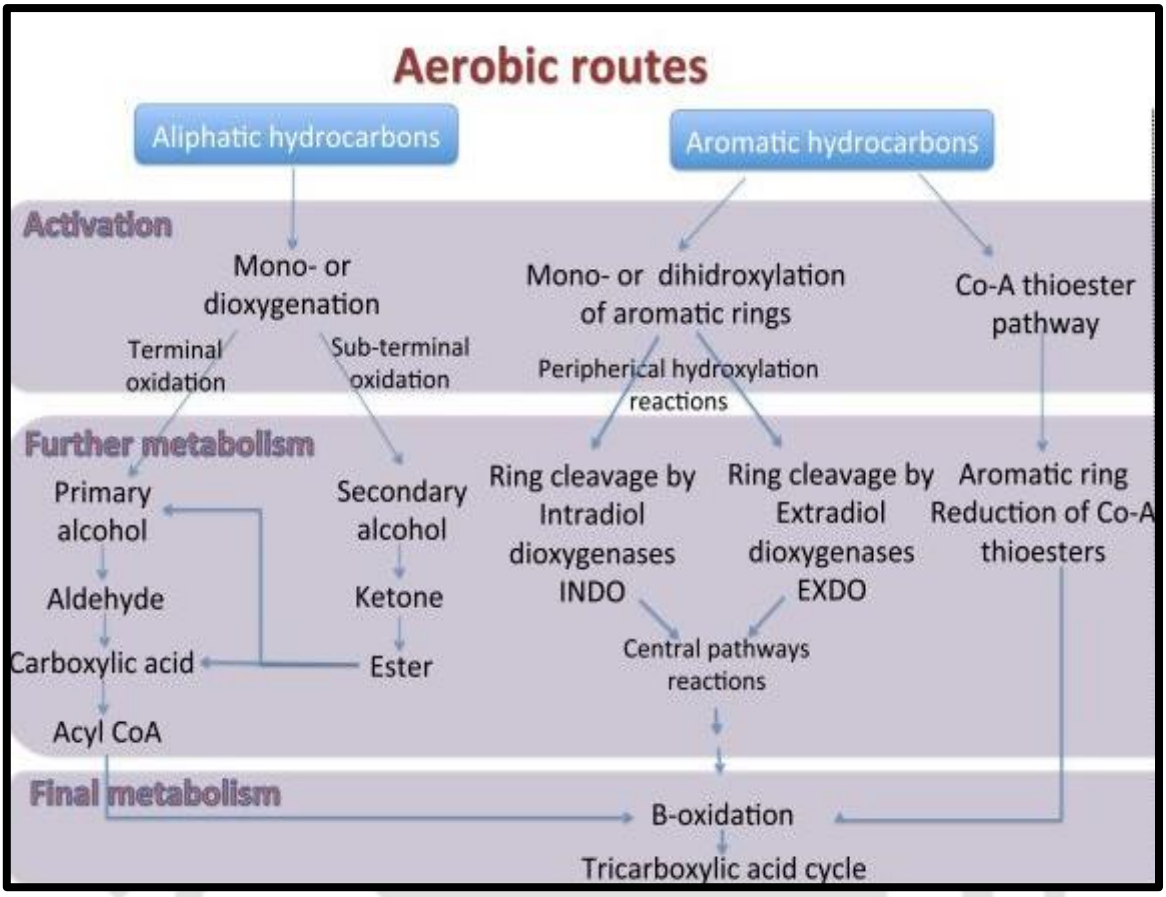

Figure 2.3. Schematic representation of hydrocarbon catabolism under aerobic conditions (Sierra-Garcia and de Oliveira, 2013)

Similarly, *Pseudomonas putida* G7 has been characterized for the presence of genes responsible for aromatic hydrocarbon degradation. The microbe contains a NAH7 plasmid coding for two operons: (1) nal operon coding for upper half pathway (Naphthalene → Salicylate), and (2) sal operon coding for lower half pathway (Salicylate → Pyruvate)(Miyazawa et al., 2020; Peng et al., 2008), as shown in **Figure 2.4**. Another PAH catabolizing operon has also been explored in a few genera, such as *Ralstonia* sp. U2, *Comamonas testeroni* strain GZ42 and *P.stutzeri* AN10, comprising nag operon for the first half of the pathway and nahGTHINLOMKJY operon for the second half of the pathway (Peng et al., 2008).

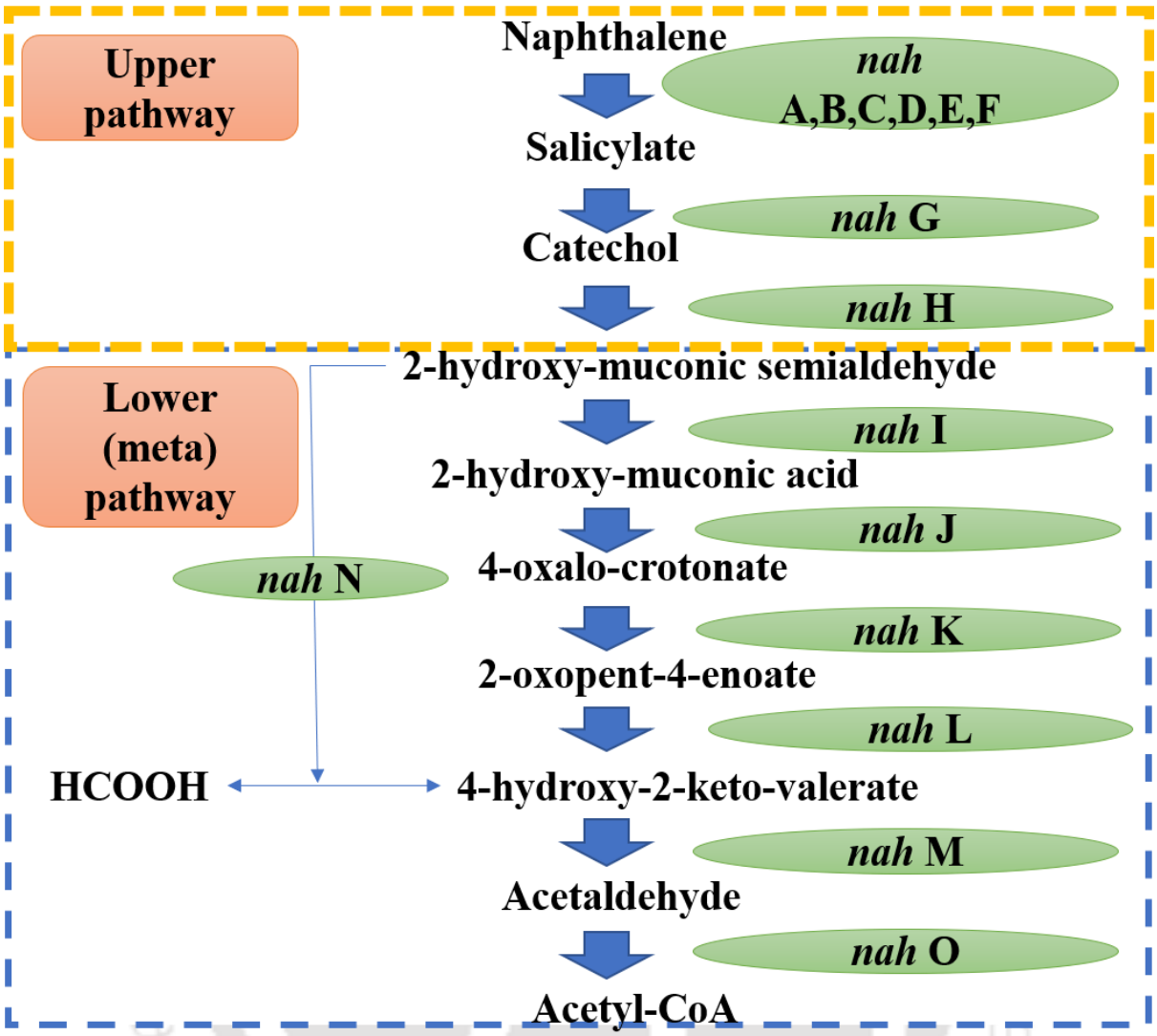

Figure 2.4. General naphthalene degradation pathway and genes coding NAH7 plasmid (Grimm and Harwood, 1999)

However, in the absence of oxygen, a few micro-organisms opt for an anaerobic pathway of hydrocarbon degradation **(Figure 2.5)**. This anaerobic pathway occurs through (a) fumarate addition; (b) hydroxylation under anoxic conditions; (c) carboxylation; (d) reverse methanogenesis; or (e) hydration (Laczi et al., 2020). Few major enzymes involved in this process are listed as; alkyl succinate synthase (Ass) (Simister et al., 2016), methyl-CoM reductase (Mcr) (Scheller et al., 2010), ethylbenzene dehydrogenase benzylsuccinate synthase (Bss) (Rabus et al., 2019), and naphthyl-2-methyl succinate synthase (Nms) (Selesi et al., 2010).

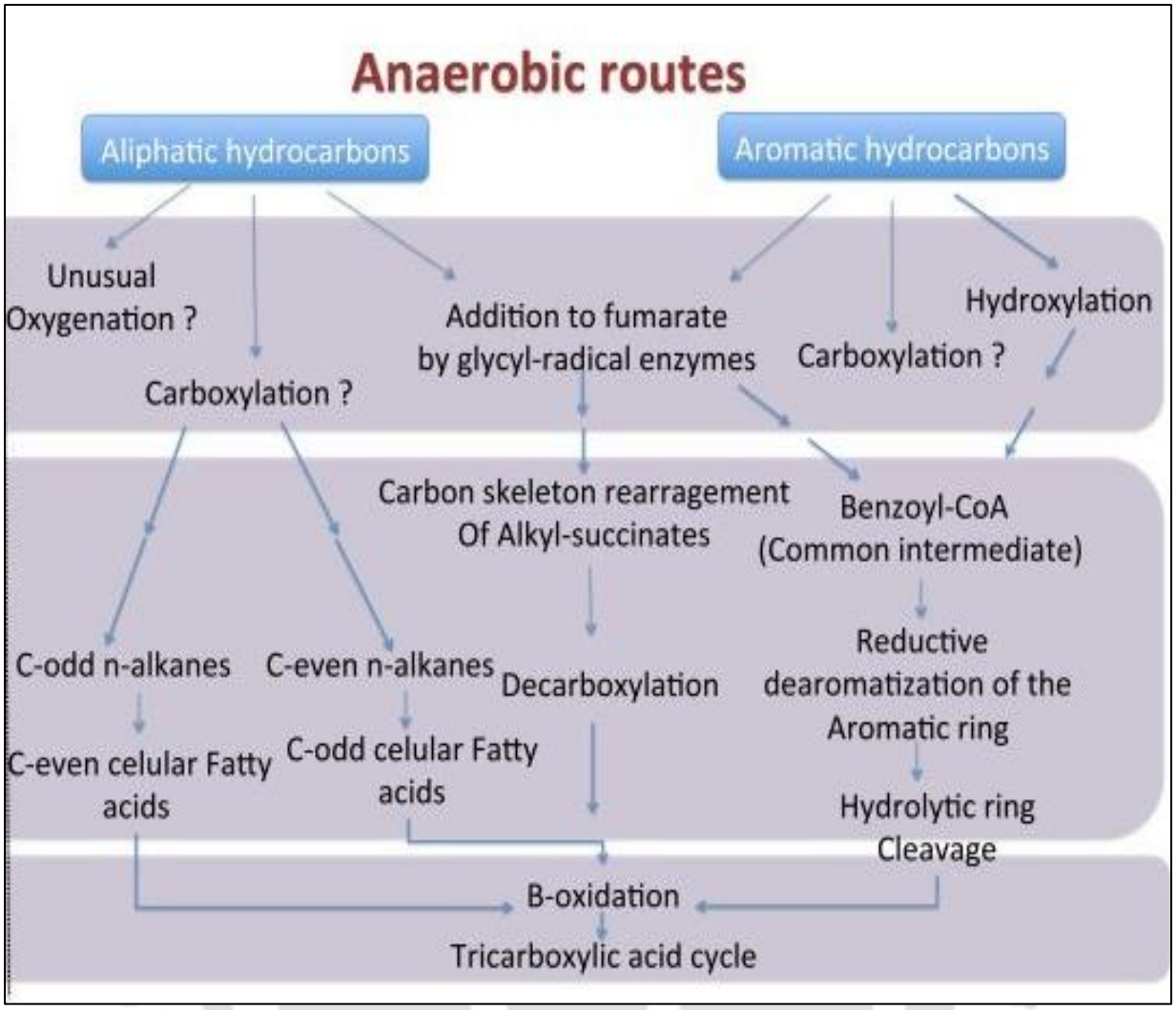

Figure 2.5. Schematic representation of hydrocarbon catabolism anaerobically (Sierra-Garcia and de Oliveira, 2013)

The natural degradation of crude oil contaminants by the inherent microbes without human intervention is called natural attenuation (Agnello et al., 2016). Natural attenuation is a continuous process contributing to ecosystem biodegradation. However, the process is slow and less effective due to the stress and toxic effect of hydrocarbons on the biodegradation ability of microbes. On the other hand, bioremediation is a manual engineered intervention to the natural endlessly occurring biodegradation phenomenon. Bioremediation intends to improve this naturally existing process overall to enhance the rate by many folds. This improvement is achieved by training the combating biological agents with adequate nutrition and stimulating their metabolic machinery for higher activity and yield. In order to

improve this naturally existing process, researchers have utilized techniques such as (1) isolation and screening of potential inherent microbial consortium, (2) bio stimulation referring to the supplementation of optimized nutrients for improved biomass growth and biodegradation, (3) bioaugmentation where the contaminant site is supplemented with exogenous hydrocarbon-degrading microbes in order to complement the existing inherent microbial consortia.

2.4.2. Isolation of oil degraders and exploration of their biodegradation ability

The most economical solution is to exploit inherent microbes inhabiting the oil-contaminated sites to restore the natural ecosystem and biodegradation of contaminants. Studies revealed that the inherent bacteria been acclimatized to the toxicity of the hazardous compound play a major role in the biodegradation due to their inherently gained resistance (Council, 1993; Paliwal et al., 2012). Thus, research targeted the isolation and identification of these microbes and understanding their potential role in biodegradation. In this regard, ample research has enlightened the different inherent microbes and their potentiality in biodegradation. More than 80 genera of bacteria have been isolated from oil-contaminated sites and reported for their potential petroleum biodegradation ability (Ejaz et al., 2021). The isolation and screening of oil-degrading bacteria occur in two major steps: (1) Enrichment culture system and (2) Sub culturing to solid agar.

The enrichment culture system focuses on favoring the population of a certain group of bacteria over the total microbial titer of the sample. The process provides favorable physiological conditions stimulating the growth of targeted bacteria by providing particular nutrients. The technique aims to enhance the population of the desired set of bacteria that previously had limited counts to a detectable level to isolate them in further steps (Madhuri et al., 2019). Most of the enrichment media are minimum salt media (MSM), such as Bushnell Haas broth which lacks any carbon source, thus keeping the room for choosing a specific C source for targeted population growth. Various isolation studies for petroleum biodegrading microbes were performed using MSM media with crude oil as the sole C source for enriching only oil-degrading bacterial population (Datta et al., 2018; Datta et al., 2020; Ejaz et al., 2021). They are enumerated after enrichment of the desired bacterial population using serial dilution and solid agar plating techniques. Briefly, the overnight enriched bacterial culture is serially diluted by

five to seven folds and plated on solid agar plates containing only crude oil as a C source. The growth of bacteria is observed visibly after 24 to 48 hr of incubation based on their hydrocarbon utilization ability. Based on the source of isolation, such as soil, oil spill, petroleum industry effluent, the isolation and optimization studies of crude oil degraders have been summarized in **Table 2.4.**

However, these studies are limited to the culture-dependent microbes, which only contribute to a small percentage of inherent microbiota at the contaminated site. Many scientific findings have emphasized the need to unveil the uncultivable microbes, as they play a major role in *in-situ* biodegradation (Shekhar et al., 2020). Various meta-genomics, transcriptomics and proteomics-based unconventional approaches have been explored to understand this sheer miscellany of the microbial community. Few such potential degrading yet difficult microbial culture communities include Firmicutes, Actinobacteria, Proteobacteria, and Bacteroidetes (Pal et al., 2019; Sar et al., 2019).

Table 2.4. Case studies summarizing the isolation of oil-degrading microbes from various sources, their isolation techniques and oil biodegradation efficacy

S.No.	Source of isolation	Isolation procedure used	Bacteria isolated	Optimization condition for crude oil biodegradation	Biodegradation efficiency	Ref
1.	Seawater samples from Teluk-Batik beach, Malaysia	Enriched in MSM supplemented with 0.5 % (v/v) Tapis Light Crude Petroleum Oil (TLCO) and incubated at 24°C, 197 rpm for 7 days 3 serial enrichments were performed using 15 mL inoculum in fresh MSM, followed by isolation of TLCO degraders on solid nutrient agar plates	*Bacillus tropicus*, *Bacillus licheniformis* and *Bacillus subtilis*	Different concentrations of palm oil mill effluent discharge (POME FD) (0.1, 0.25, 0.5, and 1 %, v/v) were added to MSM media supplemented with TLCO (0.5 and 1.0 %, v/v)	POME FD dosage of 0.25 % with 1 % TLCO was obtained as optimum concentration for achieving 95.23 % of oil biodegradation efficiency within 40 days	(Sayed et al., 2021)
2.	Textile effluent	50 ppm of 4-Aminobiphenyl (4-ABP) was supplemented to 100 mL of Nutrient broth, and 1mL textile effluent was used as inoculum. The culture was incubated at 37 °C, 120 rpm for 7 days and 5 repetitive subculturing were performed followed by spread plating after serial dilution (10^{-1} to 10^{-4}).	*Brevibacterium* sp. GA245	Biodegradation of 4-ABP supplemented in MSM media was optimized by varying factors: pH (3, 5, 7 and 9), temperature (30, 50, 70 and 90 °C) and concentration of 4-ABP (50 ppm, 100ppm, 150 ppm and 200 ppm)	50 ppm of 4-ABP at pH7, and 30°C showed maximum biodegradation of 76 %, which was further improved to 82. 2% upon addition of biosurfactant (2.5 g/L)	(Femina Carolin et al., 2021)

3.	PAH-contaminated river sediment samples from Anhui Province, East China	Sediments samples were mixed in sterile water in a 1:9 w/v ratio and mixed in an orbital shaker for 5 h at 30°C, 150 rpm. Enrichment was performed using 1 % (v/v) of culture in sterile MSM with 50 ppm PHE and incubated at 30 °C, 150 rpm for 7 days. Sub-culturing was performed for 5 repetitive cycles with gradual 50 ppm PHE addition in each cycle. After the 5^{th} cycle, the bacteria culture was serially diluted to 10^{-7} folds and later spread on the MSM agar medium coated with the PHE solution and incubated at 37 °C for 3 days to obtain single colonies.	*Diaphorobacter nitroreducens* MK027365.1	Culture medium pH (4, 5, 6, 7, 8, 9, and 10), temperature (20, 25, 30, 35, and 40°C); initial PHE concentrations (100, 200, 300, and 400 ppm) were varied in MSM to obtain the maximum PHE biodegradation.	100 % biodegradation was obtained at optimized conditions of PHE concentration of 100 ppm at 30°C and pH 7.0 after 72 h of incubation	(Wang et al., 2020)
4.	Petroleum oily sludge (POS) from an oil refinery plant Shazand, Iran	The sample was incubated in sterile mineral Bushnell-Haas medium (MBHM) with 5 % (w/v) POS supplementation at 30 °C for 7 days. Subculturing was done using 5 % (v/v) inoculum in fresh MBHM followed by streaking on Nutrient agar for colonies isolation.	*Acinetobacter radioresistens* KA2 and *Enterobacter hormaechei* KA3	Different concentrations of kerosene oil (1, 2, 3, 4 and 5 %, v/v) and pH (5, 6, 7, 8, and 9) were added to the MBHM inoculated with the selected bacterial consortium incubated for 7 days at 30 °C.	Kerosene oil was biodegraded by 66.35 % at neutral pH by the selected consortium	(Kooliva nd et al., 2020)

5.	Petroleum hydrocarbons-rich sludge (PHRS)	5 % (w/v) PHRS was enriched in sterile Bushnell-Haas (BH) media and incubated at 30 °C for 7 days. 5 % (v/v) inoculum was sub-cultured in fresh BH supplemented with 1 % crude oil (v/v) for 3 consecutive cycles. Afterward, serial dilution and plating was performed on Mueller Hinton agar to isolate single colonies	*Sphingomonas olei* KA1 and *Acinetobacter radioresistens* KA2	Different concentrations of crude oil (1, 2, 3, 4, and 5 %, v/v) supplemented in BH media at different pH 4, 5, 6, 7, 8, and 9 were incubated at 120 rpm for 7 days	70.86 % crude oil was biodegraded using 2 % initial oil concentration in BH medium (pH 7) by a mixed consortium in 7 days of incubation	(Kooliva nd et al., 2019)
6.	Lubricant contaminated soil and contaminated soil from the locomotive depot, Ukraine	The bacterial strain was isolated using the serial dilution method followed by the spread plate technique using agar containing 200 ppm of phenol incubated at 28°C for 5 days.	*R. aetherivorans* UCM Ac-603	Different concentration of phenol (200-2000 ppm) was supplemented in MSM media and incubated at various incubation period based on bacterial phenol assimilation rate.	100 % phenol biodegradation occurred when an initial phenol concentration of 1750 ppm was added to the MSM within 4 days	(Nogina et al., 2020)

7.	Soil contaminated with oil or salt or aromatics, Kazakhstan	MSM with C substrate as tetradecane, pristane, cyclohexanone, biphenyl, and 4-tert-amylphenol at pH 6.3 were incubated at 30°C, and 130 rpm for the enrichment and subsequently serial dilution and spread plating on nutrient agar were incubated for 6 days for bacterial isolation	*Curtobacterium* sp. SBUG 2094, *Rhodococcus* sp. SBUG 2075, *Rhodococcus* sp. SBUG 2031	0.25 % (v/v) of individual substrates were supplemented to MSM medium and incubated at 30°C and 130 rpm	100 % biodegradation of tetradecane substrate was obtained for *Curtobacterium* sp. and *Rhodococcus* sp. SBUG 2075, and almost 96 % degradation of pristane was reported for *Rhodococcus* sp. SBUG 2031 within 5 days of incubation	(Mikolasch et al., 2019)
8.	Fuel oil-polluted coastal marine sediments of Penang Island	Samples at a concentration of 1 % (w/v) were enriched in ONR7a, and Bushnell Hass mineral salts (BHMS) media containing 1% (v/v) engine oil as the sole carbon source and incubated at 30°C for 10 days after that 4 consecutive subculturing using fresh media and 5 % (v/v) inoculum were performed followed by streaking to obtain single colonies on BHMS agar and ONR7a agar.	*Chryseobacterium* sp. AJ0 and *Escherichia* sp. UIWRF0110	10 % (v/v) of bacterial inoculum was added to 10 mL of fresh engine oil and incubated at 150 rpm and 37°C for 7 days.	*Escherichia* sp. UIWRF0110 efficiently biodegraded up to 90 % of oil while *Chryseobacterium* sp. AJ0 showed 84 % biodegradation efficiency within 7 days of incubation at 150 rpm and 37°C.	(Abbas et al., 2018)

9.	Oil-polluted coastal sediment, Bohai Bay, China	Fresh MSM containing 0.5 % (w/v) crude oil were inoculated with 10 % (v/v) of well homogenized 10 g contaminated soil sample and incubated for 7 days at 170 rpm and 30°C. Subsequently, 3 sets of subculturing were done with a gradual increase in substrate concentration by 0.5 % in fresh MSM containing 10 % previously enriched culture. For isolation of single colonies, serial dilution-based spread plating was done on MSM agar plates and incubated at 30 °C for 48 h.	*Lysinibacillus* sp. HDB-1; *Bacillus flexus* HDB-2; *Pseudomonas mendocina* HDB-3; *Pseudomonas alcaligenes* HDB-4; *Bacillus thuringiensis* HDB-5; and *P. alcaligenes* HDB-6	A mixed bacterial consortium at a 5 % (v/v) concentration was inoculated to 1.5 % (w/v) crude oil containing medium and incubated at 30°C and 180 rpm for 14 days.	5 % (v/v) inoculum prepared using mixed bacterial consortium exhibited crude oil (1.5 %) biodegradation ability of 80.64 % within 14 days of incubation	(Tian et al., 2018)
10.	Crude oil contaminated soil in Turkey	1 % (v/v) of fully homogenized soil sample (20 %, w/v) was inoculated into fresh MSM media supplemented with 100 ppm of diethyl phthalate (DEP) and incubated for 5 days at 150 rpm and 30°C. 3 subsequent subculturing was performed with a gradual increase in DEP concentration followed by serial dilution and spread plating on MSM agar plates containing 100 ppm DEP for 5 days, maintained at 30°C.	*Pseudomonas putida*	1 % (v/v) bacterial inoculum was added to MSM media supplemented with yeast extract (0.5 %, w/v) and 100 ppm DEP, incubated at 150 rpm and 30°C for 5 days	Bacteria exhibited the DEP biodegradation efficiency of 85.5 % in 5 days of incubation at pH 7.0 and 30°C.	(Çevik et al., 2019)

11.	Polyaromatic hydrocarbon contaminated farmland soil, Shanghai, China	Enrichment of bacteria was performed using an equal volume of soil slurry and minimal media containing 100 ppm PAHs and incubated for 4 weeks at 28°C under shaking. The serially diluted culture was further repetitively spread plated on agar plates containing phenanthrene or pyrene as a C source, incubated for 2-3 weeks at 28°C static to isolate single colonies.	*Mycobacterium gilvum* SM 35, *Bosea thiooxidans* DSM 9653, *Arthrobacter pokkalii* P3B162, *Paenibacillus cookii* LMG 18419, *Sphingobium barthaii* KK22, *Bacillus megaterium* WH13, *Bacillus cereus* BDU5 and *Rhodococcus corynebacterioides* B1	The bacterial hydrocarbon biodegradation study was performed by incubating overnight enriched bacterial culture in fresh MM liquid culture containing individual or mixture PAHs as the sole carbon source (10 mM for benzo [a]pyrene and 20 mM for the other PAHs) incubated under shaking at 160 rpm, 28°C for 4 weeks.	PAH removal efficiencies of 82, 92, 69 and 64 % for *Bosea thiooxidans*, *Mycobacterium gilvum*, *Arthrobacter pokkalii* and *Paenibacillus cookii*, respectively, were obtained	(Zeng et al., 2019)

12.	Oil exploration sediments from a deep-water channel	Hydrocarbon degraders were enriched in 30 mL ONR7 medium with 1 %(w/v) crude oil or 10 g/L mixture of hydrocarbons as C source, inoculated with 1 g sediment sample. Two successive sub-culturing was done using 1 % (v/v) inoculum from the previous culture in the same media every 3 weeks, followed by spread plating on ONR7 agar medium to obtain single bacterial colonies.	*Halomonas*, *Pseudomonas* and *Pseudoalteromonas* and *Rhodococcus*	10% (v/v) of inoculum was added to ONR7 medium containing 2 % model oil as a C source and incubated at 20°C for 2 weeks.	~30 % of crude oil was biodegraded by a consortium isolated from the sediment	(Gontikaki et al., 2018)
13.	Oil contaminated beach sediments, Beijing	Enrichment of sediment isolates was prepared in marine broth 2216 followed by subculturing in MSM media using 2 % (v/v) inoculum for the isolation of hydrocarbon degraders	*Bacillus algicola*, *Rhodococcus soli*, *Isoptericola chiayiensis*, and *Pseudoalteromonas agarivorans*	Bacteria were inoculated to MSM media supplemented with 1 % (v/v) crude oil as C source, incubated at 28°C for 14 days at 180 rpm	Isolates effectively biodegraded >85 % of crude oil within 14 days of incubation	(Liu et al., 2018)

14.	An aged stockpile of soil from gas work site contaminated of PAHs, Australia	Enrichment was done in Bushnell Hass (BH) mineral salts medium supplemented with phenanthrene as the sole C source incubated at 28°C for 6 days, followed by spread plating on Bushnell Hass agar plates, supplemented with 1% (w/v) phenanthrene as substrate	*Rhodococcus* sp., *Achromobacter* sp., *Oerskovia paurometabola*, *Pantoea* sp., *Sejongia* sp., *Microbacterium maritypicum* and *Arthrobacter equi*	2 % of hydrocarbon (naphthalene (NAP), phenanthrene (PHE) and pyrene (PYR)) were supplemented to bacterial culture and incubated for 5 days	Bacteria showed significant hydrocarbon degradation activity, as also confirmed by their C12O activity analyses	(Haleyur et al., 2018)
15.	Activated sludge from waste water treatment plant, Saudi Arabia	Enrichment was carried out using Bushnell Haas medium (BH) supplemented with 1 % (v/v) olive CO, as the sole carbon source comprising 1 % (w/v) sludge suspension incubated for 7 days at 60 rpm. Successive subculturing was performed in the same medium composition every 7 days for 2 successive months, followed by streak plating on BH-CO and incubation at 37°C for 1–2 days.	*Stenotrophomonas rhizophila* DWCoil-2B, *Sphingobacterium* sp. DWCoil-7G, *Pseudomonas libanensis* DWCoil-5E, *Pseudomonas poae* DWCoil-6F and *P. aeruginosa* DWCoil-1A	1 % (v/v) cooking oil was supplemented to synthetic waste water comprising isolated bacterial consortium in bioreactor	~80 % decrease in the oil and grease content of the waste water was obtained within 9 days of incubation using the consortium	(Nzila et al., 2017)

2.5. Biosurfactant: an effective tool of bioremediation of crude oil

Bioremediation of crude oil is a complex process with many underlying pathways which work simultaneously to achieve maximum biodegradation. One such pathway involves the production of biosurfactants in order to break the hydrocarbons into smaller units for easy accessibility and bioavailability to the microbes. The biosurfactants can be produced by degrading microbes at the contamination site (in-situ), or biosurfactants can be produced separately (ex-situ) and applied at the site along with microbes. This section discusses the properties of biosurfactants, factors affecting the production of biosurfactants and optimization of biosurfactants production, particularly for ex-situ bioremediation.

Biosurfactants are amphiphilic surface-active compounds released by microbes as biometabolites comprising a polar head group with a non-polar fatty acid tail (Jahan et al., 2020). Such structural characterization aids the formation of micelles, emulsification and foaming activity in a non-polar and polar liquid mixture. These chemical molecules possess silent features such as decreasing the surface tension of the oil-liquid interface, improving the solubility and hence bioavailability of non-polar compounds such as hydrocarbons into water and soil environment (Patowary et al., 2018). Biosurfactants can reduce the surface tension of the liquid, where the reduction increases with an increase in the concentration of biosurfactants. However, this reduction in surface tension value halts beyond a certain biosurfactant concentration, called as critical micellar concentration (CMC). There are various techniques to determine the CMC value of biosurfactants, but the major exploit is the Du-nouy ring and Wilhelmy Plate method using tensiometer instrumentation. CMC is the minimum concentration of any biosurfactant responsible for causing the maximum reduction in the surface tension. Above CMC value, the amphiphilic biomolecules of biosurfactant from a micellar structure with hydrophobic heads form the core, and hydrophilic tails constitute the outer shell towards the aqueous phase **(Figure 2.6)**. The biosurfactant entraps the non-polar agents within the micellar hydrophobic core, thus making it more bioavailable within the solvent.

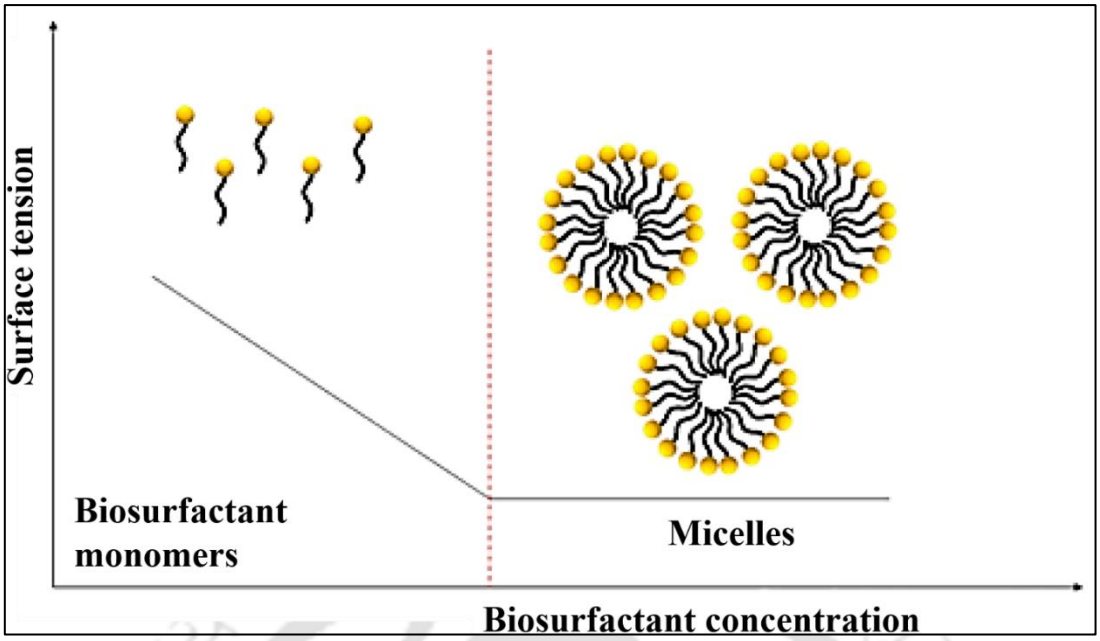

Figure 2.6. Schematic representation of reduction in the surface tension with an increase in biosurfactant concentration and micelle formation at and above CMC value of biosurfactant

The CMC value determines the efficacy of the biosurfactant. When the biosurfactant concentration is < CMC, the biomolecules act on the water and oil interface, reducing the surface tension and mobilizing the oil. On the other hand, when the concentration is above CMC value, the biomolecules tend to aggregate into the micellar structure, thus entrapping the oil within the core and increasing its bioavailability or solubility within the aqueous phase. Biosurfactants are proven to have very low CMC and high stability with no loss in activity in a broad range of pH, temperature, and salinity, thereby restricting the reliance on non-biodegradable chemical surfactants. These biosurfactants are also rich in antimicrobial and anti-viral activities (Akbari et al., 2020; CHOOKLIN and SAIMMAI, 2020). A comparative change in the CMC value of various biosurfactants in their crude and purified form has been listed in **Table 2.5.**

Table 2.5. List of various types of microbial biosurfactant and their reported CMC values

Biosurfactant	Microbial origin	Quality	CMC (mg/L)	Ref
Rhamnolipid	*P. aeruginosa* IGB83	Pure	27	(Bodour and Miller-Maier, 1998)
	P. aeruginosa (ATCC 9027)	Purified	30	(Renfro et al., 2014)
	P. aeruginosa J4	Purified	50	(Whang et al., 2008)
	P. aeruginosa KVD-HR42	Partial purified	100	(Deepika et al., 2016)
	P. aeruginosa	Crude	127	(Câmara et al., 2019)
	B. kururiensis KP23T	Purified	180–220	(Tavares et al., 2013)
	B. kururiensis LMM21	Purified	80–100	
	Bacillus Lz-2	Crude	240	(Li et al., 2015)
	P. fluorescens	Partial purified	290	(Abouseoud et al., 2010)
Surfactin	*B. licheniformis* JF-2	Purified	10	(Lin et al., 1994)
	B. licheniformis	Purified	15	(Jenny et al., 1991)
	B. subtilis MG495086	Crude	40	(Datta et al., 2018)
	B. subtilis ATCC 21332	Purified	45	(Whang et al., 2008)
	P. aeruginosa PG1	Purified	56	(Patowary et al., 2017),
	B. subtilis MJ01	Partial purified	60	((Veshareh et al., 2019)
	Brevibacillus sp. AVN13	Purified	80	(Vigneshwaran et al., 2021)
	B. subtilis N3-1P	Crude	180	(Zhu et al., 2020)
Trehalolipids	*M. luteus* BN56	Purified	25	(Tuleva et al., 2009)
	Rhodococcus sp., *PML026*	Purified	250	(White et al., 2013)
Flavolipid	*Flavobacterium* sp. MTN11	Partially purified	300	(Bodour et al., 2004)

Biosurfactants are classified as low molecular weight (glycolipids and phospholipids) and high molecular weight (lipopeptides and complex polymeric compounds) based on their structural

composition. Glycolipids can be further categorized as Rhamnolipid, Sophorolipids, Trehalose lipids and Mannosylerythritol lipids (MEL). These biosurfactants are majorly produced by *P. aeruginosa, P. alcaligenes, P. desmolyticum, R. erythropolis, Arthrobacter, Mycobacterium, Nocardia, R. ruber, R. opacus,* and *Micrococcus luteus* (Christova et al., 2013; Gein et al., 2011; Jadhav et al., 2011; Muthusamy et al., 2008; Niescher et al., 2006; Oliveira et al., 2009; Tuleva et al., 2009; Zaragoza et al., 2013). These glycolipids have proven to improve the bioremediation of hydrocarbons by mobilization and solubilization of otherwise persistent hydrocarbons. Similarly, Lipopeptides have also been subdivided into Surfactins, Iturins, Amphisin, Fengycins, Viscosin, Subtilisin, Polymyxins, and Putisolvin. *Bacillus* spp., *Serratia* spp., *Acinetobacter* spp., *Agrobacterium* spp. *Streptomyces* spp., *Halomonas* spp., *Marinobacter* spp., and *Pseudomonas* spp. are major producers of lipopeptide biosurfactants (Chang et al., 2011; Coutte et al., 2017; Datta et al., 2018). Among various lipopeptides, surfactin is highly potential in the emulsification of hydrocarbons.

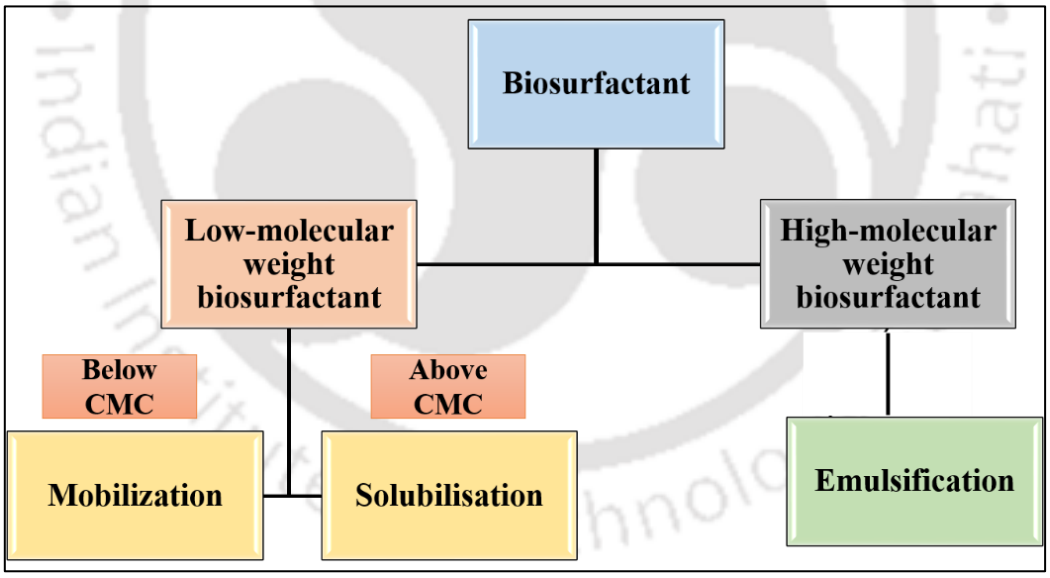

Figure 2.7. Biosurfactant classification based on their molecular weight and mode of action

Biosurfactants act on poorly bioavailable contaminants by either mobilizing them, solubilizing them or emulsifying them based on their chemical composition **(Figure 2.7)**. In a typical mobilization phenomenon, biosurfactants present in concentration below their CMC reduce the capillary force between oil and soil, reducing the interfacial tension between soil-oil improving its mobility for

bacterial action (Lin et al., 2017; Ma et al., 2018). Gradually, when biosurfactant concentrations rise above CMC, micellar structures are formed, entrapping the non-polar entity within the core, thus solubilizing it. A similar observation was made by Li et al. while exploring the solubility of pyrene, naphthalene and phenanthrene in the presence of rhamnolipid biosurfactant released by *Bacillus* Lz-2. With an increase in the biosurfactant concentration above CMC, a linear increase in the solubility of these compounds was reported (Li et al., 2015). High molecular weight biosurfactants are preferably stable in forming a highly stable emulsion of non-polar and polar compounds, e.g., oil-in-water emulsion. This characteristic feature is essential in refineries' oil washing and recovery operation. Datta et al. has reported the applicability of surfactin biosurfactant produced by *Bacillus* spp. in MEOR operation and oil washing, owing to its remarkable emulsification activity of > 65 % (Datta et al., 2018; Datta et al., 2020). Apart from this, biosurfactants are also involved in modifying the cell surface hydrophobicity of microbial cell membrane, enhancing its affinity to non-polar substrates (e.g., contaminants)(Kaczorek et al., 2018; Zhong et al., 2015). Thus, such biosurfactant properties have been extensively utilized for remediation of hydrocarbon contaminated sites, such as soil washing and oil recovery (Gupta, 2021; Ramesh and Sakthishobana, 2021).

There have been many debates on the behavior of biosurfactant production to be growth-associated or non-growth-associated. Various studies support that biosurfactants production is a characteristic feature of hydrocarbon-degrading microbes; however, some studies suggest that not all hydrocarbon-degrading strains are biosurfactant producers (Patowary et al., 2017; Wu et al., 2019). Even after decades of research in this field, the exact biosurfactant production pathway is unclear as the process varies from microbial strain to strain. Few studies hypothesize the biosurfactant production process to be induced during stress conditions; however, there is evidence where contradictory results have been reported (Chakraborty et al., 2012; Santos et al., 2016). However, every literature supports the role of biosurfactant in hydrocarbon degradation by microbial bioremediation (Abdulsalam et al., 2016) (Akbari et al., 2020; Datta et al., 2018; Jimoh and Lin, 2020; Parthipan et al., 2017; Patowary et al., 2017). Hence, it is a vital part of microbial bioremediation and environmental clean-up. Nevertheless, the challenge lies in the limited availability of such proficient bioremediation tools at the site of action, owing to its low microbial productivity. Recently, various researchers are emphasizing optimization for

the maximum biosurfactant production in order to simultaneously achieve maximum degradation as they are highly dependable processes (Datta et al., 2018; Ghazala et al., 2019; Haloi and Medhi, 2019; Jimoh and Lin, 2019; Jimoh and Lin, 2020; Ohadi et al., 2017; Vigneshwaran et al., 2018).

Understanding the basic underlying principle behind the biosurfactant production pathway by the biodegrading microbes is the key to designing a successful production model. Presuming the biosurfactant to be a growth-associated product, optimizing the microbe growth is mandatory to achieve higher productivity. The associated culture conditions and physiological parameters play a vital role in effective culture growth. With the interest of looking into media composition and understanding the role of each physiological parameter, we have described the major factors controlling biosurfactant production. Based on these major factors, their associated optimization techniques are elaborated with their associated merits and demerits.

2.5.1. Factors regulating microbial biosurfactant production

A high yield of biosurfactants is a must for competing with the commercial surfactant and being eligible for industrial production. Maximizing biosurfactant production is controlled by two factors: (1) improving the strain classed as strain engineering and (2) optimizing the culture conditions, classed as process optimization. Various studies put forward that maximum biosurfactant production is at the optimized microbial growth conditions, signifying the metabolite to be growth-associated (Devaraj et al., 2019; Yaraguppi et al., 2020). Understanding the effect of each media component and its impact on process conditions is crucial before designing an optimization model. In this regard, various researchers have restricted the role of major parameters: Carbon source, Nitrogen source, their respective concentration, culture pH, temperature, and other salt concentration as the deciding factors governing the overall microbial production effectiveness.

2.5.1.1. pH

The pH factor is regarded as one of the major factors controlling microbial growth and thereby biosurfactant production. Most of the biosurfactant production studies are conducted in the pH range of 4-10, where pH 7 is the most preferred choice as most microbial enzymes are effective at this pH.

Hence, the best-known biosurfactant producers are neutrophiles (Datta et al., 2018; Jimoh and Lin, 2020; Suganthi et al., 2018). Microbes that prefer acidic, neutral and basic environments for their growth are termed acidophiles (pH<7), neutrophiles (pH 7) and alkaliphiles (pH>7), respectively. Culture pH immensely controls the production and bioavailability of biosurfactants in the culture media. Durval et al. observed an acidic change in culture pH from 7.2 to 6.5, with increased release in biosurfactant in the culture media after 48 h of incubation (Durval et al., 2019). On the contrary, Dikit et al. observed an increase in pH from 7 to 7.5 with the increase in the biosurfactant production ability of the bacterium *Marinobacter hydrocarbonoclasticus* ST1 (Dikit et al., 2019). In correspond to these studies, it was concluded that the biosurfactant production was significantly higher in the pH range of 6-8 and was found to be drastically reduced outside this range (Jimoh and Lin, 2019).

However, the exception exists in the case of acidophiles and alkaliphiles, where the microbes are well equipped with suitable aids for surviving in such extreme conditions (Datta et al., 2018). Furthermore, Lingquing et al. suggested that pH aided microbial cell growth in *P. aeruginosa* during the early incubation stage and played a critical role in biosurfactant production in the later stages of growth. It was reported that bacteria tend to internalize the biosurfactant within the cell or on the surface in mild basic or neutral pH, hence in the first 24 h, the pH was maintained at pH7-7.5, however, post 24 h, rhamnolipid production initiated, and they changed the biosurfactant medium to 6-6.5 for extracellular release of biosurfactant (Zhu et al., 2012). Hence, pH plays an influential role in biosurfactant production and its release in the given cultural conditions.

2.5.1.2. Temperature

Temperature is another critical parameter that decides the fate of microbial growth and metabolism. Based on the preference of microbial growth over their surrounding temperature, they are classified as psychrophiles (capable of growth at low temperature < 20°C), mesophilic (suitable growth in the range of 25-45°C), and thermophilic (prefers growth at extreme temperature range >45°C). Since biosurfactant is a growth-associated metabolic product, the most preferred temperature for the maximum biosurfactant production is highly driven by the fact that microbe growth should be the highest in the range of temperature provided. Most of the biosurfactant producers (*Pseudomonas* sp.,

Bacillus sp., *Paenibacillus* sp.) are mesophilic (Jie et al., 2019; Jimoh and Lin, 2020; Yaraguppi et al., 2020).

However, a certain thermophilic bacterium such as *Bacillus subtilis* MG495086 was a highly efficient biosurfactant producer in the thermophilic condition, i.e., 62.5°C temperature, reducing the surface tension 29.85 mN/m endorsing their suitability in enhanced oil recovery applications (Datta et al., 2018). Another *Bacillus* species, *B. licheniformis*, also exhibited excellent biosurfactant production and emulsification activity, reducing the surface tension from 72 to 23.8 mN/m at a high temperature of 50°C (Daryasafar et al., 2016). Similarly, few of the prevailing biosurfactant producers in cold climate includes species of genus *Rhodococcus*, *Bacillus*, and *Pseudomonas* (Cai et al., 2014; Malavenda et al., 2015). Hence, temperature also is crucial for the growth of bacterium and thus their biosurfactant production ability.

2.5.1.3. Carbon (C) source

Carbon act as the primary source of energy for microbial growth and metabolite production. Aside from being vital for biomass growth, C acts as the building block for the synthesis of biosurfactants. Microbes can produce biosurfactants by utilizing a broad range of substrates varying from simple sugars, hydrocarbons and a few fatty acids in used/waste frying oil (Datta et al., 2018; Sharma et al., 2019). Every biosurfactant structural synthesis requires polar substrates, which are involved in the synthesis of polar head group, and non-polar substrates, such as hydrocarbon and oil, which are involved in synthesizing lipidic non-polar tails (George and Jayachandran, 2013). Most bacteria utilize simple sugars such as glucose and sucrose as C sources for maximum biosurfactant production due to their easy metabolism. However, these C sources are not cost-effective for bulk production and are often disregarded for scale-up studies. Hydrocarbons are a complex C source and often cause the production of biosurfactants in the process of their catabolic assimilation. Hydrocarbon-rich waste crude oil and fatty acid-rich used vegetable oils have gained immense attention for their inherent waste-to-wealth concept (Chen et al., 2018; Jimoh and Lin, 2020; Lan et al., 2015; Sharma et al., 2019).

Various studies support the suitability of these slowly assimilating C sources for the production of secondary metabolites such as biosurfactant (Cai et al., 2014; Dikit et al., 2019; Nur Asshifa et al., 2017;

Omarova et al., 2019; Ramos et al., 1995; Xu et al., 2018). The carbon catabolite repression (CCR) phenomenon improvises microbe's ability to prefer one C source over the other. CCR is a mechanism where less preferred substrate assimilation is restricted due to inhibition of the genes required for its expression in the presence of a more preferred substrate (Magnus et al., 2017). This phenomenon is evident in the case of hydrocarbon-degrading microbes, where no biosurfactant production is observed in the presence of polar substrates such as glucose. These polar substrates are more involved in promoting growth in the bacteria and were found to interfere with biosurfactant production (Klekner and Kosaric, 1993).

While looking for a suitable C source, another factor to keep in mind for the bulk production of the metabolite is the availability and cost of the nutrient source. For instance, waste, spent crude oil, or discharged sludge could be a suitable low-cost C source for the biosurfactant. Nevertheless, the challenges such as toxicity and poor microbial assimilation rate diminish its use as the sole C source for biosurfactant production. Hence, apart from type C sources, their concentration also plays a vital role in their suitability for microbial utilization. Various studies suggest the inhibitory impact of excess of the concentration of C source and propose the need to optimize the concentration of substrate prior to use (Datta et al., 2018; Ohadi et al., 2017; Ravi, 2019; Vigneshwaran et al., 2018). Hence, a low-cost C source with a fast assimilation rate and non-interfering is suitable for the biosurfactant production pathway.

2.5.1.4. Nitrogen (N) source

Opting for a suitable N source is a significant factor for biosurfactant production as microbes use N sources as their building units for biosurfactant synthesis (e.g., lipopeptides) similar to C sources. Studies revealed that microbes could utilize organic and inorganic nitrogen sources for their metabolism (Sharma et al., 2019). Major organic N source preferred by microbes for biosurfactant production includes peptone, beef extract, and urea and yeast extract (Dikit et al., 2019 259). Microbes also show a significant preference towards nitrates form of N over the ammonium ion. Due to the complexity reduction of nitrate salts to their respective nitrites form, which gets further reduced to ammonia and later integrates to the glutamine–glutamate pathway (Sharma et al., 2019). Thus, in comparison to easily

assimilated form of ammonium ion as N source, nitrates are preferred as it creates a nitrogen limiting environment due to its slow assimilation rate, leading to improved biosynthesis of biosurfactant. Davis and group also revealed the importance of ammonium ion as N source in the cell growth and nitrate form of N source in biosurfactant production (Davis et al., 1999).

Additionally, few amino acids are also found to be enhancers in the biosurfactant production ability of microbes. Apart from the source, nitrogen concentration plays an important part in biosurfactant production. Lower availability of N source might lead to pre-cell death leading to accumulation of biosurfactant production. On the other hand, excess of N in the media deviates the overall metabolic flux towards cellular growth and division, causing an exponential growth of the cell and diminishing biosurfactant production (Lan et al., 2015). Overall, the N source plays an important role in the production, and its concentration also controls the fate of microbial biosurfactant biosynthesis.

2.5.1.5. C/N ratio

An optimum concentration of carbon to nitrogen in the media aids the overall biosurfactant production. Most studies revealed that a high C to N ratio supports the high biosurfactant yield (Jimoh and Lin, 2019; Saimmai et al., 2013; Sharma et al., 2019). It is suggested that a high C/N ratio leads to restriction in cell growth and promotes cell metabolism for metabolites production. Joy et al. also observed a similar effect of C/N ratio on biosurfactant production by *Achromobacter* sp. (PS1) using lignocellulosic biomass as C source and the mixture of sodium nitrate and beef extract as N source. While modifying the C/N ratio from 6.2 to 12.5 range, it was reported that varying C/N ratio from 6.2-8.3 range, there was an increase in rhamnolipid production with increase in C/N ratio, emphasizing the importance of N limitation on the biosurfactant synthesis. However, when the ratio was further varied in the range of 8.3-12.5, there was a decline in biosurfactant production (Joy et al., 2019). It was due to poor assimilation of C source in the limitation of N source (Santos et al., 2016). It supports that the concentration of N in the media should be lesser than the C, however too low N source also limits the metabolism of C and thereby decreases the biosurfactant production. Summarily, the C/N ratio is a highly sensitive parameter, which varies from strain to strain and the chemical type of C and N source used.

2.5.1.6. Other factors

Even though the factors mentioned earlier play a key role in biosurfactant production, studies also suggest the importance of optimizing other non-essential reaction conditions based on further application. Few such factors are discussed in the sections below.

Salinity plays a vital role in the structural stability of *Halobacterium* and various other marine bacteria that require a salt concentration of 100-150 g/L for their survival (Oren, 2008). Despite the geographical region, the average salinity of sea water is 3.5 % (35 g/L). Hence, exploration of such halotolerant microbes is required for the oil-spill remediation and microbial enhanced oil remediation application (Darvishi et al., 2011). Since most marine bacteria are well adapted to such salinity, studies have revealed the synergistic effect of salinity on the biosurfactant-based emulsification activity (Vecino Bello et al., 2012). However, beyond the optimized condition, the emulsification activity is compromised with an increase in salt concentration; hence, the tolerance of bacteria to salinity levels needs to be tested for better results. Deng et al. studied the effect of salt concentration on the biosurfactant production ability of *Achromobacter* sp. A-8, reporting the decrement in emulsification activity when the salt concentration is increased beyond 10 g/L (Deng et al., 2020). Likewise, a moderately halophilic bacterial strain, *Bacillus subtilis* MG 495086, was found to exhibit maximum growth at 6 g/L salinity, where further increase in salt concentration decreased the reduction in surface tension (Datta et al., 2018). Though most of the fresh water and soil bacteria are not tolerant to high salinity concentration, the crude biosurfactant extracted from these bacteria are well stable at extreme pH, temperature and salinity and hold a potential role in the *in-situ* remediation and oil recovery studies (Chen et al., 2018; Jie et al., 2019; Jimoh and Lin, 2020; Joy et al., 2019).

Optimized inoculum size also plays a vital role in the overall production of biosurfactants. Studies revealed that with an increase in inoculum size, there is an increase in the overall biosurfactant production. However, further increases in microbial concentration can lead to depletion in dissolved oxygen beyond certain optimum concentrations. It occurs due to the overgrowth of microbes, resulting in increased cellular respiration, negatively affecting biomass growth and metabolite production (Suganthi et al., 2018). Jimoh *et al.* stated a similar decrease in the biosurfactant production ability of

Paenibacillus sp. D9 when the inoculum size was increased above 1.5 % (v/v) (Jimoh and Lin, 2019). Sharma et al. also supported the importance of using a small inoculum size of 2 % (v/v) for higher biosurfactant production, when the incubation time was as low as 48 h, stating it exerted lesser pressure on cellular metabolism and the overall cost of production remains effective (Sharma et al., 2018). Overall, the inoculum size should be appropriate so it does not cause either substrate feedback inhibition (i.e., higher substrate availability than a requirement) or substrate limitation during incubation due to excessive growth.

Agitation speed ensures the proper availability of oxygen and substrate throughout the culture volume to prevent dead zones. It plays an important part in the case of an immiscible or poorly miscible substrate such as oils and sludge samples as a C source. Since these substrates limit the overall dissolved oxygen transfer rate, optimized agitation is required to make oxygen available for the microbes present in the culture. Usually, fast dividing aerobic cultures require a higher agitation rate than facultative and anaerobic cultures. Studies revealed that a high agitation rate favored biosurfactant production (Bertrand et al., 2018; Brumano et al., 2017; Fonseca et al., 2007). However, where low agitation limits microbial growth due to poor availability of dissolved oxygen, high agitation leads to cell membrane disruption due to high shear force. As observed by Asshifa et al., the oxygen transfer rate in a diesel enriched culture medium was highest at 500 rpm agitation rate compared to 400 and 600rpm, leading to the highest biosurfactant production by *P. aeruginosa* USM-AR2. It was stated that volumetric mass transfer coefficient 'k_La' was found to increase from 48.21 (at 400 rpm) to 70.38 h^{-1}(at 500 rpm). However, it decreased 65.31 h^{-1} at 600rpm, leading to a decrease in biomass and biosurfactant production. It was due to restriction in an increase in area 'a', suggesting the limitation in the role of agitation rate in overall oxygen transfer (Nur Asshifa et al., 2017). At a high agitation rate >500 rpm, some *Bacillus* sp. were found to form endospores, resulting in decreased surfactin productivity (Ha et al., 2018). Another issue with biosurfactant production is the foam formation with increased agitation, limiting the overall biosurfactant productivity (Shaligram and Singhal, 2010). Hence, it is important to analyze the best-suited agitation rate for maximum microbial growth and biosurfactant production.

Incubation time plays a crucial role in cases of secondary metabolite production. Since the release of biosurfactants varies from the early exponential phase to the stationary phase, it is always important to

understand the relation between the bacterial growth profile and its biosurfactant release profile. Since biosurfactant metabolite production is growth associated in a few species and non-growth associated in some, it is not easy to predict its time of extracellular release. Thus, the incubation period plays an important role in biosurfactant production because during the late stationary phase, microbes internalize the biosurfactant within the cell, leading to a drop in the biosurfactant production and hence the overall productivity (Durval et al., 2019). Abdulsalam et al. reported a similar trend of increasing biosurfactant production until 144 h, which decreased after 168 h (Abdulsalam et al., 2016).

Similarly, a decrease in biosurfactant concentration (up to 0.5g/L) was observed after 72 h of incubation by *B. subtilis* MG495086, stating that bacterial cells tend to consume the biosurfactant as a secondary carbon source during the late stationary phase (Datta et al., 2018). Such loss of metabolite productivity makes the entire production system forfeited. Hence, it is essential to extract the released metabolite from the culture medium at an optimized time interval, i.e., before cells enter the late stationary phase. Although many studies have reported the essential factors that play a crucial role in maximizing biosurfactant production, it is also clear that these factors vary from strain to strain. Any suitable combination of these parameters cannot be concluded as best suitable. Hence, the need for an optimization model particular for each strain makes the entire production of biosurfactant time and cost-effective.

2.5.2. Optimization designs for maximizing biosurfactant production

Optimization is a scientific approach to regulate each culture parameter so that their integration provides the best output response. Various researchers have critically investigated the importance of media composition and culture reaction conditions in bulk microbial biosurfactant production. The most conventional culture condition optimization technique employed was “one factor at a time approach” (OFAT). However, this technique involves numerous experiments diluting its overall accuracy and making the entire model time-consuming and expensive. Later, various optimization models were developed with computational tools in mathematical and statistical analysis. These models are more accurate, robust and efficient in predicting response and hence are gaining more attention by present research communities. Optimization design aims to understand the impact of each experimental variable

on the final output response (Bertrand et al., 2018). **Figure 2.8** depicts the hierarchy of development of optimization model designing, where the pioneer optimization model is One-factor-at-a-time (OFAT). Later, with a consistent emphasis on the role of an interdisciplinary approach, various mathematical and statistical models have been designed for successful optimization. In the section below, a detailed understanding of the most widely employed model designs targeted for maximum biosurfactant production has been discussed, along with an attempt to understand the basics of each model with insights into their pros and cons.

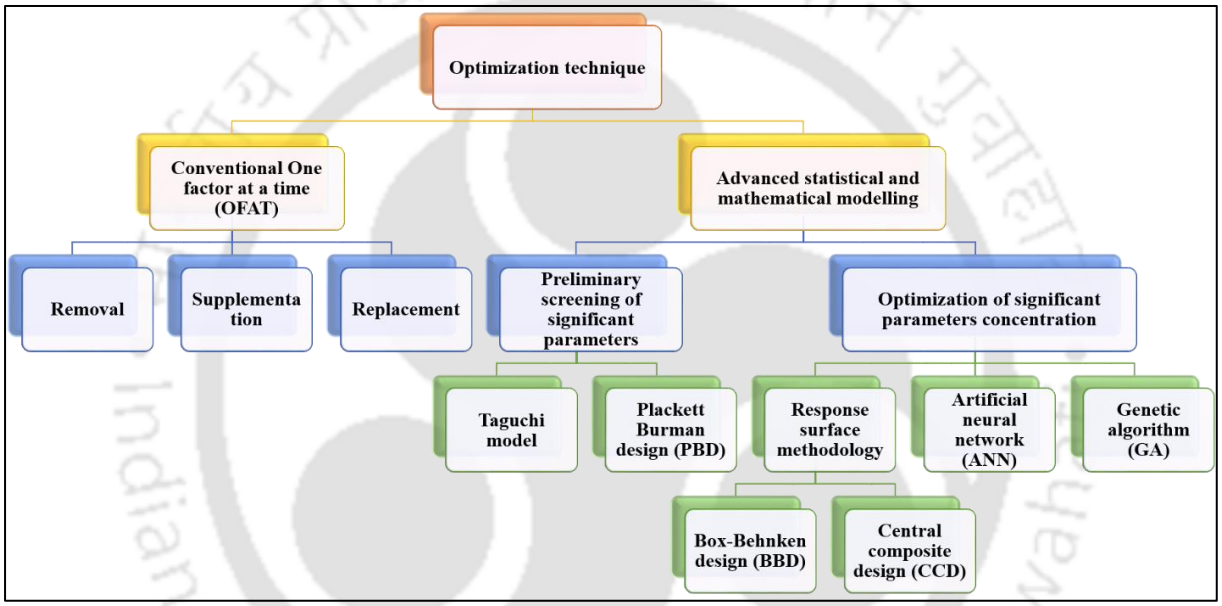

Figure 2.8. The schematic representation of the hierarchy of development of optimization techniques (Adapted with permission from (Singh et al., 2016))

2.5.2.1. One- factor-at-a-time (OFAT)

OFAT is the most classical optimization technique researchers practice for primary factors, owing to its ease of operation. In the OFAT technique, only one factor is varied in each experimental trial keeping the other factors constant. Since only one variable is explored simultaneously, sequentially optimizing each factor is needed. For example, pH is initially optimized in most cases, followed by temperature; further, the C source and N source are optimized based on the optimized pH and temperature. Various studies support using the OFAT model to optimize biosurfactant production (Parthipan et al., 2017;

Sharma et al., 2019). The OFAT technique is further performed in three sequential steps: (1) Removal, (2) Supplementation, and (3) Replacement technique (Singh et al., 2016). The fundamental removal technique is to analyze the effect of each parameter when it is absent from the culture medium. This technique is mostly used to design the composition of the culture medium. Initially, the interest component is removed from the system, and the control model analyzes the change. The essential components are segregated for further optimization (Singh et al., 2008).

In the supplementation technique, the importance of any component (e.g., carbon or nitrogen source) is analyzed when it is supplemented to the minimal salt medium. To date, this technique is widely utilized in optimizing the suitable C and N source during the media designing experiments. For example, in the basic biosurfactant optimization technique, researchers have confined the major nutrient supplementation beneficial for the biosurfactant production as C and N. Hence, all the techniques optimize these nutrients separately compared to other macronutrient types. Finally, upon selecting and shortlisting the major factors playing an important role in governing the overall product outcome, these factors are varied in a defined range, as in case of pH and temperature, or replaced with low-cost nutrients in case of C and N source optimization studies, hence termed 'replacement.'

OFAT technique has been used as a preliminary optimization technique to sort major controlling parameters (Hema et al., 2019; Joy et al., 2019). The overall experimental trials to be performed are expressed in **equation 2.3,**

Total number of trials = [Number of factors to be studied × (Number of levels - 1) + 1] **(2.3)**

Overall, such expression causes an increase in the number of experimental trials making the process time-consuming, laborious and non-economic. Discouragingly, this technique lacks the study of the interaction between two independent parameters and does not minimize the noise caused due to random experimental errors, making the outcomes comparably compromised. Other drawbacks associated with OFAT include the Domino effect, which concludes that error in one experimental parameter can cause inconclusive optimized results.

In this regard, various researchers proposed a statistical approach in the late 1960s as a suitable solution to lacunas of the classical OFAT model. Design of experiment (DOE) is a statistical technique exploring a set of variables and gaining information about their cumulative effect on the response. This technique was more acceptable as it could consider various controllable and noise factors. An advanced mathematical and statistical model could gain more insights into the possible relation between independent parameters in limited experimental trials. When a DOE technique utilizes all the factors and their possible combinations, it is termed 'full factorial designing'; on the other hand, using only a few factors and choosing only significant combinations is termed 'partial factorial designing.' Due to the interventions of mathematical model fittings, the suggested solution is more precise and accurate than OFAT. In l991, Silveria et al. supported the accuracy of the DOE optimization model as it resulted in 1.3 times improved response output than the conventional OFAT model (Silveira et al., 1991).

2.5.2.2. Plackett burmann design (PBD)

PBD model involves 2-level factorial designing where each variable is varied at two levels (+1,-1). In a typical PBD design, only the essential parameters are considered, ignoring the non-essential ones. There are two categories of variables- real and dummy. The real variable is varied to its highest and lowest levels, whereas dummy variables are kept constant throughout the process design. The overall statistical variance of dummy variables is used to estimate the experimental error. The total number of experimental trials in a typical PBD with "n" essential variables is obtained as "n+1". The contribution of each variable is given by **equation 2.4,**

$$E_X = 2 \times \frac{\sum Y_{XH} - \sum Y_{XL}}{N} \quad \textbf{(2.4)}$$

E_X, Y_{XH}, Y_{XL}, and N represent the effect of variable X, the yield of variable X at a high level, the yield of variable X at a low level, and the total number of trials performed, respectively. Sunkar et al. utilized the PBD technique to design the culture media for *Bacillus cereus* HM998898 using Gingley oil as a C source. Assuming no interaction within variables, 7 media components (KNO_3, Oil, K_2HPO_4, KH_2PO_4,

$MgSO_4 \cdot 5H_2O$, $FeSO_4 \cdot 7H_2O$ and NaCl) were optimized using an 8-run PBD design. The significance of each factor was obtained using equation 2.4, where the average difference between the high and low levels was considered. In the order of their importance from Pareto plot analysis, 3 variables were obtained, namely, (1) KNO_3, (2) K_2HPO_4 and (3) Gingley oil, which under optimized condition yielded 11.32 g/L of biosurfactant (Sunkar et al., 2019).

Similarly, Yaraguppi *et al.* also screened the significant culture media components involved in the biosurfactant production by *Bacillus aryabhattai* ZDY2 using crude oil as substrate. Among the 8 variables (Yeast extract, $NaNO_3$, KCl, Glucose, NaCl, KH_2PO_4, $MgSO_4 \cdot 7H_2O$, and Crude oil), 3 factors were obtained as significant ($p < 0.05$) based on regression analysis, namely $NaNO_3$, yeast extract and crude oil. It was reported that among the 3 significant variables, crude oil was most significant with E_X = 1.485, followed by yeast extract (E_X = 1.4) and $NaNO_3$ (E_X = 1.01). It was concluded that *B.aryabhattai* ZDY2 positively used crude oil as the sole C source and organic and inorganic N source for the maximum biosurfactant production, yielding 5.88 g/L biosurfactants (Yaraguppi et al., 2020).

Overall, this technique decreases the total experimental trials immensely, making the design implementation simple, easy, quick, cost-effective, and statistically efficient. However, due to the lack of incorporating the interaction within the essential factors, this technique is restricted to the study of mutually exclusive parameters and does not mask the effect of one another (Biniarz et al., 2018). The technique is mostly used to screen essential variables, which can be further optimized using more statistically robust techniques (Câmara et al., 2019).

2.5.2.3. Taguchi model

The Taguchi model, developed in the late 1950s by Genichi Taguchi, is a robust optimization model preferred when the optimizing factors are too many and the involved noise quotient is high. It is a 3-level (+1, 0, -1) statistical modelling, where the interaction between essential variables is explored, unlike PBD. In addition, the noise factors are also incorporated in the design of the experiment. However, the Taguchi model only analyzes the main factors, with no interactions.

It is used when the target is to obtain the best optimal design in the range of specification provided but is more centric to the mean of the provided parameters. The advantage is its ability to incorporate the

noise factors while designing the most suitable optimized condition. The noise factor here means the factors which are not predefined or controllable during the culture conditions. In general, the numbers of experimental trials to be done by Taguchi design can be expressed in **equation 2.5**,

$$\textbf{Total experimental trial} = 1 + (\textbf{Parameters studied}) \times (\textbf{Levels} - 1) \quad (2.5)$$

An orthogonal array is selected in a typical Taguchi model to find the minimum number of experiments required to analyze the optimal conditions. The total experiments to be conducted are determined as the suffix to 'L' For instance, for three parameters with three corresponding levels, the L9 orthogonal matrix is chosen.

In a recent study by Raza and co-workers, using the Taguchi model, rhamnolipid biosurfactant production by *Pseudomonas putida* was optimized using waste frying oil as a C source. L9 orthogonal matrix was chosen, with 9 experimental trials were suggested for the optimization purpose. The 3 major factors studied include C source, fermentation set up and the incubation time. The optimized model enhanced the biosurfactant yield from 3.4 to 4.1 g/L (Raza et al., 2020). Similarly, Haloi and the group reduced the effect of uncontrollable parameters on the glycolipid production by *Achromobacter* sp. TMB1 by optimizing 3 parameters with 4 levels each. These included: C source, N source, and inducer concentration using an L16 orthogonal matrix. Taguchi model summarizes the contribution of each parameter studied, making it suitable to understand the role of each parameter in the overall biosurfactant contribution. For example, in the above study, yeast extract as an inducer played a vital role in maximum biosurfactant production (Haloi and Medhi, 2019). With the presence of large experimental factors to be studied, this techniques endeavors advantages such as; 1) lesser number of experiments, 2) time and cost-effective, and 3) highly precise. The only disadvantage with this model is that the number of parameters to be studied must be significantly higher than the noise factors.

2.5.2.4. Response surface methodology (RSM)

RSM is an optimization technique that uses mathematical regression analysis such as ANOVA and statistical experimental design to formulate optimized conditions in the presence of a set of inter-

dependable parameters/factors. This design obtains the best outcome using finite experimental runs, reducing noise factors. The unique feature of RSM is its surface plot-based representation of output results. The response obtained is expressed in terms of a simple, mathematical expression with associated regression analysis. One such general quadratic response expression is mentioned as **equation 2.6,**

$$\boldsymbol{Y(X) = A_0 + \sum_{i=0}^{N} A_i X_i + \sum_{i<j}^{N} A_{ij} X_i X_j + \sum_{i=0}^{N} A_{ii} X_i^2} \quad \textbf{(2.6)}$$

Here, Y(X) stands for the predicted response, A_i X_i represented the linear expression as the effect of each variable on response factor, A_{ij} X_i X_j represented the interaction between independent variables and their role in response output, and A_{ii} X_i^2 represented the square terms.

RSM provides a quantitative analysis of each factor on the response output. In RSM, we can study the effect of 2 or more process parameters within a range and predict the optimized yield, which is not necessarily one of the experimental trial conditions performed. In the case of biosurfactant production, RSM uses optimization designs such as CCD or BBD to formulate a statistically valid optimization model **(Figure 2.9)**.

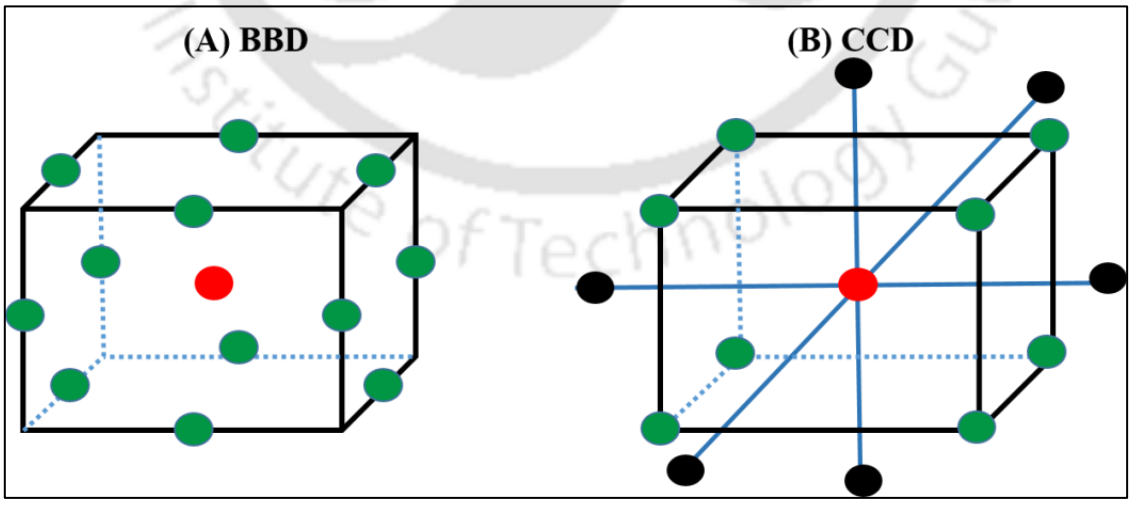

Figure 2.9. RSM optimization designs using (A) BBD and (B) CCD design models

2.5.2.4.1. Box -Behnken Design (BBD)

In this model, each factor is studied at 3 levels, two factorial points and one centric point. Centric point is often replicated for error evaluation. In this regard, El-Housseiny et al. explored the effect of pH, temperature and inoculum size on the rhamnolipid production concentration. Each factor was studied at 3-levels. Upon using the RSM-BBD model, the optimized conditions were obtained as pH 8, 30°C with the inoculum size of 1 %, reporting a remarkable yield of 46.85 g/L (El-Housseiny et al., 2019). RSM techniques are unique for their ability to deduce the correlation within the variables and their integrated effect on the overall output response. In this regard, Ghazala et al. explored 4 variables (Glucose, Glutamic acid, temperature and salinity) to evaluate their impact on the biosurfactant synthesis by *Bacillus mojavensis* I4. A set of 29 runs were performed to analyze the possible reaction among the 4 variables, each varied at 3 levels (+1, 0, -1). RSM-BBD analysis provided a second-order polynomial equation expressing the biosurfactant yield in terms of all 4 variables and their interaction. It was observed that apart from salinity, all the other three factors positively affect the biosurfactant yield. Among them, the Glucose and Glutamic acid coefficients were 0.49, whereas the coefficient for temperature was 0.16, describing the importance of C and N sources on the overall production of biosurfactants. Temperature also played an important role (coefficient = 0.16); however, salinity inversely affected the overall productivity. The model proposed the optimal biosurfactant yield of 4.12 g/L at 3 % glucose concentration, 0.6 % glutamic acid concentration, 35°C temperature and 10 g/L salinity (Ghazala et al., 2019).

Similarly, Jimoh et al. observed the inter-relation between C source, N source and trace elements on the overall biosurfactant production ability of *Paenibacillus* sp. D9. Waste canola oil was used as a C source and KNO_3 as an N source. BBD design expressed the significant integrated effect of N source and metal supplementation on the overall biosurfactant yield. The optimized concentrations for all three variables were obtained as 5, 2 and 1 % for C, N and metal supplementation, respectively, yielding 5.31 g/L of biosurfactant concentration. The model suggested the constitutive effect of high canola oil concentration and N-trace element interaction, positively driving biosurfactant production. On the other hand, C-trace elements concentration and C-N interaction negatively repressed the overall yield of biosurfactant (Jimoh and Lin, 2020).

Hence, the BBD technique statistically expresses the importance of the significant role played by individual factors and their inhibitory or inducing effect on other variables. Such insights help examine the media composition and other physical parameters in a finite number of runs, making the entire design statistically relevant and time and cost-effective. However, the BBD model is highly sensitive to mismeasure of experimental runs or missing data points as the number of runs is highly restricted. Hence, the entire model is compromised with loss or wrong data points.

2.5.2.4.2. Central composite design (CCD)

Among all the RSM designs, CCD is the most employed design. It utilizes a second-order model fitting equation to analyze effect of each variable on output and each other. RSM-CCD factorial design is a more advanced tool for optimization study, where each variable is explored at 5-levels. There are two factorial design points, two axial points and one centric point, as shown in **Figure 2.10**. Studying each variable at 5 levels ensures that losing data or mismeasurement will not affect the entire model design, unlike BBD, making the entire design highly robust. A typical experiment runs in the CCD model can be expressed as **equation 2.7**,

$$\textit{Number of experimental runs} = 2^N + 2N + C_N \qquad \textbf{(2.7)}$$

N is the number of independent variables, and C_N represents the total number of replica tests performed for the centric point (Cornell and Khuri, 1987; Sahoo and Barman, 2012). In the case of the experimental design for CCD and BBD model for three independent variables, the number of runs in the BBD model is 15, which increases to 20 in CCD optimization. It is due to the point analysis beyond the maxima and minima user range.

In a biosurfactant production study, 3 variables (pH, Temperature and C source) were optimized using the RSM-CCD technique using 20 sets of equations. A quadratic equation was obtained to determine each variable's constitutive effect and interaction with the response factor. The optimal biosurfactant concentration was obtained as 6.3 g/L in the presence of 3.89 % paraffin oil as C source, pH 7.73 and 62.5°C incubation temperature (Datta et al., 2018). Similarly, Khademolhosseini et al. analyzed the

biosurfactant production ability of *Pseudomonas aeruginosa* HAK01 using 5-level factorial designing considering C source concentration, inoculum size and salinity as 3 variables. The optimization experiments revealed the sensitivity of strain to high salt concentration, yielding 2.07 g/L of biosurfactant in the presence of 22.9 g/L sunflower oil as C source, 2.77 % (v/v) inoculum size and a very low salt concentration of 0.19 % (w/v) (Khademolhosseini et al., 2019).

Another study utilized the 5-level factorial designing to optimize biosurfactant production using *Pseudomonas aeruginosa* UCP 0992 in the presence of corn-steep liquor and vegetable oil residue, as low-cost C and N substrate, keeping into consideration 4 reaction parameters: agitation speed, incubation time, aeration, and inoculum size. It was reported that using optimal conditions of 1 vvm aeration rate, 225 rpm agitation rate, 3 % inoculum size and 120 h of incubation, a remarkably high biosurfactant yield of 26 g/L was achieved (Silva et al., 2018). Even though CCD optimization techniques yield the most suitable optimized condition, its numerous experimental runs make the entire process time-consuming and laborious. Apart from all the mentioned advantages, there exist associated disadvantages of RSM. To list a few, RSM uses second-order polynomial order for response analyses, which loses its precision with an increase in variable counts and their levels. Hence, it is restricted to the prediction of low levels of parameters. In a biological system, like bioreactors, many complex reactions with unknown kinetics decrease the reproducibility of predicted responses.

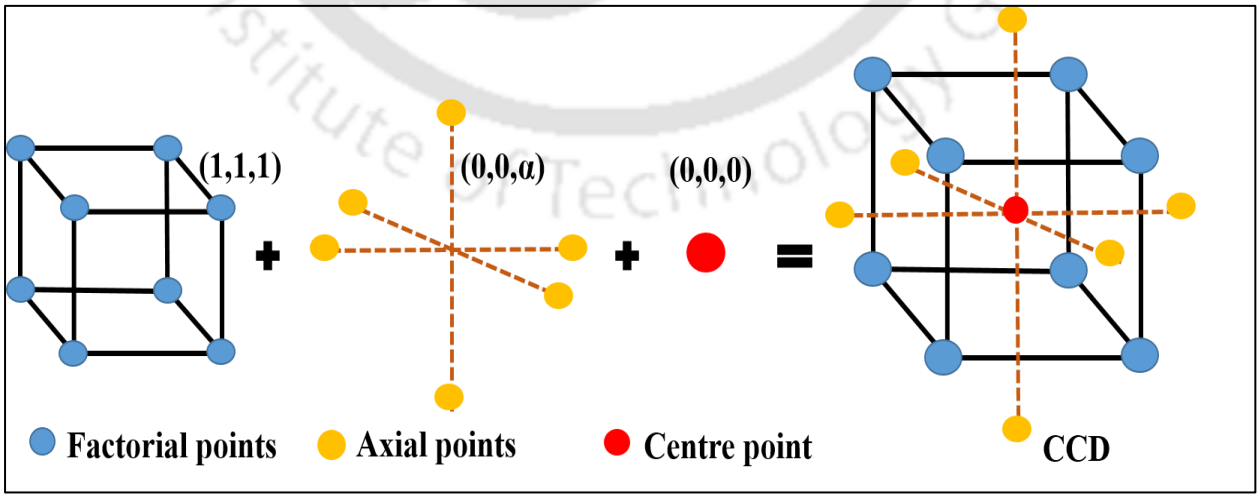

Figure 2.10. 5-level factorial design in CCD optimization technique showing two factorial design points, two axial points and one centric point

In such cases, two or more models are integrated to screen out significant variables from the rest, decreasing the strain on further optimization models. For instance, Biniarz et al. exploited the PBD optimization technique to screen parameters essential for biosurfactant production, followed by further optimization using the CCD technique. Primarily, the media formulation was done by studying 11 different media constituents. It was followed by analyzing media additives, which were performed using CCD. The three significant variables, namely glycerol, tryptone and leucine, were chosen as major elements in media formulation for the maximum biosurfactant by *Pseudomonas fluorescens* BD5, yielding 610.4 ± 5.9 mg/L of biosurfactant. These 3 factors were further optimized using the CCD technique, resulting in a two-fold increase in biosurfactant yield of 1187 ± 13.0 mg/L. Hence, an enhanced biosurfactant production was obtained using an integrated optimization model (Biniarz et al., 2018).

Joy et al. also explored the advantage of CCD after the OFAT optimization study for biosurfactant production using *Achromobacter* sp. (PS1). Initially, the lignocellulose hydrolysate streams comprising C_5 and C_6 residues were screened using OFAT technique as C source, and the optimal biosurfactant concentration was obtained as 3.3 g/L; however, the authors further optimized the concentration of C source and other 5 factors ($NaNO_3$, yeast extract, $FeSO_4$, Phosphate and agitation rate) using CCD technique, using C_6 hydrolysate as optimal C source. The CCD optimization further improved the overall rhamnolipid yield to 5.46 g/L (Joy et al., 2019). Hence, the RSM model has been extensively explored to maximize metabolite production and optimization studies. Integration of optimization techniques has been proven to improve the biosurfactant yield by many folds and should be further explored for more robust model development. Nevertheless, its inability to unwind complex biological interactions which are not linearly dependent has caused a lacuna in its suitability for living systems. It has opened doors for further research in this domain.

Table 2.6 reports various optimization models explored for maximizing the overall biosurfactant production ability of different bacterial species. In contrast to tremendous improvement in biosurfactant productivity using various optimization techniques, each technique possesses certain limitations. The optimization techniques involve a lot of experimental trials, which are time-consuming, labor-intensive and expensive. It is also evident that every optimization result mentioned in the literature is uniquely

restricted to the strain, media and physiological parameters used and cannot be generalized. In addition, the shake flask results do not fit in bioreactor-based experiments in most cases. Due to many uncontrollable parameters in the shake flask can provide exceptionally different results if controlled in the reactor. Hence the optimization results vary at different scale studies. Since biological species consist of complex metabolic pathways which may undergo mutation based on an external change in the environment leading to under-expression or overexpression of output yield, it is suggested to look into mutagenic species as well as control to understand the insights of external optimization on the internal metabolic activity of biological species. Another factor is the restriction of optimization techniques to liquid-based medium. There is a scarcity in the availability of information regarding the optimization model for solid-state or semi-solid-state models. Furthermore, most optimization models aim to increase overall productivity, which deviates with a change in any media component.

Table 2.6. List of optimization models used for maximizing biosurfactant production by various bacterial species in the presence of mentioned reaction parameters

Optimization model	Substrate	Bacteria studied	Optimized Reaction Parameters	Biosurfactant concentration	Ref.
OFAT	Oily sludge	*Shewanalla chilikensis, Bacillus firmus,* and *Halomonas hamiltonii*	pH 7.0, 35°C, 1 % oily sludge as substrate 15 % inoculum size, 7days incubation time	152 mg/g	(Suganthi et al., 2018)
OFAT	Kitchen waste oil	*Pseudomonas aeruginosa*	pH 8.0, 35 °C, 2.0 g/L yeast extract concentration,10 % (v/v) inoculum size	NA	(Chen et al., 2018)
OFAT	*Parthenium hysterophorus* biomass	*Pseudomonas mosselii* F 01	pH 6.0, 35 °C, 3 % (w/v) biomass substrate, 96 h incubation time glucose and yeast extract as C and N source	1.94 g/L	(Devaraj et al., 2019)
OFAT	Molasses	*Marinobacter hydrocarbonoclastic* us ST1	pH 7.0, 30 °C, 5 % (v/v) inoculum size, 2.5 % (w/v) molasses and 0.3 %(w/v) sodium nitrate, 72 h incubation time	6.25 g/L	(Dikit et al., 2019)
OFAT	Waste frying oil	*Bacillus cereus* BCS0	2 % (w/v) frying oil and 0.12 % (w/v) peptone, 250 rpm and 48 h	3.5 g/L	(Durval et al., 2019)

OFAT	Rapeseed oil	*Pseudomonas aeruginosa* KT1115	pH 7.5, 37°C, 1 % (v/v) inoculum size, 180 rpm and 8 days incubation time, 60 g/L rapeseed oil, 6 g/L $NaNO_3$, 3 g/L yeast extract, 1 g/L KH_2PO_4, 1 g/L Na_2HPO_4, 0.1 g/L $CaCl_2 \cdot 2H_2O$, 0.1 g/L $MgSO_4$	44.39 g/L	(Jie et al., 2019)
OFAT	Diesel fuel	*Paenibacillus* sp. D9	pH 7.0, 30 °C, C/N (ammonium sulfate) ratio of 3:1, 4.0 mM $MgSO_4$, and 1.5 % (v/v) inoculum size	4.11 g/L	(Jimoh and Lin, 2019)
OFAT	Dextrose	*Achromobacte*r sp. (PS1).	pH 7.0, 30 °C, 120 rpm, C/N ratio 8.3 using sodium nitrate and beef extract	4.13 g/L	(De Meester et al., 2016)
PBD	Glycerol	*Pseudomonas aeruginosa*	pH 7.37, 30.17 °C, C/N ratio of 32.35, 9.36 % (v/v) Glycerol concentration of and 10.26 days incubation time	0.88 mg/L	(Câmara et al., 2019)
PBD	Gingley oil	*Bacillus cereus* HM998898	KNO_3 (1 g/L), Gingley oil (2 mL), K_2HPO_4 (2.5 g/L), KH_2PO_4 (0.75 g/L), $MgSO_4 \cdot 5H_2O$ (0.5 g/L), $FeSO_4.7H_2O$ (0.005 g/L) and NaCl (0.025 g/L)	11.32 g/L	(Sunkar et al., 2019)
RSM-BBD	Waste canola oil	*Paenibacillus* sp. D9	pH 7.0, 30°C, waste canola oil (2 % v/v), 2 g/L KNO_3, and 48h incubation time	5.31 g/L	(Jimoh and Lin, 2020)
RSM-BBD	Glucose	*Bacillus subtilis* MJ01	1.49 g/L Yeast extract; 7.62 g/L KH_2PO_4; 33.68 g/L K_2HPO_4; 11.9 g/L Glucose	1.14 g/L	(Veshareh et al., 2019)

RSM-BBD	Glucose	*Bacillus mojavensis* I4	35 °C, 3 % (w/v) glucose, 0.6 % (w/v) of glutamic acid, 10 g/L Salinity	4.12 g/L	(Ghazala et al., 2019)
RSM-CCD	Whey and vinasse	*Lactococcus lactis* CECT-4434	15 % (w/v) whey, 3 % (w/v) vinasse, 1 % (w/v) sucrose, 1.5 % (w/v) yeast extract	0.11 g/L	(Vera et al., 2018)
RSM-CCD	Glucose	*Bacillus brevis*	pH 8.0, 33 °C, 10 days incubation time and 8.5 g/L glucose	NA	(Mouafi et al., 2016)
RSM-CCRD	Vegetable oil	*Pseudomonas aeruginosa* UCP 0992	0.5 % (w/v) corn steep liquor, 4.0 % (w/v) vegetable oil, 1.0 vvm aeration rate, 3.0 % (v/v) inoculum size, 225 rpm and 120 h incubation time	26 g/L	(Silva et al., 2018)
RSM-CCD	Light Paraffin oil	*Bacillus subtilis* MG495086	pH 7.7, 62.4 °C, 96 h and 3.8 % (v/v) of light-paraffin oil	6.3 g/L	(Datta et al., 2018)
RSM-CCRD	Glucose	*Bacillus subtilis* BR-15	pH 7.0, 37.5 °C and 72 h incubation time, 2.17 % (w/v) glucose, 0.5 % (w/v) yeast extract and 4 % (v/v) inoculum	1.72 g/L	(Sharma et al., 2020)
RSM-CCRD	Glycerol	*Bacillus amyloliquefaciens* SAS-1	pH 7.0, 37.5 °C, 4 % (v/v) inoculum size, 72 h incubation time, 5 % (v/v) glycerol, and 0.5 % (w/v) Yeast extract	2.40 g/L	(Sharma et al., 2020)
RSM-CCD	Poultry slaughter greasy effluent	*Pseudomonas aeruginosa* ATCC 10145	30°C, 48 h incubation time, 1.2 vvm aeration, 600 rpm, and 1.0 g/L inoculum concentration	5.37 g/L	(Borges et al., 2015)

RSM-CCD	Sunflower oil	*Pseudomonas aeruginosa* HAK01	144 h incubation time, 25 g/L of C, 4 % (v/v) inoculum size, 2.5 % (w/v) salinity	2.07 g/L	(Khademolhosseini et al., 2019)
RSM-CCD	Glucose	*Bacillus amyloliquefaciens* IT45	pH 6.8, 30 °C, 48 h incubation time, agitation rate 200 rpm, 25 g/L glucose syrup, 15 g/L yeast extract, and 2 g/L calcium chloride	5.5 g/L	(Lima et al., 2020)
RSM-CCD	Brewery waste	*Bacillus subtilis* N3-1P	pH 6.41, 27°C, 7 % (v/v) brewery waste, 6.22 mg/L ammonium nitrate, agitation 150 rpm	0.66 g/L	(Moshtagh et al., 2019)
OFAT -RSM-CCD	Industrial rice-straw hydrolysate	*Achromobacter* sp. (PS1)	30 °C, 8 days incubation time, Total sugars 40 g/L, sodium nitrate 6.0 (g/L), yeast extract 2.0 (g/L), ferrous sulphate 0.2 (mg/L), phosphate 1000mM, and agitation 100 rpm	5.46 g/L	(Joy et al., 2019)
OFAT-RSM	Glucose	*Planococcus* sp. MMD26	pH 7.0, 48 h incubation time,2.5 % (w/v) salt concentration, 4 % (w/v) glucose, and 1 % (w/v) ammonium nitrate	NA	(Hema et al., 2019)
PBD- RSM-CCD	Glycerol	*Pseudomonas fluorescens* BD5	20–100 g/L glycerol, 15 g/L tryptone, 10 g/L Leu/Val, 0.5 g/L K_2HPO_4, 0.1 g/L $MgSO_4$,50 mg/L $Fe_2(SO_4)_3$, 100 mM MOPS	1.19 g/L	(Biniarz et al., 2018)
PBD-RSM-CCD	Crude oil	*Bacillus aryabhattai* ZDY2	pH 7.0, 35°C, 4 days incubation time, 200 rpm, 4.0 % (v/v) crude oil, 0.7 % (w/v) yeast extract and 3 % (w/v) $NaNO_3$	8.86 g/L	(Yaraguppi et al., 2020)

2.6. Recent expansions in the bioremediation of crude oil

2.6.1. Design of Microconsortium for effective crude oil bioremediation

Micro-consortium is an associative term referred to a symbiotically or cooperatively inter-linked population of two or more microbes of different genera or taxa, co-inhibiting under the same physiological condition. The term is often misunderstood with mixed culture; however, the key concept is the cooperative interaction mandatory for the consortium, unlike mixed cultures. Nature is abundant with effective microbial communities, yet their contribution remains un-highlighted due to the presence of interfering species along with symbiotic ones. Hence, comes the need to look into designing a stable micro-consortium. In agreement with this, various researchers have also suggested the upper hand of the consortium over single bacterial bio-degradative activity (Birolli et al., 2020; Jannat et al., 2021; Krainara et al., 2020).

Co-cultivation of a set of microbes with diverse metabolic enzymatic activity and adaptability towards physiological factors ensures improved stability and expands the possibility of secondary metabolite production (Hoshino et al., 2019). The co-cultivation of biosurfactant producing and hydrocarbon-degrading bacterial cultures confer a mutualistic effect on the overall biodegradation activity of individual bacteria. The biosurfactant improves the bioavailability of hydrocarbons, increasing their desorption from the contaminated sites, further aiding the catalytic activity of hydrocarbon degraders for the remediation. Nevertheless, it is not the sole mutual activity of hydrocarbon degraders and biosurfactant producers that leads to hydrocarbon remediation. Studies have revealed the presence of non-hydrocarbon degrading species at the contamination site along with those mentioned above major ruling microbes (Alves et al., 2019; Ebadi et al., 2017; Wanapaisan et al., 2018). These non-degraders thrive on the intermediates released during the primary hydrocarbon catabolism.

In order to design a micro-consortium, two approaches are commonly exploited, namely the “Top-down” and “Bottom-up” approaches. The first case focuses on exploring a diverse and complex microbial population, followed by screening and shortlisting selective species of interest which act as key contributors in the microconsortium, for example, sorting only hydrocarbon-degrading microbes from the diverse oil-contaminated environmental site. The top-down approach puts forward the naturally selected, interlinked, inherent microbial communities. However, the presence of non-

cultivable complex microbial communities in the top-down prevents researchers from understanding the complete metabolic activities and pathways involved in the process. In contrast, the second approach focuses on "bottom-up" designing, where each microbe in the consortium (need not to be of the same place of origin) is selected with required traits and later enriched in the microbial consortium (Ibrar and Zhang, 2020). The advantage of the bottom-up approach lies in its inclusivity with engineered microbes as a part of the consortium, making it the most adapted technique in the synthesis of synthetic consortium (Tuleva et al., 2009; Zaragoza et al., 2013). **Figure 2.11** depicts the two conventional approaches explored in the design of microconsortium. Overall, the challenging part in consortium design is the unavailability of accurate information regarding the genomics, metabolic fluxes and catabolic enzymes involved in the biosynthesis of the product of interest, limiting the designing of synthetic consortium. Advancement in metabolic engineering, system biology, metagenomics, and single-cell techniques is required to successfully design a robust and stable microbial consortium.

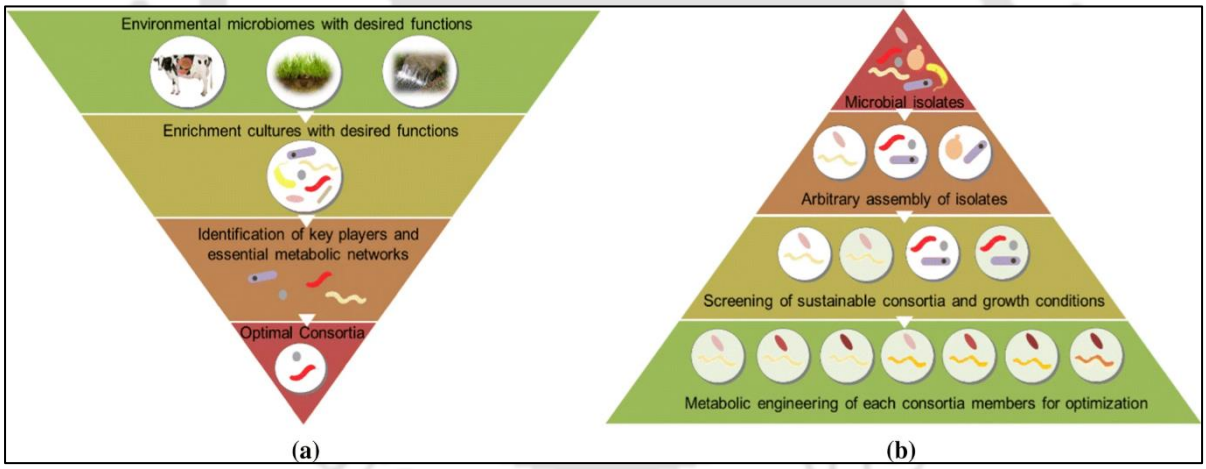

Figure 2.11. A basic top-down (a) and bottom-up (b) approaches for synthetic consortia construction (Adapted from (Che and Men, 2019))

2.6.2. Criteria of designing microbial consortium

A microbial consortium involves complex underlying inter-microbial interactions dependent on the molecular and metabolic pathways involved; hence a thorough knowledge of these aspects is vital in the rational designing of the microbial consortium. While designing a petroleum-utilizing consortium,

choosing a potential biosurfactant producer and hydrocarbon degrader is crucial. Though a consortium rich in numerous potential degraders with the capabilities mentioned above are promising candidates, the results are often contradictory to expectations. Rizzo et al. investigated one such incongruity in consortium designing. Three biosurfactant-producing strains (*Joostella* sp. A8, *Pseudomonas* sp. A6, and *Alcanivorax* sp. A53) were explored for their hydrocarbon degradation ability in pure culture and in the consortium. While performing the study on pure culture indicated that each strain was grown significantly in mineral medium with diesel oil supplementation exhibiting biodegradation efficiency of 26.8 %, 38.2 %, and 52.7 % by *Joostella* sp. *Pseudomonas* sp. and *Alcanivorax* sp., respectively. During the co-culture study of *Joostella* sp. with *Pseudomonas* sp. (J-P) and *Alcanivorax* sp. (J-A), however, the biodegradation activity of 99.4 % in the case of the J-A consortium and 99.2 % by the J-P consortium was reported. Their study witnessed strong competitiveness in the J-P consortium, where an abundance of *Joostella* sp. decreased with an increase in the growth of *Pseudomonas* sp.. (Rizzo et al., 2018). Hence, it is important to analyze the growth behavior of each strain with their co-inhabiting species before using them in a consortium. Interaction within co-inhabiting species is the major governing factor in consortium functioning. These interactions can be majorly classified as positive (+, beneficial), negative (-, detrimental) and neutral (0, no effect). **Table 2.7.** summarizes the various modes of microbial interactions within two species in a consortium.

Table 2.7. Various modes of microbial interaction within co-inhabiting species *[Symbols: Beneficial (+), Detrimental (-), and No effect (0)]*

Mode of interaction	Microbe A	Microbe B
Mutualism	+	+
Commensalism	0	+
Parasitism/ Predation	-	+
Competition	-	-
Amensalism	-	-
Neutralism	0	0

Various researches report the suitability of mutualism (+, +) and commensalism (+, 0) as the major interactions involved in cumulative growth and robustness of microbial consortium. Mutualism is the interaction within two microbes where both are benefitted from one another. The best example is cross-feeding, where there is an exchange of metabolic products between the two species. Commensalism is a one-way interaction, where one species is benefited whereas the other is neither benefitted nor negatively affected. For instance, non-hydrocarbon degraders survive on the intermediate metabolites produced by the key species. The benefits involved in every co-species interaction are intended for (1) cell growth, (2) substrate utilization, and (3) balancing of redox factors such as Nicotinamide adenine dinucleotide (NADH), Nicotinamide adenine dinucleotide phosphate (NADPH). Major microbial interaction reported in bioremediation involves syntrophy, bio-film formation and detoxification, as shown in **Figure 2.12.**

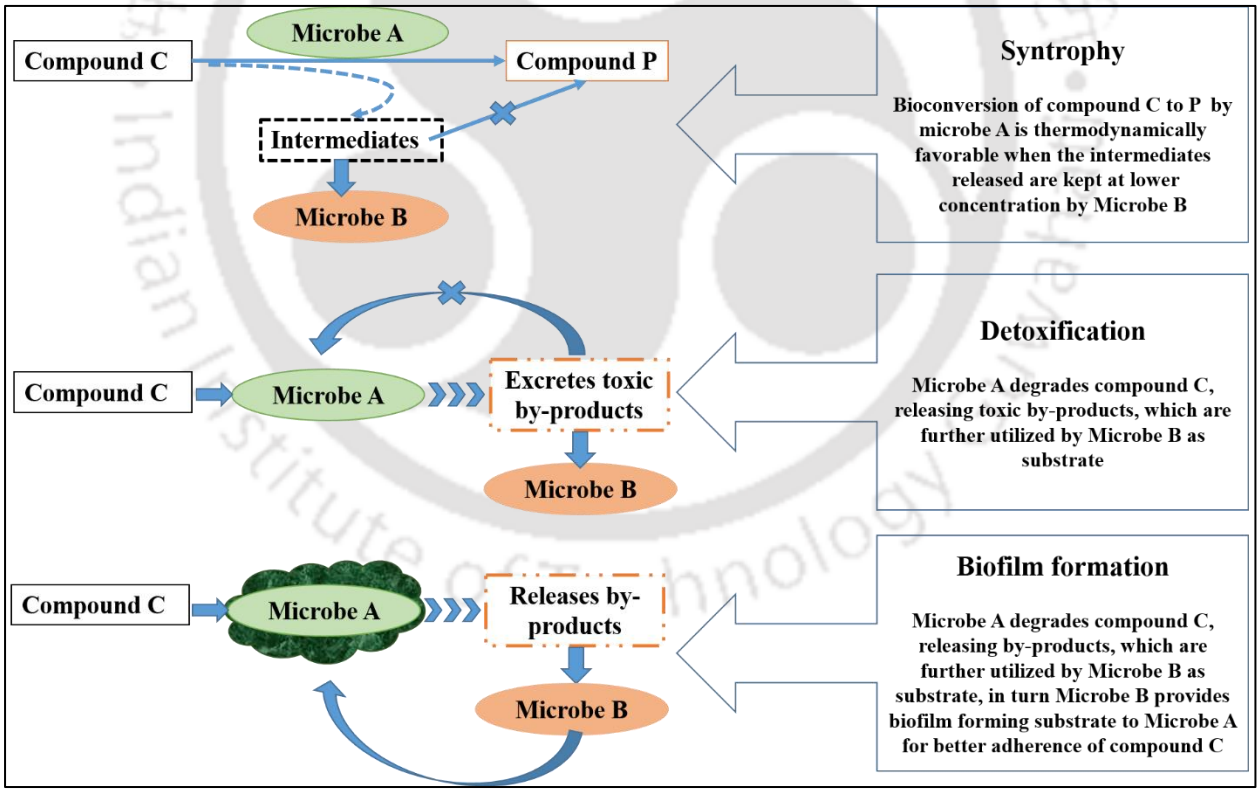

Figure 2.12. Various modes of positive microbial interaction using syntrophy, detoxification and biofilm formation

Like pure bacterial culture, a consortium's biodegradability and secondary metabolite productivity depend on physiological conditions. Hence, a designed bacterial consortium needs to be optimized to obtain the appropriate culture growth condition to achieve optimal results. Suganthi et al. isolated 3 hydrocarbon degraders (*Shewanalla chilikensis* MG452729, *Halomonas hamiltonii* MG452731, and *Bacillus firmus* MG452730) from oily sludge and used these isolates as a consortium for further bioremediation studies. Culture conditions such as pH, incubation time, temperature, biomass concentration and oily sludge concentration were optimized using the OFAT technique. The authors explored the bacterial growth, selective enzyme activity and biosurfactant yield as response factors for the analyses. The optimized culture condition obtained were: pH 7, 35 °C, 1 % (w/v) oily sludge concentration, 15 % (v/v) biomass concentration and 7 days of incubation time. Under the optimized condition, authors reported 96 % biodegradation of total petroleum hydrocarbon concentration and remarkably high hydrocarbon degradative enzyme activity, i.e., 68 U/mL oxidoreductase activity, 80 U/mL lipase activity 46 U/mL catalase activity (Suganthi et al., 2018). Summarily, the use of syntrophic microbes that share either mutualistic or commensalism-based interaction is the preliminary screening criteria of microbes before considering consortia members. Later, the growth conditions of microbes are optimized to achieve cumulative maximum growth and metabolite production.

2.6.3. Advantage of the microbial consortium over pure isolates

Crude oil and other petroleum products are chemically complex hydrocarbons with diverse aliphatic and aromatic structural compositions. Various researchers have debated a single microbial system (axenic) to utilize such a complex substrate as their energy source. In this regard, Kumari et al. used a diverse mixture of microbes, namely, *Ochrobactrum anthropic* IITR07, *Pseudomonas mendocina* IITR46, *Pseudomonas aeruginosa* IITR48, *Microbacterium esteraromaticum* IITR47, and *Stenotrophomonas maltophilia* IITR87. The ability of crude oil bioremediation was analyzed in three modes (1) Axenic culture, (2) Microconsortium, and (3) Consortium supplemented with rhamnolipid JBR- 425. Focusing on major contributors of crude oil, i.e., polyaromatic hydrocarbons (PAH), the axenic culture showed the highest naphthalene degradation by IITR47 strain (80.4 %), which increased to 97.3 % when used in the consortium. Similarly, phenanthrene was highest biodegraded by 67.1 % by

strain IITR48, which raised to 96.5 % when performed by microconsortium. Other PAH such as benzo(b)fluoranthene and fluorene also showed 1.4 folds and 1.6 folds higher biodegradability in the consortium than axenic culture. The authors highlighted the role of coordinated metabolic activity in the consortium that led to better results (Kumari et al., 2018). **Table 2.8.** summarizes the comparative change in biodegradation ability of compounds by a few bacterial species when grown in microconsortium over axenic culture.

Table 2.8. Comparison of biodegradation ability of various toxic compounds by pure (axenic) culture and their consortium

S.no.	Compounds	Microbes used	Reaction conditions	Efficiency	Ref
1.	Natural rubber	*Rhodococcus pyridinivorans* **Consortium** (indigenous soil-inhabiting microbes including *Rhodococcus pyridinivorans*)	Incubated in MSM supplemented with dried latex glove pieces (0.6 %, w/v) as a sole carbon source at 30 °C, 150 rpm for 4 weeks.	9.36 % 18.38 %	(Nawong et al., 2018)
2.	Saturated fractions of oily sludge Aromatic fractions of oily sludge	*S. acidaminiphila* *B. megaterium* *B. cibi* *P. aeruginosa* *B. cereus* **Consortium** (all the strains as mentioned earlier) *S. acidaminiphila* *B. megaterium* *B. cibi* *P. aeruginosa* *B. cereus* **Consortium** (all the above-mentioned strains)	Incubated with 1 % oily sludge as the sole carbon source, kept at 100 rpm, and 30 °C for 40 days.	91.7 % 89.0 % 89.7 % 86.7 % 88.4 % 90.7 % 33.2 % 39.6 % 64.3 % 39.5 % 40.3 % 51.8 %	(Cerqueira et al., 2011)

3.	Phenanthrene	*Bacillus* sp. ASP1 *Pseudomonas* sp. ASP2 *Stenotrophomonas fsmaltophilia* ASP3 *Staphylococcus* sp. ASP4 *Geobacillus* sp. ASP5 *Alcaligenes sp.* ASP6 **Consortium** (all the strains mentioned above)	Incubated with Phenanthrene (300 ppm) using 4 % (v/v) inoculum at 37°C, and 150 rpm for 120 h	29 % 38.66 % 52 % 38 % 43 % 43 % 76 %	(Patel et al., 2013)
4.	Crude oil	*Raoultella ornithinolytica* PS *Bacillus subtilis* BJ11 *Acinetobacter lwoffii* BJ10 *Acinetobacter pittii* BJ6 *Serratia marcescens* PL **Consortium** (all the strains as mentioned above)	Incubated in 10 % (v/v) inoculum, 0.4% crude oil (w/v), 30 °C,180 rpm for 10 days	83.5 % 81.1 % 75.80 % 74.90 % 70.00 % 94.00 %	(Bidja Abena et al., 2019)
5.	Bisphenol A	*Pseudomonas knackmussii* Consortium (Inherent microbes from contaminated river sediment, predominantly *Pseudomonas knackmussii)*	Basal salt medium (BSM) supplemented with 10 ppm of BPA,150 rpm at 30 °C	100 % in 7 days 100 % in 28 h	(Peng et al., 2015)

6.	Octachlorodibenzo -p-dioxin (OCDD)	*P. mendocina* NSYSU **Consortium** (Inherent microbes from contaminated soil with bioaugmentation of *P. mendocina* NSYSU)	NB broth, room temperature (20 °C) for the 65-day incubation	68 % **62 %** (reduced due to competition with indigenous microbes)	(Tu et al., 2014)

Along with metabolic activity, increased biosurfactant production was also reported by Alves et al. during co-culturing of biofilm-forming bacterial strains *Pseudomonas aeruginosa* ATCC 27853 with model biosurfactant producing *Pseudomonas* sp. While during the axenic study, the overall rhamnolipid production was reported to be 53.5 mg/L, a 2.4 times increase in the biosurfactant yield (i.e., 129 mg/L) was stated in the presence of co-culturing with biofilm-forming *Pseudomonas aeruginosa*, expressing its role as inducer and stimulator in the consortium (Alves et al., 2019). Hence, microbes complement one another in a consortium by acting as an inducer or stimulator of essential metabolic pathways.

Interestingly, apart from improved biosurfactant production, different isoforms of biosurfactant have also been reported during consortia study over axenic growth. Ibrar et al. constructed a microbial consortium to enhance the overall biodegradation activity and biosurfactant yield in this approach. More than 60 % biodegradation of glyceryl tributyrate (GT) was obtained by using a microconsortium comprising 4 strains of *Lysinibacillus* spp. (HC_B, HC_C, HC_4, and HC_4L), *Paenibacillus* sp. (HC_A), *Gordonia* spp. (HC_8A) and *Cupriavidus* sp. (HC_D). Whereas the axenic growth of *Cupriavidus* sp. exhibited poor biodegradative activity of 30-45 %, the other bacterial species (*Lysinibacillus, Paenibacillus,* and *Gordonia*) exhibited 45-60 % biodegradation. Thus, heptapeptide isoforms during consortium growth led to increased emulsification and biodegradation activity (Ibrar and Zhang, 2020). Kanaly et al. also reported new metabolic activity in *Rhodanobacter* sp., which otherwise could not grow on benzo[*a*]pyrene as the sole substrate. On the other hand, as a part of the consortium, by the action of mineralization and solubilization of benzo[*a*]pyrene by other members of the consortium, it could utilize intermediates of catabolism and hence was reported to be actively participating in the overall degradation, exhibiting a two-fold higher biodegradative activity (Kanaly et al., 2002). Such induction of new metabolite production elucidates the assertive effect of microconsortium over pure cultures.

Consortium also reveals commensalism within members, where one species initiates the degradation of contaminant present, so that rest co-surviving species can thrive on catabolic metabolites released in the environment and degrade the contaminant more effectively. Wanapaisan and the group also suggested a synergistic effect of the microbial consortium over pure culture. In this study, pyrene

hydrocarbon was used as a model high molecular weight contaminant to analyze the bioremediation activity of consortium procured from mangrove sediments. The study stated that the inherent sediment microconsortium was primarily enriched with *Mycobacterium* spp. strains (PO1 and PO2), capable of utilizing pyrene as a C source. However, the other components of the consortium, i.e., *Novosphingobium pentaromativorans* PY1, *Ochrobactrum* sp. PW1 and *Bacillus* sp. FW1 strains were not able to grow in pyrene enriched agar. Such different growth patterns of various consortium components revealed the co-existence of non-pyrene degraders. Further bioinformatics study explained the occurrence of genes in strains PY1 and PW1 responsible for the catabolism of intermediates of the pyrene degradation pathway. However, strain FW1 lacked genes involved in the biodegradation of pyrene or its intermediates. Interestingly, FW was responsible for the assimilation of pyrene, improving its bioavailability for other bacteria due to its ability to produce biosurfactants. Hence, such diverse bacteria in the consortium (PO1, PO2, PY1, PW1 and FW1) led to > 80 % pyrene degradation within 72 h of incubation, which was more than 2 folds higher than the biodegradation activity of axenic *Mycobacterium* spp. (PO1, PO2) (Wanapaisan et al., 2018).

Though indigenous microbes are major bioremediating agents; however, the low bioavailability and biotoxicity of hazardous contaminants at high concentrations, the biodegradation is severely compromised. Exogenously augmented microbes add the genetic and metabolic diversity to the contamination site, and hence significant tolerance is attained by the consortium, and their degradation capability is also broadened. Hence, in a few cases, augmenting the contaminated site with new microbes is vital to improving overall survivability and thus bioremediation activity (Yuan et al., 2018). Ebadi et al. explored the bioremediation activity in a harsh salt-rich contaminated site. Consortia enriched with oil-degraders and biosurfactant producers, *Pseudomonas aeruginosa* strains (T4, T27, T30, and E1) were prepared. The obtained results stated that in the presence of 30 g/kg of initial crude oil concentration, with an increase in salinity from 0 to 300 mM, the biodegradation rate constant, k (day^{-1}) of inherent consortium varied from 0.002 to 0.0009, which got modified to 0.0049 to 0.0035, expressing the augmenting role of *Pseudomonas* strains. In concordance, the authors also investigated the effect of catabolic enzyme dehydrogenase in the given experimental conditions. The results reported an approximate 2 fold boost in the enzyme activity in the case of bio augmented (6.35 ± 0.62 µg g^{-1} h^{-}

^{1}) than inherent consortium (3.41± 0.59 µg g^{-1} h^{-1}) (Ebadi et al., 2017). Various researchers have also reported the enhancement in the catabolic and degradative enzyme activity in the presence of metabolically enriched consortia (Loureiro et al., 2020; Suganthi et al., 2018).

Thus, the microbial consortium is highly significant in the overall biodegradation of contaminants over pure cultures due to the cooperative and mutualistic effect among members that leads to an increase in metabolic activity and sometimes induces the production of novel pathways for the contaminant degradation and metabolite production. The development of synthetic microbial consortium has been successfully exploited in various environmental remediation and industrial metabolite production applications. Nevertheless, potential insight in this domain is challenging due to the unavailability of smart system biology, bioinformatics and metagenomics tools.

2.7. Integrated physiochemical techniques assisted crude oil biodegradation

Crude oil bioremediation has come up as a simple, eco-friendly and economic process; however, one should not rule out the advantages of other physiochemical techniques. Various researchers nowadays are proposing the advantage of merging existing physio-chemical techniques with biological methods; a few examples are discussed below. Before subjecting the contaminated site for bioremediation purposes, these strategies have been used as a pre-treatment strategy. The advantage of these strategies includes, effective at high hydrocarbon concentration, rapid action, and the generated by-products are easily accessible by the later bioremediation treatment (Yap et al., 2011). Chemical oxidation strategies focus on removing organic compounds from the contaminated sites (Martinez-Pascual et al., 2015). On the other hand, photooxidation-based strategies are more effective towards aromatic organic compounds-based remediation (Tamai et al., 2017). The Electrokinetic-bioremediation technique deals with the remediation of aliphatic and aromatic hydrocarbons (Fan et al., 2015; Ramadan et al., 2018). Biosurfactant-mediated biodegradation technique is widely used as pre-treatment during soil washing or flushing prior to microbial biodegradation to effectively mobilize hydrocarbons (Szulc et al., 2014). Adsorption-assisted bioremediation technique is used for oil-contaminated sites with high initial oil concentration (> 5% w/w) as it rapidly reduces the toxicity effect on the microbial biodegradative action (Vasilyeva et al., 2020; Wang et al., 2020).

2.7.1. Photo-oxidation assisted bioremediation

This technique involves using light irradiation to break down hydrocarbons and other long chains into polar derivatives, improving their bioavailability for microbial biodegradation. This technique is majorly utilized for PAH-contaminated sites. In a study, Bacosa et al. explored the role of photooxidation using solar irradiation and microbial biodegradation in the bioremediation effectiveness of crude oil contaminated surface water from the Deepwater Horizon site. They stated that where biodegradation played a key role in alkanes' bioremediation, photooxidation was vital for polyaromatics bioremediation. Almost 70 % enhancement in the 4-5 ring aromatic compounds resulted from photooxidation activity (Bacosa et al., 2015). Vergeynst et al. studied the effect of photooxidation-assisted biodegradation of crude oil immobilized onto adsorbent as thin oil film. They reported that major factors involved in overall oil bioremediation included dissolution, microbial biofilm formation, and photooxidation. Biofilm was predominated by major oil degraders such as *Oleispira, Alkanindiges* and *Cycloclasticus.* Though microbial biodegradation activity was limited due to poor nutrient availability, simultaneous photooxidation occurrence caused almost complete (97 %) biodegradation of PAHs similar to alkanes, which otherwise have poor solubility hence lesser biodegradation rates within 112 days (Vergeynst et al., 2019).

However, though photooxidation has been proved to increase the bioremediation of PAH in crude oil, few studies also suggested their inhibitory role for the biodegradation of other crucial components of crude oil, i.e., pristanes and phytanes (Bacosa et al., 2015). Wang et al. explored an integrated photocatalytic-biological degradation system to remediation PAHs. A microcapsule was designed with a consortium entrapped within the capsule and coated with $Ag_3PO_4@Fe_3O_4$. The study revealed that microcapsule removed 944.1 mg/ kg PAHs present in the contaminated soil within 30 days (Wang et al., 2019). In addition, various studies have also stated the applicability of photocatalysts such as TiO_2 for the photooxidation of aromatic hydrocarbons using UV irradiation. The photocatalysts excite the electron to the conduction band, creating a hole site which in the presence of water or O_2 forms reactive oxygen species such as *OH or O_2^- which leads to oxidation of hydrocarbons. Zhang et al. used UV irradiation for the photocatalytic degradation of Phenanthrene, Pyrene and Benzo[a]pyrene by reducing their half-lives (h) by 4, 3.2, and 3.5 folds at the contaminated site (Zhang et al., 2008). However, these

studies cannot be integrated with microbial bioremediation as UV light for irradiation is harmful to microbial growth.

2.7.2. Chemical oxidation assisted bioremediation

This technique involves using chemical agents to break down hydrocarbons and other long chains into polar derivatives, improving their bioavailability for microbial biodegradation. The use of chemical agents such as H_2O_2 persulfate has also gained attention in this aspect. The Fenton oxidation reaction uses H_2O_2 and Fe^{2+} ions to release OH* radicals that further mineralize hydrocarbons **(equation 2.8 to 2.14)** (Bajagain et al., 2018).

$$H_2O_2 + Fe^{2+} \rightarrow OH^* + OH^- + Fe^{3+} \quad \textbf{(2.8)}$$

$$OH^* + Fe^{2+} \rightarrow OH^- + Fe^{3+} \quad \textbf{(2.9)}$$

$$RH + OH^* \rightarrow H_2O + R \quad \textbf{(2.10)}$$

$$R^* + Fe^{3+} \rightarrow R^+ + Fe^{2+} \quad \textbf{(2.11)}$$

$$H_2O_2 + Fe^{3+} \rightarrow OOH^* + H^+ + Fe^{2+} \quad \textbf{(2.12)}$$

$$H_2O_2 + OH^* \rightarrow OOH^* + H_2O \quad \textbf{(2.13)}$$

$$OH^* + OH^* \rightarrow OOH^* + OH^- \quad \textbf{(2.14)}$$

Thus, initial oxidation using physiochemical agents reduces the contaminant's initial concentration to low-risk values and improves their bioavailability for bacterial metabolism. Zhen et al. explored the modified Fenton process using suitable chelating agents to maintain the oxidizing activity of H_2O_2 at neutral pH. For this, ferrous sulfate and sodium citrate with H_2O_2 were used in the ratio of 1:1:100. The resulting TPH removal rate was reported as 4.73–24.26 %, with improved inherent microbial dehydrogenase and polyphenol oxidase activities (Zhen et al., 2021). In another study, the hydrocarbons were primitively chemically oxidized using oxidants such as persulfate and permanganate. It was reported that a week-long pre-oxidation of substrate led to complete removal of poly-aromatic hydrocarbons and almost 92 % removal of aliphatic hydrocarbons in 2 months' incubation. To this treated substrate, biochar supported zero-valent iron oxide nanoparticle adsorbent system was used for the biosorption assisted biodegradation study. During the biodegradation study, it was suggested that

biochar on the nanoparticle helped enhance the overall metabolic activity of inherent soil microbes (Mora et al., 2020).

Another study used persulfate ($S_2O_8^{2-}$, PS) to oxidize soil contaminants using Fe^{2+} as an activator in the form of nano zero-valent iron (ZVI). The activator was loaded to porous the biochar (BC) in the mass ratio of 3:1 to prevent loss in activity due to aggregation, forming BC-nZVI as a sustained source of Fe^{2+}. An optimized PS concentration of 15 % (w/v) was applied to TPHs polluted soil for 60 days. The initial oxidation of TPH occurred by the generation of SO_4^{*-} and HO^* radicals within 6 days, followed by the microbial biodegradation process. Compared to control carrying nZVI/PS groups, the BC-nZVI/PS groups could increase the soil microbial metabolic activities during the remediation period. A gradual TPH degradation into smaller units was reported in the presence of a BC-nZVI/PS mediated biodegradation study (Zhang et al., 2020). Hsia et al. explored the use of electron supplementation in the form of sulfate for the effective anaerobic bioremediation of ground water. A sulfate releasing bio-barrier was prepared using magnesium sulfate blended with rice husk and polylactic acid as carrier and binder, respectively. The released sulfate was acted as an electron acceptor by the sulfate-reducing bacteria growing faster and remediating ~70 % of methyl tert-butyl ether and 92 % of toluene within 120 days of incubation (Hsia et al., 2021). Hence, an amalgamation of chemical pre-treatment, such as oxidation with physical sorption, has shown tremendous improvement in the overall biodegradation activity of microbes.

2.7.3. Electrokinetic-bioremediation

The use of electric current has shown promising effects on increasing the electro-osmosis of bacterial cells and water hydrolysis, thereby increasing the mass transfer and oxygen availability, respectively, thus creating a favourable aerobic environment with more bioavailability hydrocarbons in the contaminated soil. However, such current may adversely affect soil pH and temperature, causing detrimental effects to inherent microbes. In response, Huang et al. explored alternating current applied to the contaminated soil with an inherent microbial consortium. A 50Hz electric field was applied to 2-D stable anodes connected to AC, providing a uniform electric field to hydrocarbon contaminated soil kept in a methacrylate made rectangular cell (160 × 90 × 160 mm^3). In the initial 35 days, continuous

biodegradation was observed; however, after 35-63 days, no significant change in the microbial biodegradation was achieved attributed to the limitation of nutrient concentration within the system. Thus, it bio-stimulated the overall degradation process by adding nutrients as soil additives to the treated soil. After 77 days of treatment, the results reported that a 16.5 % TPH biodegradation microbial action was raised to 50.9 % when electrokinetic treatment was added to the biological system. The treatment was continued to reduce the TPH concentration < 1 mg/g dry soil (permissible concentration), and 0.94 mg/g dry soil was achieved after 119 days of treatment (Huang et al., 2021).

Another study also explored the suitability of using electrokinetic coupled with biosurfactant-mediated bioremediation of hydrocarbon contaminated soil. The rhamnolipid biosurfactant was produced from bacteria *Pseudomonas aeruginosa* PF2, and its purified solution was exploited for the soil washing of contaminated soil at different concentrations of 1, 2, 3, 4 CMC value, pH (3–9), and time (4, 12, 24, 36 h). The maximum desorption of hydrocarbons: pyrene (85 %), anthracene (86 %), and phenanthrene (87 %) were reported at pH value of 6, 3×CMC and desorption time of 24 h. Thus, obtained desorbed solution was used for remediation using electrokinetic treatment. Magnetite Nanoparticles Modified Graphite (MNMG) electrode was used for the application. Almost complete oxidation of pyrene, anthracene and phenanthrene was obtained at pH 5 and 6 h when subjected to 3 V voltage and 25 ppm electrolyte concentration (Pourfadakari et al., 2019).

2.7.4. Biosurfactant mediated biodegradation

Feng et al. explored the synergistic application of biosurfactants to aid the inherent microbial biodegradation of petroleum hydrocarbons. Sophorolipid (SL) was applied to the contaminated soil at a 1.5 g /kg soil concentration. The addition of SL enhanced the bioavailability of hydrocarbon by increasing their desorption from soil particles. Additionally, the bacteria exhibited stimulated growth in the presence of SL as a co metabolite. A 57.7 % biodegradation was reported when the inherent bacterial consortium was augmented with SL, whereas in control, 44.5 % biodegradation was achieved after 30 days (Feng et al., 2021). Another integrated approach was performed by Wei et al., investigating the role of biosorbent biochar (BC), rhamnolipid (RL) biosurfactant and coated urea as external N sources. The 3 agents together led to 80.9 % degradation of hydrocarbons within 50 days of incubation. The

authors attributed the results to the 3 aspects: sustainable retaining of the substrate, increased solubilization and bioavailability of hydrocarbon from biochar by the RL and improved biodegradation ability of bacteria in the presence of N source stimulant. The other combinations, i.e., BC+RL and BC+N, resulted in 32.3 %, 73.2 %, biodegradation of hydrocarbons (Wei et al., 2020).

However, Zhen et al. dismissed the addition of RL and BC as separate entities during the integrated approach stating the risk associated with biodegradation of RL by inherent microbes or RL non-specific adsorption to clay soil particles hindering its emulsification activity as a whole in the system. Hence, the authors used rhamnolipid modified biochar (RL-BC) as a soil amendment for the 3 months' incubation-based hydrocarbon contaminated soil biodegradation study. Though modification of rhamnolipid reduced the surface area of pristine biochar, it increased its oxygen content. Thus, the biodegradation ability of hydrocarbon and the biodiversity of inherent microbes increased in modified bagasse (Zhen et al., 2021).

2.7.5. Adsorption assisted bioremediation

The use of adsorbents has become a promising strategy for rapidly removing toxic hydrocarbons from contaminated sites. Studies have shown the potential advantage of using an adsorbent as a carrier for bacterial biodegradation-based applications with the emerging immobilization strategies. Naloka et al. explored the use of high-density polyethylene (HDPE) made plastic balls as a carrier for the immobilization of hydrocarbon degraders, *Rhodococcus ruber* S103, *Mycolicibacterium parafortuitum* J101 and *Mycolicibacterium austroafricanum* Y502 for the simultaneous adsorption and bacterial biodegradation of fuel oil contaminated synthetic water. In the lab-scale study with an initial fuel oil concentration of 3000 ppm, > 50 % removal within 24 h was reported by the bacterial consortium immobilized plastic balls. In addition, 64 % adsorbed oil was reported to be biodegraded within 7 days by the bacterial syntrophic action. It was revealed that balls provided a non-toxic carrier system for the consortium to build biofilm to reduce exposure to fuel oil toxicity (Naloka et al., 2021). However, the poor biodegradability of plastic balls is the limitation of such a bioremediation system.

Biosorption has come up as the best detoxification technique to reduce the harmful effect of high concentrations of contaminants on biological species. Biosorption involves using bio-origin waste as

an adsorbent for contaminant immobilization. The initial surface adsorption is a very quick process and only lasts for a few minutes. This way, the contaminant concentration for the microbial encounter reduces to a tolerable level, allowing them to more effectively metabolize them as their substrate, overall improving the extent of biodegradation. In most cases, these biosorbent are organic molecules with appreciable adsorption capacity and effective substrate bed formation property. This way, the adsorbed biosorbent is used up by microbes as their secondary substrate and acts as a carrier for the sustained release of contaminant as a substrate for microbial metabolism.

Trichloroethylene (TCE), a common landfill leachate contaminant remediation, was explored using biochar packed columns with naturally occurring biofilm-forming microbes present in the leachate. The microconsortium colonizing on the biochar showed the dominance of biofilm-forming and TCE degrading microbes such as *Desulfitobacterium* spp., *Desulfuromonas* spp. and *Sulfurospirillium* spp. and very least population of pathogenic microbes such as *P. aeruginosa* and *E. coli*. With an initial TCE concentration of 35 ppm, > 99 % removal of TCE was reported by the simultaneous action of adsorption and biodegradation (Siggins et al., 2020). A magnetic loofah sponge biochar (MagLsBC) was explored in a similar study to remediation PAH-contaminated sediments. MagLsBC observed a significant 31.9 % reduction in PAH content after 350 days of incubation. In addition, the loofah was enriched with *Chloroflexi, Acidobacteria, Euryarchaeota,* and *Proteobacteria, a* phylum that is well reported for aromatic compound degradation (Hao et al., 2021).

Another concurrent biodegradation study of 4-Nitrophenol was performed using Acacia gum with immobilized *Pseudomonas* sp. YPS3. Within 6 h, >98 % contaminant biodegradation was reported at pH 7, 37°C, with an initial contaminant concentration of 30 ppm (Kalaimurugan et al., 2021). Fang et al. explored the advantages of using a combination of natural polymers such as alginate, chitosan, and their composite to immobilize *Cupriavidus nantongensis* $X1^T$ for the removal of Chlorpyrifos (20 ppm) contaminants. The study revealed that a composite of chitosan with alginate improved the adsorption capacity of alginate by 1.7 folds achieving 96.6 % biodegradation within 24 h by the immobilized cells (Fang et al., 2021).

2.8. Challenges associated with microbial bioremediation

The major challenge in the ineffectiveness of various bioremediation tools at the actual contaminated site are listed below:

1. The concentration of crude oil at the contaminated site is above the tolerance limit for bacterial growth (Mulligan et al., 2001; Sharma, 2012; Vidali, 2001).

2. Lack of nutrient availability and trace elements at the site: N and P are the major limiting nutrients in the contaminated site impeding biodegradation. Though crude oil is a rich C source, it lacks essential minerals and traces elements required for microbial growth (Cubitto et al., 2004; Vidali, 2001).

3. Weathering of Crude oil: Factors such as the incorporation of dumped garbage and debris along with suspended materials and loss of light hydrocarbons due to solar irradiation, causing concentration of by-products and heavy hydrocarbons with increased toxicity, diminishing the quality of spilled oil for microbial consumption (Ron and Rosenberg, 2014; Sorkhoh et al., 1990).

4. Microbes exhibit a slower biodegradation rate: As soon as the oil gets spilled into soil or water, it forms a thick layer impeding the mixing of oxygen and sunlight to the inhabiting microbes, thus limiting their overall biodegradation abilities.

5. Incomplete biodegradation and resistance towards asphaltenes: Incomplete bioremediation is a hazard as the non-sequestered residual contaminant gets more bioavailable and increases the chances of toxicity.

6. Occurrence of competing microbes: Various simultaneous competing processes apart from biodegradation by inherent microbes leads to reduced efficacy of key hydrocarbon degraders.

7. The unsustainability of laboratory bioremediation experiments in the field sites: Biostimulation leads to eutrophication, whereas bioaugmentation shows poor sustainability in the in-situ environment (Santos et al., 2016).

In this direction, researchers have put forward to use microconsortium approach in improving the biodegradability efficacy. Also, the exploitation of integrated strategies such as adsorption and photodegradation-assisted biodegradation can improve efficacy. The use of biosurfactants as additives can be explored in improving the solubility of hydrocarbons. Similarly, injecting steam into heavy fuel oil contaminated sub-surface soil aids in improving microbial activity of degradation. A microbial

encapsulation-based strategy has also been explored in a few case studies to protect microbial consortiums from contaminant toxicity (Muthusamy et al., 2008). Also, bio-augmentation using exogenous and genetically modified hydrocarbonoclastic microbes can be used to pump up the overall degradability. Recent in-situ remediation techniques involve sparging-slurping followed by biostimulation using nutrients and biosurfactants (Akbari et al., 2018).

2.8.1. Research gaps

The possible research gaps in the microbial bioremediation of crude oil include:

1. Biodegradation efficiency varies greatly on the bioavailability of oil and affinity of microbes
2. Spilled sites are always nutrient derived, and the addition of nutrients externally sometimes leads to eutrophication
3. Asphaltic residues remain unaffected by biodegradation
4. High initial oil concentration or supersaturated oil concentration at the spilled site inhibits the biodegradation process and extends the lag phase by 2-4 weeks
5. Limited biodegradability and relatively longer treatment time required

2.8.2. Hypothesis

Based on these challenges, we hypothesize that crude oil bioremediation can be enhanced by isolation, screening and identifying inherent oil degraders and optimization of parameters such as pH, Temperature, and crude oil concentration that limits their biodegradation ability. Understanding their aliphatic and aromatic hydrocarbon biodegradation and biosurfactant production ability can further aid in designing microconsortium. Further immobilization of potential oil-degrading consortiums into suitable carriers would prevent toxicity and improve their growth, which will help in improving their crude oil biodegradation ability.

2.9. Conclusions

With the emerging industrialization and urbanization, the risk of exposure of the environment to toxic chemicals is severe. The use of biological agents such as bacteria, fungi and plants and their products in enzymes and other exudates has gained interest. It has been immensely explored for the degradation, detoxification or transformation of these toxic compounds, highlighting the importance of the bioremediation technique. Microbes being the most primitive form of life, are well equipped with the required machinery for remediation of toxic contaminants. It is due to the presence of effective catabolising enzymes like alkane hydroxylases and mono- or di-oxygenase extracellular by-products like biosurfactants and emulsifiers. Inherent microbes at the contamination site play a major role in the *in-situ* bioremediation of contaminants; however, their efficacy reduces with the emergence of xenobiotics and other high molecular weight compounds. Various researchers focus on genetic and metabolic engineering techniques as an effective solution to this problem. In addition to this, studies also revealed the synergistic advantage of integrating physio-chemical and biological techniques systematically in order to achieve the best results. Hence, in order to maximize the rate of bioremediation, an integrated approach should be followed, which includes (1) understanding the *in-situ* microbial community, (2) using metagenomics tools to analyze the active metabolic pathways, (3) using metabolic and genetic engineering techniques to uplift the overall microbial population size and enzyme activity. (4) Providing suitable chemical and physical amendments to aid microbial activity.

Chapter 3

Exploring the crude oil biodegradation and biosurfactant production abilities of isolated *Agrobacterium fabrum* SLAJ731

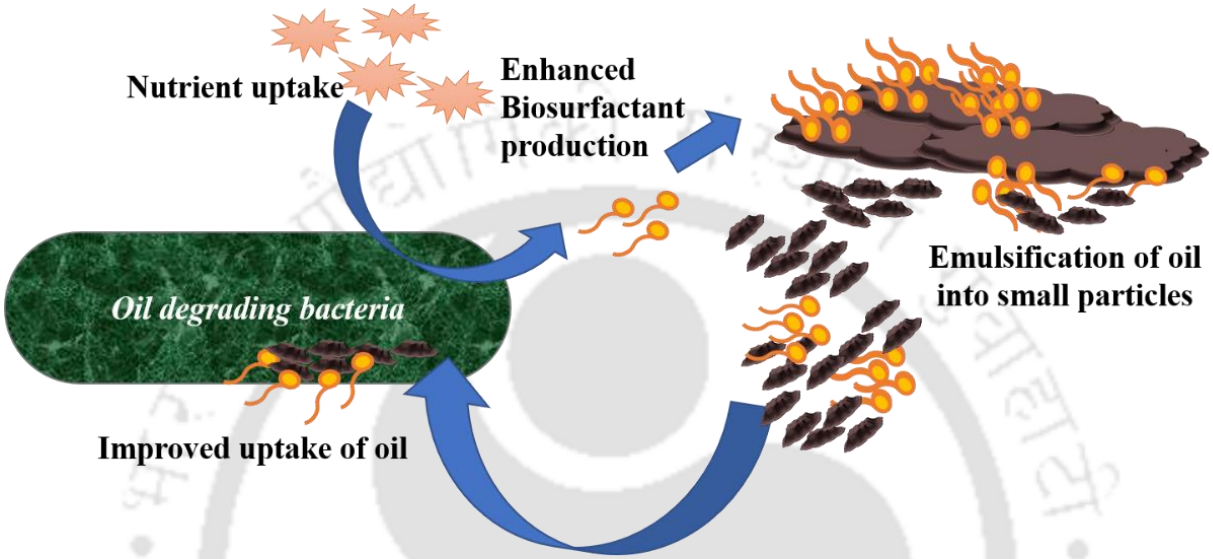

(Biocatalysis and Agricultural Biotechnology 21, 101322, 2019 (Sharma et al., 2019))

This chapter discusses the screening of previously isolated *Agrobacterium fabrum* SLAJ731 for its biosurfactant production and oil-degrading abilities. The culture conditions were optimized to maximize the biosurfactant production using one factor at a time technique. Under optimized culture conditions, the growth, oil biodegradability, surface tension reduction, biosurfactant concentration, and enzyme activity were studied. The obtained biosurfactant was characterized and scrutinized to analyze their promising potential in oil biodegradation and enzyme activity induction.

3.1. Introduction

Crude oil is composed of various hydrocarbons, heavy metals, non-metals, and other particulate matter and is utilized as the foremost value-added substrate to meet energy demands. The mishandling of crude oil during extraction, transportation and accidental spills lead to hazardous exposure of its toxic

components into the environment (Hou, 1982). The complex composition of spent crude oil makes it poor-biodegradable. Toxicity of the components of crude oil, including particulate matters, polyaromatic hydrocarbons, volatile organic matters, and oil mist, poses a serious threat to the environment (Bhattacharya et al., 2019). Therefore, various environmentalists are working across the globe to remedy this alarming hazardous exposure.

The major issue in the biodegradation of spent crude oil is its hydrophobic nature, as it causes a decrease in its bioavailability for natural attenuation. Among various reported physio-chemical techniques (Arivalagan et al., 2014; Pugazhendhi et al., 2018; Saxena et al., 2018), researchers have reported bioremediation of crude oil as the most efficient, economical and eco-friendly approach (Thulasinathan et al., 2019). Bioremediation mediates the employment of biological agents (i.e., bacteria, fungi or algae), which increase the bioavailability of oil by secreting biosurfactants upon utilizing them as carbon (C) source (Saravanakumar and Kathiresan, 2014; Saxena et al., 2018; Sharma et al., 2019). Unlike synthetic detergents, biosurfactants are economical in production, work at extreme temperature and salinity ranges, and are biodegradable (Fai et al., 2015). These lucrative advantages stimulate the optimization of biosurfactant production to maximize the biodegradation of crude oil. Various bacterial strains including *Bacillus* sp., *Pseudomonas* sp., *Rhodococcus* sp., *Brevibacillus* sp., *Lysinibacilllus* sp., *Stenotrophomonas* sp., have been explored for their role in biosurfactant production and crude oil degradation; however, the biosurfactant production was not found to be very impressive, i.e., 0.1 to 6 g/L. However, scant attention has been given to the biosurfactant production ability of the *Agrobacterium* genus.

Furthermore, alongside emulsifying activity of biosurfactants, the rate of biodegradation of crude oil is also attributed to the enzyme activity of certain oil-degrading enzymes such as alkane hydroxylase (AH). The activation of hydrophobic crude oil involves oxygenation of its aliphatic and aromatic residues, which is catalyzed by AH (Hou, 2017). The enzyme oxidizes alkanes (medium-chain length mostly C_5 to C_{16}) into alcohols, which are further metabolically oxidized to aldehydes and ketones and later fluxed to the β oxidation pathway for the production of energy and other metabolic products (Hou, 2005; Hou, 2006).

In the present study, the ability of the rhizosphere inhabiting *Agrobacterium* spp. to produce biosurfactants has been explored. Culture conditions, i.e., pH, temperature, C, Nitrogen (N) and C: N ratio for the maximal production of biosurfactant, were optimized. Further, the biosurfactant was characterized using various instruments like Fourier-transform infrared spectroscopy (FTIR), Liquid chromatography-mass spectroscopy (LC-MS), Tensiometer, and Nuclear Magnetic Resonance (^{1}H NMR). In this study, we have observed that the role of glucose was not only limited to enhancing cell density. Interestingly, this study explores the synergistic effect of co-substrate glucose on the present strain's crude oil degradation and biosurfactant production ability in terms of enzyme activity of AH.

3.2. Materials and methods

3.2.1. Microbial strain and chemicals used

In this study, a gram-negative bacterium *Agrobacterium fabrum* SLAJ731 was used, which was earlier isolated by our group from a core sample of the Assam oil field, India. Crude oil (API gravity 34.97°) used in this study was obtained from IOCL, Noonmati, Assam India., in sterile sampling bottles and stored at 4°C till further use. Bushnell Hass (BH) media (Himedia M350-500G) was used for all optimization studies. Nutrient Broth (M002-500G), Luria Bertani (LB) media (M1245-500G), Nicotinamide Adenine Dinucleotide Hydride (NADH, RM393), n-hexadecane (RM2238-100ML), Yeast extract (RM027-500G) Glucose (MB037-500G), 3-[(3-Cholamidopropyl) dimethyl ammonio]-1-propanesulfonate (CHAPS, MB084), Trifluoroacetic acid (RM874), Acetonitrile (AS029), n-hexane (AS097), Methanol (AS059) and Ethyl acetate (AS051), were purchased from Himedia, India. Deuterated chloroform (570699), and Sinapinic acid (85429) were procured from Sigma, India. MiliQ (18 MΩ, Millipore system) water was used throughout the experiments.

3.2.2. Screening for biosurfactant production

Pre-culture of *A. fabrum* SLAJ731 was used as inoculum (1 %, v/v) in sterile BH media supplemented with 1 % (v/v) hexadecane as a model C source, at 30 °C and 150 rpm for 24 h. After incubation, the culture was centrifuged at 8000 rpm for 10 min at 4 °C. The supernatant was collected and explored for

screening of biosurfactant production ability of the bacteria using drop collapse test, oil displacement test and emulsification activity (E_{24}) (Datta et al., 2018).

3.2.2.1. Drop collapse test

Drop collapse test examines the destabilizing ability of oil droplets by the action of biosurfactant. In this assay, 2 µL of oil was added to the cleaned glass slide and allowed to equilibrate at 37 °C for 1 h. Next, 5 µL of cell-free supernatant was added to the oil droplet and left for 1 min. The collapsing of oil drop indicated the reduction in the interfacial tension between the polar and non-polar solvents interface, indicating positive surface activity of the biosurfactant (Persson and Molin, 2004).

3.2.2.2. Oil displacement test

The oil displacement test examines the ability of biosurfactants to displace the oil layer by lowering its surface tension. For this, 100 µL of oil was poured on 20 mL of distilled water in a Petri plate, and a uniform oil film was allowed to form. 10 µL of cell-free supernatant was added to this oil film, and immediately, the diameter of the clear zone formed was measured. The diameter of the clear zone is directly proportional to the surface activity of the biosurfactant (Morikawa et al., 1993).

3.2.2.3. Emulsification activity

E24 technique is used to determine the emulsion forming ability of biosurfactants in the non-polar and polar solvent system (Datta et al., 2018). Estimation of E_{24} was performed by mixing an equal volume of n-hexane (non-polar solvent) with the obtained cell-free supernatant. The mixture was vigorously homogenized for 2 min and left at room temperature for 24 h. Later, the height of the emulsion layer formed in the mixture was measured, and the E_{24} was calculated using **equation 3.1**,

$$E_{24} = \frac{\text{Height of emulsified layer (mm)}}{\text{Total height of liquid column (mm)}} \times 100 \qquad \textbf{(3.1)}$$

3.2.3. Optimization of biosurfactant production

Upon confirming the ability of the present strain for biosurfactant production, its culture conditions were optimized using the one-factor-at-a-time approach (OFAT) as discussed in Chapter 2, section 2.5.2.1 (Devaraj et al., 2019; Jimoh and Lin, 2019; Parthipan et al., 2017). In each case, the 24 h grown culture of *A. fabrum* SLAJ731 was used as inoculum (5 %, v/v) at 1.4×10^7 CFU/mL and incubated in BH broth at listed pH, temperature and 150 rpm for 24 h **(Table 3.1)**. After incubation under each listed condition, the cells were pelleted down by centrifugation at 8000 rpm for 10 min at 4 °C and weighed for the dry biomass estimation. The obtained supernatant was tested for E_{24}.

3.2.4. Biosurfactant extraction and characterization

The bacterial culture was grown in sterile BH media with optimized C and N (as per the C: N ratio obtained) and maintained at optimized conditions for 144 h. At the end of the incubation period, the cells were harvested using centrifugation at 8000 rpm for 10 min at 4°C. Next, the solvent extraction technique using an equal volume of ethyl acetate: methanol (4:1) and cell-free supernatant was exploited for biosurfactant extraction, as also reported by our group (Gudiña et al., 2015; Sharma et al., 2019). In this regard, the obtained supernatant was initially acid precipitated (pH 2) and incubated overnight at 4°C using 6M HCl. Later, it was solvent extracted, and the organic layer was vacuum evaporated using rotary vacuum evaporation, leaving behind a crude biosurfactant. Thus, obtained biosurfactant was weighed gravimetrically and stored at room temperature for further characterizations using FTIR spectroscopy (Perkin–Elmer, Spectrum two), ^{1}H NMR spectroscopy (MERCURY PLUS, VARIAN), and LC-MS (Waters, Q-Tof Premier) and Tensiometer (Data physics, DCAT 11EC).

3.2.4.1. Functional group analyses

The functional group analyses of the crude biosurfactant were performed using FTIR and NMR spectroscopy. FTIR spectroscopy works based on identifying the chemical groups and functional groups present in the molecule of interest. FTIR spectroscopy uses infra-red radiation to vibrate and rotate molecules within the compound at a specific frequency recorded by the detector as a peak intensity. The nature of the peak (stretching/bending) and its intensity describe the chemical groups present in the

chemical structure of the compound of interest. FTIR has been a widely accepted identification and characterization technique employed to study biosurfactants. Briefly, 10 µL of crude biosurfactant was mixed with 100 mg of anhydrous KBr and then compressed into a thin film/ pellet, which was analyzed using an FTIR spectrophotometer (400-4000 cm^{-1}). The spectra resolution was set to 4 $cm^{-1,}$ and the scan rate was maintained to 32 scans (Elazzazy et al., 2015).

The NMR technique is an analytical technique used to determine the structure of any compound based on its magnetic spin orientation in an external magnetic field applied. Crude biosurfactant sample was prepared in deuterated chloroform and analyzed using in 400 MHz ^{1}H NMR Spectrometer equipped with an Oxford superconducting magnet of frequency 400 MHz (9.4 Tesla) with a probe capacity of 5 mm. The obtained chemical shifts (δ) of NMR absorptions were recorded in ppm scale relative to tetramethylsilane (Zou et al., 2014).

3.2.4.2. Surface tension measurement

The cell-free supernatant was also studied for the determination of critical micelle concentration (CMC) of the crude biosurfactant based on reduction of surface tension of water upon sequentially adding varying concentrations of crude biosurfactant till inflection point was reached using a tensiometer (Data physics, DCAT 11EC) at 25 °C using a Du Nouy ring method (Pandey and Pattanayek, 2013).

3.2.5. Biodegradation analysis of crude oil

The ability of *A. fabrum* SLAJ731 to biodegrade crude oil was performed by inoculating at 1.4×10^{7} CFU/mL inoculum (5 %, v/v) in sterilized BH media (100 mL) under optimized experimental parameters. The experimental setups were prepared as described in **Table 3.1**. In order to study the effect of optimization on the oil biodegradation ability, a comparative experimental setup was kept with no glucose, imitating sub-optimal condition. The cells were harvested using centrifugation upon incubation, and the supernatant with residual crude oil was recovered and extracted in organic solvent (n-hexane) thrice. Later, the organic layer, comprising residual oil, was pooled and subjected to vacuum evaporation to recover residual oil. Thus, obtained residual oil was quantified gravimetrically. The overall oil biodegradation was calculated using **equation 3.2**;

$$\textbf{\textit{Oil degradation}}\ (\%) = \frac{(\textbf{\textit{Amount}}_{\textbf{\textit{initial oil}}} - \textbf{\textit{Amount}}_{\textbf{\textit{residual oil}}}) \times 100}{\textbf{\textit{Amount}}_{\textbf{\textit{initial oil}}}} \quad \textbf{(3.2)}$$

Furthermore, the extracted residual crude oil was analyzed using FTIR spectroscopy and Gas chromatography-mass spectrometry (GC-MS) analyses to elaborate the change in its chemical composition. For GC-MS study (model 7890B, Agilent Technologies), DB5 column (30 m × 0.25 mm × 0.25 μm) used. The injector temperature was maintained at 280 °C with a split ratio of 1:10. The initial oven temperature was maintained at 80 °C for 2 min and increased at ramping of 5 °C/min to 280 °C, followed by a hold for 30 min. The detector was maintained at 300 °C, and the Helium (carrier gas) flow rate was maintained at 1 mL/min. On the other hand, the aqueous layer was studied for biosurfactant production, as discussed in section 3.2.4. In addition, the chemical oxygen demand (COD) was also estimated to determine the dissolved organic content (Clesceri et al., 1998; Sajna et al., 2015).

Table 3.1. Experimental designs for the study of the biodegradation of crude oil using *A. fabrum* SLAJ in the presence of co-substrate

Experimental setups	**Culture parameters (Incubation conditions: pH 6, 30°C and 150 rpm for 144 h)**
With glucose (Optimal condition)	BH media + Glucose (1 % w/v) + Crude oil (1 % v/v) + Yeast extract (1 % w/v) + Inoculum (5 % v/v)
Without glucose (Sub-optimal conditions)	BH media + Crude oil (1 % v/v) + Yeast extract (1 % w/v) + Inoculum (5 % v/v)
Abiotic control	BH media + Crude oil (1 % v/v) + Yeast extract (1 % w/v)

3.2.6. Determination of alkane hydroxylase activity

One of the major enzymes involved in crude oil degradation is alkane hydroxylase. Alkane hydroxylase is involved in the oxidation of hydrocarbons into their alcoholic derivatives **(equation 3.3)** (Elumalai et al., 2017)

$$RH\ (Alkane) + O_2 + H^+ + NADH \xrightarrow{Alkane\ hydroxylase} ROH(Alcohol) + H_2O + NAD^+ \quad \textbf{(3.3)}$$

After incubation, the pelleted bacterial cells were initially washed with sterile distilled water twice and later re-dissolved in 20mM Tris-HCl (pH 7.4). Further, the cells were lysed using sonication at 4°C for 15 min to obtain crude protein extract. The lysate was centrifuged at 10000 rpm at 4°C for 30 min to recover debris-free crude protein extract. Obtained pelleted debris was dried overnight oven to calculate the dry biomass. The total protein was estimated using QuantiPro BCA assay kit (Sigma, India, Cat no. 100134331) using BSA as standard (de Andrade et al., 2016; Hasan et al., 2018; Pandey et al., 2012; Pandey and Pattanayek, 2011; Pandey and Pattanayek, 2013).

The crude protein extract was studied for alkane hydroxylase assay. The reaction mixture comprised 0.1 mM Nicotinamide adenine dinucleotide (NADH) as a cofactor, CHAPS hydrate (0.15 % (*w/v*), pH 7.4), 10 µL of hexadecane as substrate (1 % hexadecane in 80 % DMSO) and 50 µL of crude enzyme extract. The alkane hydroxylase enzyme activity was analyzed based on a decrease in NADH concentration during the oxidation of hexadecane to hexadecanol by AH enzyme present in the crude extract. Such consumption of NADH per minute was estimated as measuring absorbance at 340 nm, signifying the successful oxidation of the substrate (Jauhari et al., 2014; Meng et al., 2017; Singh and Tiwary, 2017).

3.2.7. Statistical analysis

The statistical analyses were carried out using OriginPro 8.5. All the experiments were performed in triplicates, and their values were reported as average ± standard deviation. Statistically, a significant difference was considered when the significance level, p, was <0.05, using analysis of variance (ANOVA).

3.3. Results and discussion

The biosurfactant production ability of the present bacterial strain, *A. fabrum* SLAJ731, was evaluated using standard screening methods such as oil drop collapse activity, oil displacement method, and emulsification index. The bacterial strain showed positive results for all tests mentioned above with an oil displacement diameter of 1.5 ± 0.3 cm, causing flat morphology of oil drop with few seconds of adherence and a remarkable E_{24} of 50 ± 2.5 % within 24 h of incubation. Hence, upon validating the present strain for biosurfactant production, its culture conditions were optimized.

3.3.1. Optimization of culture conditions for biosurfactant production

In order to enhance the biosurfactant production ability of the present strain, the culture conditions were optimized based on pH, temperature, C, N and C: N ratio **(Table 3.2). Figure 3.1** shows the optimization results for the earlier parameters and selections of the best conditions based on the E24 value and dry biomass yield, which responds to biosurfactant synthesis ability and cell growth. The optimized conditions for the present strain were obtained as pH 6, temperature 30°C (mesophilic), glucose as C source, yeast extract as N source and C: N ratio of 2:1.

Table 3.2. Culture conditions investigated for the optimization of the biosurfactant production

Factors	Values	Experimental conditions
pH (a)	4.0, 5.0, 6.0, 7.0, 8.0, and 10.0	C= Glucose (1 %); T = 37 °C
Temperature (b)	20°C, 30°C, 40°C, 50°C and 60°C	C= Glucose (1 %); pH = optimized (a)
C source (c)	Glucose, Sucrose, Glycerol, Molasses, Crude oil, and Hexadecane (C16)	pH = optimized (a); T = optimized (b)
N source (d)	Yeast extract, Urea, Ammonium sulphate, and Sodium nitrate	pH = optimized (a); T = optimized (b); C= optimized (c)
C:N ratio (w/w)	1/1,1/2, 1/3, 1/4, 1/5, 2/1, 3/1, 4/1, and 5/1	pH = optimized (a); T = optimized (b); C= optimized (c); N= optimized (d)

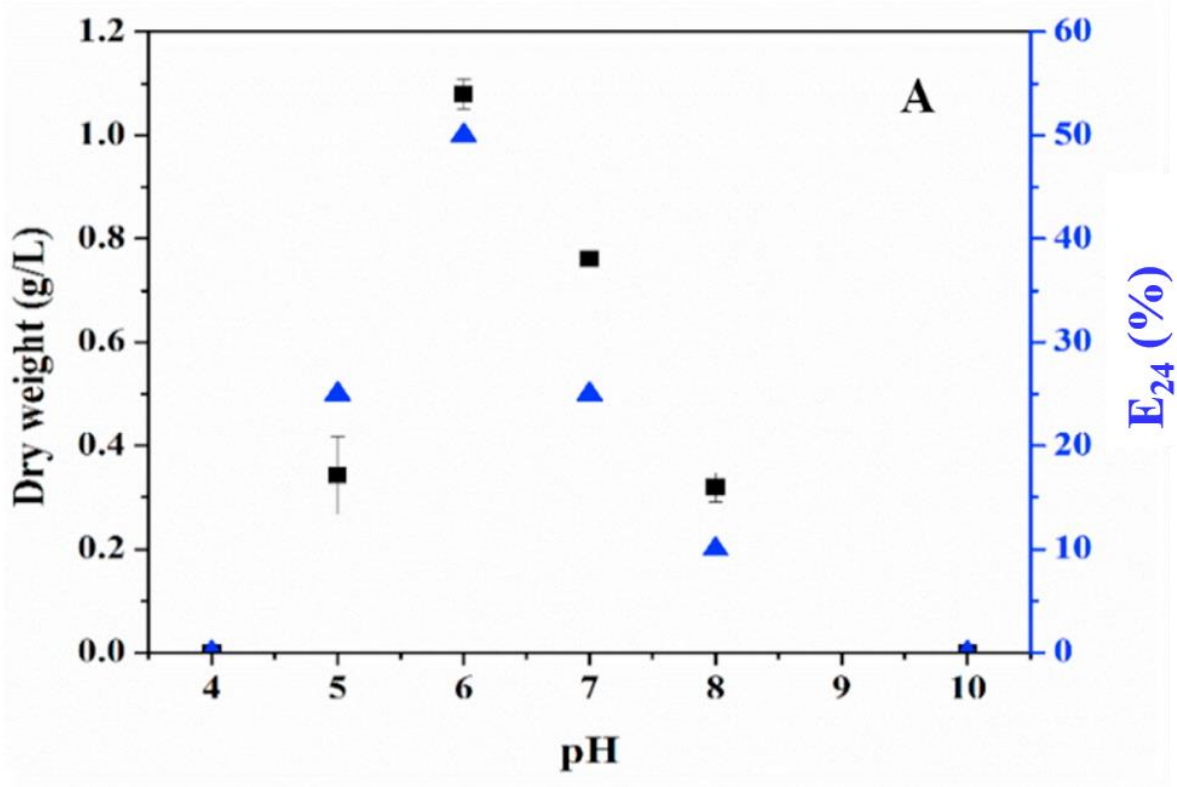

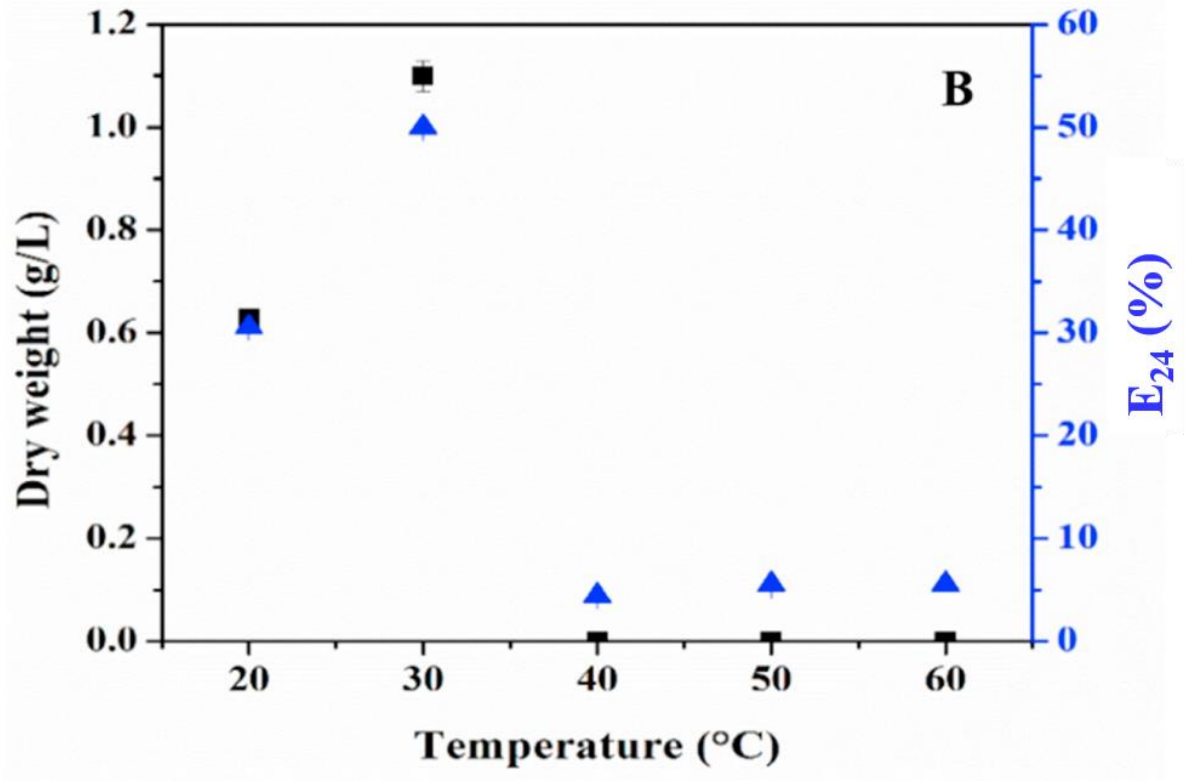

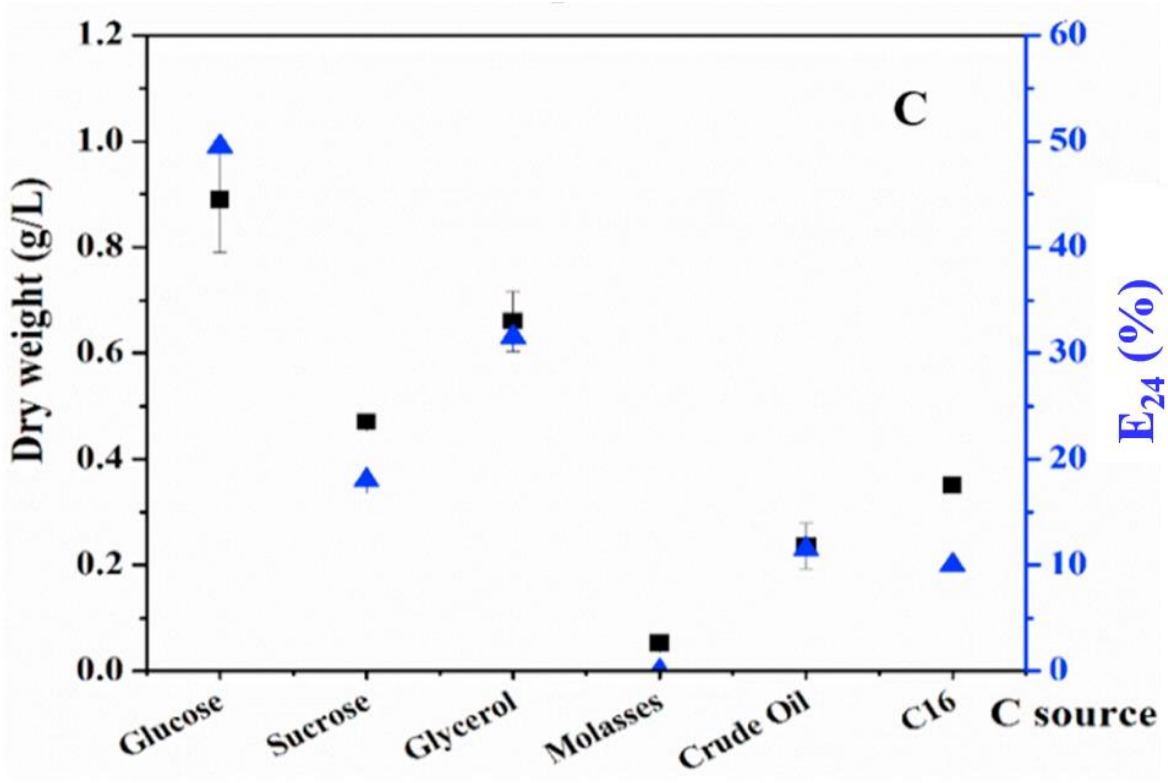

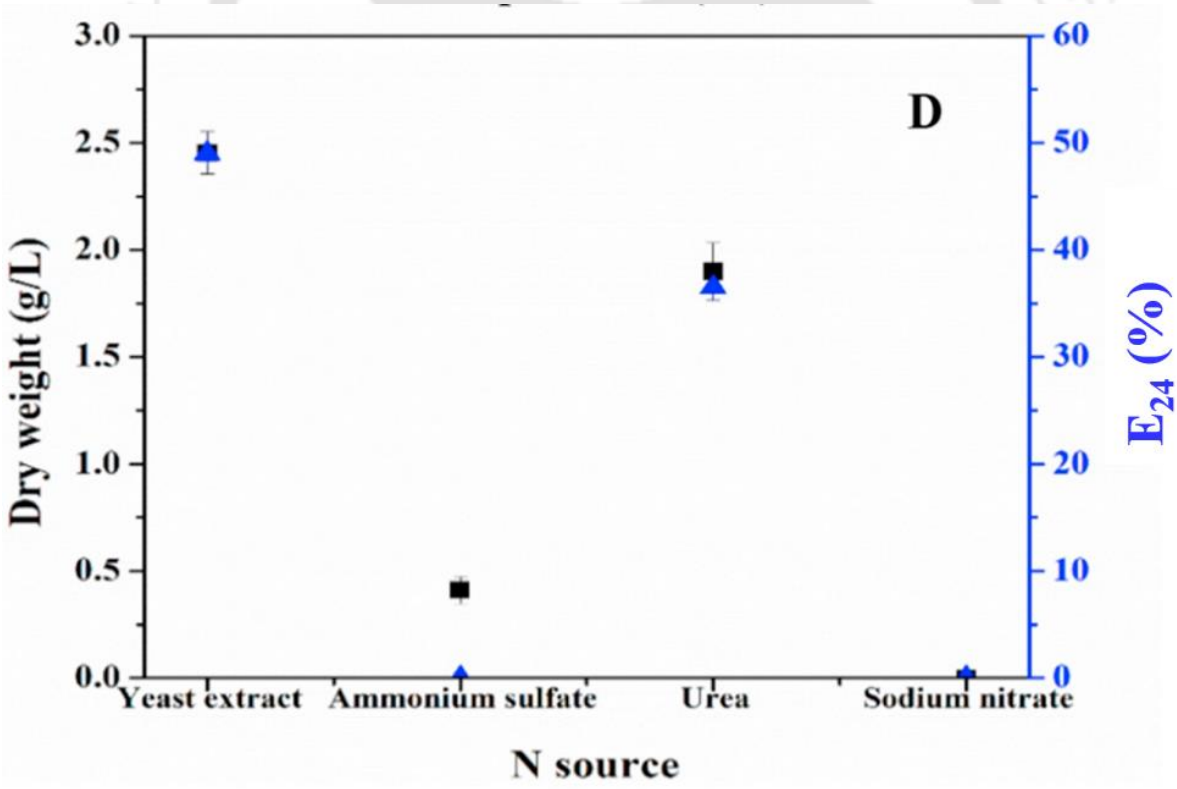

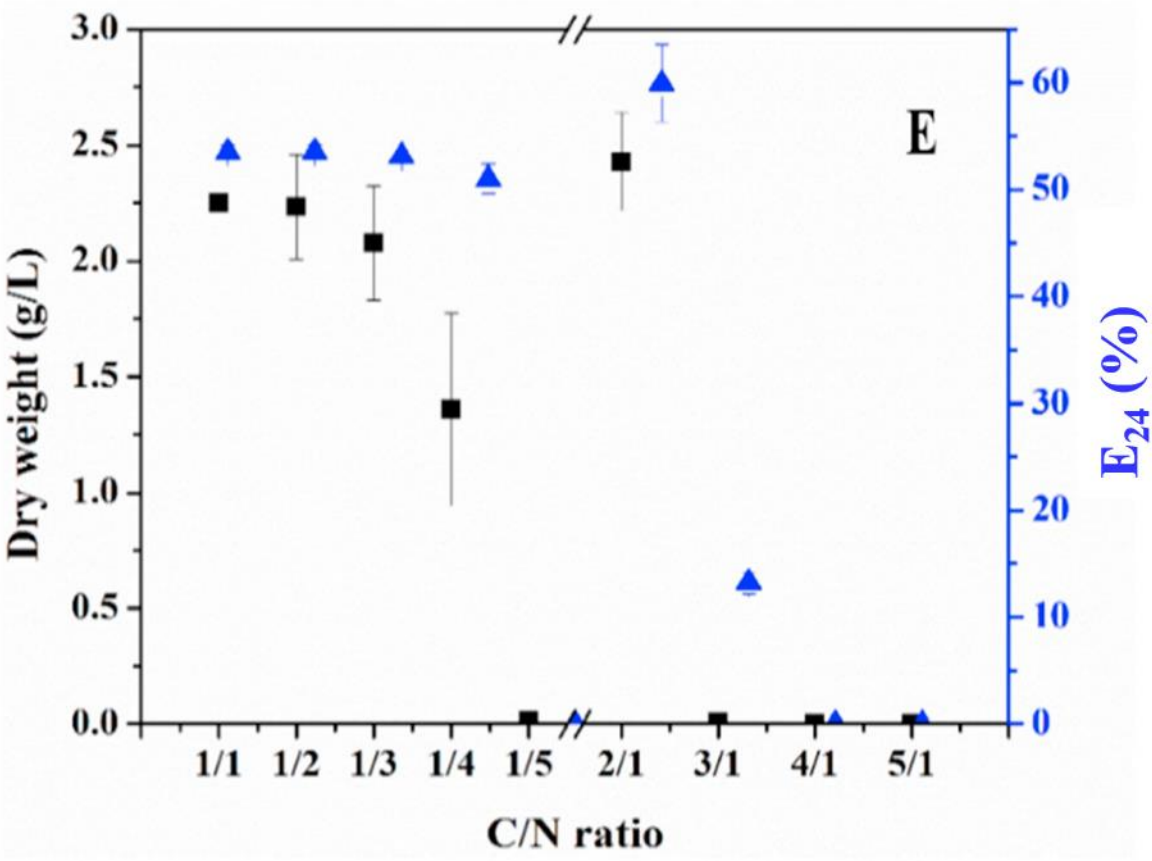

Figure 3.1. Effect of different culture parameters (A) pH; (B) Temperature; (C) C sources; (D) N sources; and (E) C: N ratio, on the biosurfactant production ability of *A. fabrum* SLAJ731

Under these optimized conditions, *A. fabrum* SLAJ731 was studied for its growth behavior (based on dry biomass) and subsequent biosurfactant production, which was analyzed by a change in surface tension, E_{24} and biosurfactant yield analyses as shown in **Figure 3.2**. It was observed that cells showed a short lag phase (~6 h) and exhibited a specific growth rate of 0.01 h^{-1}, reaching the maximum cell mass of 16.7 ± 0.2 g/L within 96 h of incubation. Parallelly, residual substrate (glucose) analysis was performed to understand the effect of substrate on bacterial growth. It was observed that glucose was consumed at 0.14 ± 0.1 g/L/h and completely depleted after 144 h. On the contrary, the biosurfactant yield increased from 48 h to 120 h at the rate of 0.07 ± 0.02 g/L/h, suggesting the biosurfactant as a secondary metabolite produced during the stationary phase. This rapid onset of extracellular biosurfactant production during the stationary phase was due to the release of cell-bound biosurfactant, as reported in a few other studies (Thavasi et al., 2011). Hence, E_{24} activity increased with an increase

in biosurfactant production and the maximum E_{24} was found to be 65 ± 0.2 % at 144 h. Similarly, the surface tension followed the reverse trend concerning E_{24} and reached 32 ± 0.5 mN/m from 72 ± 0.4 mN/m within 144 h of incubation.

Under these optimized conditions, the overall crude biosurfactant yield was obtained as 5.77 ± 0.3 g/L, which is found to be complementary to other reported strains (**Table 3.3**). **Table 3.3** summarizes various recent literature reports on biosurfactant production utilizing oily substrate as the only 'C' source. Compared to the reported values, our strain produced a notable biosurfactant upon utilizing waste crude oil as the C source. Utilizing spent crude oil as a C source for biosurfactant production is economical and eco-friendly, as its degradation decreases the detrimental effects of its exposure to the environment.

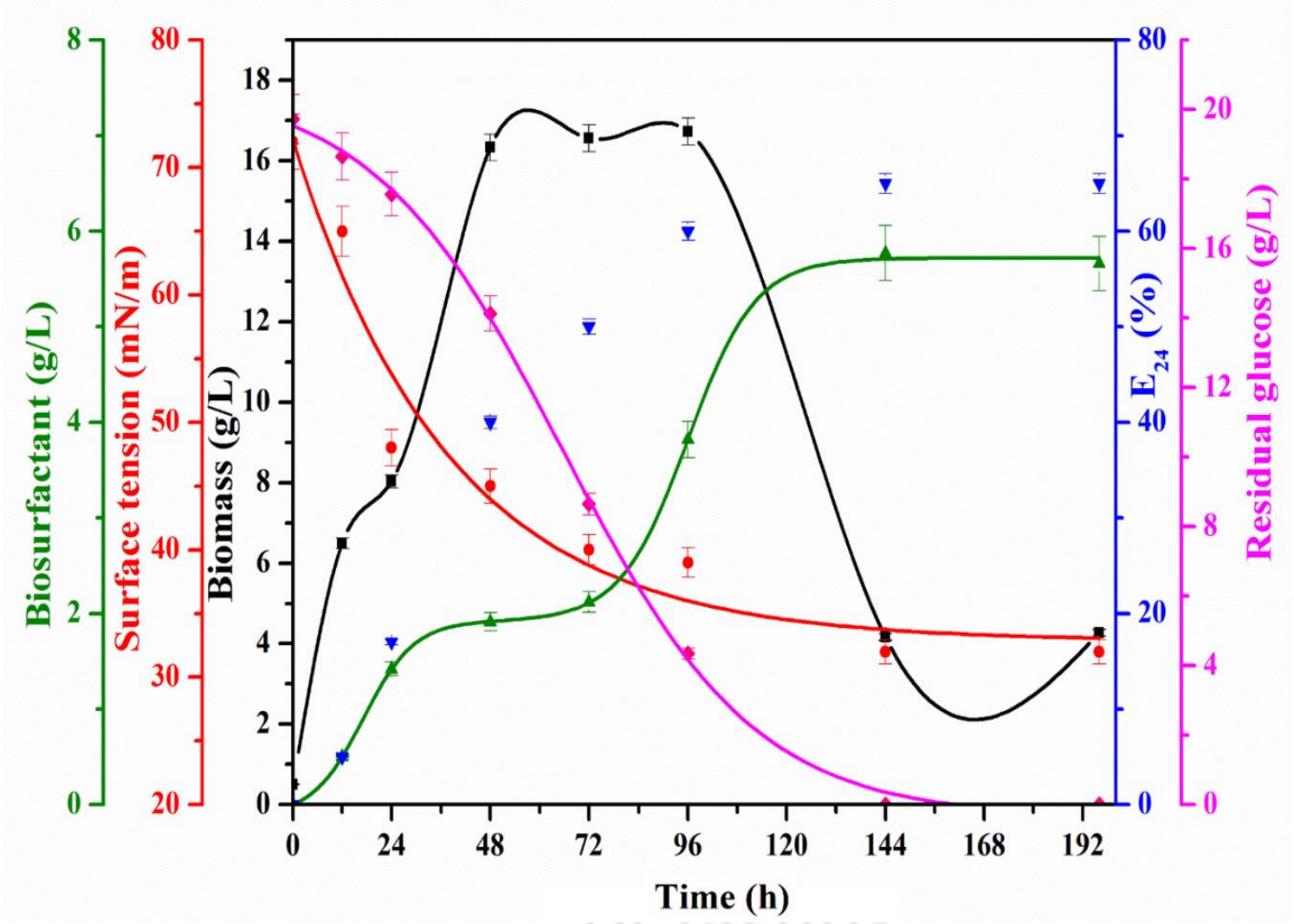

Figure 3.2. Biomass growth, biosurfactant, surface tension, residual glucose and E_{24} profile under optimized conditions of pH 6 and 30 °C using 2:1 ratio of glucose: yeast extract in BH medium

Table 3.3. A summarized literature of biosurfactant production utilizing oil-based C sources

Bacteria	Substrate	Biosurfactant type	Biosurfactant yield (g/L)	E_{24} %	Surface tension (mN/m)	Ref.
Agrobacterium fabrum SLAJ731	Glucose	Lipopeptide	5.77	65	32	Present study
	Crude oil	Lipopeptide	4.15			
Lysinibacillus sphaericus IITR51	Glycerol	Rhamnolipid	1.6	48	52	(Gaur et al., 2019)
Bacillus subtilis MG495086	Light-paraffin oil	Surfactin	6.3	72.5	29.9	(Datta et al., 2018)
Serratia marcescens	Glycerol	NA	1.4	NA	28.4	(Almansoory et al., 2017)
Brevibacillus sp. AVN 13	Used engine oil	Lipopeptide	1.3	72	36	(Vigneshwaran et al., 2018)
Bacillus pumilus 2IR	Glucose and crude oil	Lipopeptide	1.1	NA	34	(Fooladi et al., 2018)
Staphylococcus capitis	Diesel oil	Lipopeptide	0.1	NA	39.9	(Chebbi et al., 2018)
Bacillus cereus SNAU01	Peanut oil cak	Lipopeptide	NA	65	NA	(Nalini et al., 2016)
Pseudomonas aeruginosa KVD-HR42	Karanja oil	Rhamnolipid	5.9	NA	30.1	(Deepika et al., 2016)
Pseudomonas cepacia	Soybean waste frying oil	Rhamnolipid	5.2	NA	29.8	(e Silva et al., 2014)
Acinetobacter junii B6	Iranian light crude oil	Glycolipid	NA	51	38	(Ohadi et al., 2017)
Pseudomonas cepacia CCT6659	Waste frying oil	Rhamnolipid	8	90	25	(Rita de Cássia et al., 2017)
Brevibacterium luteolum	Mineral oil	Lipopeptide	NA	NA	27	(Unás et al., 2018)
Streptomyces sp. DPUA1566	Soybean waste frying oil	Lipopeptide	1.9	NA	28	(Santos et al., 2019)

3.3.2. Characterization of the produced biosurfactant

Based on the different functional groups present in the crude biosurfactant, its chemical nature was investigated in **Figure 3.3(A)**. **Table 3.4** lists the various spectra peak positions and their functional group's assignment for the crude biosurfactant. Similar peaks were observed in reported literature for lipopeptide biosurfactants. These characteristic peaks indicated the produced biosurfactant to be lipopeptide in nature (Nalini et al., 2016).

Table 3.4. List of major FTIR spectra peaks and their assignment for crude biosurfactant

Peak position (cm^{-1})	**Functional group assignment**	**Ref**
3442	Aliphatic primary amine (-NH)	(Rayeni and Nezhad, 2018)
1717	Amine group	(Bao et al., 2014)
1645	Fatty acid linkage (-C=O-NH)	(Khopade et al., 2012)
2933-2853	Aliphatic –CH group of the long fatty acid chains	(Kiran et al., 2017)
1465-1387		

Similarly, the NMR analysis showed the presence of peaks at position δ = 7.1-7.5, signifying the C=O-NH signals of the peptide moiety bonding with the fatty acid chain. Likewise, the peaks at chemical shift δ = 2.1-2.5 represented the $CH_2C=O$ as a bond, in **Figure 3.3(B).** These peaks are similar to peaks reported for the lipopeptide nature of biosurfactants (Datta et al., 2018). Hence the biosurfactant produced by *A. fabrum* SLAJ731 was classified as lipopeptide in nature. The molecular weight spectrum suggested the presence of fragmentation ions for $C_{12}[M + H]^+$ (m/z = 994) and $C_{13}[M + H]^+$ (m/z = 1008) surfactin isomers, as shown in **Figure 3.3(C).** The m/z 976, 863 and 685 represented C_{12} isomer in the fragmentation ions of $[M - 18 + H]^+$, $[M - (Leu/Ile + 18) + H]^+$ and $[(H)\ Leu/Ile - Leu/Ile\ (OH) + H]^+$, respectively (Tang et al., 2010). In addition, peaks at 781, 667 and 567 corresponded to $[M+H-Asp]^+$, $[M+H - Val]^+$ and $[M+H-Leu]^+$, respectively. The actual fragmentation was observed as 894⟶781⟶667⟶567⟶454⟶341⟶113, as reported by Chen et al. for the C_{13} surfactin isomer (Chen et al., 2017). Similarly, CMC of crude biosurfactant was obtained as the point of inflection at

the lowest concentration at which the surface tension of water reached its minimum value. The produced lipopeptide showed a CMC of 650 ± 10 mg/L, reducing surface tension from 72 mN/m to 34 ± 0.5 mN/m **(Figure 3.3(C)).** Similar results have been reported in the literature, exhibiting present lipopeptide has a decent CMC value (Santos et al., 2019).

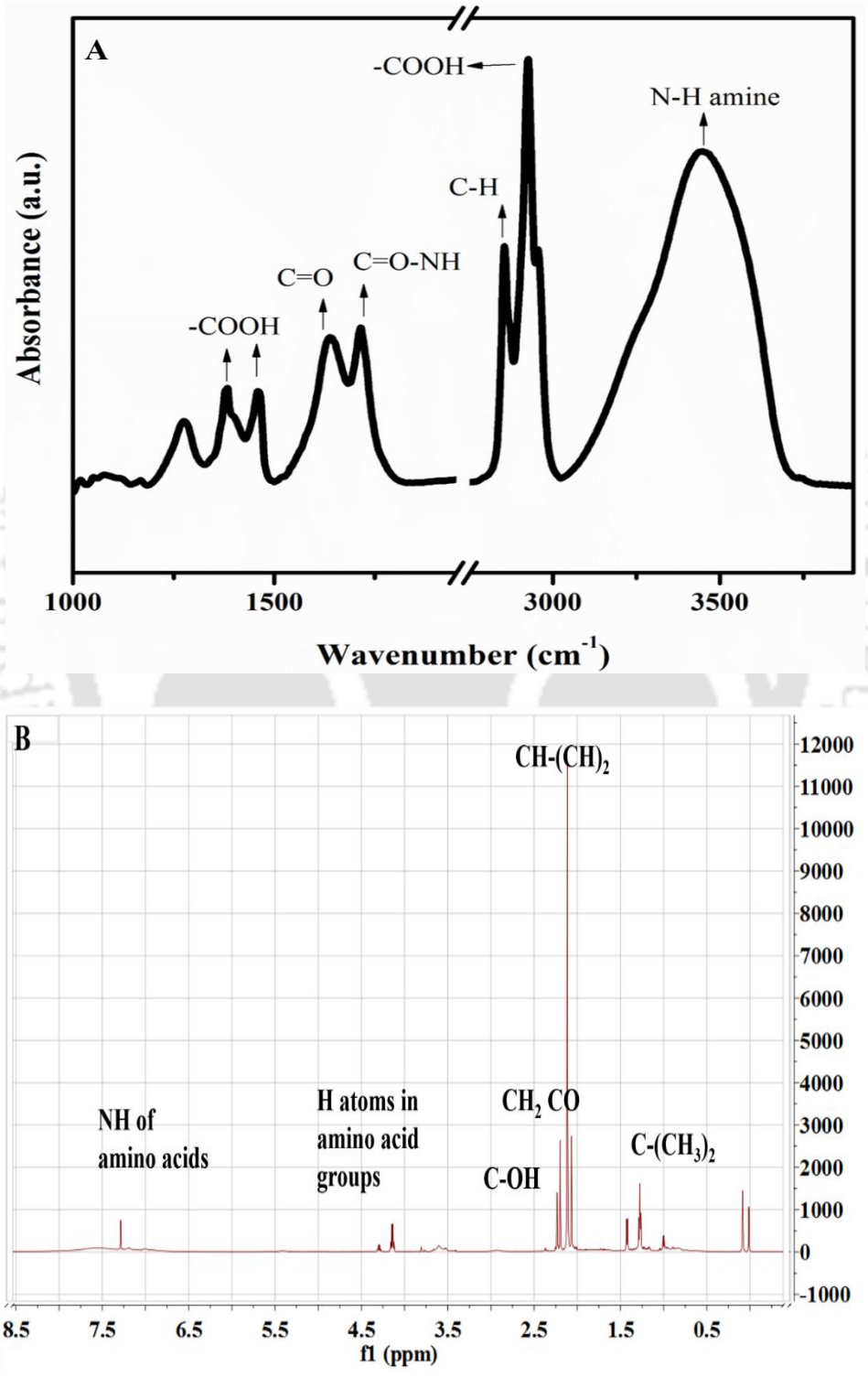

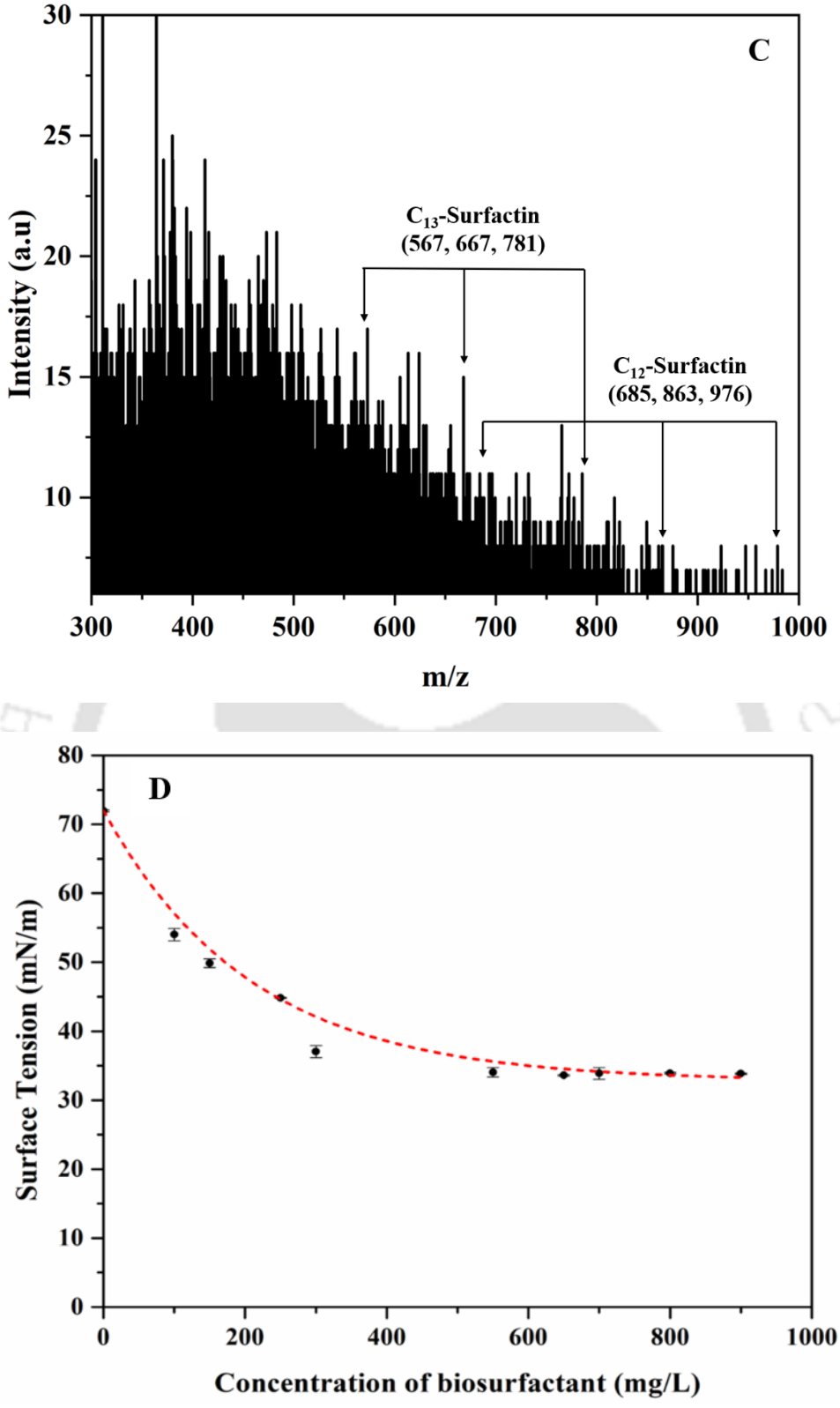

Figure 3.3. Characterization analyses of crude biosurfactant using (A) FTIR, (B) ^{1}H NMR spectroscopy (C) LC-MS analysis, and (D) Surface tension measurement for CMC determination. The functional group analyses confirmed the lipopeptide nature of biosurfactant

3.3.3. Biodegradation analysis of crude oil

The crude oil biodegradation ability of *A. fabrum* under optimized experimental parameters was explored. The experimental setups were (A) crude oil supplemented under optimized experimental parameters, (B) control-1: crude oil under optimized experimental parameters without glucose (sub-optimal condition) and (C) control-2: with no inoculum under optimized experimental parameters without glucose (abiotic), as mentioned in **Table 3.1.** As shown in **Figure 3.4(A)** and **(B)**, it was observed that sets (A) and (B) followed a similar growth pattern; however, the specific growth rate was ~1.7 folds higher for the set (A) (μ=0.1 ± 0.04 h^{-1}) as compared to set (B) (μ=0.06 ± 0.01 h^{-1}). Upon completion of 144 h, the residual oil and produced biosurfactant in the supernatant were examined using gravimetric and chromatographic methods. These studies were carried out with an abiotic sample taken as control. Similarly, the change in the organic content of the culture after biological treatment was assessed using COD measurement. It was observed that a complete reduction in the COD value from initial value of 2131 ± 2.3 and 1066 ± 1.6 mg/L was obtained for set up A, crude oil supplemented with a co-substrate, glucose and B, only crude oil after bacterial biodegradation.

In order to study the kinetics of substrate (crude oil) utilization and product (biosurfactant) formation, the samples were taken at a regular interval of 24 h. The residual crude oil and the produced biosurfactant in the culture were estimated by n-hexane extraction and ethyl acetate extraction methods. The crude oil degradation rate was higher in the presence of glucose (0.004 ± 0.001 g/L/h) as compared to its absence (0.002 ± 0.001 g/L/h), as shown in **Figure 3.4**. The overall degradation of crude oil was obtained as 58 ± 5% in the presence of glucose and 40 ± 4 % in its absence. Similarly, after 6 days of incubation, the biosurfactant yield was obtained as 2.5 ± 0.5 g/L in the absence of glucose, which was enhanced to 4.15 ± 0.2 g/L in the presence of glucose.

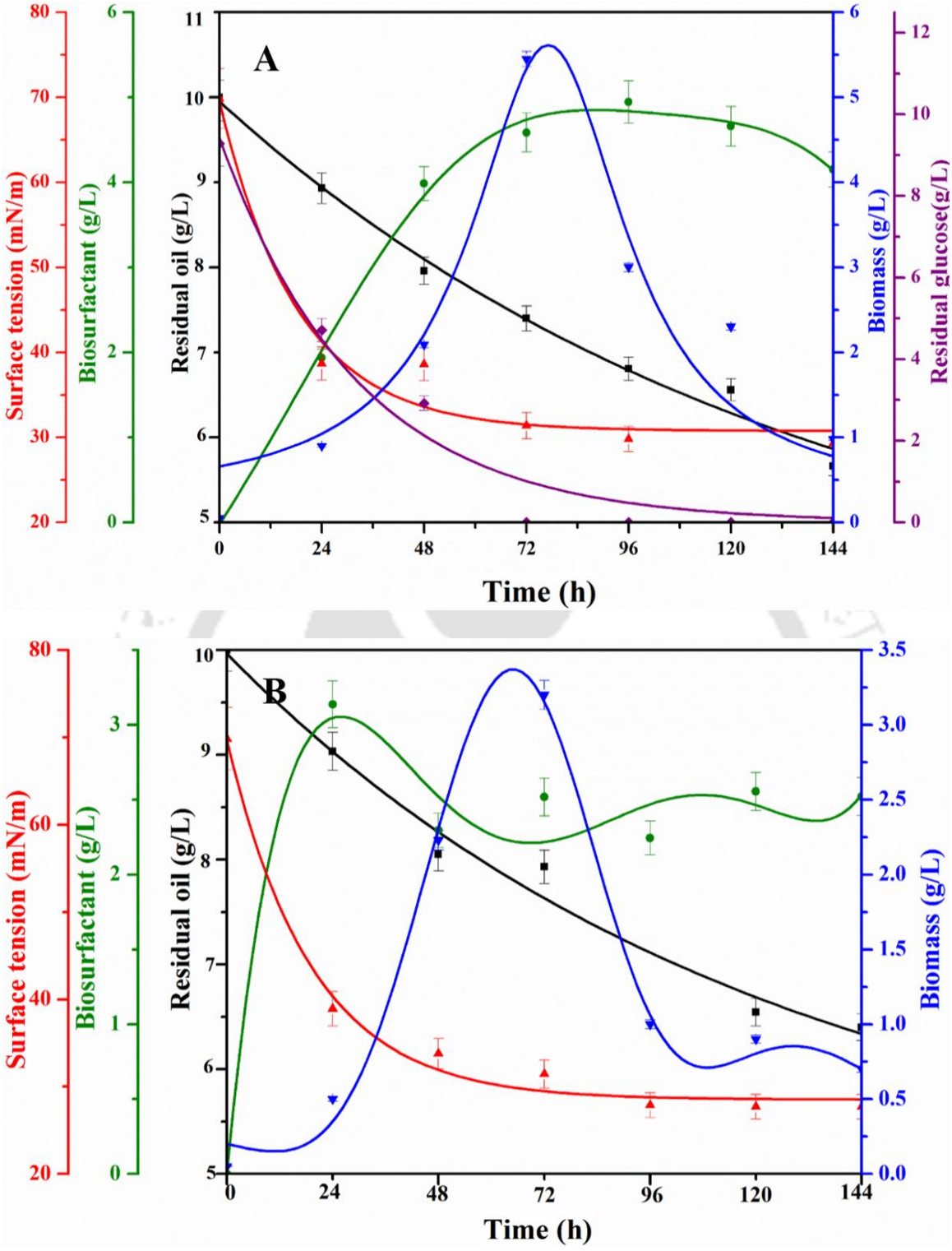

Figure 3.4. Biomass growth, biosurfactant, surface tension, residual glucose and crude oil degradation profile under optimized conditions with (A) 1 % glucose supplemented with 1 % crude oil in BH medium (B) Control: only 1 % crude oil

An FTIR analysis of the residual crude oil was performed to analyze the degradation further. **Figure 3.5** shows the change in peak area in the range of 2200-400 cm^{-1}. Peaks at 1465 cm^{-1}, 1450 cm^{-1}, and 1375 cm^{-1} suggest a -CH_2 group and a -CH_3 group of alkanes, respectively. A peak at 1601 cm^{-1} shows the presence of C=C bonds of aromatic groups, and peaks at 880 cm^{-1}, 830 cm^{-1}, and 742 cm^{-1} indicate the presence of aromatics out of a plane, *i.e.*, "oop" bonds of the residual crude oil. Upon comparing the peak area of the mentioned peaks, the overall decrease was the highest in the presence of glucose, i.e., about 65 %, which agreed with gravimetric analysis.

The GC-MS analysis of residual crude oil was also studied based on a peak area (intensity) reduction as tabulated in **Table 3.5.** Based on reported literature, the aliphatic hydrocarbons were assigned as mass to charge ratio of ((m/z) 57, 71, 141) and aromatic hydrocarbon were represented by m/z=155, 156, 169, 170, 193, 207. The oil degradation represented as a decrease in peak intensity was found to be maximum in glucose as co-substrate.

Table 3.5. Comparison of degradation of crude oil based on major peaks obtained in GC mass spectroscopy

m/z values	Abiotic (Relative peak area)	With Glucose (Relative peak area)	Without Glucose (Relative peak area)	Potential hydrocarbons (Nicolescu, 2017; Pavlova and Papazova, 2003)
57.09	69973196	41182613	78065789	C_4H_9 •, C_2H_5–CO•
57.09	125993034	9377268	13484307	
57.09	94018675	4620738	12645811	
71.1	36334662	20418554	41127582	C_5H_{11} •; C_3H_7–CO•
71.1	86930680	1.44E+08	1.39E+08	
71.1	36000612	16944259	36984645	
155.12	58081211	8689569	0	C_6H_5 = C_6H_5 + •
155.12	38740650	8466431	0	
156.13	39326048	23212930	44422321	C_2-Naphthalenes
156.13	48945095	15757929	56498782	
169.12	37245806	4882136	35661249	C_3-Naphthalenes
169.12	33824212	8490820	18552434	
170.16	68845816	21264980	63239168	
193.12	31715735	21270316	36633184	C_1-Phenanthrenes
207.13	31349933	4624913		C_2-Phenanthrenes

The changes in peak intensity are attributed to the breakdown of compounds into their subsequent subunits. The GC-MS analysis showed 47 % degradation of aliphatic hydrocarbons (m/z = 57, 71, 141) (Nicolescu, 2017) and a 70 % decrease in aromatic hydrocarbon (m/z=155, 156, 169, 170, 193, 207) contents (Pavlova and Papazova, 2003) in the presence of co-substrate glucose, however, in the absence of any co-substrate, the decrease in aliphatic and aromatic compositions was obtained as 27 % and 34 %, respectively relative to abiotic. Hence, the chromatogram based peak area analysis revealed that

microbial consumption of crude oil components occurred more effectively in the presence of glucose than in its absence. The reduction in the total peak area of the crude oil incubated in the presence of glucose was about 58 %, which also complemented the FTIR and gravimetric analyses. Conclusively, based on the gravimetric and spectroscopic analyses, it was established that the natural degradation of oil components was lesser than microbial biodegradation. However, the present *Agrobacterium* strain showed comparatively better degradation in the presence of glucose (optimized C source). Hence, the presence of glucose intensified the biodegradation ability of oil by the present strain. Similar results have been reported in literature stating that the presence of glucose increases crude oil degradation (Farag et al., 2018; Jeroh et al., 2011; Khan et al., 2006). However, scant attention has been paid to the mechanism involved, and hence the bottleneck remains. Hence, this study gives an insight into the relationship involved in biosurfactant production and oil degradation in the presence of glucose.

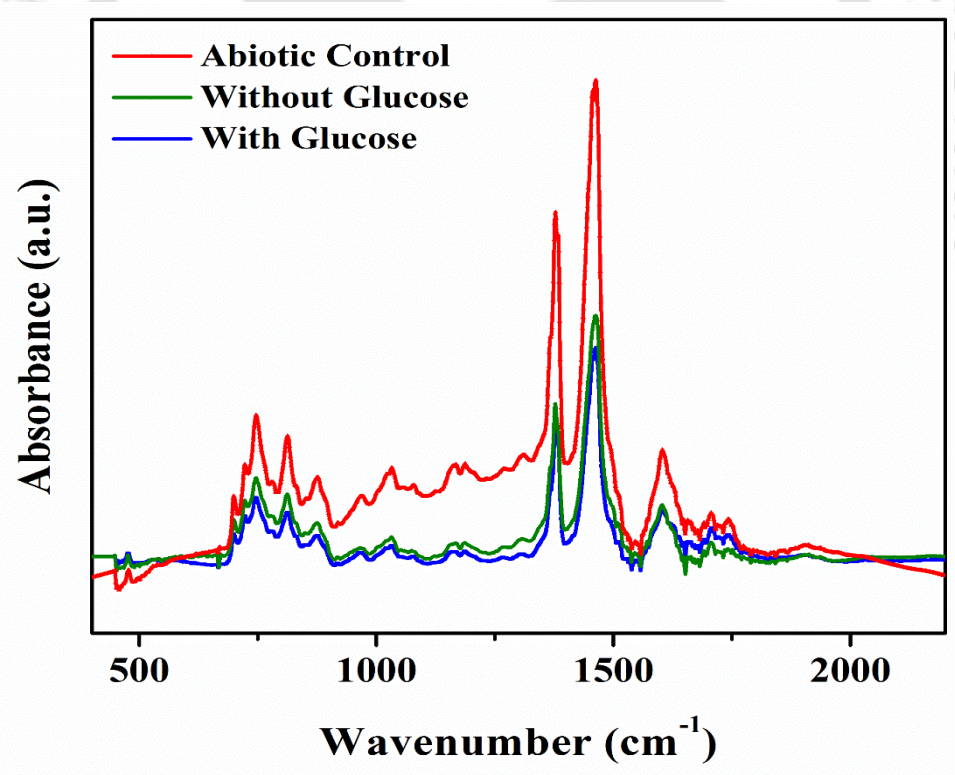

Figure 3.5. FTIR analysis of residual crude oil signifying the reduction in peaks due to biodegradation presence and absence of glucose compared to the abiotic loss

3.3.4. Relation between biosurfactant production and crude oil degradation

In order to understand the effect of glucose in the degradation of crude oil, a graph of biosurfactant production with oil degradation was plotted. From **Figure 3.6**, it was anticipated that biosurfactant production enhanced significantly ($p < 0.05$) in the presence of glucose. Even though there was lesser biosurfactant production in the initial 48 h, which could be due to the utilization of available glucose as a C source; however, with the depletion of glucose in the media, subsequent enhanced biosurfactant production crude oil utilization was observed. On the other hand, in the control containing only crude oil, no significant change ($p > 0.07$) in biosurfactant production was observed with a change in oil degradation. It revealed a breakthrough, *i.e.*, glucose significantly enhances biosurfactant production and crude oil degradation.

Biosurfactants are natural emulsifying tools produced by bacteria using polar and non-polar substrates. A general lipopeptide biosurfactant production involves a 5 staged process: (1) Glycolysis of substrate for the biosynthesis of acetyl CoA; (2) Amino acid biosynthesis; (3) TCA cycle; (4) Biosynthesis of fatty acids; and (5) Amino acid-lipid bio-assembly (Sharma et al., 2022). Thus, the presence of Glucose as simple sugar acted as catalysing agent in the biosurfactant production, improving the crude oil emulsification and hence overall biodegradation. However, biosurfactant is not the sole factor involved in oil degradation. Hence, we further explored the role of the AH enzyme.

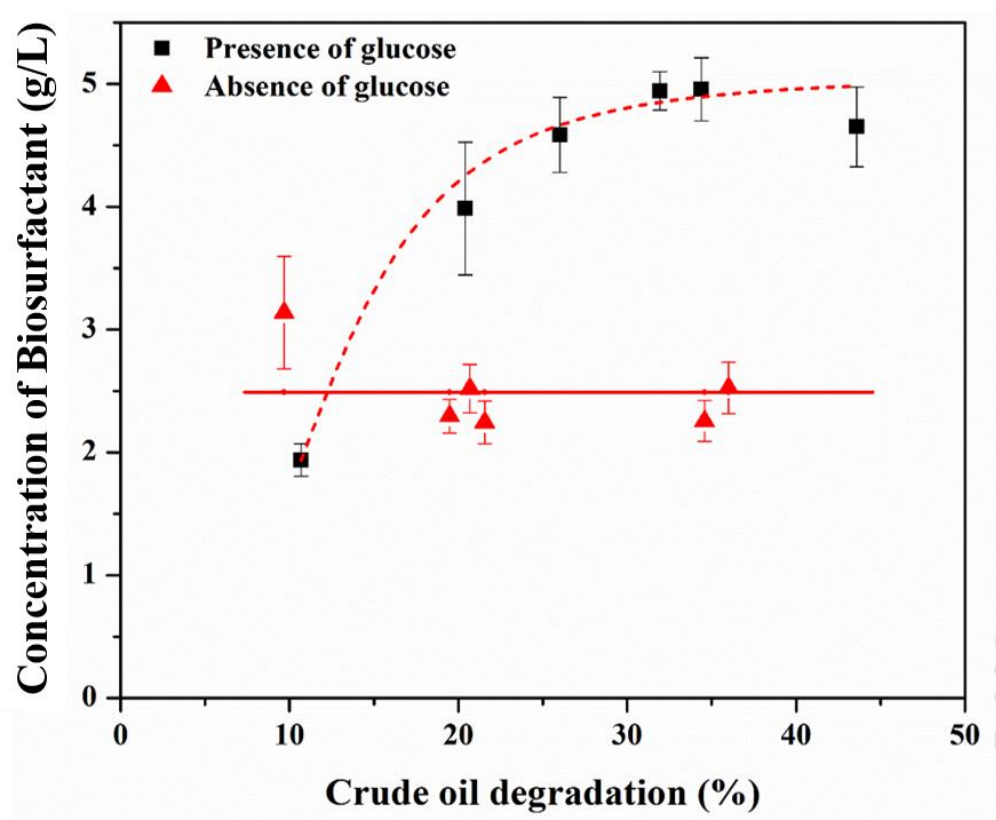

Figure 3.6. Study of the effect of crude oil biodegradation efficiency with bacterial biosurfactant production in the presence and absence of co-substrate: glucose

3.3.5. Determination of alkane hydroxylase activity

The principal cause for microbial degradation of crude oil components is the activity of degradative enzymes. Jurelevicius et al have also reported the presence of alkB gene responsible for AH enzyme in *Agrobacterium* genus (Jurelevicius et al., 2013). To analyze the biodegradation ability of the present strain, AH was focused. The present strain synthesized AH both extracellularly (eAH) and intracellularly (iAH). The activity of AH is regulated by the presence of 'C' substrate in the media. Hence, we performed a comparative study on the effect of glucose-supplemented crude oil on the activity of AH.

It was observed that in the presence of glucose, the AH enzyme activity remained active both extracellularly and intracellularly. However, the maximum enzyme activity was observed at 72-96 h of incubation, with an iAH enzyme activity of 9 ± 0.1 U/mL and eAH enzyme activity of 4.5 ± 0.02 U/mL. In contrast, in the absence of glucose, the maximum extracellular enzyme activity was found at day 1,

i.e., 4.0 ± 0.1 U/mL (which decreased gradually afterward), whereas the maximum intracellular activity was observed at day 2 (3.4 ± 0.2 U/mL). Interestingly, the presence of glucose enhanced the overall extracellular AH activity. It was anticipated that it was due to the availability of cofactor (NADH) regeneration system during the catabolism of glucose to gluconic acid, as also supported in the literature (Iyer and Rajkumar, 2019). The substrate continuously provided NADH for the effective activity of extracellular expressed AH. Furthermore, we observed that constitutive expression of both intracellular and extracellular AH activity was required for better degradation of crude oil, as experienced in the presence of glucose than its absence.

3.3.6. Relationship between AH and oil degradation and biosurfactant production

To understand the cause of oil degradation in the presence of glucose, we studied the enzyme activity of eAH hydroxylase, one of the key enzymes in the hydrocarbon degradation pathway. From **Figure 3.7(A),** it was inferred that eAH activity initially increased significantly ($p < 0.01$) with an increase in the oil degradation ability, signifying that the oil degradation ability of *A. fabrum* is regulated by the activity of eAH. However, no significant change ($p > 0.12$) in the activity of eAH in control (containing only crude oil) suggested that the presence of glucose enhanced the activity of eAH. It could be explained in terms of depletion of the cofactor, NADH. Furthermore, eAH activity was also responsible for the production of biosurfactants. It was observed that the AH activity increased with an increase in biosurfactant, as shown in **Figure 3.7(B).** Summarily, the presence of glucose showed an overall enhancement in the activity of eAH, which in turn uplifted the biosurfactant production and crude oil degradation compared to control.

Similarly, it was observed that the iAH activity got upregulated by ~ 2 folds in the presence of glucose with crude oil (9.0 U/mL) than the control (3.4 U/mL). Interestingly, the expression of iAH enhanced the biosurfactant production, as shown in **Figure 3.7(C).** However, the decrement in intracellular activity occurred as the cells reached their death phase. In the absence of glucose, biosurfactant production was independent of iAH activity preassembly due to the lower activity of iAH. The iAH activity showed a similar trend for crude oil degradation in the presence and absence of glucose (data not shown). It revealed that both iAH and eAH regulated the biosurfactant production ability of the

present strain. Summarily we hypothesized that a suitable co-substrate such as glucose aided the balance of redox potential, which upregulated the biosurfactant production pathway and hydrocarbon degradation pathway.

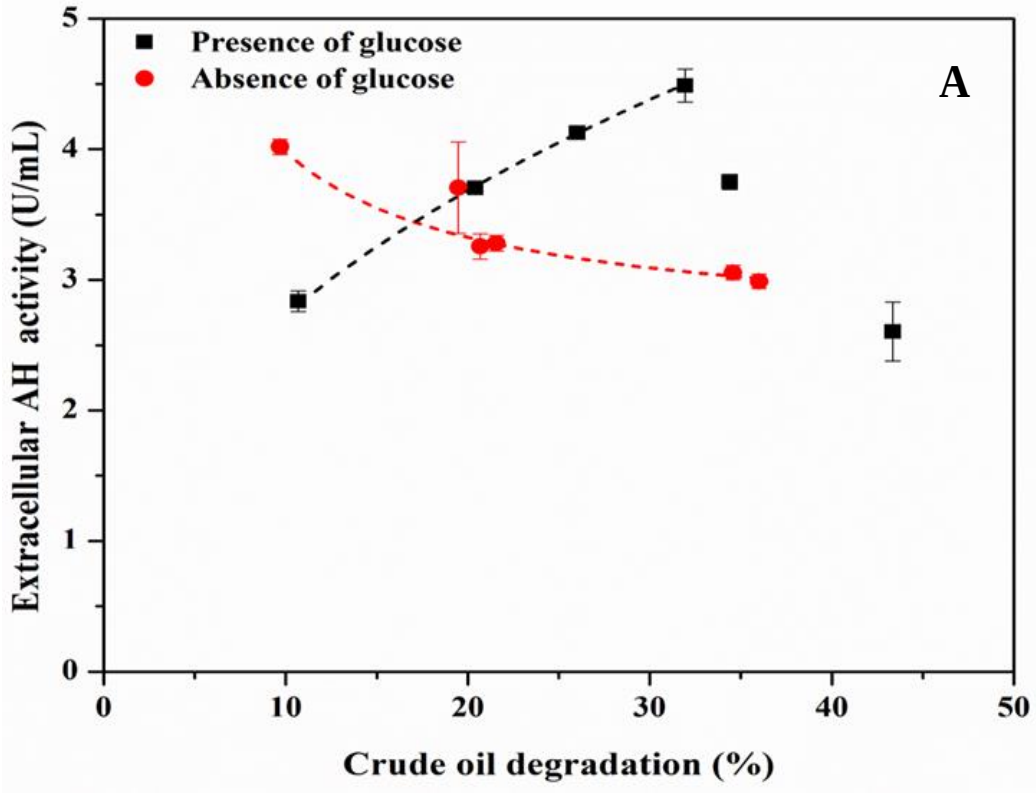

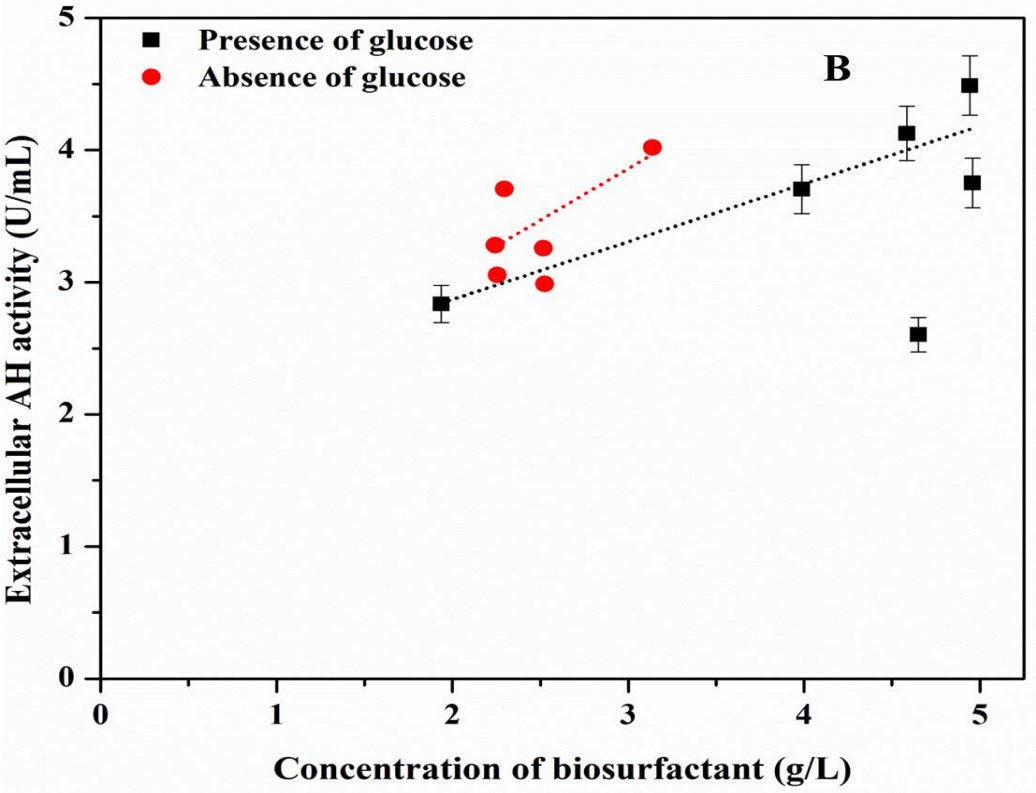

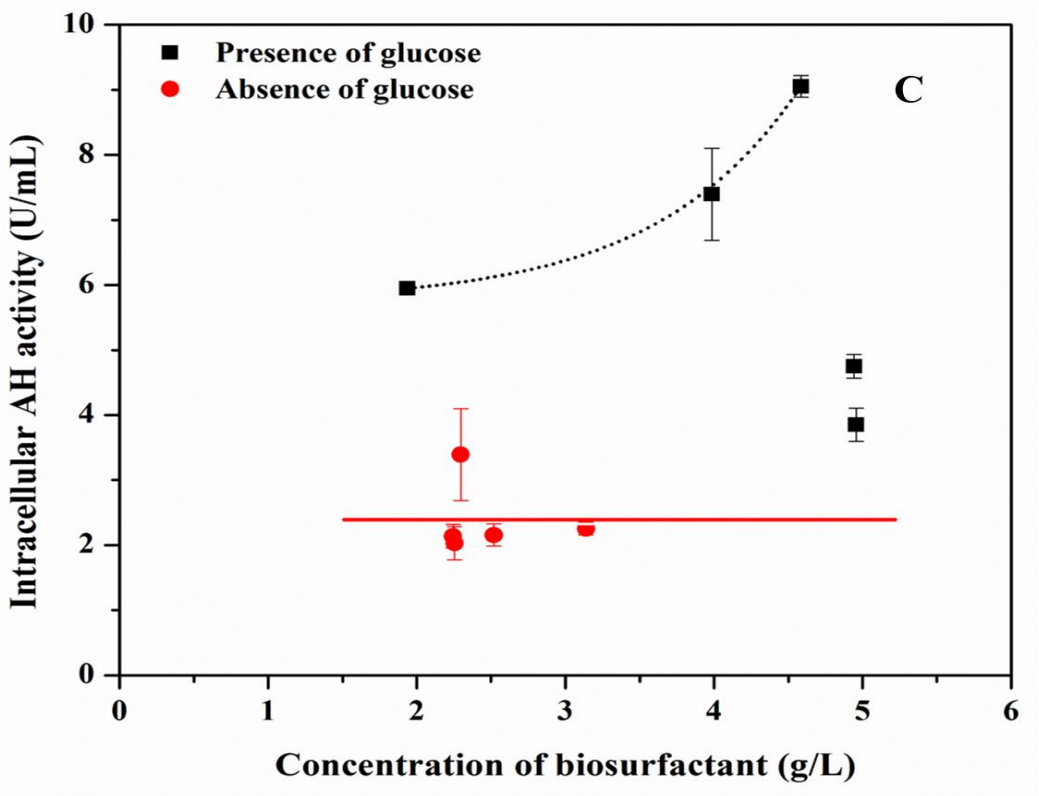

Figure 3.7. Study of the effect of (A) extracellular Alkane hydroxylase (eAH) activity on crude oil biodegradation; (B) extracellular Alkane hydroxylase (eAH) activity on biosurfactant production; and (C) intracellular Alkane hydroxylase (iAH) activity on biosurfactant production

3.4. Conclusions

In this study, *Agrobacterium fabrum* is explored for its ability to produce biosurfactants and biodegrade crude oil. Screening experiments such as oil displacement assay, drop collapse test and E_{24} confirmed the biosurfactant production ability of the present bacterium. Further, optimization studies revealed that the mesophilic strain showed the maximum biosurfactant production of 5.77 ± 0.3 g/L at pH 6 and 30 °C using glucose and yeast extract at a C: N ratio 2:1. The strain was also found to degrade crude oil by synthesizing AH. The bacteria showed an enhanced biosurfactant production in the presence of co-substrate glucose. Similarly, the bacterium showed augmented crude oil biodegradation of 58 ± 5 % within 6 days of incubation in the presence of glucose. The crude oil degradation was further confirmed by investigating the regulation of the AH enzyme activity. Upon supplementing with crude oil, glucose uplifted the biodegradative metabolism and the biosurfactant production by enhancing the AH activity. Moreover, it was revealed that cofactor availability was the major driving force responsible for the overall metabolism. These outcomes suggest glucose-rich feedstock can be used as a C source to augment crude oil biodegradation. The obtained results postulate the suitability of the present strain in the field of enhanced oil recovery, bioremediation, biodegradation and other industrial purposes.

Chapter 4

Biosurfactant mediated crude oil biodegradation by isolated *Bacillus subtilis* RSL 2

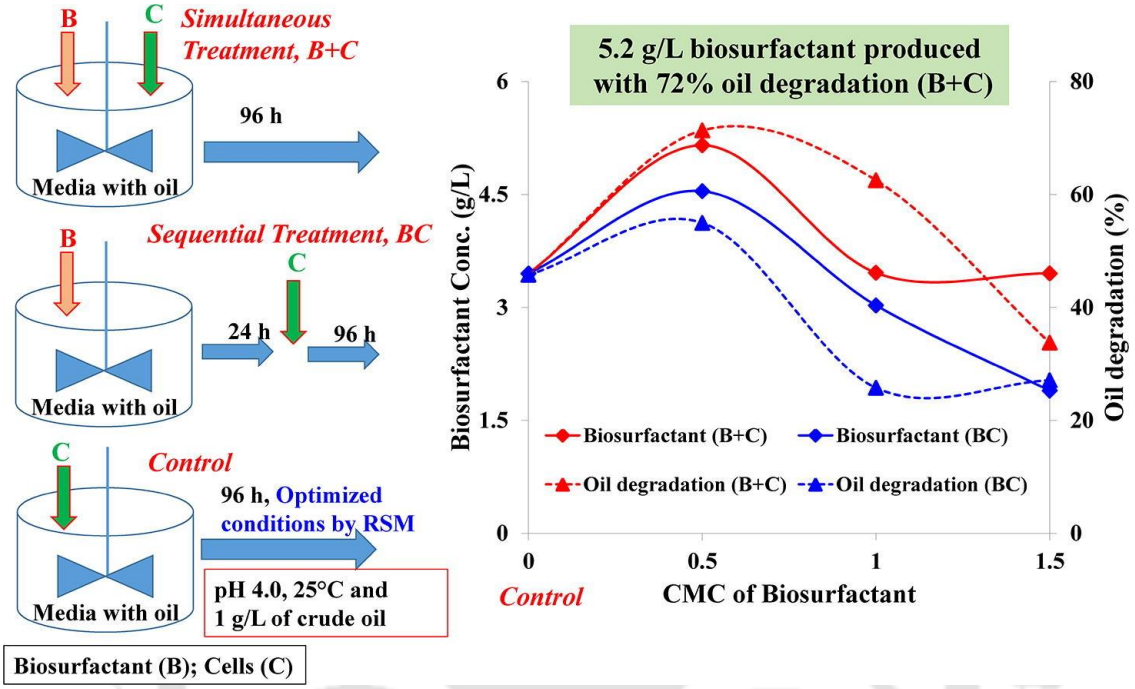

(Bioresource technology 307, 123261, 2020 (Sharma et al., 2020))

This Chapter discusses the effect of biosurfactant as stimulant in crude oil bioremediation. Isolated oil-degrading strain, *Bacillus subtilis* RSL 2 was optimized for the maximum oil degradation and biosurfactant production using Response surface methodology. The produced biosurfactant was characterized and investigated for its effect on microbial oil degradation in two modes (a) sequential (BC) and (b) simultaneous (B+C) inoculation. The study aimed to explore the surface activity of crude biosurfactant in alteration in surface wettability of a hydrophobic substrate (crude oil) making it more bioavailable for biodegradation activities of oil-contaminated sites.

4.1. Introduction

In the previous Chapter 3, the need to optimize bacterial growth conditions for maximizing biosurfactant production to achieve effective crude oil biodegradation ability has been elaborated. This Chapter puts forward crude biosurfactant as an inherent bio stimulating tool for mediating the bacterial crude oil biodegradation. Biosurfactant is a growth-associated metabolite produced by microbes during their oil utilization phase. It is established that microbes apply this metabolite as a tool to emulsify the heavy chains of crude oil to make it more bioavailable for effective utilization (Akbari et al., 2018). Various researchers have worked on this line to improve the production of biosurfactants to achieve a higher degradation of spilled crude oil (Patowary et al., 2018). Biosurfactants known to emulsify crude oil majorly effectively comprise isoforms of Lipopeptides and Rhamnolipids (Bai et al., 2017; Datta et al., 2018; Lin et al., 2017; Sharma et al., 2019; Sharma et al., 2019). However, commercially available synthetic surfactants are more favored for oil degradation due to their high efficiency (Jin et al., 2019; Kaczorek and Olszanowski, 2011). To date, very scarce literature certifies the use of biosurfactants in oil-contaminated sites (Saravanan et al., 2020; Sharma et al., 2020). Hence, a deeper insight is required to improve biosurfactant-mediated crude oil biodegradation effectiveness.

In this direction, an attempt has been made towards an amalgamated biosurfactant-assisted microbial oil biodegradation approach. Inherent oil degraders were isolated and optimized for maximum biosurfactant production. Further, to unveil the role of biosurfactants in oil utilization, the produced biosurfactant was supplemented with crude oil in varying concentrations, and resultant effects on microbial oil degradation were investigated.

4.2. Materials and methods

4.2.1. Chemicals and reagents

Crude oil contaminated sludge samples were obtained from IOCL, Noonmati, Assam in sterile sampling bottles and stored at 4°C till further use. The chemicals and reagents with their source information have been mentioned in previous chapters. The remaining chemicals are Ammonium nitrate (101188), Ammonium sulfate (101217), Urea (108486), and Iron nitrate hydrated (103883) were purchased from Merck, India. Diidomethane (RM2766) was purchased from Himedia, India.

4.2.2. Isolation and screening of bacterial isolates

Local sludge samples were initially enriched in LB broth. These enriched bacteria were incubated in BH media with 1 % (*v/v*) crude oil as the only carbon source for a week. Further, single colony isolation was performed using the conventional serial dilution technique in sterile phosphate bovine serum (PBS, pH 7.4) followed by streak- plate technique using 1 % crude oil-enriched BH agar. Isolated single colonies were inoculated in sterile BH media with 1 % (*v/v*) crude oil as sole carbon source and incubated at 37 °C, 180 rpm for 24 h. The obtained isolates were screened based on surface-active properties, i.e., emulsification activity (E_{24}) and oil displacement activity, as stated in Chapter 3, section 3.2.2. Further, the isolates were also analyzed for decreased surface tension using Tensiometer, as stated in Chapter 3, section 3.2.4.2.

4.2.3. Identification of selected isolates

Based on the preliminary screening results, the selected isolates were further studied for the genomic DNA (gDNA) isolation procedure provided in the Himedia HiPurA bacterial gDNA purification kit (MB505-50PR) protocol. The obtained gDNA was amplified using universal primers 27F (forward primer) and 1492R (reverse primer). Europhins, India, performed the 16S rRNA sequencing. Further, the obtained sequences were compared with the Basic Local Alignment Search Tool (BLAST), and the phylogenetic tree was constructed using National Center for Biotechnology Information (NCBI) neighbor-joining tree construction and analysis tools (Datta et al., 2018; Mehetre et al., 2019).

4.2.4. Optimization of nitrogen source

The optimal strain was selected for further optimization studies among the isolated strains. In this regard, firstly suitable nitrogen source (1 %, *w/v*) was scrutinized in the presence of 1% crude oil as the sole carbon source at pH 7.0 and 37°C in sterile BH media. Different nitrogen (N) sources included yeast extract, ammonium nitrate, ammonium sulfate, urea, and iron nitrate. The growth of strain was examined by measuring optical density (O.D.) at 600 nm using a spectrophotometer (Cary 100 UV–vis spectrophotometer) for every 24 h up to 7 days (Datta et al., 2018). Based on the increased turbidity of culture media, biomass growth was estimated, and the optimum N source was selected. Furthermore,

the concentration of the selected nitrogen source was also optimized by varying its concentration from 0.5 % to 2 % (*w/v*) at pH 7.0 at 37°C for 7 days. After incubation, the biomass growth was also analyzed in terms of dry cell weight and biosurfactant production was studied in terms of surface tension reduction of cell-free supernatant, as mentioned in Chapter 3, section 3.2.4.2.

4.2.5. Optimization of culture conditions

Optimization of bacterial culture conditions was performed to understand the interaction among various culture conditions to maximize the overall crude oil degradation and biosurfactant production using an empirical technique, Response surface Methodology – Central Composite Design (RSM-CCD) tool (Design Expert, version 7.0) statistical tool, as discussed in Chapter 2, section 2.5.2.4.2. In this design, we studied the effect of three independent variables (pH, temperature and crude oil concentration) to explore the probable interaction among them for the maximum biosurfactant production. In this regard, biosurfactant concentration was considered to be the response output. The range studied for independent variable pH, temperature, and crude oil concentration were 4.0 to 8.0, 25-45°C, and 1-5 g/L, respectively. A set of 20 experiments were suggested, and the experiments were performed at the mentioned conditions for 7 days in sterile BH media with an optimized N source. At the end of incubation, cultures were centrifuged and obtained cell-free supernatant was further analyzed for biosurfactant concentration (Response parameter).

4.2.6. Estimation of produced biosurfactant

After the incubation period, the cells were harvested and solvent extracted as reported in section 3.2.4 (Gudiña et al., 2015; Sharma et al., 2019; Sharma et al., 2019). Thus, obtained biosurfactant was weighed gravimetrically and stored at room temperature for further characterizations. Henceforth, the obtained biosurfactant concentrations were incorporated in the Design-Expert software modeled with RSM-CCD tools. The data were examined using a two-way analysis of variance (ANOVA) to obtain the optimized culture conditions.

4.2.7. Estimation of residual crude oil

The cells were harvested upon incubation, and the cell-free broth was analyzed to estimate residual crude oil and COD as mentioned in Chapter 3, section 3.2.5.

4.2.8. Study of biosurfactant production utilizing crude oil under optimized conditions

The selected strain was incubated at thus optimized pH, temperature and crude oil concentration to analyze its degradation and biosurfactant production ability. The strain's oil consumption ability and growth characteristics were analyzed based on biomass, surface tension, residual oil, and extracellularly released biosurfactant every 24 h till 7 days. Briefly, each day samples were centrifuged at 8000 rpm and 4°C for 10 min. The obtained pellet was utilized for biomass and enzyme alkane hydroxylase (AH) assay. AH is responsible for the oxidation of alkane hydrocarbons to their alcoholic derivatives using NADH as a cofactor. The cell-free supernatant was studied for surface tension measurement, biosurfactant production (Chapter 3, section 3.2.4) and residual crude oil estimation (Chapter 3, section 3.2.5) (Sharma et al., 2019).

4.2.9. Estimation of Alkane Hydroxylase Activity

The intracellular alkane hydroxylase activity was spectrophotometrically estimated using the protocol mentioned in Chapter 3, section 3.2.6.

4.2.10. Biosurfactant characterization studies

The crude biosurfactant extracted using solvent extraction and evaporation was further characterized by analyzing the chemical functional groups using Fourier transform spectrophotometer, attenuated total reflectance (Make: Perkin-Elmer Spectrum Two) ATR- FTIR mode (4000-400 cm^{-1}). The molecular weight of the crude biosurfactant was estimated using Matrix-assisted laser desorption ionization time-of-flight mass spectrometry (MALDI-TOF-MS) analyses (Sharma et al., 2022). In addition, the Du-Nouy Ring method in Tensiometer was opted to determine inflation point of surface tension reduction with increase in biosurfactant concentration (CMC), as mentioned in Chapter 3, section 3.2.4.2. The crude biosurfactant was further analyzed for its surface wettability based on water

contact angle measurement at 25°C and 1 atm on the Goniometer (Make: HOLMARC) (Datta et al., 2018). Surface energy (γ_{ij}) is other key parameter that determines the intermolecular forces present at the solid-liquid interfaces. It is calculated using equation as stated below

$$\boldsymbol{\gamma_{ij} = \gamma_i + \gamma_j + 2\theta[(\gamma_i^d \gamma_j^d)^{\frac{1}{2}} + (\gamma_i^p \gamma_j^p)^{\frac{1}{2}}]} \quad \textbf{(4.2)}$$

Where γ_i^d is expressed as surface energy due to the dispersive component of liquid and γ_i^p is expressed as surface energy due to the polar component of liquid. Similarly, γ_j^d is expressed as surface energy due to the dispersive component of solid and γ_j^p is expressed as surface energy due to the polar component of solid (Hasan et al., 2018). Also, θ act as an interaction parameter (~1). Also, the thermal stability of crude biosurfactant was studied using thermogravimetry analysis (TGA) (Netzsch, Model: STA449F3A00) (Datta et al., 2018).

4.2.11. Biosurfactant assisted biodegradation studies

In order to enhance the oil degradation ability of the strain, crude biosurfactant was supplemented in media, and the system's performance was analyzed. For this, three concentrations of crude biosurfactant were explored viz. 0.5 CMC, CMC and 1.5 CMC. The experiment was performed in two setups (1) biosurfactant was mixed with oil containing media for the first 24 h followed by bacterial inoculation (5 %, *v/v*; 1×10^8 CFU/mL) for 96 h (Biosurfactant → cells, "BC"), and (2) crude biosurfactant co-cultured with bacteria in oil containing media (Biosurfactant + cells, "B+C") for 96 h at 25°C, 180 rpm. After incubation, cultures were centrifuged to analyze the residual oil and biosurfactant concentration from the supernatant, and the recovered pellet was used for biomass estimation, as mentioned above. The residual oil was further quantified using GC-FID (Varian 450, Sil-8 CB column, 30 m × 0.25 mm × 2.5 µm) analysis. The injector temperature was maintained at 250°C, and the detector temperature was maintained at 280°C. The oil samples were prepared in hexane with an injector volume of 1 µL. Also, helium gas was used as carrier gas maintained at a 1:50 split ratio. In addition, the overall oven

temperature was programmed as an initial temperature of 60°C for 5 min, which was raised with the ramping of 5°C/min to 280°C with a hold time of 15 min (Mahesh et al., 2019).

4.2.12. Statistical analysis

The statistical analyses of experimental data were performed by OriginPro 8.5 software, as mentioned in Chapter 3, section 3.2.7.

4.3. Results and discussion

4.3.1. Isolation, screening and identification studies for selected strains

The biosurfactant production ability of isolated bacterial strains was evaluated using standard screening methods such as oil displacement, surface tension reduction, and E_{24}. The selected bacterial strains showed positive results for all tests mentioned above, as tabulated in **Table 4.1**. These selected bacterial strains were then identified using the 16S rRNA sequencing technique, and their phylogenetic tree was obtained using the NCBI neighbor-joining tool as represented in **Figure 4.1.** The selected strains were identified from the figure as (A) *Acinetobacter* sp. SRL_72524, (B) *Klebsiella pneumoniae* SRL_52525, (C) *Enterobacter* sp. SRL_93721, and (D) *Bacillus subtilis* RSL2.

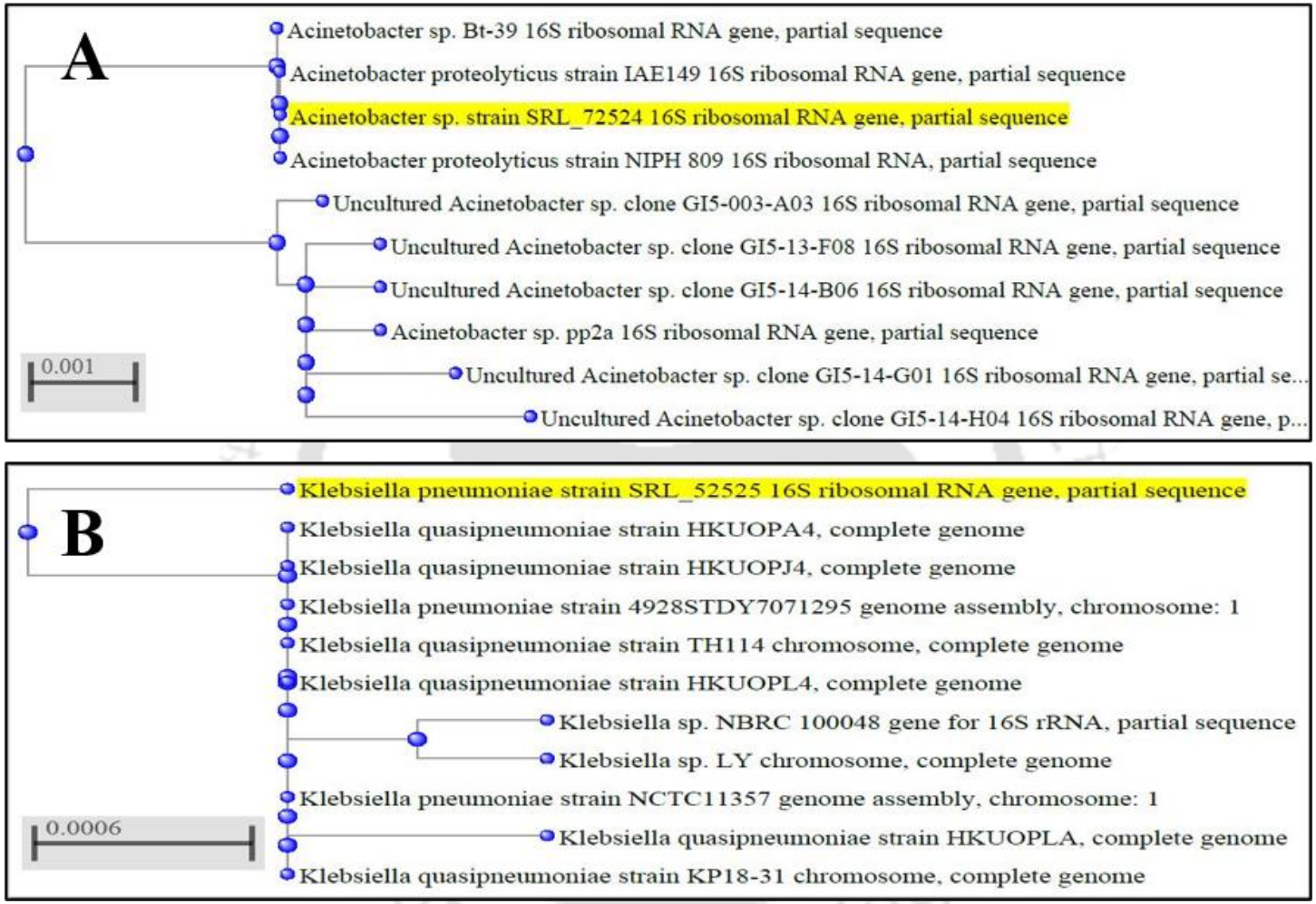

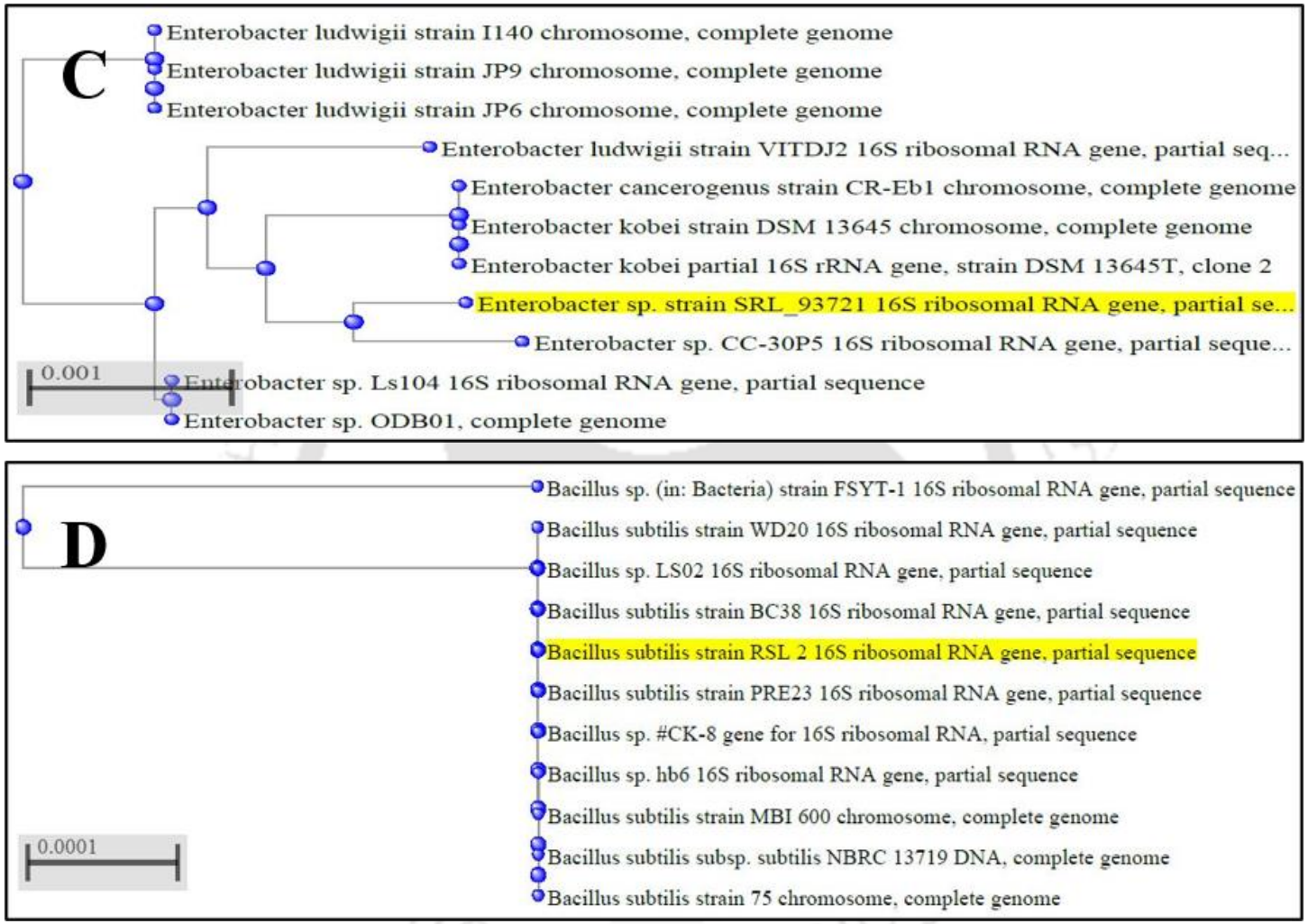

Figure 4.1. Phylogenetic tree obtained using NCBI neighbor-joining tool for selected bacteria (A) *Acinetobacter* sp. SRL_72524, (B) *Klebsiella pneumoniae* SRL_52525, (C) *Enterobacter* sp. SRL_93721, and (D) *Bacillus subtilis* RSL2

It was observed that strain RSL-2 belonged to *Bacillus* sp., strain 93721 belonged to *Enterobacter* sp., strain 52525 belonged to *Klebsiella* sp., and strain 72524 belonged to *Acinetobacter* sp. The 16S rRNA sequences for the abovementioned strains were submitted to the NCBI GenBank sequence database, with GenBank accession number *Bacillus subtilis* RSL 2 (MK734048) (Ravi, 2019), *Enterobacter* sp.SRL_93721 (MK752685), *Klebsiella pneumonae* SRL_52525 (MK752681), and *Acinetobacter* sp SRL_72524 (MK752684). Among the selected strains, *Bacillus subtilis* RSL2 exhibited high surface-active properties such as 57 % $E_{24,}$ positive oil displacement activity and reduced the surface tension to 40 ± 1 mN/m Hence, interpreting from the preliminary test, *Bacillus subtilis* RSL2 was chosen as a potential biosurfactant producing strain for further studies.

Table 4.1. Preliminary test for screening of isolated bacteria for biosurfactant production ability

Strain	NCBI accession no.	Oil displacement	Emulsification activity(E_{24})	Surface tension (mN/m)
RSL-2	MK734048	+	57 %	40 ± 1
93721	MK752685	+	45 %	41 ± 1
72524	MK752684	+	45 %	42 ± 1
52525	MK752681	+	45 %	44 ± 1

4.3.2. Optimization of Nitrogen source

The effect was different N sources on the growth and biosurfactant production ability of *Bacillus subtilis* RSL 2 was further analyzed. The maximum OD_{600} was observed as follows:

Yeast extract > Iron nitrate > Ammonium sulfate > Ammonium nitrate > Urea

Furthermore, the yeast extract concentration was optimized by varying its concentration from 0.5 % to 2 % (*w/v*). The effect of yeast extract concentration on the growth and biosurfactant production ability of *Bacillus subtilis* RSL 2 was analyzed based on the biomass and surface tension reduction abilities at the end of incubation, as shown in **Figure 4.2.** 1.5 % yeast extract was optimal N concentration for the growth of bacterial cells and reduction of surface tension.

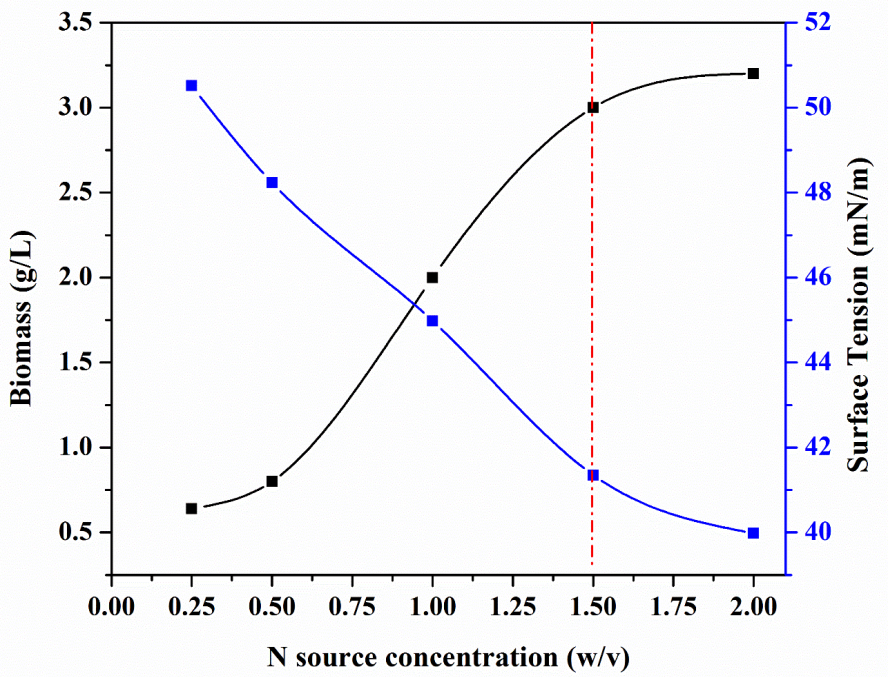

Figure 4.2. Optimization of yeast extract (N source) concentrations for *B. subtilis* RSL2

Biosurfactants are surface-active bio-molecules, which reduces the surface tension of culture media (Sharma et al., 2019). Hence, the biosurfactant production was estimated in terms of the surface tension reduction of culture media. In concordance to obtained results, various literature also supported the ability of *Bacillus* sp. to produce higher biosurfactant in the presence of organic N sources such as yeast extract (Gudiña et al., 2015; Liang et al., 2018; Parthipan et al., 2017) Parthipan *et al.* explored the biosurfactant production ability of *Bacillus subtilis* A1 using 2 % sucrose and 3 % yeast extract for the production of 4.85 g/L of biosurfactant (Parthipan et al., 2017). Similarly, Liang *et al.* supplemented 2 % yeast extract to produce biosurfactants (Liang et al., 2018). However, an effective microbial growth and biosurfactant production using crude oil and comparatively lesser yeast extract concentration made the entire process economic.

4.3.3. Optimization of culture conditions

Effect of pH (A), temperature (B) and crude oil concentration (C) (in the presence of pre-optimized N source) on the overall biosurfactant production ability of bacterial strain was analyzed using RSM-CCD methodology. Sets of 20 experiments were designed using RSM-CCD, and their predicted and

experimental output values are listed in **Table 4.2**. **Figure 4.2** shows the optimization study done for the above parameters and selecting the best conditions based on the biosurfactant concentration as the response. After completing all experiments, biosurfactant concentration was used as a response and obtained interaction was fitted as a quadratic model equation to predict optimized conditions. The fitted model predicted the concentration of biosurfactant using the following quadratic **equation 4.3**:

$$\boldsymbol{Biosurfactant\ concentration} = +\mathbf{12.05247} - \mathbf{1.01235} \times \boldsymbol{A} - \mathbf{0.33823} \times \boldsymbol{B} - \mathbf{0.63442} \times \boldsymbol{C} + \mathbf{1.87500}\boldsymbol{E} - \mathbf{003} \times \boldsymbol{A} \times \boldsymbol{B} + \mathbf{0.056250} \times \boldsymbol{A} \times \boldsymbol{C} + \mathbf{6.25000}\boldsymbol{E} - \mathbf{004} \times \boldsymbol{B} \times \boldsymbol{C} + \mathbf{0.057850} \times \boldsymbol{A}^{\mathbf{2}} + \mathbf{4.59443}\boldsymbol{E} - \mathbf{003} \times \boldsymbol{B}^{\mathbf{2}} + \mathbf{0.057850} \times \boldsymbol{C}^{\mathbf{2}} \quad \textbf{(4.3)}$$

Where biosurfactant concentration (g/L) was controlled by factors A, B and C, which represented pH of the culture media, the temperature of incubation and crude oil concentration, respectively.

Table 4.2. Experimental setup design by RSM-CCD with predicted and obtained responses (Biosurfactant concentration)

S.No.	Experimental design			Predicted concentration (g/L)	Actual concentration (g/L)
	pH	Temperature (°C)	C (g/L)		
1	4	25	1	3.20	3.25
2	8	25	1	2.34	2.36
3	4	45	1	3.03	3.04
4	8	45	1	2.32	2.34
5	4	25	5	3.01	3.02
6	8	25	5	3.05	3.07
7	4	45	5	2.89	2.90
8	8	45	5	3.08	3.06
9	2.63	35	3	2.88	2.84
10	9.36	35	3	2.31	2.30
11	6	18.18	3	3.30	3.25
12	6	51.82	3	3.18	3.18
13	6	35	0	2.35	2.30
14	6	35	6.36	2.84	2.84
15	6	35	3	1.94	1.97
16	6	35	3	1.94	1.96
17	6	35	3	1.94	1.95
18	6	35	3	1.94	1.94
19	6	35	3	1.94	1.90
20	6	35	3	1.96	1.93

According to ANOVA analysis, the quadratic model was found to be significant ($p \leq 0.0001$) with an insignificant lack of fit ($p \geq 0.082$). The model's reliability was a low coefficient of variation (CV = 1.51 %) and a high Adeq precision value of 49.53. The Model R^2 and F-value were 0.997 and 374.15, respectively. The Predicted R^2 value (0.9811) was also found to agree with the Adjusted R^2 value (0.9944). Both pH and initial oil concentration ($p \leq 0.0001$) influenced the biosurfactant concentration. In contrast, temperature ($p \geq 0.0001$) was insignificant for two-way interaction. Hence, factors A, C,

AC, A^2, B^2, and C^2 were significant model terms. Overall, the optimized condition for biosurfactant production was pH 4.0, 25°C using 1 g/L crude oil. At these optimized conditions, the actual biosurfactant concentration (3.6 g/L) was more prominent than the predicted concentration (3.2 g/L).

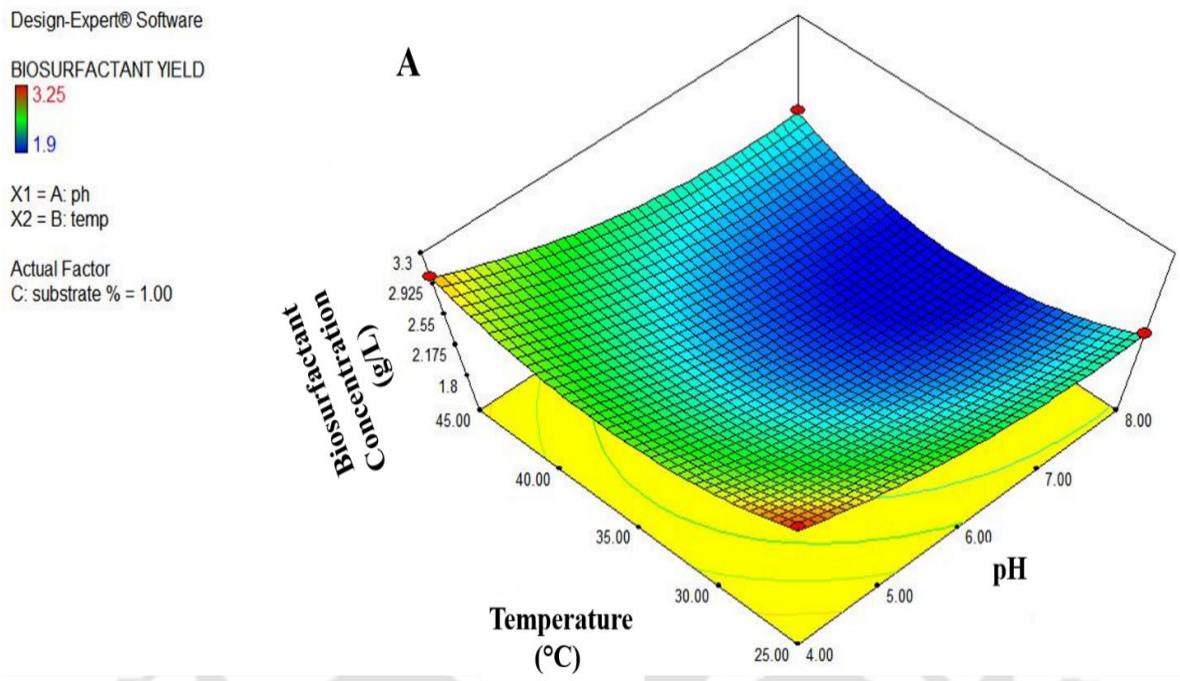

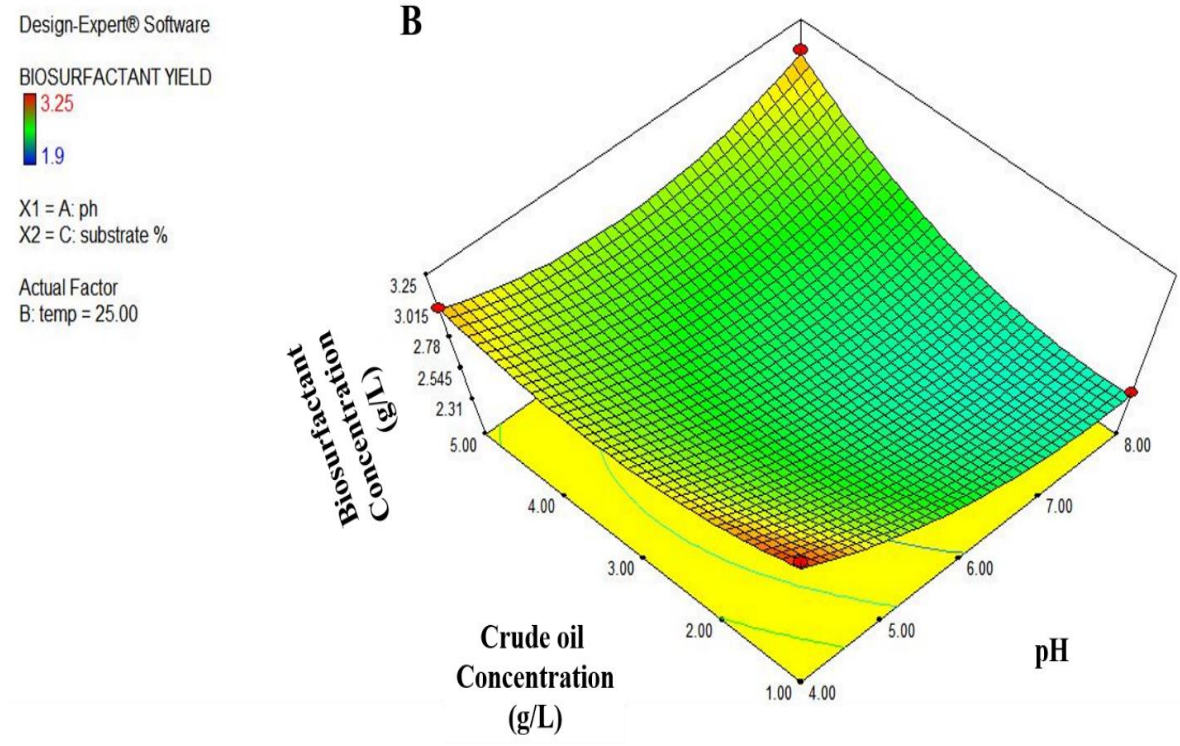

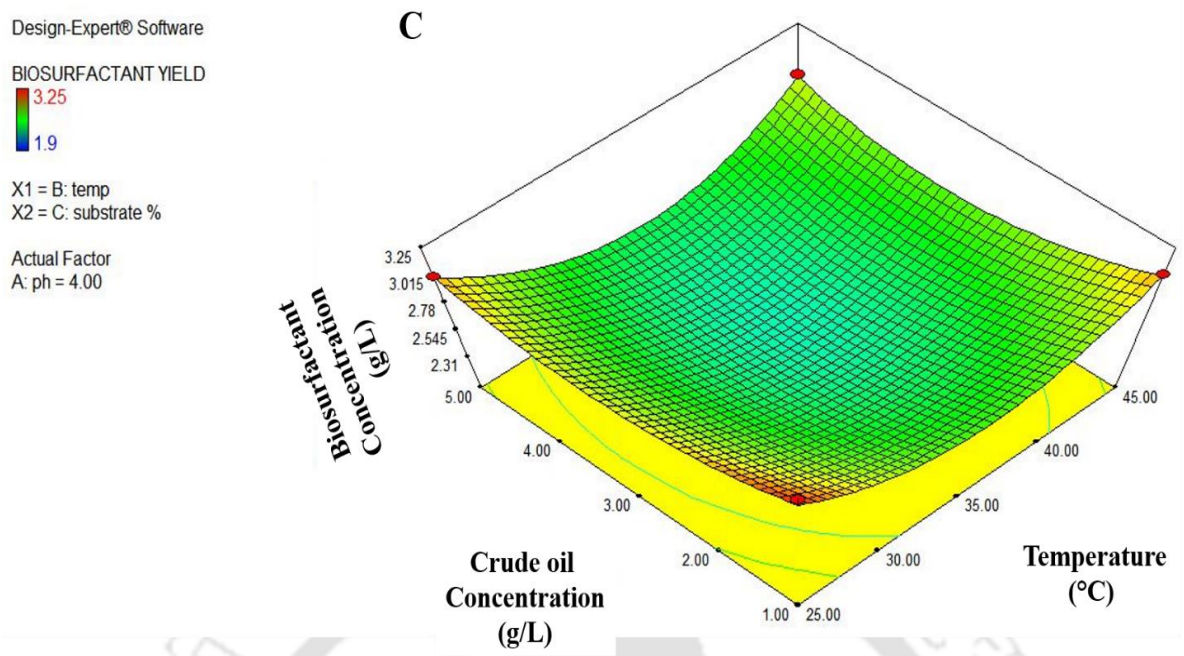

Figure 4.3. Response surface plots for the maximum biosurfactant concentration considering: (A) Temperature and pH as the parameters at constant crude oil concentration; (B) Crude oil concentration and pH as the parameters at constant temperature; and (C) Crude oil concentration and temperature at constant pH

4.3.4. Study of crude oil degradation and biosurfactant production under optimized conditions

Under the optimized conditions (pH 4.0, 25°C and 1 g/L crude oil), *B. subtilis* RSL2 was studied for its growth and subsequent production of biosurfactant, which was analyzed in dry biomass surface tension and biosurfactant concentration, as shown in **Figure 4.4**. The residual crude oil reflected the oil degradation ability of the strain. The specific growth rate (μ) was obtained as 0.08 h^{-1}. It was observed that biomass reached a stationary phase after 3rd day of incubation. Also, the biosurfactant concentration increased rapidly till the 3rd day. It later maintained the same until the 7th day, suggesting that biosurfactant was released primarily within the exponential phase as a growth-associated metabolite. Such rapid onset of extracellular biosurfactant production during the exponential phase agrees with the trend of surface tension reduction, which reached an inflation point of 38 mN/m after the 3rd day. The overall crude biosurfactant concentration was obtained as 3.6 ± 0.3 g/L after the 7th day of incubation. Datta *et al.* also referred to biosurfactant as a primary metabolite, produced during the exponential-

growth phase of *B. subtilis* MG 495086 using 3.8 % *(w/v)* of light paraffin oil as C source, producing 6.3 g/L of biosurfactant (Datta et al., 2018). Similarly, Parthipan *et al.* reported biosurfactant production (4.85 g/L) as a growth-associated metabolite by bacterium *B. subtilis* A1, using 2 % sucrose and 3 % yeast extract as C and N source (Parthipan et al., 2017). Likewise, *B. licheniformis* AL 1.1 strain showed 0.86 g/L of purified lipopeptide biosurfactant within 24 h using glucose as C source at 30°C (Coronel-León et al., 2015).

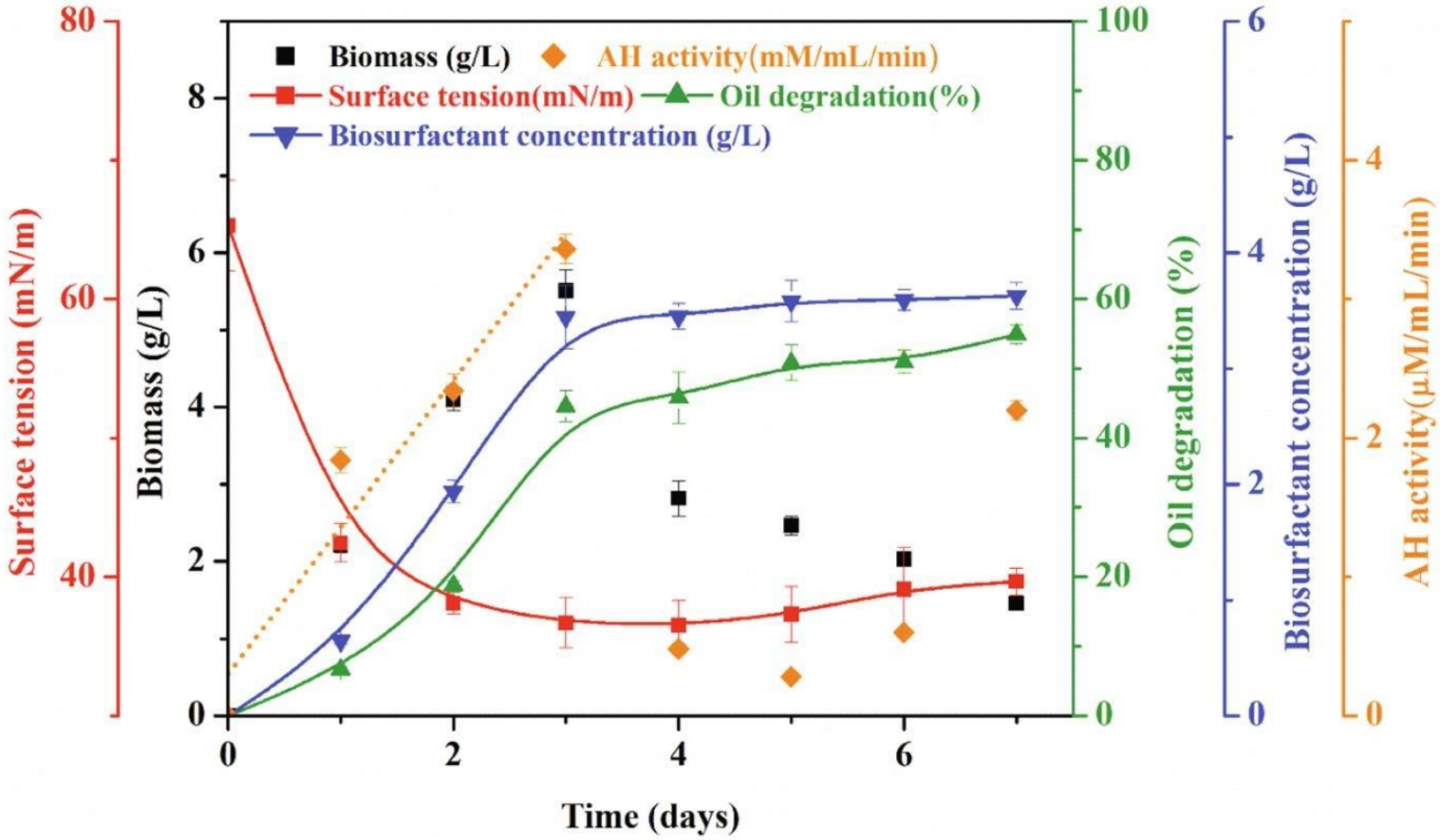

Figure 4.4. Study of growth, biosurfactant production and oil degradation under optimized conditions of pH 4.0, 25°C and 1 g/L of oil in BH media with oil to yeast extract ratio of 1/15

With the release of biosurfactant since the early bacterial exponential phase, there was a simultaneous increase in bacterial oil degradation ability, which reached 45 % on the 3rd day. After that, a significantly lower change in oil degradation was observed (55 ± 2 %), which was in agreement with no more increment in biosurfactant production and death phase of biomass. A similar 33 ± 5 % removal in the soluble COD was obtained on the 3rd day of incubation which increased to 67 ± 5 % by the end of incubation. It suggested the importance of biosurfactant presence in microbes' overall oil degradation ability. This observation correlates with intracellular oil-degrading enzyme activity. Conclusively, based on the gravimetric analysis of crude oil degradation and biosurfactant production, it was established that the present *Bacillus* strain showed comparatively better biodegradation activity using waste crude oil as the sole carbon source.

4.3.5. Estimation of Alkane hydroxylase enzyme activity

The principal cause for bacterial degradation of crude oil components is the catalytic activity of hydrocarbon catabolizing enzymes. The principle enzyme, i.e., AH, was focused on analyzing the present strain's oil biodegradation ability. AH oxidizes long-chained hydrocarbons (C_5-C_{16}) to their alcoholic by-products (Sharma et al., 2019). The hydroxylation activity of this enzyme is majorly regulated by the availability of substrate (alkanes) and cofactor (NADH) (Ji et al., 2013). Arslan *et al.* also reported that the expression of the alk gene depends on nutrient availability. They stated that the higher availability of nutrients improved microbial growth and, in turn, their catabolic activity. Metabolically active cells showed higher enzyme activity (Arslan et al., 2014). In agreement, the findings revealed that the overall enzyme activity was high during the exponential phase, causing higher degradation of crude oil in the early exponential phase, till 72 h (3 days). However, with the late stationary phase, the enzyme activity reduced presumably due to the death phase of biomass. It is also reflected as poor oil degradation in this phase. Hence, the overall activity of AH played a crucial role in the biodegradation of crude oil as its overexpression increased the overall degradation by many folds. **Figure 4.3 (**dotted line) depicts the linear relationship between oil degradation, biomass production and biosurfactant production with increase in alkane hydroxylase activity during exponential phase. Parthipan *et al.* also reported similar improved alkane hydroxylase activity (188 µmole/min/mg) during

the exponential phase (48-72 h), which gradually declined as the cell reached death phase (Parthipan et al., 2017). Conclusively, it is suggested that AH plays vital role in overall biodegradation of crude oil, as alkane contributes to the major contents of crude oil.

4.3.6. Characterization of produced biosurfactant

The biosurfactant was characterized for its ability to reduce surface tension till its inflation point, i.e., CMC of the biosurfactant. The crude biosurfactant showed a value of 0.5 g/L CMC (**Figure 4.5(A)**), decreasing surface tension to 38 ± 0.5 mN/m. The chemical nature of crude biosurfactant was also analyzed using FTIR spectroscopy. Based on the major transmittance peaks recorded in the spectra, different functional groups present in the crude biosurfactant were identified (**Figure 4.5(B)**). Furthermore, the chemical nature of the biosurfactant was investigated by comparing its assigned functional groups with existing literature suggesting it to be lipopeptide in chemical nature **(Table 4.3).** The crude biosurfactant was characterized using MALDI-TOF analyses as shown in (**Figure 4.5(C)**). The presence of peaks at m/z 1044, 1058 and 1074 suggested the presence of C_{14}-surfactin $[M+Na]^+$, C_{15}-surfactin $[M+Na]^+$, C_{15}-surfactin $[M+K]^+$, respectively. Similar peaks were reported by Price et al. from the crude biosurfactant produced by *Bacillus subtilis* B-41086 (Price et al., 2007). Various reports have reported the occurrence of $C_{13\text{-}15}$ surfactin peaks in the *Bacillus* genus MALDI-TOF analysis (Hoefler et al., 2012; Yang et al., 2015).

Table 4.3. Major peaks positions from FTIR spectra of crude biosurfactant

S.No.	Peak positions (cm^{-1})	Functional group assignment	Ref
1	1640	Amine group	(Balan et al., 2016)
2	1535	Fatty acid linkage (-C=O-NH)	(Habib et al., 2020)
3	3042-2855 and 1200-1400	Aliphatic –CH group of the long fatty acid chains	(Velioğlu and ÜREK, 2015)
4	1054	C-O stretch	(Kiran et al., 2017)

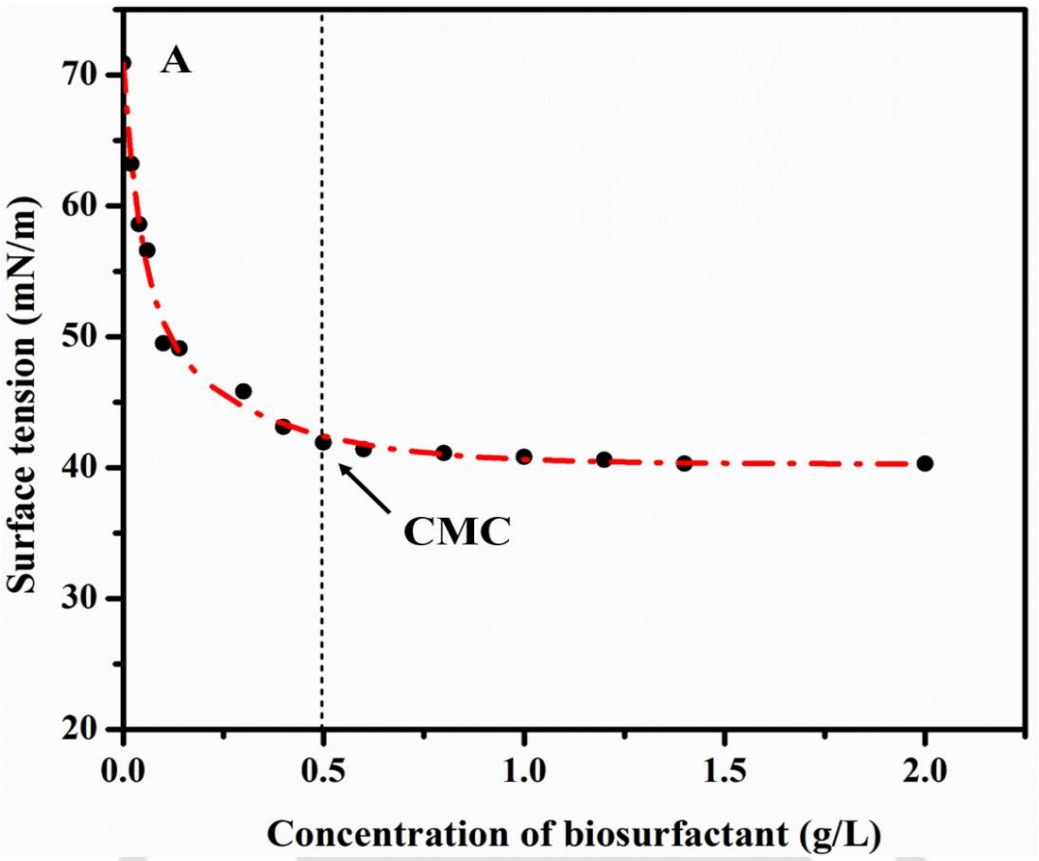

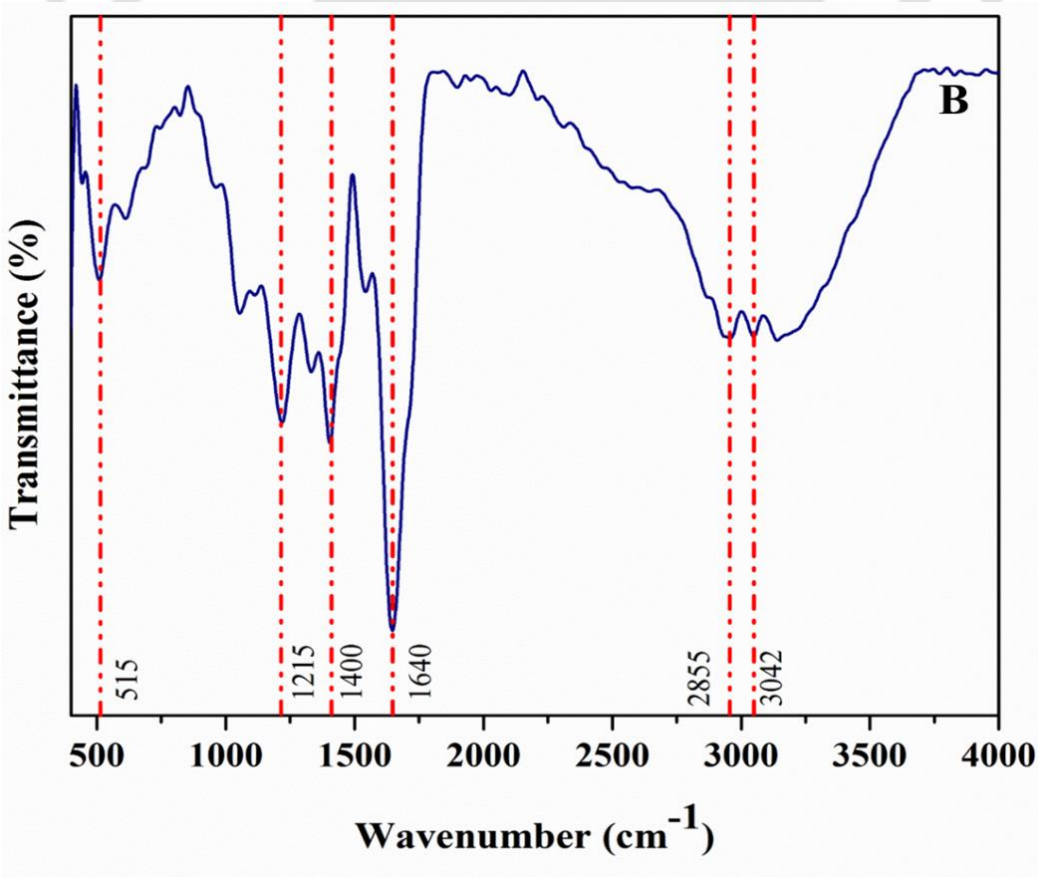

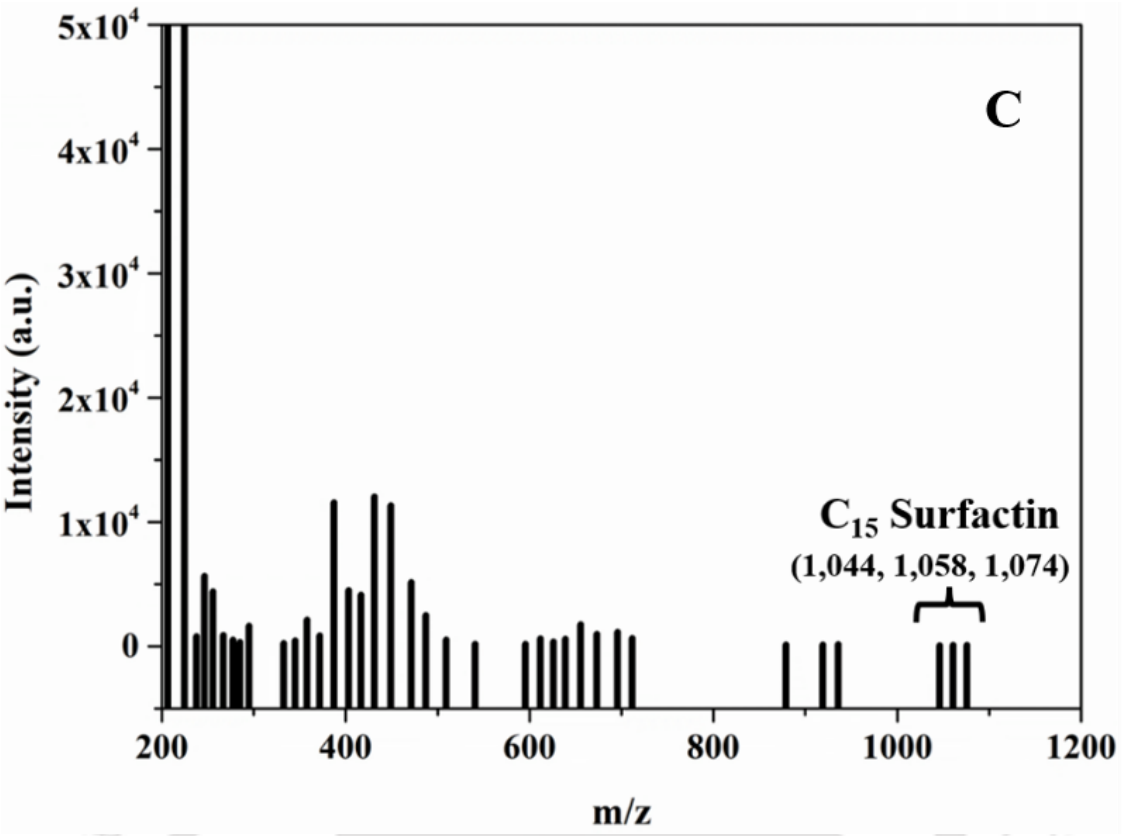

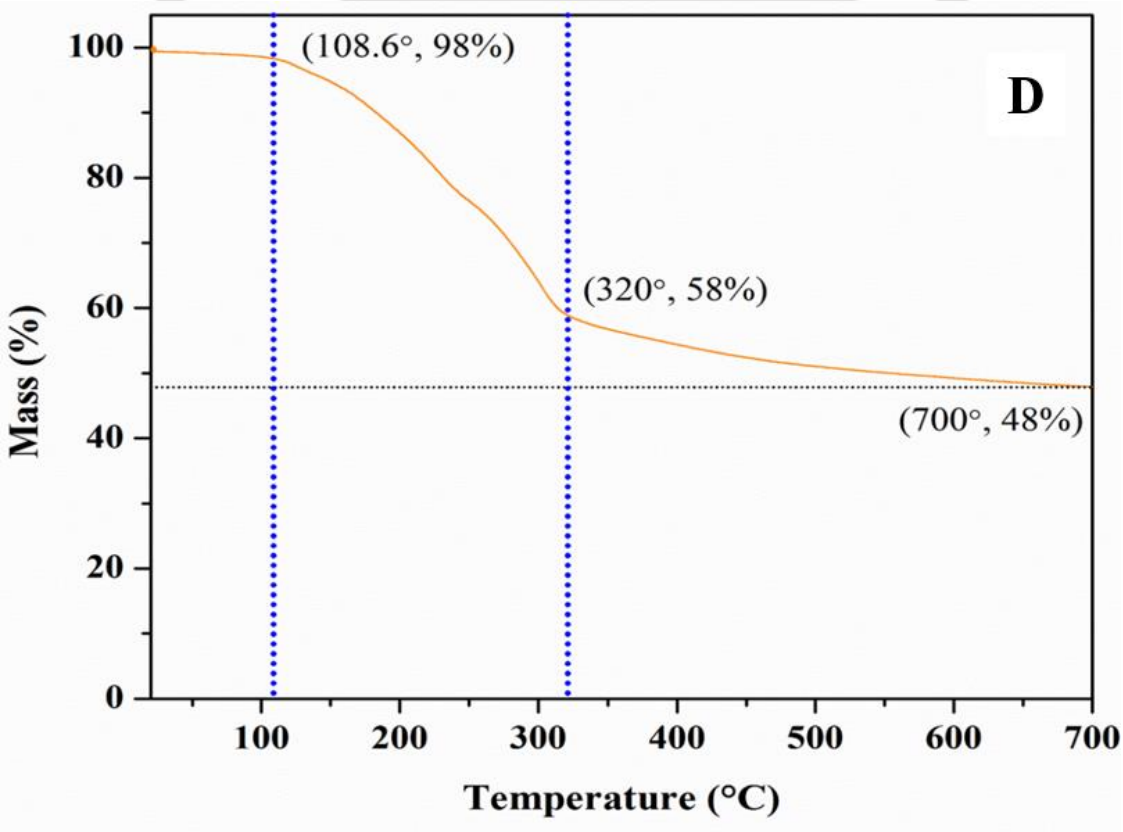

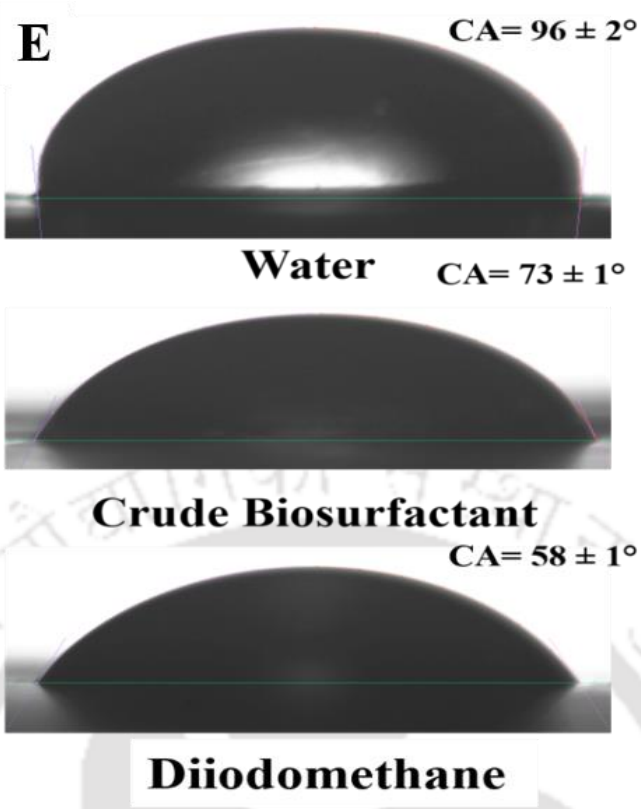

Figure 4.5. Characterization analyses for crude biosurfactant using (A) Surface tension measurement to determine the CMC value, (B) Functional group analysis using FTIR, (C) Molecular weight analysis using MALDI-TOF-MS, (D) Thermal stability analysis using TGA, and (E) Wettability study on paraffin using water, crude biosurfactant, Diiodomethane

The thermal stability of biosurfactant was studied by heating it at the rate of 10°C/min in the temperature range of 20-700°C in an inert atmosphere (**Figure 4.5(D)**). The biosurfactant showed three-phase thermal degradation. The initial phase showed a negligible loss in mass (~98 %) due to moisture removal till 109°C; there was a 58 % decrease in mass till 320°C. It was due to the loss of thermos-labile components of biosurfactants such as lipids. However, the biosurfactant retained ~48 % of its mass till 700°C, signifying that 50 % of biosurfactant composition is thermos-tolerant. Interestingly, produced biosurfactant showed excellent stability till ~110 °C with negligible mass loss, nominating its importance for in-situ oil recovery and remediation processes, where the maximum temperature reaches up to 100°C.

Further, the wettability characteristic of crude biosurfactant was studied on a hydrophobic surface (paraffin) using contact angle and surface energy (**Figure 4.5(E**)). The contact angle of the biosurfactant on the surface was compared with that of water and diiodomethane (MI) as controls. The hydrophobic paraffin surface resulted in a water contact angle of 96 ± 2°, indicating poor wetting behavior. On the other hand, the produced biosurfactant showed moderate wettability with a contact angle of 73 ± 1° representing the improved wettability due to the interfacial interaction of amphiphilic biosurfactant molecules. The contact angle of MI was found to be 58 ± 1°. The solid surface energy was calculated based on the measured water contact angle of liquids, water, biosurfactant solution, and MI. The surface energy of the hydrophobic paraffin surface was estimated to be 30 ± 1 mJ/m^2, which agreed to the literature for a hydrophobic surface of solid (Hasan and Pandey, 2016; Hasan et al., 2018; Pandey and Pattanayek, 2013). However, in case of moderate wettability ($\theta = 73 \pm 1°$), surface energy was increased to 35 ± 1 mJ/m^2. It indicated that the produced biosurfactant improved solid-liquid interfacial interactions on a hydrophobic surface. This property enables better interaction with oil (hydrophobic) and is helpful in oil washing and oil recovery applications.

4.3.7. The implication of biosurfactants in biodegradation behavior

The bacterial culture was explored for its ability to degrade crude oil in the presence of biosurfactants. Two modes were studied, (1) sequential biosurfactant injection in oil-containing media for an initial 24 h followed by bacterial inoculation (BC), (2) simultaneous biosurfactant and bacterial inoculation (B+C) in oil containing media. Also, crude biosurfactant concentrations, i.e., 0.5 CMC, CMC and 1.5 CMC, on the oil degradation ability of bacterial culture were studied. It was observed that in the case of simultaneous biosurfactant assisted biodegradation (B+C), there was improved bacterial growth, biosurfactant production and crude oil degradation as compared to sequential inoculation (BC).

Figure 4.6 shows the profile of biosurfactant, biomass and oil degradation at different biosurfactant concentrations in both modes. In both cases, enhanced oil degradation was observed at 0.5 CMC concentration due to increased oil mobilization by biosurfactant, making it more bioavailable for microbial biodegradation. In the case of simultaneous feed of biosurfactant and oil, the maximum oil degradation of 72 % was obtained, 1.6 folds higher than control, i.e., without biosurfactant. In

agreement, 1.5 folds increased biosurfactant concentration of 5.2 g/L was also achieved. However, in the case of sequential feeding (BC) of biosurfactant followed by microbes, the system's performance was lower than simultaneous feed (B+C), i.e., 55 % oil degradation and 4.5 g/L of biosurfactant. It indicated the role of biosurfactants towards both oil availability and microbe's efficacy, which is explored in section 4.2.8. of cell surface hydrophobicity.

The GC-FID chromatograms for the recovered residual oil after biosurfactant-assisted biodegradation studies are shown in **Appendix 4A (section S4-1.1, Figure 4A-1)**. It was observed that there was complete degradation of small chains of hydrocarbons (Retention time (RT) 0-15 min) in all the experimental cases. Also, a significant decrease (~50 %) in peak intensities for long chains of hydrocarbons compared to raw crude oil was recorded (RT = 15-51 min). In the case of simultaneous biosurfactant and oil feeding, the maximum decrease in peak intensities (degradation) was observed, which agreed to the maximum oil degradation and, in turn, biosurfactant production**.**

4.3.8. Role of concentration of biosurfactant on bio-stimulation

The biosurfactant concentration greatly influences its mode of operation in the oil-water interface. When biosurfactant is present at a concentration below its CMC, it tends to mobilize the oil improving its bioavailability towards microbes. On the other hand, when the biosurfactant concentration is at its CMC value or above, it tends to form micelles encapsulating oil within its hydrophobic core, further diminishing its bioavailability (Pacwa-Płociniczak et al., 2011). It suggested that in the case of 0.5 CMC of biosurfactant, oil molecules were mobilized, which enhanced their bioavailability and biodegradation. However, above CMC, oil molecules were entrapped in micelles and became less available to microbial degradation. Lin *et al.* also reported a reduction in biodegradation of phenanthrene (PHE) by *Sphingomonas* sp. GY2B when rhamnolipid biosurfactant was exploited above its CMC concentration (Lin et al., 2017). Similarly, Ma *et al.* also found a similar increment in PHE biodegradation by *Pseudomonas* sp. Ph6 when rhamnolipid were used below 100 mg/L, suggesting the role of CMC in substrate bioavailability (Ma et al., 2018). However, no coherent literature is available on the role of lipopeptide biosurfactants in the biodegradation of crude oil.

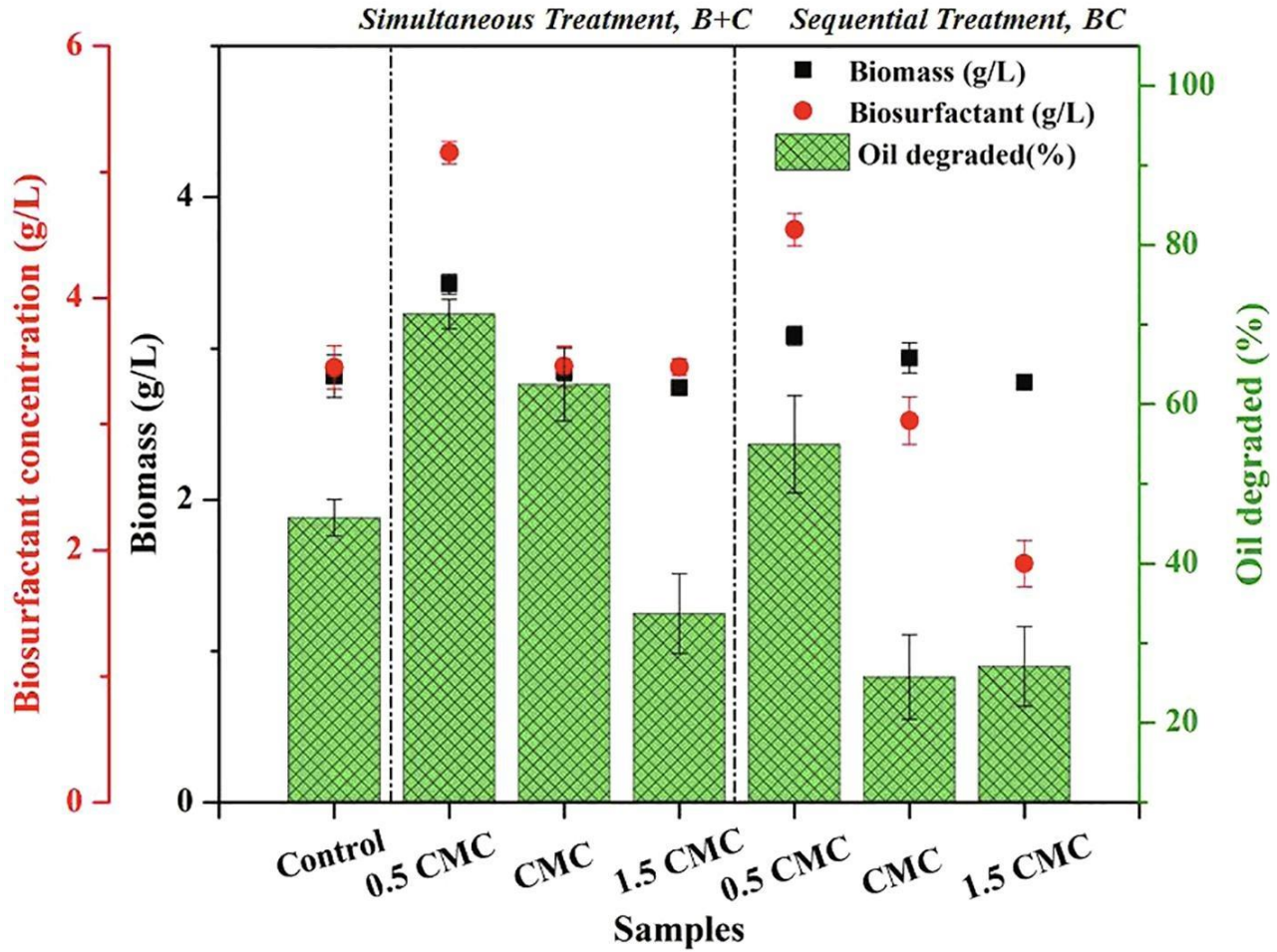

Figure 4.6. Effect on biomass growth, Biosurfactant production, and crude oil degradation in case of sequential (BC) and simultaneous (B+C) oil degradation using different concentrations of biosurfactant

4.3.8.1. Antibacterial and cell-surface hydrophobicity properties of crude biosurfactant

To estimate the growth inhibitory effects of biosurfactant concentration on bacterial growth, *B. subtilis* RSL2 was spread plated with different concentrations of biosurfactant as a well-diffusion technique, as shown in **Figure 4.7(A)**. The zone of inhibition (ZOI) obtained were 17 ± 0.3 mm for positive control (kanamycin), 10.5 ± 0.3 mm at 7 CMC, 8.1 ± 0.1 mm at 1.5 CMC, 7.3 ± 0.2 mm at CMC, and 1.2 ± 0.4 mm at 0.5 CMC concentrations of biosurfactant. Hence, lower concentrations of biosurfactants are more suitable for bacterial growth. The presence of biosurfactant at CMC and above CMC diminished the cellular metabolism by imparting the cellular growth and reducing the bioavailability of crude oil, leading to a decrease in the overall efficiency of oil degradation metabolism. Hence, the utilization of biosurfactants at optimum concentration can increase oil degradation and improved cellular metabolism in terms of higher cellular growth and biosurfactant production.

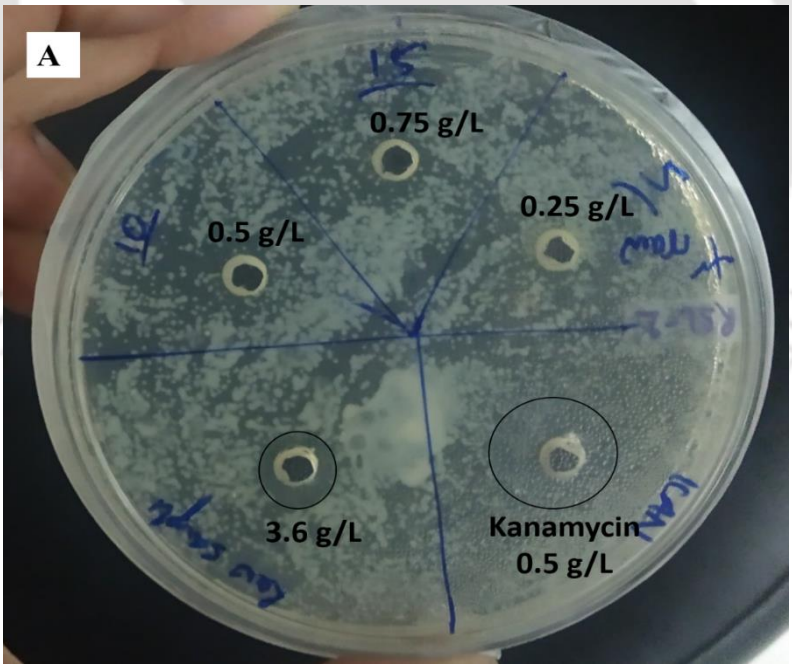

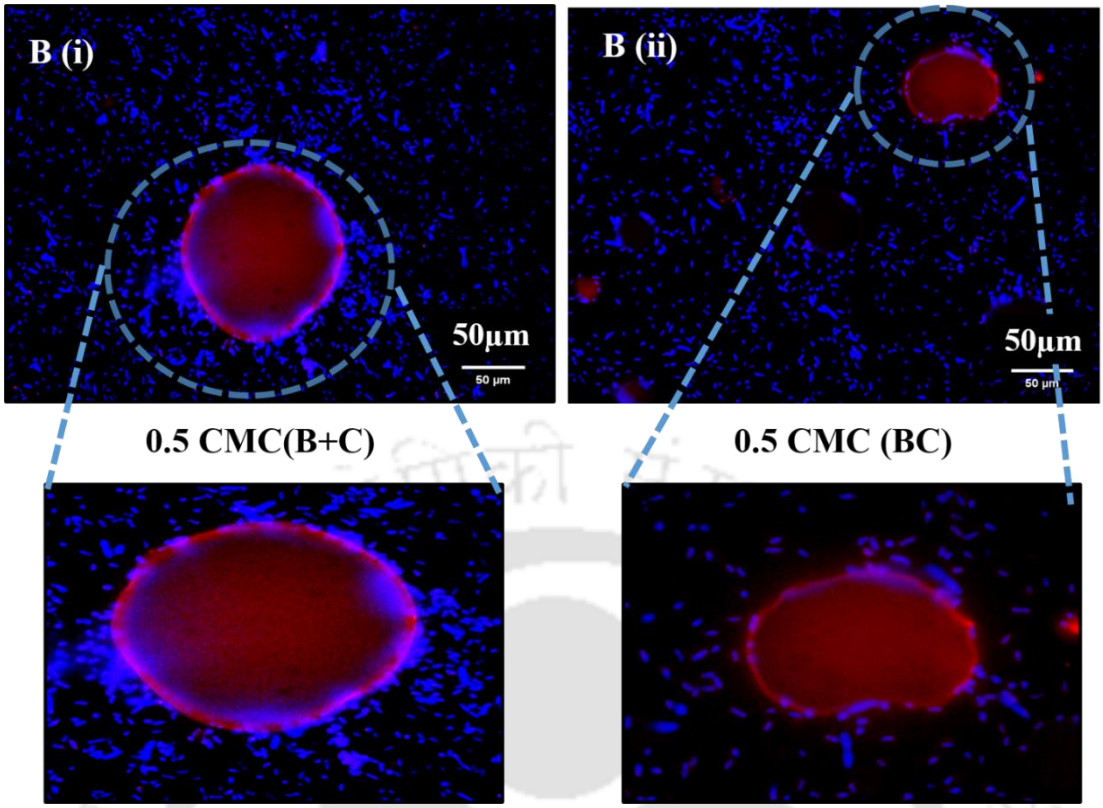

Figure 4.7(A). Growth inhibitory effect of biosurfactant with increase in concentration (0.25 g/L, 0.5 g/L, 0.75 g/L and 3.6 g/L) using Kanamycin (0.5 g/L) as control, and (B) Fluorescence image of bacterial adhesion to the hydrocarbon due to their surface hydrophobicity, aiding their overall hydrocarbon utilization (i) 0.5 CMC (B+C), i.e., simultaneous mode, (ii) 0.5 CMC (BC), i.e., sequential model

4.3.8.2. Effect of biosurfactant feeding on microbial biodegradation activity

Biosurfactant below its CMC mobilizes oil making it bioavailable for microbes. In addition, it affects the hydrophobicity of the microbial surface. This bilateral role of biosurfactant bridges the relationship between substrate and microbes for better utilization, growth and metabolism (Datta et al., 2018; Pacwa-Płociniczak et al., 2011; Sharma et al., 2019). Studies revealed that biosurfactant below its CMC value modulates the cell surface protein content contributing to modification of cellular membrane hydrophobically for better adhesion to hydrocarbons. It leads to improved oil degradation, surface tension reduction and biomass growth. When cells were incubated simultaneously with biosurfactant (0.5 CMC), there was higher cellular growth and degradation ability than sequential biosurfactant and

microbial incubation. Cell surface hydrophobicity was measured by microbial adherence to hydrocarbons (MATH) test (Kaczorek and Olszanowski, 2011). Thus, to explore the effect of biosurfactant feeding time on the bacterial cell surface hydrophobicity, fluorescence images were recorded at 0.5 CMC concentration at both sequential (BC) and simultaneous (B+C) inoculation modes. In the case of simultaneous biosurfactant feeding, more cells were observed in the vicinity of oil drops than sequential mode **(Figure 4.7(B)).** 1.5 times higher cell surface hydrophobicity was observed in the simultaneous feeding of biosurfactant and microbe than sequential inoculation, which caused improved oil-microbe's interactions and ultimately overall biodegradation**.**

Summarily, the presence of biosurfactant below CMC mobilized the oil molecules, which improved their bioavailability. Hence, the co-presence of biosurfactant with the substrate (oil) acts as a potential bio-stimulating tool to uplift the oil biodegradation ability of microbes. In addition, it is preferred to add a biosurfactant and the microbe simultaneously to modulate their CSH for maximizing oil degradation.

4.4. Conclusions

Bacillus subtilis RSL 2 was isolated and explored to produce biosurfactants and biodegrade crude oil. This strain exhibited better surface-active properties than other isolates. The maximum biosurfactant production of 3.6 ± 0.3 g/L was produced at optimized conditions as predicted by RSM-CCD. The produced biosurfactant was found to be lipopeptide with a CMC value of 0.5 g/L. The presence of biosurfactants was found to enhance the bioavailability of the oil. However, it also improved CSH when fed in simultaneous mode, i.e., oil and microbe's interactions. This strategy enhanced overall oil degradation and biosurfactant production by 1.6 folds.

Chapter 5

Design of microbial consortium and exploring their hydrocarbon biodegradation ability

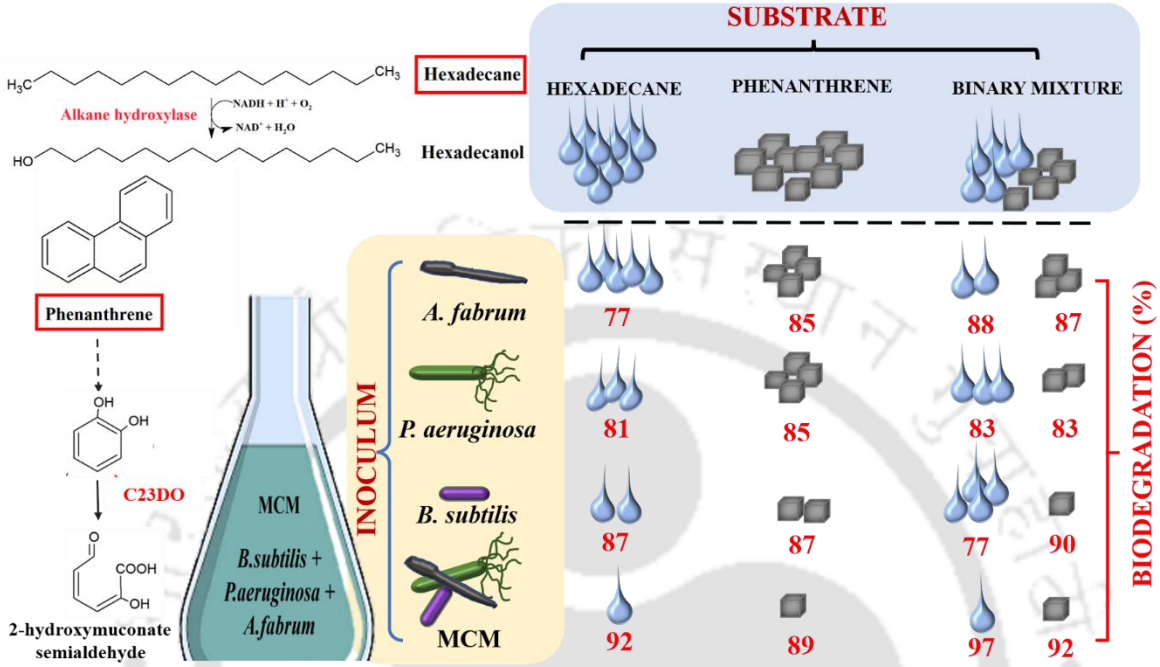

(Bioresource technology 358, 127408, 2020 (Sharma and Pandey, 2022))

This chapter discusses the biodegradation kinetics of aliphatic Hexadecane, aromatic Phenanthrene and their mixture as co-contaminants by axenic cultures of *Agrobacterium fabrum* SLAJ 731, *Bacillus subtilis* RSL2 and *Pseudomonas aeruginosa* P7815 and their consortium. The residual hydrocarbon concentration was explored for the first-order decay model, and the half-lives and decay rate were compared to estimate the biodegradation efficiency. The aliphatic catabolic enzyme alkane hydroxylase and aromatic catabolic enzyme catechol 2,3 dioxygenase in the biodegradation was examined. The chapter explores the biodegradation ability of individual bacteria using aliphatic or aromatic or both hydrocarbons as sole C source, and the change in their biodegradation ability when act as a single unit; and consortium. Thus, the overall study underscores the potential of a designed consortium in the bioremediation of crude oil and other hydrocarbon contaminated sites.

5.1. Introduction

Aliphatic and aromatic hydrocarbons are commonly found to be co-contaminated. Various studies have screened potential aliphatic and aromatic hydrocarbon degraders in bioremediation (Chettri and Singh, 2019); however, few reports also stated the inhibitory effect of co-contamination of aliphatic with aromatic hydrocarbons, thus limiting the overall biodegradability of axenic cultures (Ghorbannezhad et al., 2021). Using indigenous bacteria overcomes this lacuna as they are well acclimatized to such co-contaminant environments (Elumalai et al., 2021; Rabodonirina et al., 2019). In this direction, designing of the consortium using such indigenous bacterium has gained renowned attention in hydrocarbon bioremediation studies due to their various advantages over pure/axenic cultures, such as (a) increased metabolic diversity, (b) a broad range of degradative genes, and (c) higher tolerance and adaptability to unfavorable physiological conditions (Varjani et al., 2021). For underscoring the potential suitability and stability of consortium for hydrocarbon biodegradation, it is important to understand its axenic culture dynamics with different substrates (aliphatic, aromatic or their co-contaminant) and their interaction within the microbial communities; however, such information is limited to a few studies.

In the previous Chapter 3 and 4, the potential applicability of using inherent oil-degrading and biosurfactant-producing bacterial species; *Bacillus subtilis* RSL2, *Agrobacterium fabrum* SLAJ 731 for the remediation of crude oil were highlighted. The present chapter explored three indigenous bacteria (*Bacillus subtilis* RSL2, *Agrobacterium fabrum* SLAJ 731 and *Pseudomonas aeruginosa* P7815) based on their previously reported hydrocarbon biodegradation and biosurfactant production abilities (Sharma et al., 2019; Tiwari et al., 2017; Verma et al., 2020). Bacteria *P. aeruginosa* reported a high crude oil biodegradation rate of 0.5 g/L/day with a production of 0.35 g/L rhamnolipid biosurfactant (as discussed in Chapter 6). Thus, to combat the biosurfactant limitation, two lipopeptide biosurfactant producing bacterial strains *A. fabrum*, and *B. subtilis* were incorporated. The crude oil biodegradation rates were comparatively lesser, i.e., 0.05 and 0.15 g/L/day for *A. fabrum* and *B. subtilis*, respectively, when supplemented with crude oil as the sole C source (from previous chapters). However, A. fabrum exhibited higher biodegradation ability of aromatic fraction of crude oil than aliphatic. In addition, a simultaneous biosurfactant production of 2.5 and 3.6 g/L by *A. fabrum* and *B. subtilis*, respectively, was reported during the crude oil biodegradation study (Sharma et al., 2020; Sharma et al., 2019).

Thus, where *P. aeruginosa* exhibited high hydrocarbon biodegradation ability, the other two strains exhibited high biosurfactant production abilities, expanding the overall hydrocarbon biodegradation efficacy. Since bacteria adopt different metabolic pathways to assimilate aliphatic and aromatic hydrocarbons fractions in crude oil, a model aliphatic and aromatic C source and its binary mixture were used to understand the interaction among the two distinct metabolic pathways. Phenanthrene (PHE) was chosen as a model aromatic contaminant owing to its poor solubility of 1.24 mg/L, making it less bioavailable for microbial biodegradation and hence enlisted in the USEPA priority pollutant list. Similarly, Hexadecane (HEX) is a major component of various crude oil and diesel fuels and was opted as a model aliphatic hydrocarbon. The bacterial biodegradation study was performed in two inoculum modes, (a) individual bacterial axenic culture and (b) their consortium, with three substrates modes, (a) HEX, (b) PHE, and (c) HEX+PHE. The study aimed to gain insights into hydrocarbon degradation kinetics, bacterial growth and degradative enzyme activities in the aforementioned modes and investigate its suitability at oil-contaminated sites.

5.2. Materials and Methods

5.2.1. Chemicals

The chemicals and reagents with their source information have been mentioned in previous chapters. The remaining chemicals i.e., Phenanthrene (RM2369-25G), Hexadecane (RM2238-100ML) were purchased from HiMedia, India.

5.2.2. Microorganism and growth conditions

Three bacterial genera were individually enriched in BH agar plates with 0.1 % (v/v) crude oil as the sole C source. The plates were incubated overnight at 25°C, and single colonies were picked using a sterile loop and inoculated in sterile NB followed by incubation in a shaker incubator maintained at 180 rpm and 25°C. Later, the bacteria were recovered using centrifugation and resuspended in sterile distilled water to an OD of 1 (1.4×10^7 CFU/mL) and then used as inoculum for biodegradation studies.

5.2.3. Microbial hydrocarbon biodegradation studies

HEX and PHE were chosen as model aliphatic and aromatic hydrocarbons. Three bacterial strains, namely *Agrobacterium fabrum* SLAJ 731, *Pseudomonas aeruginosa* P7815 and *Bacillus subtilis* RSL2, were selected based on their hydrocarbon degradation ability using crude oil as their C source in previous studies (Sharma et al., 2019; Sharma et al., 2018; Verma et al., 2020). The experiments systematically studied microcosm and individual bacterial growth and biodegradation ability using an individual hydrocarbon as the sole C source. In the next step, the mixture of both the hydrocarbons was tested for biodegradation using all three bacteria and their microcosm. A similar control experiment was performed without inoculum to consider the hydrocarbon degradation due to abiotic (physical and chemical) factors such as dispersion, evaporation, dissolution, sorption, photo-oxidation, and auto-oxidation.

The bacterial inoculum was inoculated at 10 % (v/v) of concentration to sterile BH broth containing an additional 50 ppm yeast extract with HEX or PHE or both and incubated at 25 °C 180 rpm for 7 days until the bacteria reached their death phase. The average total petroleum hydrocarbon concentration at crude oil contaminated sites has been reported to be approximately in the range of 2 to 50 ppm (Gaur et al., 2021; Kriipsalu et al., 2008; KURNAZ and BÜYÜKGÜNGÖR, 2016; Nganje et al., 2007); thus initial hydrocarbon concentration was selected as 50 ppm in the case of the solo substrate and 25 ppm of each in the binary mixture. The bacterial growth was estimated by dry cell weight (DCW) measurement during the incubation period. The bacterial culture was centrifuged at regular intervals, and the pellet was recovered, washed, and allowed to dry overnight. The bacterial death was inferred from the reduction in the dry cell weight of the biomass due to cell lysis leading to the release of intracellular content, which was observed as a loss in biomass gravimetric weight (Liu, 2017). The specific growth rate (μ) was calculated using **equation 5.1**. Here X is the DCW of bacteria expressed in mg/L at a given time 't' (h), and the slope refers to μ (h^{-1}).

$$\boldsymbol{lnX = \mu t} \qquad \textbf{(5.1)}$$

Similar to the aforementioned axenic biodegradation study, an equal volume of each bacterial strain at OD of 1 was used to prepare a 10 % (v/v) bacterial inoculum to study hydrocarbon degradation using microconsortium (MCM). The degradation kinetics was analyzed by analyzing residual hydrocarbon and degradative enzymes. The cell-free supernatant's surface tension was measured using a Du Nouy ring method using a tensiometer (Dataphysics, DCAT 11 EC) at 25 °C, as discussed in Chapter 3, section 3.2.4.2.

5.2.4. Estimation of residual hydrocarbon

The cell-free supernatant was used to estimate bacterial hydrocarbon biodegradation activity at regular time intervals. The residual hydrocarbon was extracted in an equal volume of chloroform and separated using a separating funnel. The extracted organic layer was investigated for the concentration of residual HEX concentration using Gas Chromatography-Flame ionization detector instrument (GC-FID, Varian 450) equipped with Sil-8 CB column (30 m × 0.25 mm × 2.5 µm). The program used for this measurement included an injector temperature of 250 °C and detector temperature of 280 °C. 1 µL of sample previously extracted in chloroform was injected into the column. The standard curve was prepared by dissolving commercial HEX in chloroform prepared in different concentrations (0 to 50 ppm). The initial temperature of the column oven was maintained at 60 °C, raised at ramping of 20 °C/min to 190 °C followed by ramping of 10 °C/min till 280 °C. Helium gas was used as carrier gas maintained at a 1:50 split ratio.

Similarly, the residual PHE concentration was determined using a High-performance liquid chromatography instrument (HPLC, Shimadzu LC300) equipped with a PFP-C18 column (ACE®) and UV detector (254 nm). The column oven was maintained at 30 °C. The analysis used the isocratic mobile phase containing methanol: water (90:10) with 0.1 % trifluoroacetic acid (TFA) at a flow rate of 0.6 mL/min. The standard curve was prepared by dissolving commercial PHE in chloroform prepared in different concentrations (0 to 60 ppm) with a sample injection volume of 20 µL. The samples were prepared in chloroform, and an acquisition time of 30 min was maintained for each sample analysis (Wang et al., 2010).

5.2.5. Kinetics of hydrocarbon degradation

Various literature suggested the first-order exponential decay model (Hajieghrari and Hejazi, 2020) and Monod's model (Chettri and Singh, 2019) for the hydrocarbon degradation analyses. For the present study, the concentration of residual hydrocarbon at the regular time was calculated using chromatogram peak area analyses. The abiotic hydrocarbon degradation was fitted to a first-order kinetic model **(equation 5.2)** as expressed below.

$$C_t = C_0 e^{-k_1 t} \quad \textbf{(5.2)}$$

C_t and C_o refer to residual hydrocarbon concentration at the time 't' (h) and at 't = 0' and k_1 represented the abiotic hydrocarbon degradation rate. While for analyzing the biodegradation kinetics, Monod's equation was integrated with the first-order equation to represent bacterial and abiotic degradation, respectively (**equations 5.3 and 5.4**).

$$C_t = C_1 e^{-k_1 t} + C_2 e^{\frac{-k_d X t}{k_s}} \quad \textbf{(5.3)}$$

$$C_0 = C_1 + C_2 \quad \textbf{(5.4)}$$

Here, C_1 and C_2 refer to hydrocarbon (g/L) concentrations subjected to abiotic losses and microbial biodegradation, respectively. X is the concentration of biomass (g/L). k_d and k_s represent microbial hydrocarbon biodegradation rate and half-saturation constant, respectively. In the Monod equation k_s was assumed to be much greater than C ($k_s >> C$). The k_1 value was obtained by fitting abiotic data to **equation 5.2**. The microbial biodegradation data were fitted to **equations 5.3** and **5.4** to determine the values of C_2, k_d and k_s. The value of C_0 was 50 ppm for the degradation of individual hydrocarbons and 25 ppm in the case of a binary mixture. Further, the overall bacterial biodegradation percentage was calculated after 7 days of incubation period using **equation 5.5**. Here C_0 and C_t refer to the initial hydrocarbon concentration and residual hydrocarbon at day 7, respectively.

$$\textit{Overall biodegradation}(\%) = \frac{(C_0 - C_t)}{C_0} \times 100 \quad \textbf{(5.5)}$$

5.2.6. Degradative enzymes activity determination

The bacterial enzyme activity in the presence of different hydrocarbons was estimated by harvesting cells using centrifugation (8000 rpm for 10 min) at regular time intervals. The pellets were washed and resuspended in 20 mM Tris HCl (pH 7.4) in the case for aliphatic hydrocarbon-degrading enzymes estimation and 50 mM PBS buffer (pH 7.4) for aromatics degradative enzymes. Next, the cells were lysed using ultrasonication with a 20 kHz frequency (20 cycles with 10 seconds breaks). The required enzyme crude extract was then recovered using centrifugation at 11,400 rpm for 45 min at 4°C and used for further enzyme analysis.

The AH activity analysis was performed as mentioned in Chapter 3, section 3.2.6. Overall, 1 unit of enzyme activity was estimated as the enzyme responsible for the oxidation of 1 mM NADH per min . The activity of C23DO was analyzed by investigating the formation of 2-hydroxymuconic semialdehyde in the reaction mixture using catechol as substrate. It was observed as an increase in the absorbance at 375 nm. Each 1 mL reaction mixture contained 100 µL of 50 mM catechol and 100 µL of crude enzyme extract in 50 mM PBS buffer. As previously reported in the literature, the enzyme activity was expressed as a catechol (mM) concentration oxidized per minute (Elumalai et al., 2021).

5.2.7. Statistical analysis

The statistical significance of experimental data was estimated using the analysis of variance (ANOVA) technique using OriginPro 8.5 software. All biodegradation studies were performed in triplicates, and their mean value ± standard deviation is reported.

5.3. Results and discussion

5.3.1. Biodegradation of HEX

The growth and biodegradation ability of selected bacterial strains as axenic culture and consortium were investigated in the presence of 50 ppm HEX as a sole C source during 7 days of the incubation period, as presented in **Figure 5.1(A)**. A small lag phase suggested bacteria's acclimatization to initial hydrocarbon concentration. The axenic cultures showed an extended exponential phase till day 2, suggesting a slightly slower growth rate of bacteria in axenic forms. *Bacillus subtilis* RSL2 showed

higher growth among the axenic cultures than the other two genera. The μ values were obtained as 0.07 ± 0.002, 0.06 ± 0.002 and 0.05 ± 0.004 h^{-1} for *Bacillus*, *Pseudomonas* and *Agrobacterium*, respectively. In contrast, microconsortium showed the highest exponential growth within 24 h, and the μ value was found to be 0.12 ± 0.005 h^{-1} underscoring the effectiveness of selected bacterial strains in utilizing HEX as their sole C and energy source. Further, the stationary phase was not observed in the case of axenic cultures presumably due to the accumulation of toxic by-products; however, microconsortium showed the stationary phase (~ extending for 24 h). This can be related to the ability of mixed cultures to better metabolize toxic by-products (Osborne et al., 2021).

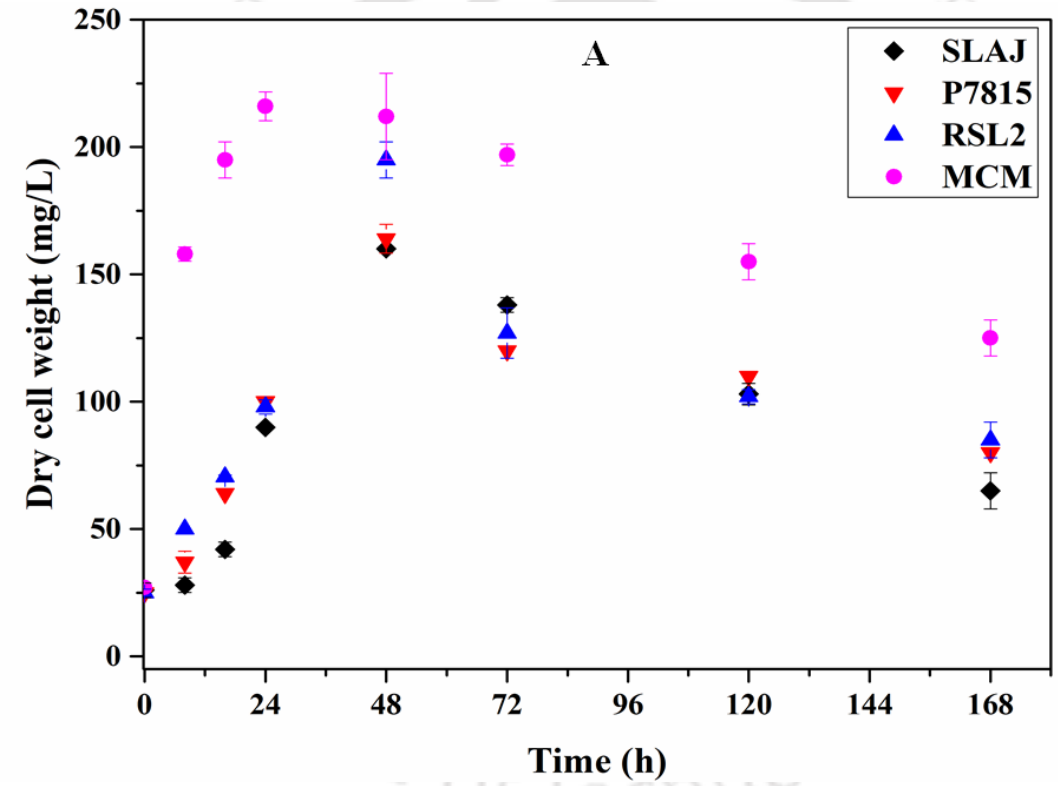

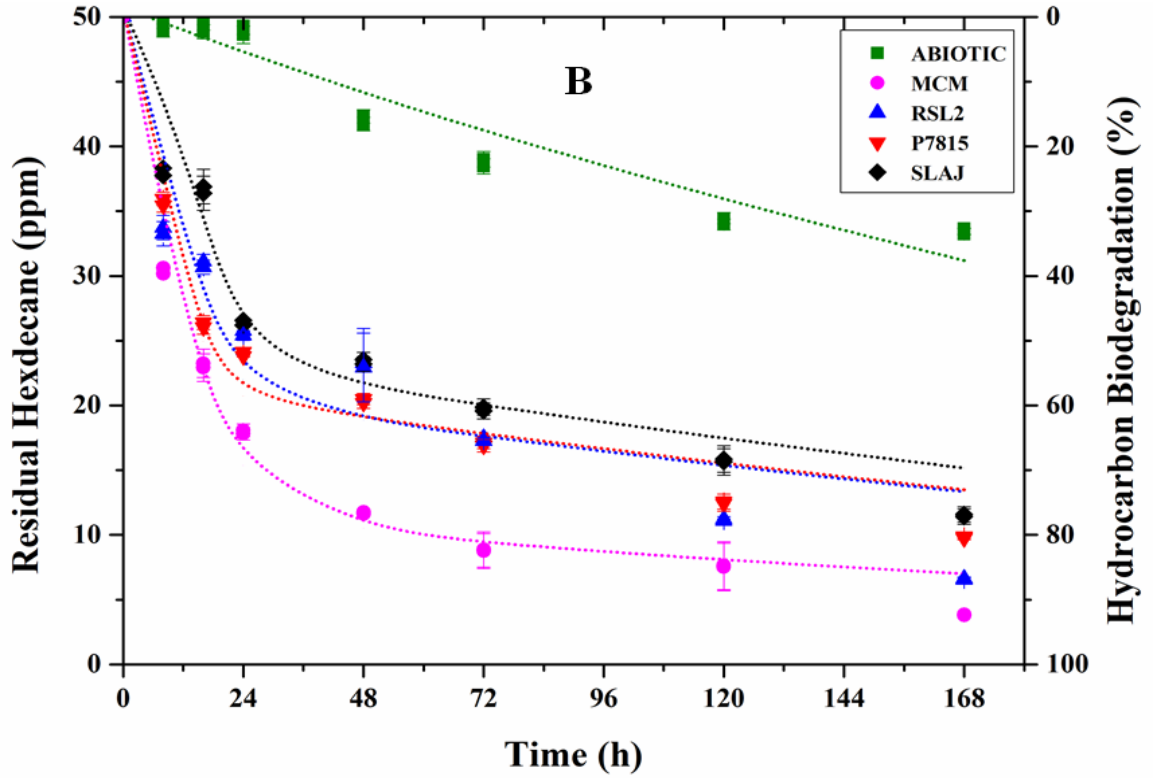

Figure 5.1. (A) Growth profile, and (B) Residual HEX concentration of axenic culture of *Agrobacterium fabrum* SLAJ731, *Pseudomonas aeruginosa* P7815, *Bacillus subtilis* RSL2 and their microconsortium (MCM) using 50 ppm of HEX as sole C source.

The residual HEX was measured to analyze the degradation behavior as shown in **Figure 5.1(B)**. The overall HEX biodegradation (%) were 77.2 ± 1.2, 80.5 ± 0.2, and 86.9 ± 0.3 % for *Agrobacterium fabrum* SLAJ731, *Pseudomonas aeruginosa* P7815, and *Bacillus subtilis* RSL 2, respectively, which further enhanced to 92.4 ± 0.3 % in case of microconsortium. In contrast, the abiotic factor led to only 33.6 ± 0.3 % loss of HEX. Thus, higher microbial growth facilitated biodegradation efficiency of the bacteria as reported in other studies (Abdel-Megeed et al., 2010; Cerqueira et al., 2011). The increased biodegradation ability of HEX in the microconsortium of *Bacillus subtilis* and *Pseudomonas aeruginosa* was reported elsewhere (Dehghani et al., 2018; Nozari et al., 2018). *Bacillus* species are found to be a better degrader of HEX as compared to *Agrobacterium* and *Pseudomonas* species. Hakima et al. reported an improved biodegradation ability of 70 % in *Bacillus* for medium aliphatic hydrocarbons (C15- C20) than *Pseudomonas* (49 %) (Hakima and Ian, 2017). Safitri et al. reported the HEX

biodegradation ability of *Bacillus subtilis* and *Pseudomonas aeruginos*a as 46.76 and 44.13 %, respectively, which increased to 47.19 % when used as a microconsortium (Safitri et al., 2018). Saimmai et al. also explored the effectiveness of biodegradation of diesel oil using a microconsortium of *Bacillus, Agrobacterium, Chryseobacterium* and *Sphingobacterium.* These observations suggest the potential synergistic contributions of *Agrobacterium, Pseudomonas* and *Bacillus* genera in hydrocarbon (alkane) biodegradation (Saimmai et al., 2012).

These findings were also supported by the reduction in surface tension data. The selected strains have been found to be biosurfactant producers during the degradation of hydrocarbons. The lowest surface tension (mN/m) was observed for microcosm (33 ± 0.5) followed by *Bacillus subtilis* RSL 2 (34 ± 0.4), *Pseudomonas aeruginosa* P7815 (44 ± 1) and *Agrobacterium fabrum* SLAJ731 (46 ± 1). The decrease in surface tension followed the reverse trend of % degradation. The lowest surface tension value in the case of microcosm corresponded to the maximum biodegradation.

Further, understanding the kinetics of HEX biodegradation in the axenic cultures and their consortium was explored. The residual concentration of HEX during the abiotic decay and biodegradation were fitted with the first-order kinetic model (equation 2) and the Monod equation combined with the first-order equation (equation 3), respectively. The experimental data fitted well with the proposed models with R^2 values ≥ 0.91. The estimated kinetic parameters for HEX degradation are summarized in **Table 5.1.** The abiotic decay rate (k_1) was 2.89E-03 ± 3.97E-06 h^{-1}. On the other hand, the biodegradation rates for the axenic cultures were enhanced by many folds and found to be 0.39 ± 0.02 h^{-1}, 0.49 ± 0.03 h^{-1}, 0.46 ± 0.02 h^{-1} for *Agrobacterium fabrum* SLAJ731, *Pseudomonas aeruginosa* P7815 and *Bacillus subtilis* RSL 2, respectively. However, the biodegradation rate of HEX in the microconsortium was reduced to 0.31 ± 0.02 h^{-1}, which suggested the possible parallel processing of HEX within the species of the microconsortium. Thus, individual bacteria encountered lesser initial HEX concentrations. Such distribution of HEX also indicated that each species followed its own pathways for HEX biodegradation. Although a reduced rate of degradation was observed **(equation 5.6)**, but the cumulative utilization (degradation) was enhanced resulting in the maximum degradation. In fact, the value of C_2 was the highest in the case of microconsortium (**Table 5.1**). The C_2 value for microcosm was increased by 1.4 to 1.5 folds as compared to that of axenic cultures.

$$\frac{1}{k_{D-MCM}} \approx \frac{1}{k_{D-SLAJ}} + \frac{1}{k_{D-P7815}} + \frac{1}{k_{D-RSL2}} \quad \textbf{(5.6)}$$

Furthermore, the time required for 90 % biodegradation (t_{90}) of 50 ppm HEX by the abiotic as well as microconsortium was calculated from the estimated kinetic parameters listed in **Table 5.3**. The t_{90} values were determined to be 34 ± 3 days for the abiotic, which decreased to 12 ± 2 days in the case of the microcosm. The t_{90} values for the axenic cultures were 23 ± 1, 20 ± 1, and 20 ± 1 days for *Agrobacterium fabrum* SLAJ731, *Pseudomonas aeruginosa* P7815 and *Bacillus subtilis* RSL 2, respectively. It indicated the suitability of the microcosm for the biodegradation of aliphatic hydrocarbons.

Table 5.1. Kinetic parameters for the integrated first order exponential decay and Monod degradation model for individual hydrocarbons as sole C substrate

Substrates	**Inoculum used**	**C_1 (ppm)**	**C_2 (ppm)**	**K_d (h^{-1})**	**K_s (ppm)**	**R^2**
Only HEX (50 ppm)	**MCM**	11.34 ± 1.50	39.38 ± 1.49	0.31 ± 0.02	765 ± 2.1	0.98
	RSL2	21.69 ± 1.35	29.02 ± 1.34	0.46 ± 0.02	385 ± 84.0	0.91
	P7815	21.93 ± 0.38	28.78 ± 0.37	0.49 ± 0.03	254 ± 35.8	0.97
	SLAJ	24.64 ± 0.06	26.07 ± 0.06	0.39 ± 0.02	312 ± 1.0	0.96
Only PHE (50 ppm)	**MCM**	8.22 ± 0.04	42.44 ± 0.04	1.94 ± 0.05	542 ± 27.4	0.99
	RSL2	10.2 ± 0.10	40.47 ± 0.18	2.24 ± 0.08	530 ± 28.7	0.99
	P7815	11.5 ± 0.26	39.15 ± 0.18	1.49 ± 0.01	615 ± 15.1	0.99
	SLAJ	13.28 ± 0.39	37.38 ± 0.31	2.05 ± 0.11	462 ± 70.3	0.99

5.3.2. Biodegradation of PHE

Bacterial growth and biodegradation ability were further explored for a model aromatic hydrocarbon, PHE. In 7-days of degradation study, individual bacterial strains and microconsortium were inoculated

in BH medium with 50 ppm of PHE as the sole C source. The bacterial growth profile is shown in **Figure 5.2(A)**. An extended growth phase till 3rd day of incubation was observed, which indicated that the selected bacterial strains preferred low molecular weight aromatic hydrocarbons to high molecular weight aliphatic hydrocarbons. The yield of biomass was higher in PHE than HEX as C source. Among the axenic cultures, a similar specific growth rate was observed in *Bacillus* with $\mu = 0.12 \pm 0.01\ h^{-1}$ and *Agrobacterium* exhibiting μ of $0.11 \pm 0.004\ h^{-1}$, followed by *Pseudomonas* exhibiting μ of $0.09 \pm 0.003\ h^{-1}$. In corroboration with present results, various studies also reported the better ability of *Bacillus* genus to utilize aromatic hydrocarbons compared to *Pseudomonas* (Das and Mukherjee, 2007; Rabodonirina et al., 2019). Further, the μ value was observed to be slightly higher in the microcosm as $0.13 \pm 0.003\ h^{-1}$.

Overall, PHE biodegradation at the end of the 7th day of incubation followed the order of *Agrobacterium fabrum* SLAJ731 (85.2 ± 1.3 %) < *Pseudomonas aeruginosa* P7815 (85.4 ± 0.6 %) < *Bacillus subtilis* RSL 2 (87.1± 0.1 %) < microconsortium (88.7 ± 0.3 %) as shown in **Figure 5.2(B)**. While only 31.86 % of the abiotic loss was observed for the PHE during the control study. The highest degradation in the case of the microcosm is related to the maximum biomass yield (**Figure 5.2(A)**). Further, the degradation was corroborated with the reduction in surface tension of cell-free culture medium. The surface tension (mN/m) values followed the same order of the % degradation as *Agrobacterium fabrum* SLAJ731 (52.04 ± 0.5) < *Pseudomonas aeruginosa* P7815 (49.4 ± 0.5) < *Bacillus subtilis* RSL 2 (47.05 ± 0.5) < microconsortium (40.1 ± 0.4).

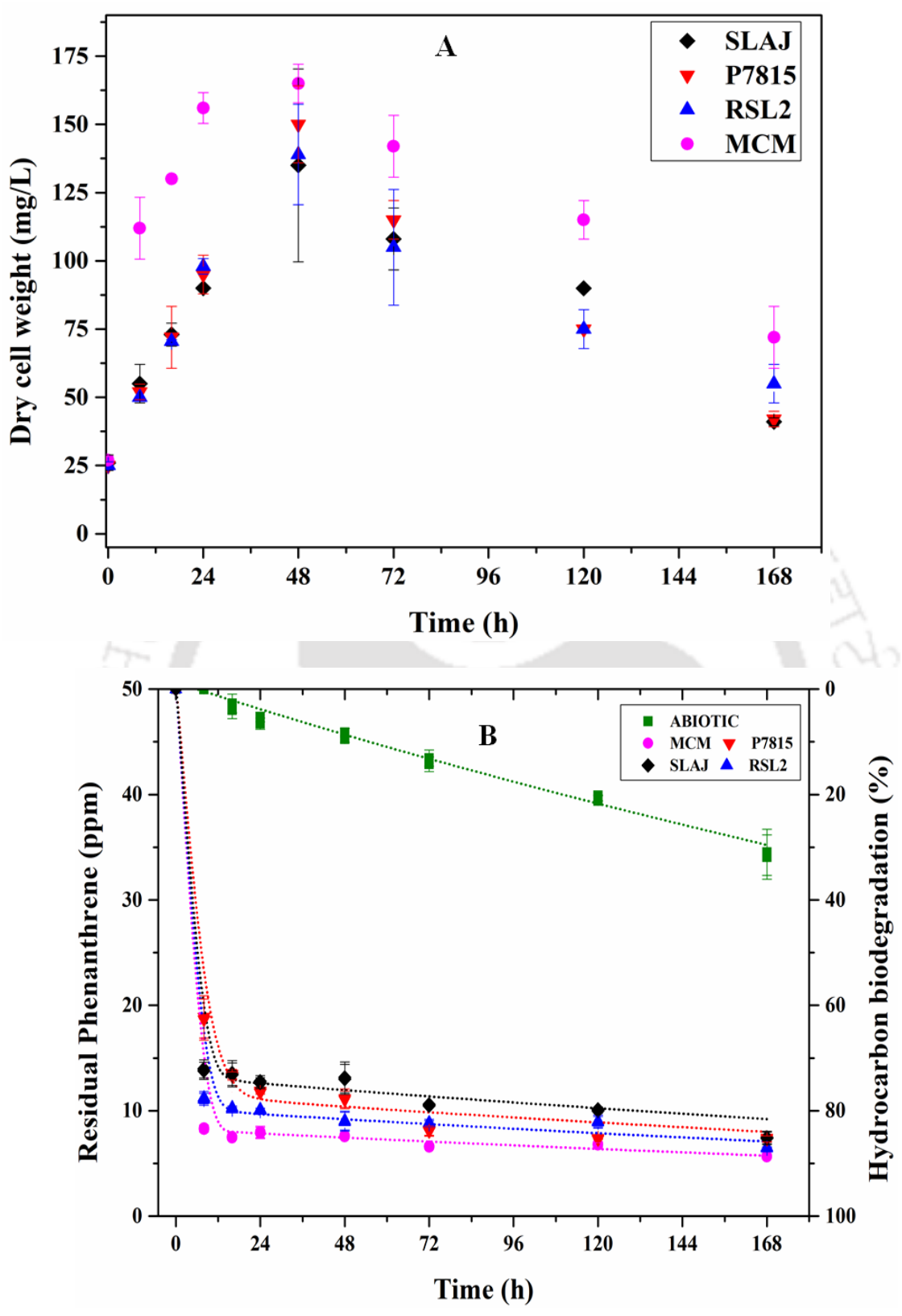

Figure 5.2. (A) Growth profile, and (B) Residual PHE concentration of axenic culture of *Agrobacterium fabrum* SLAJ731, *Pseudomonas aeruginosa* P7815, *Bacillus subtilis* RSL2 and their microconsortium (MCM) using 50 ppm of PHE as sole C source.

Similar to HEX biodegradation kinetics, first-order exponential decay kinetics fitted well for residual PHE concentration in the case of abiotic PHE degradation (R^2 = 0.99), as evidenced in different literature (Chettri and Singh, 2019; Ghorbannezhad et al., 2021). The k_1 value for abiotic PHE decay was obtained as 2.17E-03 ± 2.09E-04 h^{-1}. The Monod equation combined with the first-order equation fitted well to the microbial biodegradation with $R^2 \geq 0.99$. **Table 5.1** lists the fitted kinetic parameters for the PHE biodegradation. The k_d values for *Bacillus subtilis* RSL2, *Pseudomonas aeruginosa* P7815, and *Agrobacterium fabrum* SLAJ731 were estimated as 2.24 ± 0.08 h^{-1}, 1.49 ± 0.01 h^{-1}, 2.05 ± 0.1 h^{-1}, respectively. The obtained degradation rates were much higher as reported in the literature. Rabodonirina et al. explored the PHE biodegradation ability of *Bacillus simplex, Pseudomonas stutzeri* and *Bacillus pumilus* strains and reported the k_d value of 0.0121, 0.0083 and 0.0108 h^{-1}, respectively, using 500 mg/kg of the initial PHE concentration (Rabodonirina et al., 2019). Further, the PHE biodegradation rate in the microconsortium was found to be 1.94 ± 0.05 h^{-1} which was deciphered to be an average of the individual bacterial degradation rates **(equation 5.7)**.

$$k_{D-MCM} \approx \frac{k_{D-SLAJ}+k_{D-P7815}+k_{D-RSL2}}{3} \quad \textbf{(5.7)}$$

It suggested that PHE was serially processed by the microconsortium, where each bacteria followed the same pathways for PHE degradation in the consortium. Overall, the obtained PHE degradation rate was found to be much improved than various reported microconsortium in the literature. Bianco et al. also explored a microconsortium comprising *Achromobacter, Sphingobacterium* and *Dysgonomonas* for PHE biodegradation at the initial concentration of 50 ppm in a fed-batch bioreactor and reported the k_d value of 0.05 h^{-1} (Bianco et al., 2022). Another group studied a microconsortium of four bacterial strains, namely, *Sphingomonas cloacae* W4-1 *Rhizobium sp.* W4-2, *Pseudomonas aeruginosa* W4-3, and *Achromobacter xylosoxidants* W4-4 for the biodegradation of 200 ppm of PHE where the overall PHE degradation rate was reported as 0.023 h^{-1} (Wang et al., 2007)**.**

Furthermore, the time required for 90 % biodegradation (t_{90}) of 50 ppm PHE by the abiotic as well as microconsortium was calculated from the estimated kinetic parameters listed in **Table 5.3**. The t_{90}

values were determined to be 45 ± 5 days for the abiotic, which decreased to 10 ± 1 days in the case of the microcosm i.e., five times faster degradation. The t_{90} values for the axenic cultures were 19 ± 2, 15 ± 1, and 14 ± 2 days for *Agrobacterium fabrum* SLAJ731, *Pseudomonas aeruginosa* P7815 and *Bacillus subtilis* RSL 2, respectively. This indicated the suitability of the microcosm for the biodegradation of aromatic hydrocarbons.

5.3.3. Biodegradation of the binary mixture of substrates

With the understanding of bacterial consortium ability to biodegrade the aliphatic and aromatic hydrocarbons, a further investigation of the biodegradation ability of selected bacteria in the presence of co-contaminants was performed. For this, individual strains and microcosm were inoculated with a binary mixture of 25 ppm HEX and PHE each and incubated under previously mentioned conditions. The biomass growth profile is shown in **Figure 5.3(A)**, where the specific growth rate of microconsortium, *Agrobacterium fabrum*, *Pseudomonas aeruginosa* and *Bacillus subtilis* in the presence of co-substrates were obtained as 0.098 ± 0.003, 0.065 ± 0.003, 0.066 ± 0.006, and 0.065 ± 0.003 h^{-1}, respectively. The values of μ were found to be intermediate between individual substrates, which indicated the presence of binary substrates.

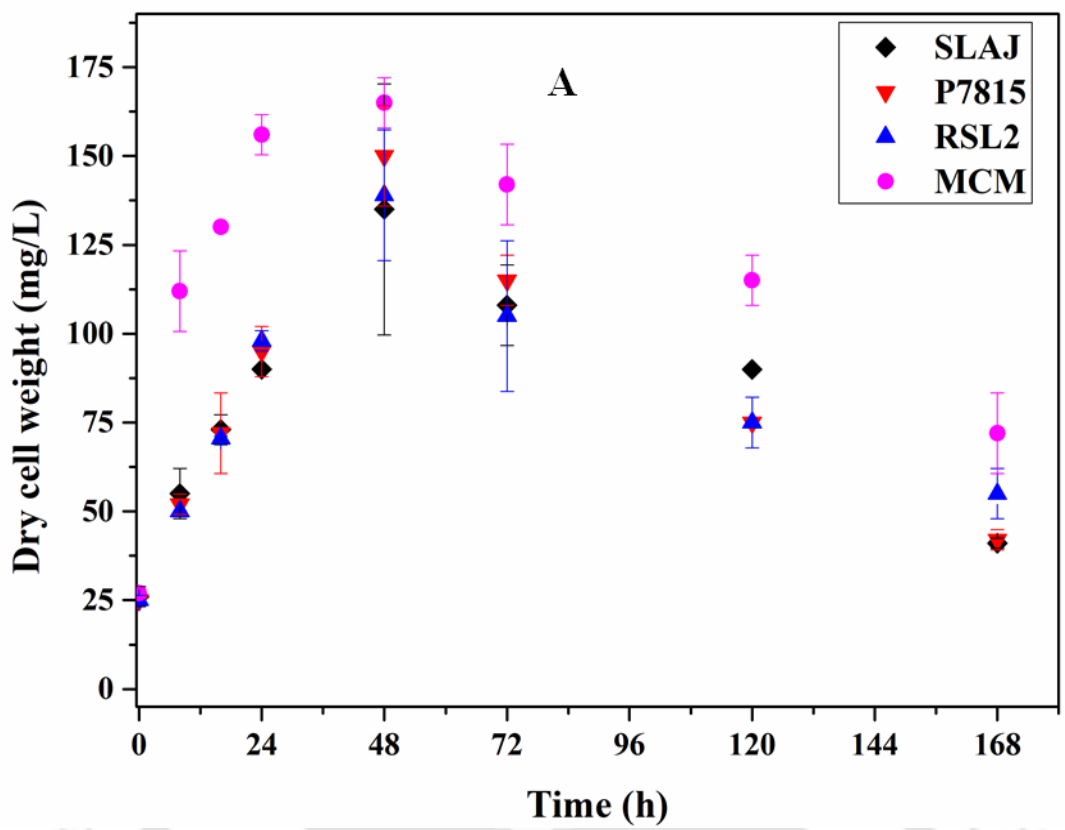

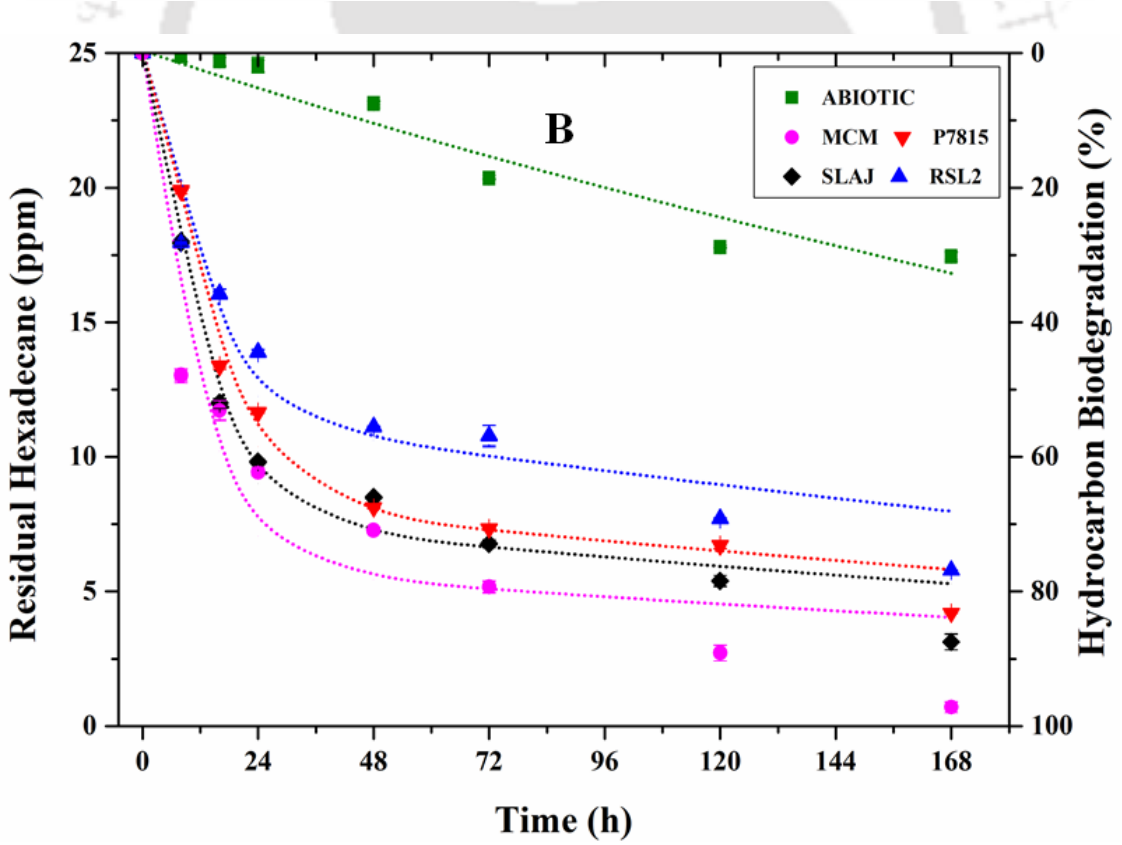

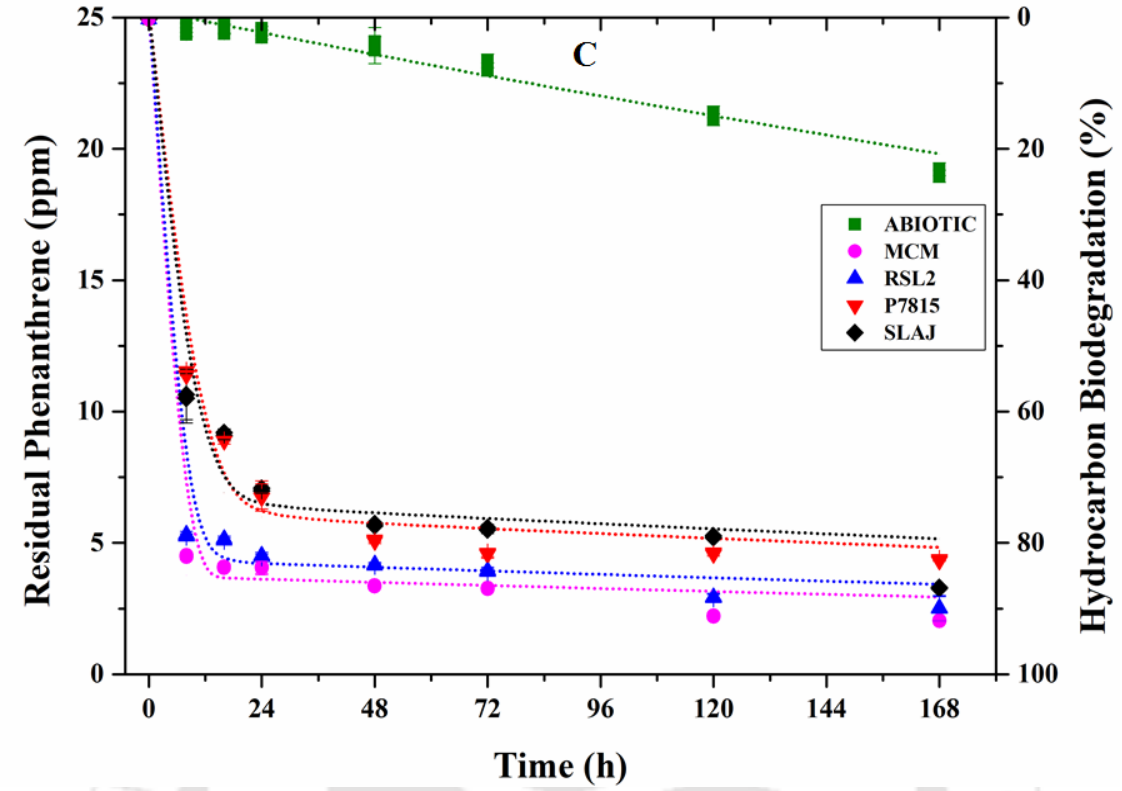

Figure 5.3. (A) Growth profile, and (B) Residual HEX and (C) PHE concentration of axenic culture of *Agrobacterium fabrum* SLAJ731, *Pseudomonas aeruginosa* P7815, *Bacillus subtilis* RSL2 and their microconsortium (MCM) using binary mixture (HEX+PHE, 25 ppm each) as sole C source

The mixed substrate biodegradation ability in the axenic cultures was also assessed based on their residual hydrocarbon concentration at regular time intervals, as shown in **Figures 5.3(B) and 5.3(C).** The kinetic data were fitted to equations 5.2 and 5.3 for abiotic and microbial degradation, respectively. The estimated kinetic parameters regulating co-substrate degradation are listed in **Table 5.2.** The abiotic with the decay rate, k_1 for HEX and PHE were 2.38E-03 ± 1.85E-05 h^{-1} and 1.45E-03 ± 8.99E-05 h^{-1}, respectively. The HEX biodegradation rates (k_d) in axenic cultures using binary substrates were obtained as 0.43 ± 0.003 h^{-1} for *Agrobacterium fabrum*, 0.38 ± 0.007 h^{-1} for *Pseudomonas aeruginosa*, and 0.41 ± 0.004 h^{-1} for *Bacillus subtilis.* Similarly, the PHE biodegradation rates (k_d) were 2.02 ± 0.1 h^{-1} for *Agrobacterium fabrum*, 1.75 ± 0.06 h^{-1} for *Pseudomonas aeruginosa* 2.46 ± 0.05 h^{-1} for *Bacillus subtilis* in the axenic cultures using binary substrates.

The k_d values in the case of microconsortium for HEX and PHE were 0.28 ± 0.003 h^{-1} and 2.14 ± 0.08 h^{-1}, respectively. Similar to the sole PHE biodegradation kinetics, in the presence of HEX as co-substrate

also the microconsortium showed a serial degradation behavior and the degradation rate was equivalent to the average of individual axenic rates. Likewise, HEX followed a parallel biodegradation pattern in the presence of PHE. Additionally, it was noted that the biodegradation rate of individual hydrocarbon in the mixture was improved in the presence of binary substrates. The degradation rates were higher for PHE as compared to that of HEX, suggesting that selected strains showed a preference for aromatic hydrocarbons over aliphatic in the mixed substrates, which could be due to bacterial machinery to utilize the PHE as discussed in the next section (Cavalca et al., 2008). In contrast, various findings state that bacteria prefer aliphatic than aromatics when present in a mixture (Tao et al., 2020; Zhou et al., 2018). This insight was deciphered by measuring the activities of key enzymes (section 5.3.4).

Table 5.2. Fitted hydrocarbon biodegradation kinetic parameters using the integrated first order exponential decay and Monod degradation model for the binary mixture of HEX and PHE as C substrate

Substrates (Binary mixture)	**Inoculum used**	**C_1 (ppm)**	**C_2 (ppm)**	**K_d (h^{-1})**	**K_s (ppm)**	**R^2**
HEX (25 ppm)	**MCM**	6.01 ± 0.04	19.07 ± 0.08	0.28 ± 0.01	401 ± 6.0	0.92
	RSL2	11.89 ± 0.07	13.20 ± 0.11	0.41 ± 0.01	377 ± 10.0	0.95
	P7815	8.62 ± 0.04	16.47 ± 0.01	0.38 ± 0.01	437 ± 48.3	0.99
	SLAJ	7.86 ± 0.11	17.22 ± 0.07	0.43 ± 0.01	387 ± 49.3	0.98
PHE (25 ppm)	**MCM**	3.58 ± 0.04	21.71 ± 0.13	2.14 ± 0.08	626 ± 95.6	0.99
	RSL2	4.35 ± 0.04	20.94 ± 0.05	2.46 ± 0.05	334 ± 1.0	0.99
	P7815	6.16 ± 0.11	19.14 ± 0.02	1.75 ± 0.06	654 ± 26.0	0.98
	SLAJ	6.56 ± 0.15	18.73 ± 0.07	2.02 ± 0.11	661 ± 195.5	0.97

In the binary mixture, the overall HEX biodegradation (%) followed the order of: microconsortium (97.2 ± 0.7) > *Agrobacterium fabrum* (87.5 ± 1.2) > *Pseudomonas aeruginosa* (83.3 ± 0.5) > *Bacillus subtilis* RSL2 (76.9 ± 0.5). The biodegradation (%) of PHE varied as microconsortium (91.9 ± 0.3) > Bacillus *subtilis* RSL2 (90.0 ± 1.83) > *Agrobacterium fabrum* (86.9 ± 0.5) > *Pseudomonas aeruginosa*

(82.7 ± 0.5). The overall degradation of individual substrates from the mixtures followed different orders as compared to that from the single substrates. This indicated the competitive utilization of substrates from their mixture. Nevertheless, the microconsortium exhibited the maximum overall biodegradation for HEX and PHE when present as co-substrates. The degradation performance was also correlated with the decrease in the surface tension, which was found to be 50.00 ± 1.0, 46.26 ± 1.0, 42.2 ± 0.5, and 40.12 ± 0.5 mN/m for *Agrobacterium*, *Pseudomonas*, *Bacillus* and microcosm, respectively. Thus, from the perspective of bioremediation of hydrocarbon-contaminated sites, the designed microconsortium has shown great potential for the remediation of contaminated soil and water systems where a mixture of aliphatic and aromatic hydrocarbons exists.

5.3.4. Insights into hydrocarbon biodegradation

Various factors account for hydrocarbon biodegradation, such as microbial load and catabolic enzyme activities. Many studies focus on optimizing bacterial growth conditions for achieving its maximum biodegradation activity (Elumalai et al., 2021; Parthipan et al., 2017). Thus, the effect of the bacterial growth rate, μ, on its hydrocarbon biodegradation ability was explored, as shown in **Figure 5.4(A).** It was observed that the hydrocarbon biodegradation was linearly dependent on the bacterial μ, where the higher biodegradation was achieved for the microbial consortium as it showed the maximum growth rate. Though biodegradation is accompanied by biomass growth, it is not only limited to higher biomass yield (Ghorbannezhad et al., 2021). Apart from the microbial load, the presence of hydrocarbon catabolizing enzymes also regulates the metabolism of hydrocarbons.

Bacterial genera such as *Pseudomonas* and *Bacillus* have been studied extensively for aliphatic and aromatic hydrocarbon degradation metabolic pathways (Meng et al., 2017). Majorly reported aliphatic hydrocarbon biodegrading enzymes are (a) Methane monooxygenase (for C1-C4), (b) Cytochrome P450 monooxygenases, (for C6-C11), and (c) Bacterial AH (AlkB) (for C5-C26), (Scoma et al., 2017). Alkane hydroxylase has been well-reported for biodegradation of HEX (C16), involving oxidation of HEX to hexadecanol, which is further converted to hexadecanal, followed by oxidation to hexadecanoic acid in the presence of AH, alcohol dehydrogenase and aldehyde dehydrogenase enzymes, respectively. The oxidized hydrocarbon is then catalyzed by acyl CoA synthetase to form acyl-CoA derivative, which

is converted to acetyl CoA via β-oxidation. This is followed by tricarboxylic acid cycle (TCA) resulting in the release of energy, CO_2 and H_2O (Meng et al., 2017) (**Appendix 5A, Figure 5A-1)**.

Similarly, major reported aromatic hydrocarbon biodegrading enzymes are (1) Dioxygenases (present in bacteria and eukaryotic algae), (2) Cytochrome P-450 monooxygenase (present in non-ligninolytic fungi, bacteria and prokaryotic algae), and (3) Peroxidases (present in ligninolytic fungi) (Hwang et al., 2007). The formation of cis-dihydrodiols by ring hydroxylation of PAHs is the most common initiation pathway followed by bacteria using dioxygenases. The diol gets further rearomatized by dehydrogenases forming diol intermediates, followed by undergoing ortho or meta cleavage by dioxygenases. This forms intermediates such as protocatechuic acid or catechol that ultimately enters in TCA cycle (Monzón et al., 2018) (**Appendix 5A, Figure 5A-2)**. However, very few bacterial also exhibited PAHs biodegradation using cytochrome P450, such as *Mycobacterium* sp. (Kanaly and Harayama, 2010). Studies have revealed that the expression of these catabolic enzymes is dependent on the substrate type. Chettri et al. explored the activity of AH and C23DO in the presence of HEX, PHE and Glucose as substrates for bacteria *N. panipatense* P5:ABC. The activity of AH was reported to be enhanced by 2.5 folds in HEX as compared to glucose. Similarly, the activity of C23DO was increased by 12 folds in PHE as compared to glucose (Chettri and Singh, 2019). This suggested the key role of AH and C23DO enzymes in the metabolism of HEX and PHE, respectively. Thus, the present study explored the activity of these key enzymes (AH and C23DO) in the biodegradation of HEX and PHE.

Figure 5.4(B) depicts the activity of the enzymes AH and C23DO during the bacterial biodegradation of HEX and PHE as sole C sources. The activity of AH was comparable with reported data. Sumarsih et al. reported AH activity in *Pseudomonas* and *Bacillus* spp. in the presence of HEX as substrate as 3.96 and 3.86 µM/min, respectively (Sumarsih et al., 2017). Another study using *Alcanivorax borkumensis* showed a maximum AH activity of 2.62 µM/min using motor oil as substrate (Kadri et al., 2018). However, the activity was C23DO was improved as compared to the literature. All three bacterial strains showed higher activity for C23DO than AH (**Figure 5.4(B)**), suggesting their potential in aromatic hydrocarbons biodegradation. This agreed with the better degradation (%) of PHE than HEX (*Agrobacterium fabrum*: HEX = 77.2 % and PHE = 85.2 %, *Pseudomonas aeruginosa*: HEX = 80.5 %

and PHE = 85.4 %, *Bacillus subtilis*: HEX = 86.9 % and PHE = 87.1 %). Singh et al. reported the maximum C23DO activity of 30.21 ± 0.61 µM/min in *Pseudomonas* spp. using PHE as substrate (Singh and Tiwary, 2017). Similarly, Tavakoli et al. explored the C23DO activity among isolated bacterial strains from oil-contaminated soil, where the highest activity was obtained for *B. cereus* spp. as 0.03 µM/min (Tavakoli and Hamzah, 2017). Thus, presents bacterial strains showed better biodegradation abilities of aromatic hydrocarbon. These findings are significant since, compared to aliphatic, aromatic hydrocarbons are relatively more stable, recalcitrant, and less degradable. Various reports have shown the antibacterial (MIC = 2 to 8 µg/mL) (Chen et al., 2018) and cytotoxic effects of (IC_{50} < 3 µM) Phenanthrene derivatives (Bisoli et al., 2020). The present study proposes a potential PHE degrading consortium as a sustainable and eco-friendly solution to such hazardous contaminants. **Figure 5.4(B)** also depicts a correlation between C23DO and AH enzyme activities and the hydrocarbon (PHE/HEX) biodegradation. It was observed that there was a linear positive correlation between the maximum enzyme activity and biodegradation efficiency. This demonstrated that the presence of active enzymes could accelerate the overall biodegradation process as reported previously (Zhao et al., 2021). The highest values of enzyme activities in the case of microcosm indicated the synergistic effects of the selected strains towards overall biodegradation.

Overall, the obtained microconsortium hydrocarbon biodegradation was comparatively higher than various *Pseudomonas* sp. and *Bacillus* sp. consortiums reported in **Table 5.3**. Since much literature supports the suitability of hydrocarbon biodegradation as a first-order exponential decay model, the kinetic rates were calculated using the same and tabulated for comparison. Thus, present study has shown the potential of designed bacterial consortium for the biodegradation of HEX and PHE, which are majorly present among the aliphatic (C_{12}-C_{20}) and aromatic (C_{10}-C_{21}) fractions of crude oil. We will be further exploring the hydrocarbon biodegradation potential of designed microconsortium using Pentadecane ($C_{15}H_{32}$) and Eicosane ($C_{20}H_{42}$) among the aliphatic hydrocarbons and Naphthalene($C_{10}H_8$) and Pyrene ($C_{16}H_{10}$) aromatic hydrocarbons in future biodegradation studies. Exploration of various other enzymes such as Alcohol dehydrogenase and cytochrome P450 will be required to understand the metabolic pathway followed by the designed MCM in the future studies. Such insights are pre-requisite to explore the suitability of MCM in the *in-vitro* crude oil biodegradation study.

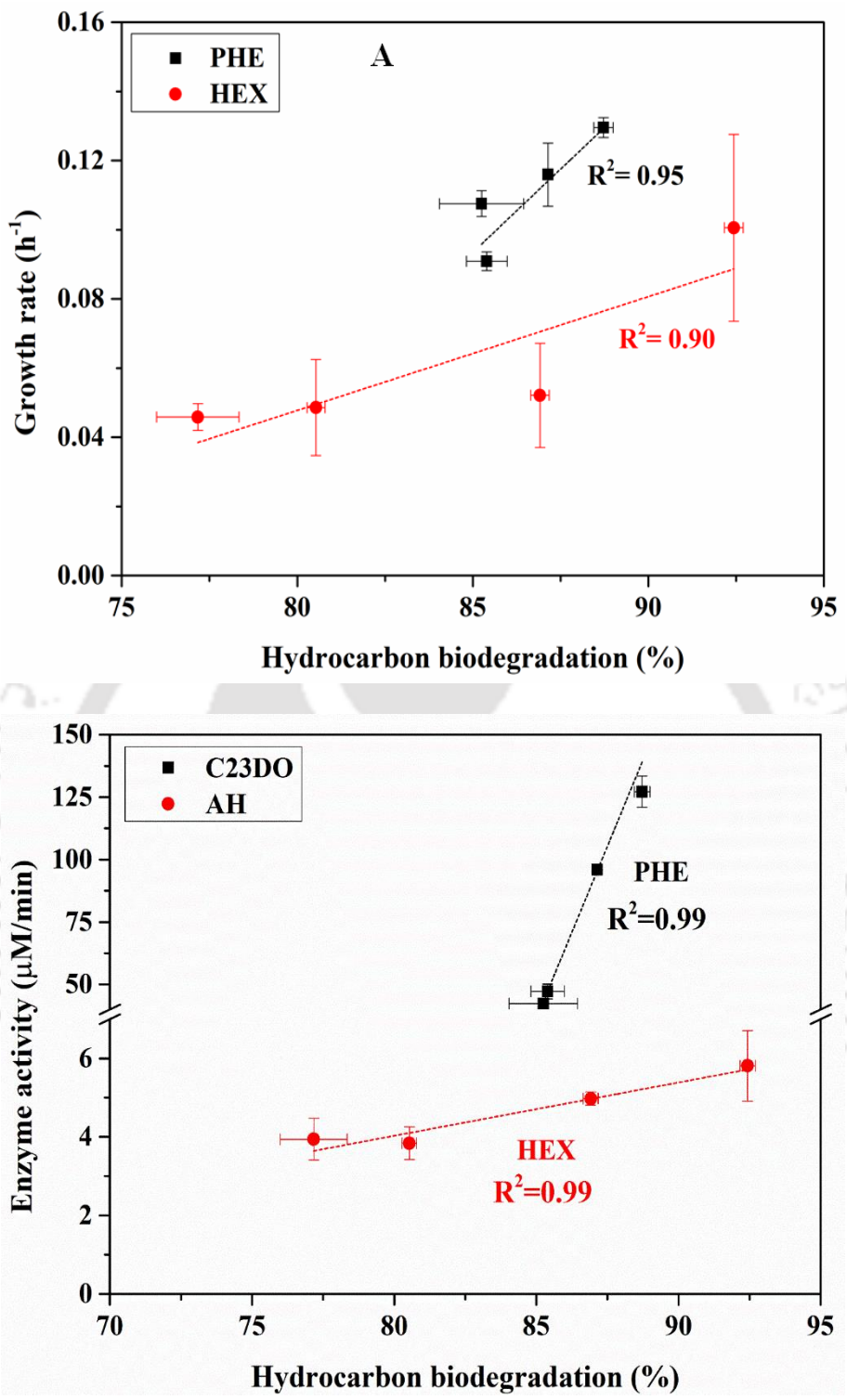

Figure 5.4. Analysing the effect of (A) bacterial growth rate; and (B) Enzyme activities of Alkane hydroxylase (AH) and Catechol 2,3-dioxygenase (C23DO) on the biodegradation of hydrocarbons (HEX and PHE)

Table 5.3. List of various bacteria explored for their Hexadecane and PHE biodegradation ability

S.no	*Inoculum studied*	Hydrocarbon	C_0	Degradation (%)	k_d (/day)	Ref
1	*Bacillus simplex* *Pseudomonas stutzeri* *Bacillus pumilus*	PHE	500 mg/kg	95.13 86.32 87.98	0.29 0.2 0.26	(Rabodonirina et al., 2019)
2	*Novosphingobium panipatense* P5:ABC	PHE	200 ppm	60	0.133	(Chettri and Singh, 2019)
3	*Pseudomonas sp.* BZ-3	PHE	50 ppm	75	0.108	(Lin et al., 2014)
4	*Achromobacter, Sphingobacterium* and *Dysgonomonas*	PHE	20 ppm	91	1.177	(Bianco et al., 2022)
5	*Sphingomonas cloacae* W4-1, *Rhizobium sp.* W4-2, *Pseudomonas aeruginosa* W4-3, and *Achromobacter xylosoxidants* W4-4	PHE	200 ppm	95	0.5547	(Wang et al., 2008)
6	*Bacillus licheniformis* STK 01, *Bacillus subtilis* STK 02 and *Pseudomonas aeruginosa* STK 03	PHE	40 mg/kg	90.34	0.0620	(Amodu et al., 2016)
7	*Delftia sp.* FM6-1 *Achromobacter sp.* FM8-1	PHE	50 ppm	na na	0.1974 0.1070	(Xu et al., 2019)
8	*Acinetobacter baumannii,*	PHE	20 ppm	48	0.0096	

	Klebsiella oxytoca,			11	0.0096	(Kim et al., 2009)
	Stenotrophomonas maltophilia,			9	0.0072	
	Microconsortium (all 3)			80	0.0264	
9	*Pseudomonas aeruginosa*	HEX	1 % v/v	63.8	0.0158	(Hajieghrari and Hejazi, 2020)
10	*Leclercia adecarboxylata* SBR14	HEX	0.3 % v/v	93.74	0.118	(Zhang et al., 2018).
	Leclercia adecarboxylata SBR45			87.79	0.103	
	Enterobacter sp. SBR27			65.66	0.069	
	Enterobacter sp. SBR28			73.27	0.087	
11	*Ochrobactrum oryzae*	HEX	3000	87.77	0.065	(Samaei et al., 2020)
	Paenibacillus lautus			80.89	0.053	
12	*Dietzia sp.* Enriched consortium	HEX	1500 mg/kg		0.056	(Akbari et al., 2021)
13	*Agrobacterium fabrum* SLAJ	HEX	50 ppm	77.17	0.30	This study
		PHE	50 ppm	85.25	2.32	
		BOTH	HEX 25 ppm	87.52	0.63	
			PHE 25 ppm	86.93	1.51	
	Pseudomonas aeruginosa P7815	HEX	50 ppm	80.53	0.66	
		PHE	50 ppm	85.35	2.66	
		BOTH	HEX 25 ppm	83.26	0.90	
			PHE 25 ppm	82.69	2.16	

Bacillus subtilis RSL2	HEX	50 ppm	86.91	0.53
	PHE	50 ppm	87.14	3.41
	BOTH	HEX 25 ppm	76.89	0.41
		PHE 25 ppm	90.00	3.60
Microconsortium (above 3)	HEX	50 ppm	92.43	1.22
	PHE	50 ppm	88.73	4.58
	BOTH	HEX 25 ppm	97.19	1.01
		PHE 25 ppm	91.87	4.38

5.4. Conclusions

Three potential inherent oil-degrading bacterial strains, *A. fabrum*, *P. aeruginosa* and *B. subtilis*, were explored to understand their aliphatic and aromatic hydrocarbon biodegradation using HEX and PHE as model hydrocarbons. The hydrocarbons were added as sole as well as a binary mixture. Further, their biodegradation potential was also explored as a consortium. The microconsortium showed high biodegradation efficiencies of 92.4 and 88.7 of individual HEX and PHE, respectively, which further increased to 97.2 and 91.9 % in the case of a binary mixture of substrates. The bacterial biodegradation kinetics fitted well to an integrated model combining first-order exponential decay and the Monod equation. The microconsortium exhibited parallel and serial assimilation for HEX and PHE, respectively. The degradation behaviour has been correlated with biomass growth and activity of key enzymes. Summarily, the designed microconsortium has shown great degradation potential of the individual and mixture of aliphatic and aromatic hydrocarbons, which can be explored for the remediation of actual oil-contaminated soil and water sites.

Chapter 6

An integrated strategy of hydrophobic surface-induced biosorption and microbial biodegradation for the enhanced crude oil remediation

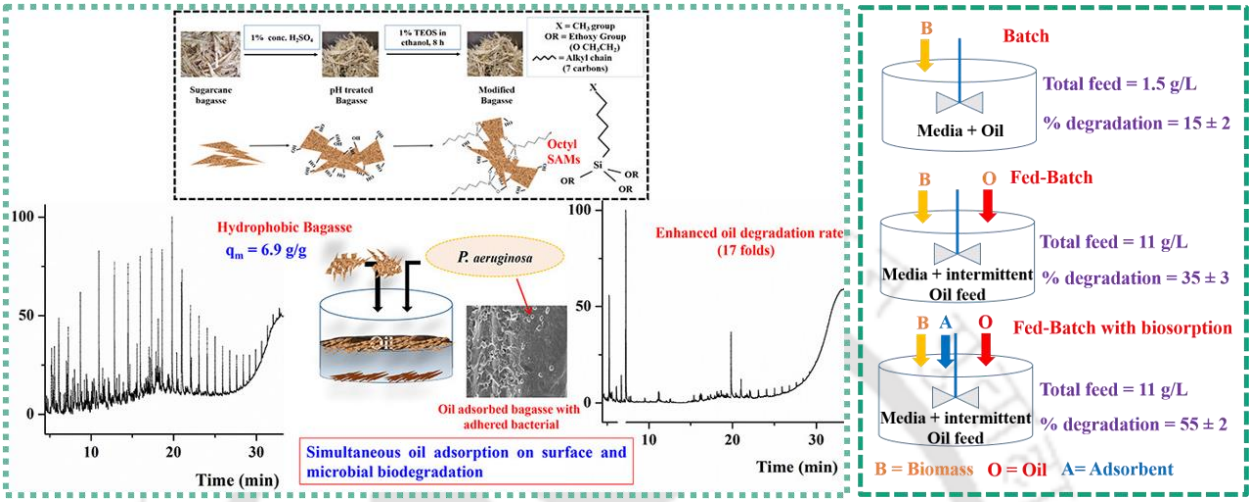

(Industrial & Engineering Chemistry Research, 60, 9378−9388, 2021 (Sharma and Pandey, 2021) and Letters in Applied Microbiology, 73(4), 471-476, 2021 (Sharma and Pandey, 2021))

This chapter discusses an integrated biodegradation strategy using a surface-induced biosorption coupled microbial biodegradation approach for effective oil bioremediation. Low-cost bagasse was used as a biosorbent, and its surface hydrophobicity was improved by forming octyl self-assembled monolayers to enhance the surface-oil interactions (adsorption). *Pseudomonas aeruginosa* was exploited for biodegradation because of its known oil degradation and biosurfactant production abilities. The integrated process proposed a kinetic model, which agreed to simultaneous biosorption and biodegradation. Using a fed-batch approach, continuous adsorption of intermittently fed oil accompanied sustained bioavailability, further decreasing the risk of substrate toxicity to the microbe. Overall, this bioremediation approach mitigates the hazardous effects of crude oil and explores it as a potential substrate for microbial degradation and biosurfactant production.

6.1. Introduction

Inherent bacterium always has the upper hand in crude oil biodegradation due to their biosurfactant production ability. Nevertheless, the harsh environmental conditions slow their biodegradation ability limiting their actual applications at the contaminated site (Sharma et al., 2019; Sharma et al., 2019). Previous chapters established that optimizing the bacterial growth condition and using suitable biostimulants can effectively improve their oil biodegradation abilities by many folds. Even though these microbes have shown effective biodegradation activity, their slow degradation rates lead to reduced efficacy. It could be due to their intolerance to higher oil concentrations (Park et al., 2021). This chapter presents an integrated remediation approach of oil biosorption coupled with microbial biodegradation. Adsorption is a rapid remediation tool for reducing the bulk oil concentration for bacterial compatibility.

Further, the biosorbent can be hydrophobically surface modified to improve the adsorption capacity. This study aimed to mitigate two major drawbacks of bacterial oil bioremediation, i.e., biotoxicity of oil at higher concentrations and limited bio affinity of oil. The study used natural biomass, bagasse, as a model sorbent. The bagasse surface was modified by forming hydrophobic octyl SAMs, which were explored for the biosorption of oil for the first time to the best of our knowledge. The hydrophobic surface induced the rapid adsorption process in the early remediation process. The subsequent remediation stage involved the integration of adsorption with slower bioremediation processes to achieve a synergistic and sustainable outcome. While hydrophobically modified adsorbent will decrease the risk of biotoxicity towards high concentrations, its oil adsorption will improve the bioavailability of the microbes. Bacteria *Pseudomonas aeruginosa* has been reported elsewhere for its effective biosurfactant production ability (Sabarinathan et al., 2021; Sharma and Pandey, 2021) and is a potential candidate for the crude oil biodegradation study. Furthermore, the performance of this integrated system was also evaluated in terms of change in microbial growth, oil degradation, and biosurfactant production activity in fed-batch mode.

6.2. Materials and Methods

6.2.1. Materials

The chemicals and reagents used for this study have been mentioned in Chapter 3. Sugarcane bagasse was obtained locally. Triethoxyoctylsilane (TEOS) was procured from Sigma (8.00658). Double distilled water (MiliQ, 18 mΩ, Millipore systems) was used throughout the experiments.

6.2.2. Preparation of biosorbent

The sugarcane bagasse was initially washed several times to remove dust and adhered impurities and later rinsed with distilled water twice before drying at 80 °C in a hot air oven. The dried bagasse was crushed into pieces, and screened with 0.5 mm sieves. The obtained bagasse was treated with a 1 % (v/v) concentration of sulphuric acid at 120 °C for 20 min to remove the hemicellulose components and expose the cellulose components of bagasse, as stated elsewhere with slight modifications (Panda and Maiti, 2019). The treated bagasse was washed several times with distilled water until neutral pH was achieved and oven-dried at 80 °C. This prepared (acid-treated) bagasse was kept in air sealed container for further use.

The acid pretreated bagasse was further chemically modified using TEOS (1 %, v/v) in ethanol under an inert atmosphere to form octyl SAMs (Hasan and Pandey, 2016; Pandey, 2021), as depicted in **Scheme 6.1.** The kinetics of TEOS functionalization on bagasse was studied for 8 h using FTIR spectroscopy. After the successful surface modification, the modified bagasse was washed using ethanol twice to remove uncoupled TEOS molecules and then dried overnight at 37 °C to ensure proper curing of octyl layer (modification) on the surface of the bagasse (Hasan et al., 2018; Hasan et al., 2018). The modified bagasse was stored at room temperature in an air-sealed container for further experiments.

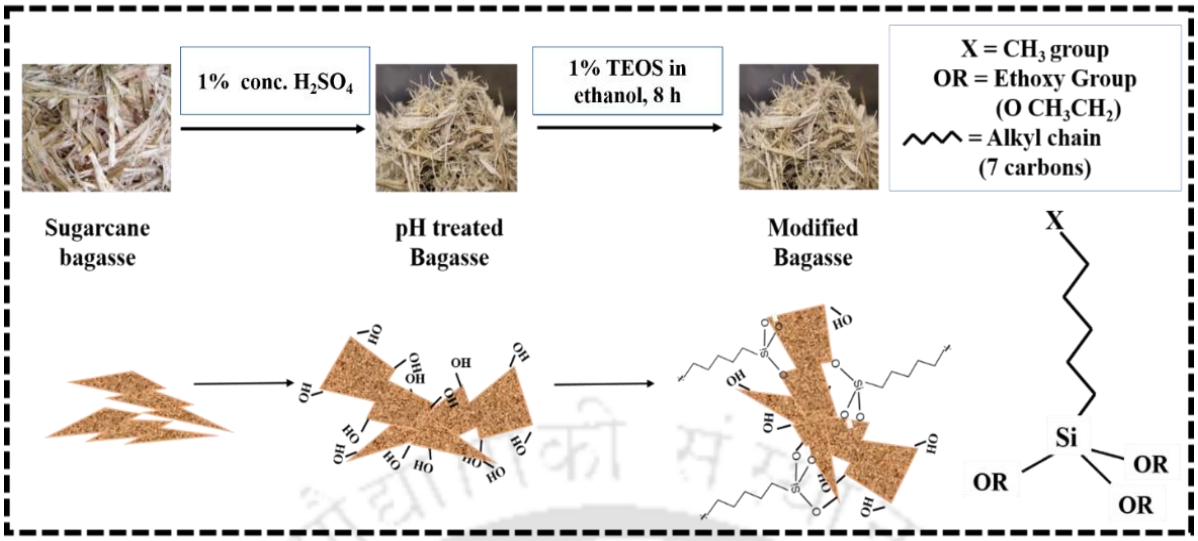

Scheme 6.3. Proposed mechanism of the surface modification of bagasse by forming octyl SAMs

6.2.3. Characterization of the prepared biosorbent (bagasse)

The prepared modified bagasse was characterized using FTIR spectroscopy to analyze the change in the chemical functional groups on the surface of the bagasse after chemical treatment and modification. The modification of bagasse was also confirmed using Energy Dispersive X-Ray (EDX, Zeiss, Model: Sigma) and Field Emission Scanning Electron Microscope (FESEM, Zeiss, Model: Sigma) analyses. The modified biosorbent was analyzed for its porosity and pore volume using Brunauer-Emmett-Teller (BET) surface area analyzer (Quantachrome, Autosorb-IQ MP). X-Ray Diffraction (XRD, Rigaku, SmartLab) analysis was performed to confirm no damage occurred to the base material after chemical treatment and modification.

6.2.4. Crude oil adsorption studies

The prepared biosorbent was initially studied for its ability to adsorb crude oil. For this, 7.52 g/L (i.e., 1 %, v/v) crude oil solution was added in water along with 5 g/L (i.e., 0.5 %, w/v) of all three types of bagasse, i.e. (1) raw bagasse, (2) pretreated bagasse, (3) modified bagasse, at 37 °C, 180 rpm for 8 h. After 8 h, the adsorbent was removed from the solution by centrifugation (Thermo-Fischer, Legend XTR), and the residual oil was quantified as mentioned in Chapter3, section 3.2.5 (Sharma et al., 2019).

The adsorption capacity for each type of biosorbent was determined using the following expression (Sharma et al., 2018).

$$q_t = \frac{(C_0 - C_t)\,V}{W} \quad \textbf{(6.1)}$$

Where q_t stands for adsorption capacity at a time 't' (mg/g), C_0 stands for the initial oil concentration (mg/L), C_t represents the concentration of oil at a time 't' (mg/L), V stands for working volume (L), and W represents the weight of adsorbent used (g).

6.2.5. Optimization of adsorbate and adsorbent concentrations

The concentration of biosorbent and initial oil was optimized using factorial designing viz. response surface methodology- central composite design (RSM-CCD) using Design Expert (version 7.0) statistical software, as discussed in Chapter 2, section 2.5.2.4.2. The biosorbent concentration was varied from 2.5 to 10 g/L, and the initial oil concentration was varied from 7.52 to 75.22 g/L. Batch experiments were conducted to investigate the interaction between adsorbent and adsorbate for maximum oil removal. In this regard, residual oil opted as response output. A set of 13 batch experiments were performed at suggested adsorbent-adsorbate concentrations at 37 °C, 180 rpm for 8 h. After the adsorption, the biosorbent was separated, and the percentage of oil removal (response parameter) was calculated, as stated in section 6.2.4 (Sharma et al., 2019).

6.2.6. Biosorbent stability/ reusability analysis

A reusability was conducted to analyze the suitability of biosorbent for repetitive application. Briefly, 10 g/L of modified bagasse was used as an adsorbent for 7.52 g/L of initial oil concentration at 37 °C, 180 rpm for 8 h. After completing each batch adsorption, the oil-adsorbed biosorbent was separated by centrifugation. The biosorbent was then solvent extracted using n-hexane to desorb the oil and oven-dried at 37 °C for overnight. This dried bagasse was then reused for a new batch of adsorption studies.

The residual oil and adsorption capacity of bagasse were analyzed for each reusability cycle to evaluate the stability of the modified sorbent.

6.2.7. Integration of bio-sorption and biodegradation

The modified bagasse-based biosorption was coupled with microbial biodegradation to analyze the synergistic effect of this integrated strategy compared to the individual biosorption and microbial biodegradation. *Pseudomonas aeruginosa* P7815 (MTCC 7815) was used for the crude oil degradation analysis due to its reported oil degradation (Sharma et al., 2019; Sotirova et al., 2009; Varjani and Upasani, 2019) and biosurfactant production abilities (Sanchez et al., 2010). The bacterium inoculum was prepared in LB broth and incubated for 12 h at 37 °C, 180 rpm. After incubation, the bacterial growth was analyzed by measuring optical density using a spectrophotometer at 600 nm. All batch oil degradation studies used this pre-culture as inoculum (5 %, v/v; 1×10^7 CFU/mL) (Sharma et al., 2019). The oil biodegradation ability of this strain was optimized by incubating bacterium with varying the concentrations of initial oil from 0.1 to 1 % (v/v) in sterile BH media at pH 7, 37 °C, and 180 rpm for 6 days. At the end of incubation, the culture was centrifuged at 8000 rpm for 10 min at 4 °C using a centrifuge. The cell-free supernatant was solvent extracted in n-hexane to obtain the residual oil, and the pellet was weighed to estimate the cell biomass (Sharma et al., 2019).

For the microbial biodegradation (control) study, 1.5 g/L of initial crude oil was added in the sterile BH broth (pH 7) and inoculated with 5 % (v/v) of bacterial inoculum at 37 °C and 180 rpm. In the case of a biosorbent assisted biodegradation strategy, 10 g/L of modified bagasse was added in 1.5 g/L of initial crude oil prepared in the sterile BH broth (pH 7) for the initial 8 h to achieve rapid adsorption followed by bacterial inoculation at 37 °C and 180 rpm. Bacterial growth and oil degradation were analyzed at regular intervals of 6 h till 24 h. The biosorbent was separated from the culture at each time interval using funnel-based gravity settling. Later, the culture was centrifuged at 8000 rpm, 4 °C, and 180 rpm. The pellet was studied for biomass analysis, and cell-free supernatant was analyzed for the surface tension and biosurfactant. The recovered biosurfactant was characterized using MALDI-TOF-MS as mentioned in section 3.2.4 (Sharma et al., 2019). The residual oil is recovered from the supernatant and gravimetrically estimated as mentioned in section 3.2.5. Further, the residual oil concentration was also

analyzed using Gas Chromatography - Flame ionization detector (GC-FID, Agilent Technologies 7890B, HP-5MS column, 60 m × 0.25 mm × 0.25 µm). For the GC-FID study, the injector temperature was maintained at 300 °C with a split ratio of 1:20. The initial oven temperature was maintained at 50 °C for 5 min and was increased with the ramping of 10 °C /min to 310 °C and held for 20 min. The detector was maintained at 300 °C, and the Helium (carrier gas) flow rate was maintained as 1 mL/min (Sharma et al., 2020).

6.2.7.1. Insights into the integrated process

The recovered biosorbent after the degradation studies were analyzed using FESEM and fluorescence imaging techniques to examine the cell-surface interaction between microbes and modified bagasse. A top surface view was monitored using FESEM to analyze the surface roughness and morphology of the microbe adhered modified bagasse. For fluorescence imaging, samples were stained using Nile Red for the oil and diamidino-phenylindole (DAPI) for the microbes. Also, extracellular alkane hydroxylase (AH) activity was investigated, as mentioned previously in Chapter 3, section 3.2.6 (Sharma et al., 2019).

6.2.8. Integrated crude oil biodegradation using fed-batch study

The bacterial inoculum (5 %, v/v) was incubated in sterile BH media (pH 7) with an initial oil concentration of 1.5 g/L at 37°C and 180 rpm. A regular batch of oil feeding was performed until the culture reached the death phase. A batch culture without intermittent oil feeding was kept as control. In the case of a fed-batch in the biosorbent study, an initial 8 h of biosorption using modified bagasse was performed. Later, the bacterial inoculum (5 %, v/v) was inoculated and incubated at 37°C and 180 rpm. The growth of bacteria was assessed using an increase in OD of the culture broth. A regular oil feed was administered, and the growth was continuously monitored. This constant oil feeding was maintained until no further OD increase was observed. Then, the bacterial biomass, oil degradation activity, and biosurfactant production ability were investigated as stated in section 6.2.7.

6.2.8.1. Microbial growth kinetics study

During the biodegradation study, biomass concentration was measured as OD_{600} at regular intervals. The oil feed rate for the fed-batch study was determined corresponding to the oil utilization rate of bacteria in the batch study (control) using **equation 6.2.**

$$\frac{dS}{dt} = -\frac{\mu X}{Y_{X/S}} - \frac{q_P X}{Y_{P/S}} - m_s X \quad \textbf{(6.2)}$$

Where S is the oil concentration (g/L), μ (= $1/X(dX/dt)$) is the specific growth rate of bacteria (day^{-1}), X is the biomass concentration (g/L). $Y_{X/S}$, $Y_{P/S}$ and $q_{P,}$ stands for the biomass yield coefficient, biosurfactant yield coefficient, and biosurfactant specific product formation rate ($g\ g^{-1}\ h^{-1}$), respectively. m_s is the maintenance coefficient and assumed as zero during the growth phase.

6.2.8.2. Oil biodegradation and biosurfactant production estimation

After incubation, the overall oil biodegradation was estimated by gravimetric analysis, as expressed in section 6.2.7. The biosurfactant concentration was estimated as mentioned in section 3.2.4 (Sharma et al., 2020; Sharma et al., 2019). The yield coefficient of biosurfactant production was also calculated using **equation 6.3** (Datta et al., 2020)

$$Y_{P/S} = \frac{\Delta P}{\Delta S} \quad \textbf{(6.3)}$$

6.3. Results and discussion

6.3.1. Surface modification of bagasse by forming the octyl SAMs

We focused on improving the oil adsorption ability of sugarcane bagasse by grafting the hydrophobic octyl groups on its surface by forming SAMs. The change in the surface chemistry of bagasse after acid treatment and chemical modification was analyzed using FTIR spectra. **Figure 6.1 (A)** depicts the change in the surface functional groups of raw bagasse after acid treatment, which is represented in the form of loss of peaks in the region 1730-1740 cm^{-1} and 1043 cm^{-1} assigned for C=O groups and C-O-C

groups of lignocellulose (Chandel et al., 2014; Zhang et al., 2017). The FTIR spectra of the octyl-modified bagasse exhibited peaks at 1028 cm^{-1} and 1056 $cm^{-1,}$ signifying the presence of Si-O-Si bonds, which confirmed the successful grafting of octyl groups on the surface (Hasan and Pandey, 2016).

The kinetics of the formation of octyl SAMs on bagasse surface was explored using FTIR. The FTIR spectra in the ranges of 900-1300 cm^{-1} and 2800-3000 cm^{-1} were chosen for this purpose, and peak areas at the different reaction time intervals are shown in **Figure 6.1 (B) and (C)).** In the 2800-3000 cm^{-1} range, narrowing down and redshift from 2900 cm^{-1} to 2890 cm^{-1} were observed with the increase in the reaction time, explaining the successful impregnation of octyl groups on the bagasse surface **(Figure 6.1 (C))**. Similarly, another spectra region from 900-1300 cm^{-1} exhibited a peak position and intensity change after the modification **(Figure 6.1 (B))**. An increase in peak intensity in the region 1040-1080 cm^{-1} represented the formation of Si-O-Si, siloxane groups (Hasan and Pandey, 2016). Moreover, there was no significant increase in peak area after 8 h of incubation, deciphering the completion of the modification (silanization) process. A similar trend was observed for the 2800-3000 cm^{-1} region. These findings indicated the completion of octyl SAMs formation on bagasse surface in 8 h, which agreed to the reported 8.5 h (Hasan and Pandey, 2016).

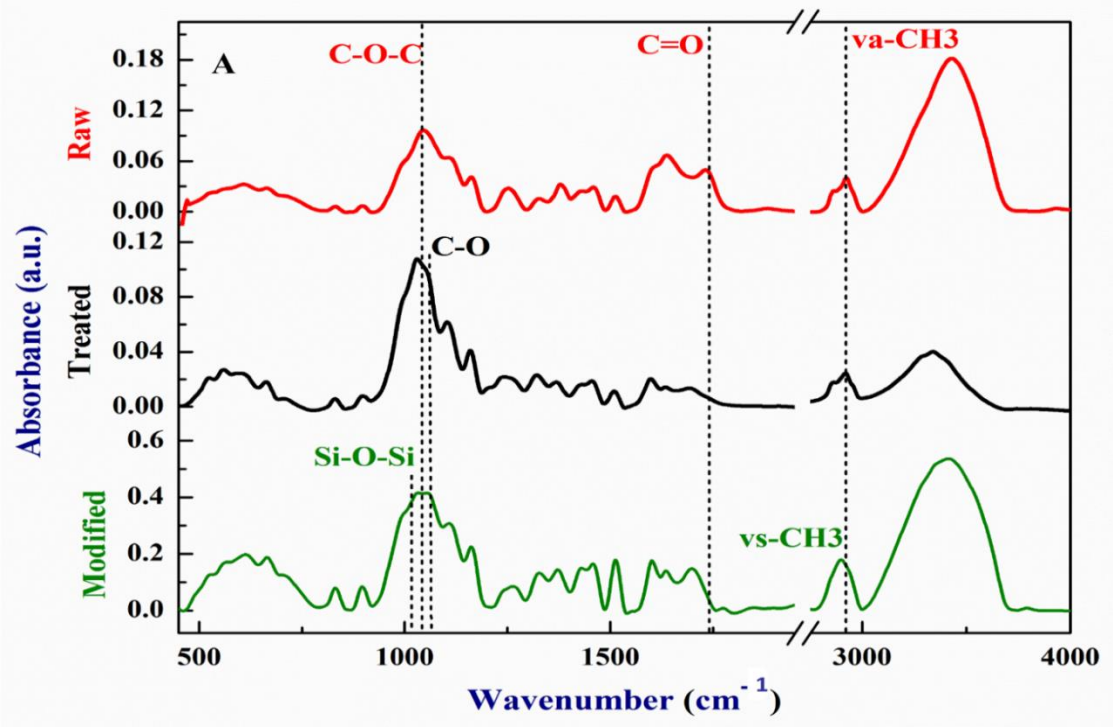

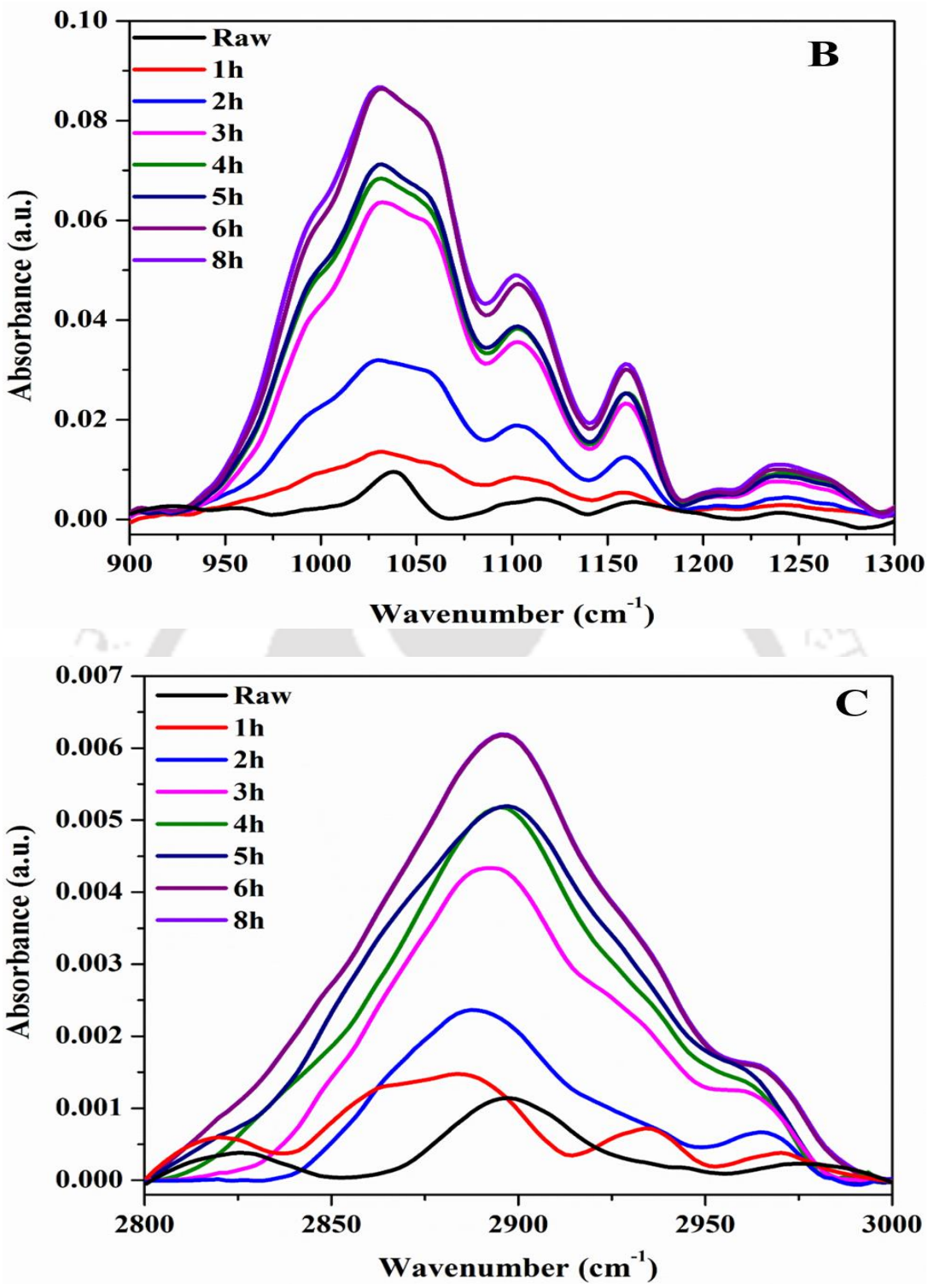

Figure 6.1. (A) FTIR spectrum of raw (red), acid-treated (black), and acid treated-surface-modified (green) bagasse; and Octyl SAMs formation by the reaction between OH groups on bagasse surface and ethoxy (C_2H_5O) groups of TEOS investigated by changes in FTIR peak intensities at the different time intervals in the region (**B**) 900-1300 cm^{-1}, and (**C**) 2800-3000 cm^{-1}

6.3.2. Characterization of the modified bagasse

6.3.2.1. X-Ray Diffraction study

The effect of acid pretreatment and octyl grafting on the crystal structure of bagasse was studied using XRD analysis. Overall, no disappearance of peaks revealed that the pretreatment did not damage the crystal structure of the base material, bagasse. Further, functionalization with octyl groups did not alter the crystal structure. **Figure 6.2** shows the diffractograms of the untreated bagasse (A), bagasse pretreated with 1 % sulfuric acid (B) and octyl modified bagasse (C). It was observed that typical cellulose peaks (15.7°, 22.6°, and 35.19°) were observed in all three cases (Kumar et al., 2014; Sofla et al., 2016); however, there was an increase in crystallinity after pretreatment, anticipated from the increased intensity. The pretreatment with acid removed the lignin and hemicellulose components from the bagasse and thus improved the crystallinity (Lv et al., 2018).

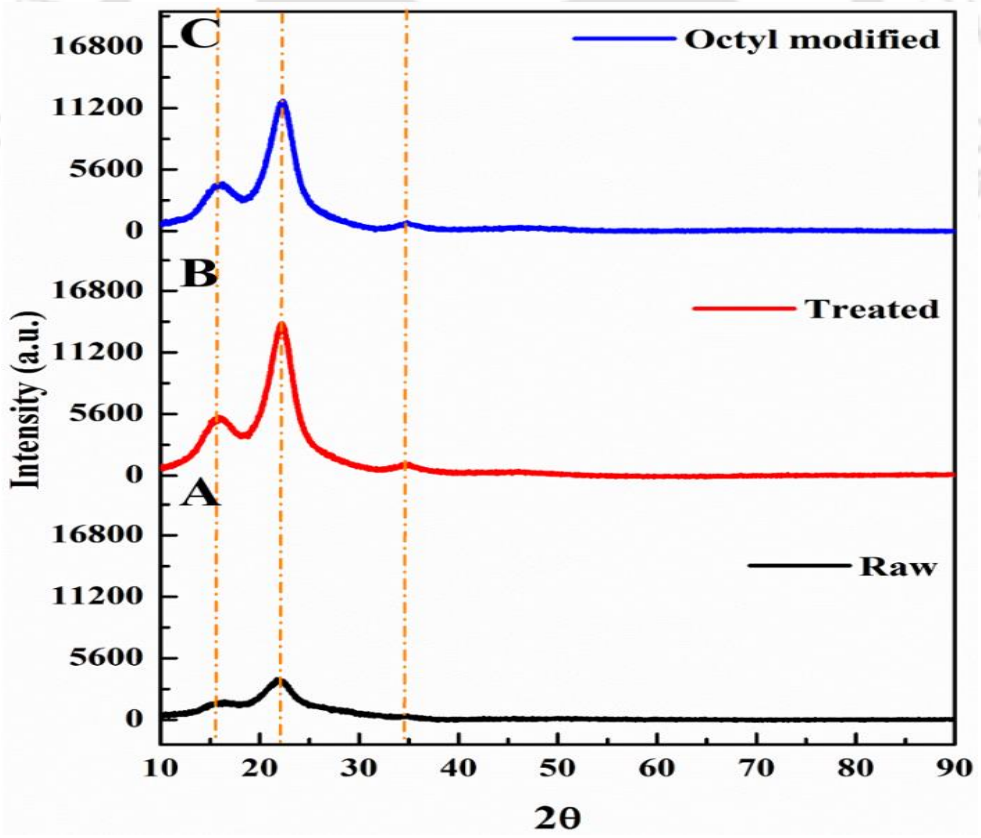

Figure 6.2. XRD analysis of (**A**) Raw, (**B**) Acid-treated, and (**C**) Octyl modified bagasse

6.3.2.2. Surface area analysis

The raw and modified bagasse surface area and pore volume were analyzed using BET. The BET isotherm curves are shown in **Figure 6.3**. Upon octyl modification, there was an increase in the overall pore size due to the grafting of the octyl groups in the pores (**Table 6.1),** as reported in previous literature (Jiang et al., 2018). Hence, such changes in the surface properties suggested the octyl groups grafting on the bagasse's surface. The specific surface area of the modified bagasse was slightly decreased. The BET analysis supported the surface modification of bagasse with octyl groups resulting in the change in adsorption isotherm curve.

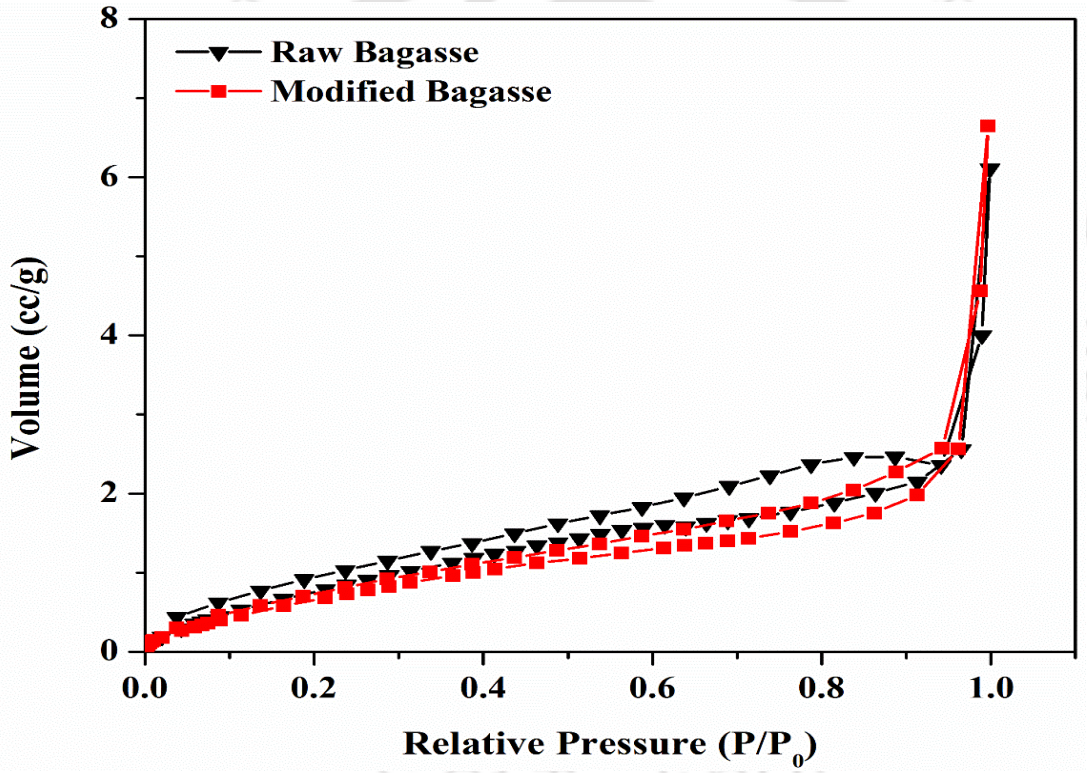

Figure 6.3. BET adsorption curves for raw and modified bagasse

Table 6.1. BET surface area analysis of the raw and modified bagasse

Samples	BET surface area (m^2/g)	Pore size (nm)	Pore volume (cm^3/g)
Raw bagasse	3.761	10.08	0.0095
Modified bagasse	3.157	13.06	0.0103

6.3.2.3. Morphology and elemental analyses

The morphology of raw and modified bagasse was studied using FESEM, and the surface elemental analysis was examined using the EDX technique. The surface of raw bagasse showed parallel and rough fibrous surfaces with superficial extractives and pith. After acid treatment and octyl modification, the surface of thus obtained modified bagasse was comparatively smooth and loose fibers without pith (**Figure 6.4(A) and (B**)). The elemental analysis of modified bagasse indicated the increase in C content and decrease in O content after surface modification. Also, Si was present only in the case of modified bagasse (**Figure 6.4(C) and (D**)). It complemented the FTIR results and confirmed the successful formation of octyl SAMs on the bagasse surface (Hasan and Pandey, 2016; Pandey, 2021).

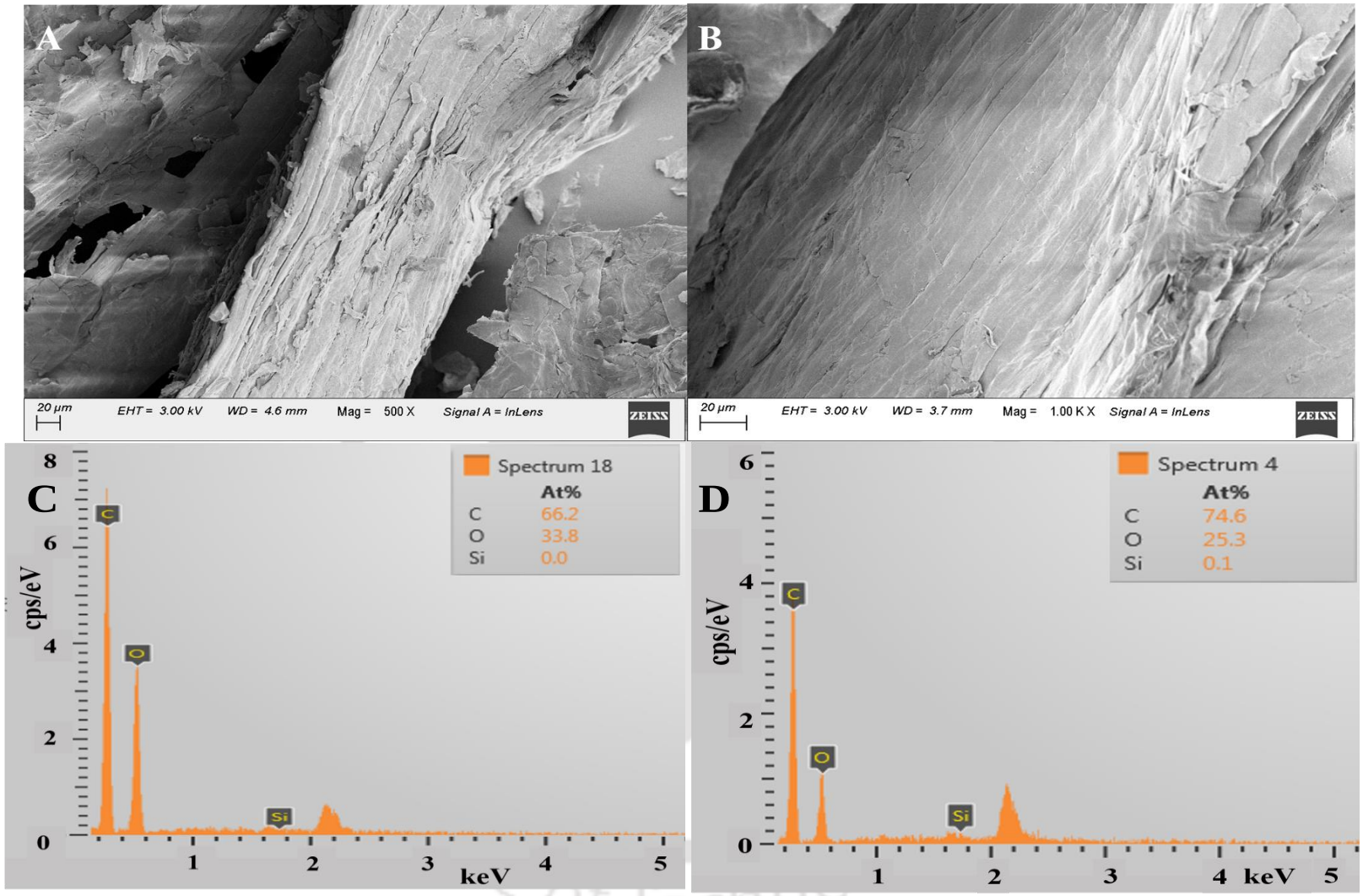

Figure 6.4. FESEM and EDX analyses of (A and C) Raw and (B and D) Modified bagasse

6.3.3. Oil adsorption study using biosorbents

Oil removal properties of raw, treated, and modified bagasse are shown in **Figure 6.5**. It was observed that the adsorption capacity of oil for all three types of biosorbents reached the maximum within 60 min of the contact time. After that, the adsorption capacity almost remained unchanged, signifying the saturation stage. The oil adsorption rate (k_a) was estimated by fitting the kinetic data to the first-order differential equation.

$$\frac{dC}{dt} = -k_a(C - C_e) \qquad [C(0) = C_0] \qquad (6.4)$$

$$C(t) = C_e - (C_e - C_0)e^{-k_a t} \qquad (6.5)$$

Here, C_0, C_e, and C(t) represent the initial oil concentration (g/L), the concentration of oil at equilibrium, and at a time 't' (h), respectively. The k_a value was found to be the maximum for the modified bagasse (4.47 ± 0.2 h^{-1}) followed by the treated (2.01 ± 0.1 h^{-1}) and raw (1.68 ± 0.1 h^{-1}) bagasse. Likewise, overall oil removal was increased from ~20 % for raw bagasse to 35 % for acid-treated, further enhancing ~85 % for the octyl-modified bagasse within 60 min of adsorption.

An improved oil adsorption capacity of acid-treated bagasse than raw bagasse is due to the loss of hemicellulose content after the acid pretreatment. Loss of peaks at 1733 cm^{-1} and 1043 cm^{-1} in the FTIR spectra (**Figure 6.1**), representing the stretching of unconjugated C = O groups, and C-O stretching in C-O-C linkages of hemicellulose content of bagasse, indicated the decrease in the polar functional groups after the acid pretreatment (**Figure 6.1 (A)**) (Chandel et al., 2014; Zhang et al., 2017). Furthermore, octyl surface modification of bagasse increased the presence of non-polar, hydrophobic octyl groups on the surface of bagasse, as indicated by the enhanced intensities of peaks in the region 2850-3000 cm^{-1} representing stretching *vs*-CH_3 (symmetric) and *va*-CH_3 (asymmetric) methyl peaks (**Figure 6.1 (A)**) (Hasan and Pandey, 2016). It indicated the significant effect of surface hydrophobicity in adsorbents' overall oil adsorption ability. Such a change in absorption capacity is because of the hydrophobic modification of bagasse that improved the oil affinity towards bagasse and improved its overall adsorption capacity. Various literature also supported the impact of surface hydrophobicity on oil adsorption ability (Pandey, 2021).

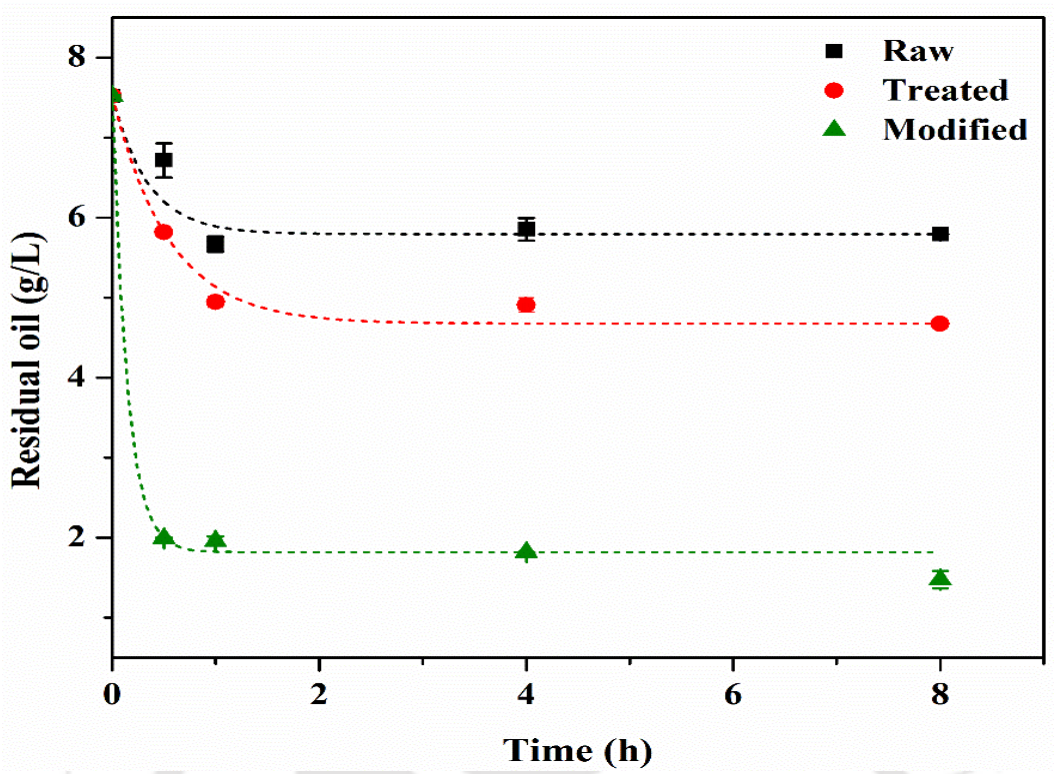

Figure 6.5. Comparative oil removal capacity in terms of residual oil concentration (g/L) of all three types of biosorbents: raw (black), acid-treated (red), and acid treated-surface-modified (green) bagasse

6.3.4. Optimization of adsorbate and adsorbent concentrations

For maximizing the removal of oil by modified bagasse, it was further optimized by varying the concentrations of adsorbent and adsorbate using the RSM-CCD factorial design technique. The adsorbent and adsorbate concentrations (g/L) were varied in the range 2.5-10 g/L and 7.52 to 75.22 g/L, respectively, to maximize the oil removal as output parameter using the Design expert RSM-CCD technique. The 13 experimental setups with respective experimental and predicted response variables are listed in **Table 6.2**. The experimental responses were fitted to the quadratic model. Predicted response values are quite in agreement with the experimental results. ANOVA was applied to the regression analysis. Correlation coefficient value was $R^2 > 0.93$. The lesser p-value and the higher F-value proved the significance of the model. From the model, initial oil concentration (factor B) was found to be significant ($p < 0.05$), hence the effect of initial oil concentration on the biodegradation of oil was further estimated using biodegradation studies.

Table 6.2. Experimental and predicted values of oil removal (%) for modified bagasse as biosorbent in RSM-CCD runs with ANOVA analysis

S. No	Bagasse concentration (g/L)	Initial oil concentration (g/L)	Experimental oil removal (%)	Predicted oil removal (%)
1	2.50	7.52	91.14	80.45
2	10.00	7.52	98.14	103.23
3	2.50	75.22	14.12	-1.37
4	10.00	75.22	42.37	42.67
5	0.95	41.37	8.75	25.09
6	11.53	41.37	78.21	72.21
7	6.25	0	100.00	102.24
8	6.25	89.24	4.72	13.44
9	6.25	41.37	44.73	43.85
10	6.25	41.37	44.39	43.85
11	6.25	41.37	42.57	43.85
12	6.25	41.37	44.39	43.85
13	6.25	41.37	43.67	43.85

ANOVA for Response Surface Quadratic Model

Source	Sum of squares	df	Mean square	F value	p-value
Model	11817.96	5	2363.59	21.57	0.0004
A-Bagasse concentration	357.66	1	357.66	3.26	0.1138
B-Initial Oil Concentration	861.13	1	861.13	7.86	0.0264
AB	112.92	1	112.92	1.03	0.3439
A^2	41.31	1	41.31	0.38	0.5586
B^2	571.71	1	571.71	5.22	0.0563
Residual	767.12	7	109.59	-	-
Lack of Fit	764.14	3	254.71	342.08	< 0.0001
Pure Error	2.98	4	0.74	-	-
Cor Total	12585.08	12	-	-	-

The response data (oil removal, %) against the input parameters (adsorbent and adsorbate concentrations) in **Figure 6.6**. The response was related to input variables by a quadratic model as follows:

$$\boldsymbol{Oil\ removal}\ (\%) = +\mathbf{78.45} + \mathbf{49.63}\,\boldsymbol{A} - \mathbf{26.74}\,\boldsymbol{B} + \mathbf{10.63}\,\boldsymbol{AB} + \mathbf{9.74}\,\boldsymbol{A^2} + \mathbf{9.97}\,\boldsymbol{B^2} \qquad (\mathbf{6.6})$$

Here A is the concentration of biosorbent (g/L), and B is the initial oil concentration (g/L). The R^2 and p-values of the model were 0.93 and < 0.05, respectively. It indicated the significance of the above model equation. The optimized conditions for the maximum oil removal were predicted to be 10 g/L of the adsorbent and 7.52 g/L of the adsorbate. Hence, further experiments were conducted at these optimized conditions.

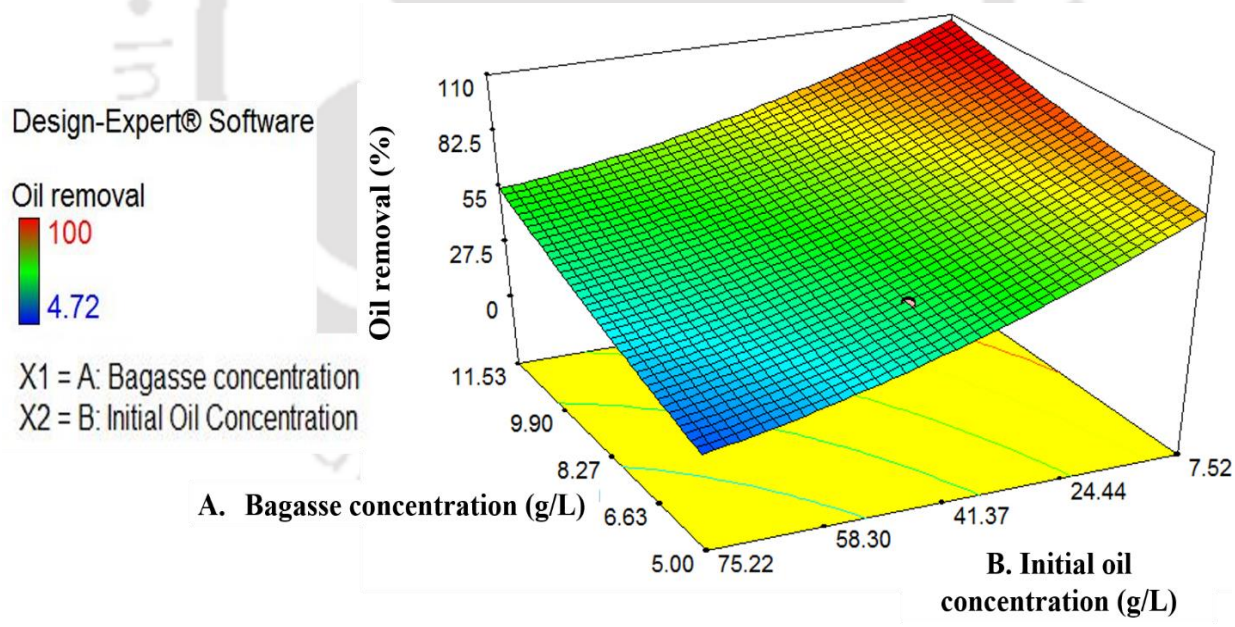

Figure 6.6. Optimization studies at pH 7, 37 °C, and 8 h of the contact time using various concentrations of bagasse (A) and Initial oil (B) as projected by Design-Expert software

6.3.5. Adsorption isotherm study

For determining the maximum oil adsorption capacity (q_m) of the modified bagasse, biosorption experiments were performed at a varying concentration of oil (7.52 to 150.4 g/L) and the obtained data were fitted to the Langmuir isotherm, which suggests the involvement of homogenous adsorption energy causing the monolayer adsorption on the adsorbent (Sharma et al., 2018; Tiwari et al., 2017). This equation is preferably considered to determine the q_m of an adsorbent.

$$q_e = \frac{q_m K_L C_e}{1 + K_L C_e} \tag{6.7}$$

Where C_e stands for the concentration of oil (g/L), q_e stands for the equilibrium adsorption capacity of adsorbent (g/g), and K_L is the Langmuir adsorption constant (L/g), signifying the binding affinity. The fitted and experimental data are shown in **Figure 6.7 (A)**. The Langmuir isotherm fitted reasonably well to the experimental data with $R^2 > 0.97$. A significantly high q_m of 6.9 ± 0.3 g/g was obtained for the modified bagasse, three folds higher than the raw bagasse (i.e., 2.5 ± 0.2 g/g). The Langmuir adsorption constant (L/g) was found to be 0.025 ± 0.002 and 0.018 ± 0.002 for the raw and modified bagasse, respectively. Such high adsorption capacity is the first report using low-cost bagasse as biosorbent for crude oil adsorption studies. The q_m value of the modified bagasse is better than the reported data using similar biosorbents (Abdelwahab et al., 2017; Behnood et al., 2016; Guilharduci et al., 2017).

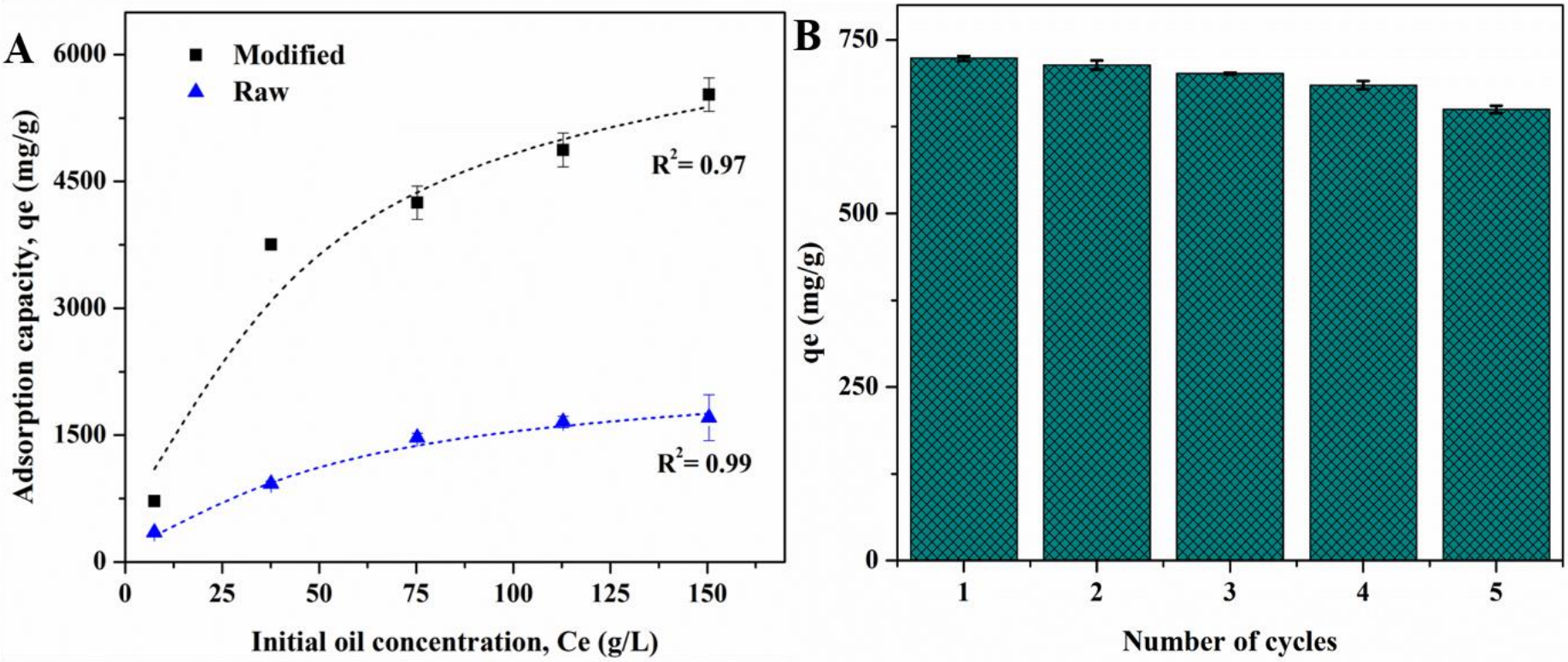

Figure 6.7. (**A**) Fitting the Langmuir adsorption isotherm to the experimental data (Dotted lines are fitted data) and (**B**) Reusability studies of the modified bagasse up to 4 cycles using 10 g/L of bagasse and 7.52 g/L of oil concentration

6.3.6. Adsorbent stability/reusability analysis

The prepared biosorbent was analyzed for the ability to adsorb oil upon reuse. After batch 1, the adsorbent was washed twice with hexane to remove adsorbed oil and dried in the oven overnight. Afterward, the same adsorbent was used for cycle 2. After repetitive adsorption-desorption till 5 consecutive cycles, up to 14 % (q_e = 650 mg/g) loss in adsorption ability was observed **(Figure 6.7 (B))**. It also indicated the stability of the modified sorbent due to the formation of covalently linked octyl SAMs. After repetitive usage, such strength and stability of the modified biosorbent suggested its potential applicability as a low-cost adsorbent for controlling and managing oil-contaminated sites.

6.3.7. Biosorption assisted biodegradation strategy

The crude oil biodegradation ability of *P. aeruginosa* was studied with varying oil concentrations at 37 °C for 6 days to explore the maximum concentration of oil that could be utilized efficiently by the bacterium. A decrease in biomass growth was observed with an increase in initial oil concentration, as shown in **Figure 6.8**. The typical concentrations of the crude oil spills in a river fall in the range of 0.2 to 5 mg/L (Ifelebuegu et al., 2017), while marine spills contribute to the concentration of about 50-100 µg/L (ppb) in seawater (Saadoun, 2015). This indicated the suitability of the *P. aeruginosa* for the remediation of oil-contaminated sites as ~ 40 % oil was biodegraded at 750 mg/L initial oil concentration. However, there was a slight decrease in the biomass growth up to 3.76 g/L (0.5 %, v/v) of oil.

Further increment in the initial oil concentration caused a sharp decline, i.e., poor oil degradation ability of microbes. It could be due to the inhibitory effect of higher initial oil concentration on the biodegradation ability of the bacteria, as evidenced by the decrease in the biomass concentration with an increase in the oil concentration. Similar toxicity effects of oil were also deciphered in literature (Jiao et al., 2016; Vigneshwaran et al., 2018). Hence, there is a need to provide microbes with oil in such an amount that it does not cause toxicity. Sustainable substrate availability is enough for microbial metabolism and should be given more attention. In this regard, a novel conjugative biosorption-aided biodegradation-based strategy was investigated.

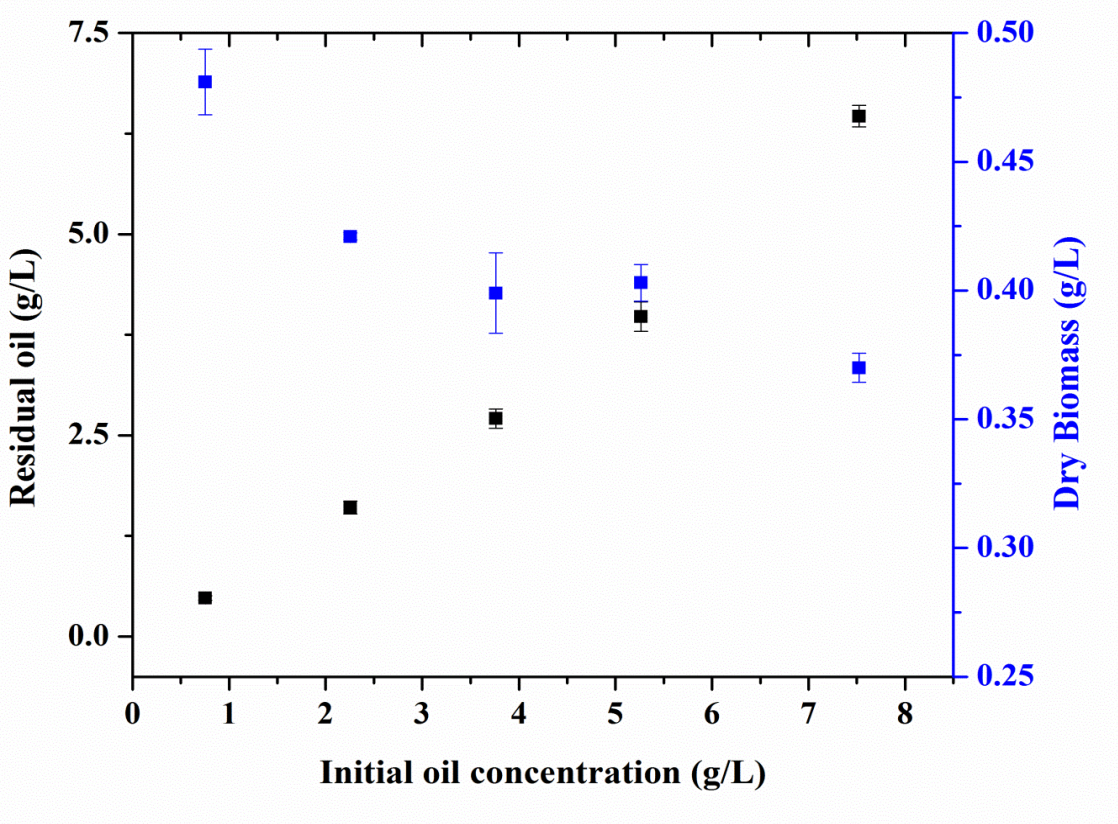

Figure 6.8. Effect of initial oil concentrations on biodegradation ability of *P. aeruginosa* P7815

6.3.7.1. Biosorption assisted microbial biodegradation strategy

The intolerance of bacterium to a high oil concentration was reduced primarily by incorporating biosorbents with an enormous oil adsorption capacity to minimize the bio-toxicity of oil. Initially, crude oil (1.5 g/L) was pre-adsorbed on the modified bagasse (10 g/L) followed by incubation of *P. aeruginosa.* The effect of biosorption on microbial oil degradation ability was analyzed by performing the oil degradation batch experiments with and without biosorbent. It was observed that, in the set containing 8 h pre-adsorbed biosorbent, there was improved cell growth, oil degradation, and biosurfactant concentration **(Figure 6.9 (B))** in comparison to control (only bacteria without bagasse) **(Figure 6.9 (A))**. The μ was found to be 0.12 ± 0.01 h^{-1} in case of the integrated process **(Figure 6.9 (B))** i.e. 1.5 folds higher than control (0.08 ± 0.01 h^{-1}) **(Figure 6.9 (A))**.

Similarly, there was a rapid decrease in residual oil up to 8 h due to the adsorption, which was further utilized through microbial biodegradation. The overall oil degradation in the integrated process was achieved as ~ 65 %, which was 4 folds greater than the control (~ 16 %). Biomass is reported to

synthesize the surface-active agents during the remediation of oils. A decrease in surface tension indicated biosurfactant synthesis (active surface metabolite). The biosurfactant profile was also monitored (Sharma et al., 2020), a growth-associated product. The maximum biosurfactant concentration for the integrated process was 0.82 g/L, while the control was 0.37 g/L. Biosurfactants are also reported to enhance the bioavailability of crude oil to microbes (Sharma et al., 2020). Biodemulsifiers were found to increase the degradation potential of hydrocarbon-degrading bacteria in ecosystems and petroleum decontamination in the marine environment (Silva et al., 2018). These observations complemented the greater oil degradation in the case of the integrated strategy.

Furthermore, the rate of microbial oil biodegradation (k_d) (**Figure 6.9 (A)**) was estimated by fitting Monod's equation stated as follows.

$$\frac{dC}{dt} = \frac{-k_d XC}{k_s + C} \approx \frac{-k_d XC}{k_s} \qquad [C(0) = C_0] \qquad \textbf{(6.8)}$$

$$C(t) = C_0 e^{\frac{-k_d Xt}{k_s}} \qquad \textbf{(6.9)}$$

Here, $C(t)$ stands for concentration of oil (g/L) at any time, t (h); C_0 refers to initial oil concentration; X refers to the concentration of biomass (g/L), and k_s represents half-saturation constant (g/L). The experimental data fitted equation 6.9 with an R^2 value of 0.90. The value of k_d and k_s was found to be 0.038 ± 0.001 h^{-1} and 17.25 ± 1 g/L, respectively. Further, to confirm the synergistic effect of the biosorption and biodegradation, the oil degradation data (**Figure 6.9 (B)**) were fitted by combining **equations 6.5 and 6.9** to predict the rates of the integrated process as follows.

$$\frac{dC}{dt} = -k_a(C - C_e) - \frac{k_d XC}{k_s} \qquad [C(0) = C_0] \qquad \textbf{(6.10)}$$

$$C(t) = -\frac{k_a C_e k_s}{(k_a k_s + k_d X)} \times \left[\left(1 - \frac{C_0(k_a k_s + k_d X)}{k_a C_e k_s}\right) e^{\frac{-t(k_a k_s + k_d X)}{k_s}} - 1\right] \qquad \textbf{(6.11a)}$$

$$C(t) = -\frac{k_a C_e k_s}{z} \times \left[\left(1 - \frac{C_0 z}{k_a C_e k_s}\right) e^{\frac{-zt}{k_s}} - 1\right] \qquad [k_a k_s + k_d X = z] \qquad \textbf{(6.11b)}$$

Here, k_a explains the rate of oil degradation due to adsorption, and k_d refers to the rate of oil biodegradation. The experimental data fitted very well to the above-combined expression **(equation 6.10)** with an R^2 value of 0.99. The values of k_a, k_d and $k_s$were estimated to be 2.15 ± 0.3 h^{-1}, 0.66 ± 0.08 h^{-1} and 3.27 ± 0.7 g/L, respectively. The rate of oil biodegradation k_d was enhanced by 17 folds in the case of biosorption-assisted microbial biodegradation strategy compared to only microbial biodegradation, which also agreed to 1.5 folds greater μ value in the integrated process.

These observations confirmed the synergistic effect of both processes. Fulazzaky *et al.* reported a similar synergistic effect of the biosurfactant producing ability of *S. marcescens* SA30 on the biosorption ability of granular sludge as biosorbent. Meng *et al*. also established a positive correlation of biosorption of petroleum hydrocarbons in the biodegradation ability of *Pseudomonas synxantha* LSH-7, suggesting a linear relationship ($R^2 > 0.90$) between biosorption of tetradecane, hexadecane, phenanthrene, and pyrene with their respective biodegradability (Meng et al., 2019).

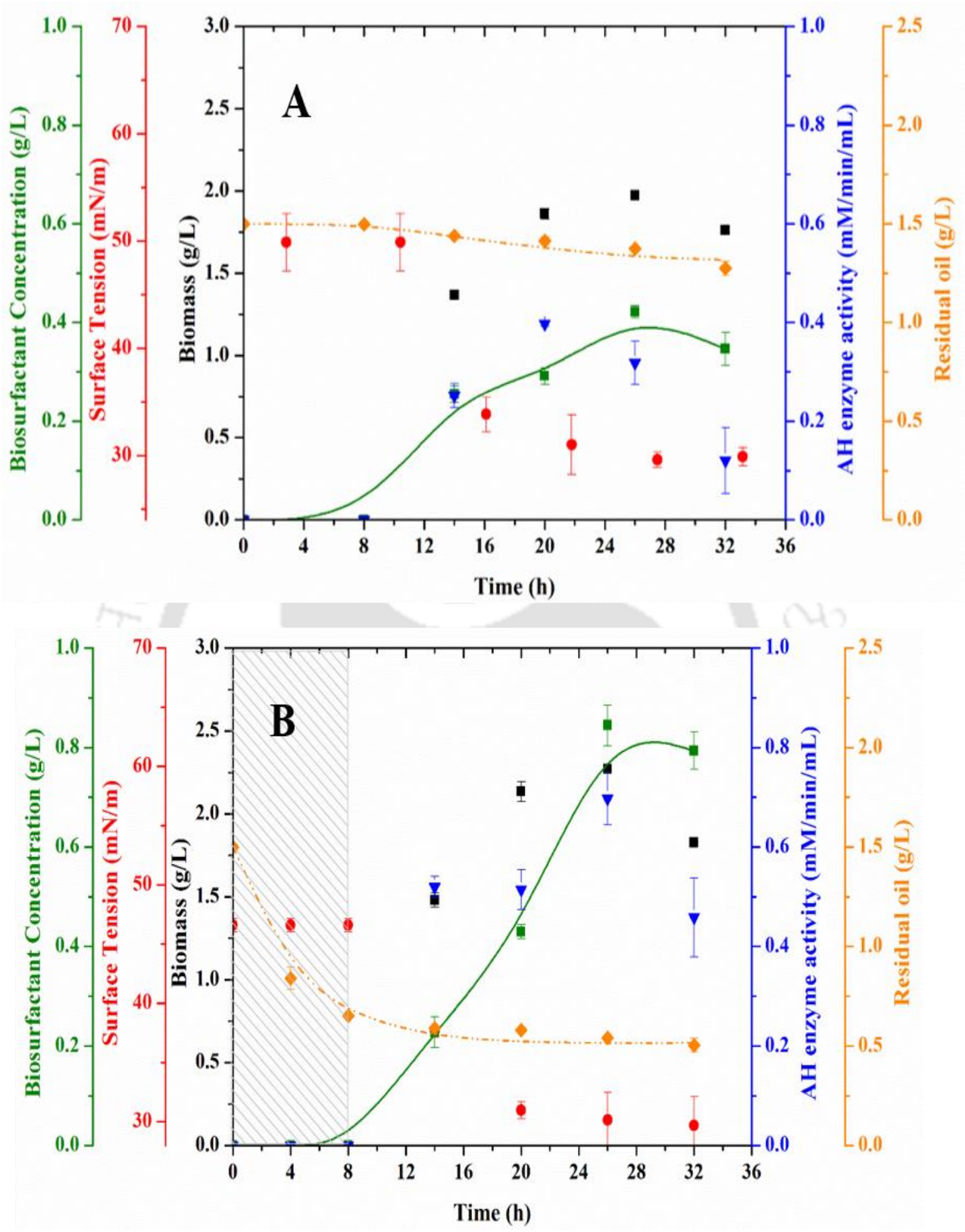

Figure 6.9. Oil degradation ability of *P. aeruginosa* within 32 h of incubation, (A) without and; (B) with bagasse. (Dotted line represents fitted data for the depletion of residual oil).

6.3.7.2. Molecular weight analysis of crude biosurfactant

The crude biosurfactant was characterized using MALDI-TOF analyses using sinapinic acid as a matrix. The mass spectra revealed the presence of a mixture of mono- and di- rhamnolipid congeners. As depicted in **Figure 6.10.** The monorhamnolipid molecules observed included Rha–C_{10}–C_{10} ($[M+Na]^+$, m/z =527; $[M+K]^+$, m/z 543), Rha–C_{12}–C_{14} ($[M+Na]^+$, m/z =611; $[M+K]^+$, m/z 626) and Rha–C_{14}–C_{14} ($[M+Na]^+$, m/z =639; $[M+K]^+$, m/z 655). Similarly, the dirhamnolipid molecules observed included Rha-Rha–C_{10}–C_{10} ($[M+Na]^+$, m/z =673; $[M-H+ Na_2]^+$, m/z 695), and Rha-Rha–C_{12}–C_{12} ($[M+Na]^+$, m/z =712) which is in concordance to various reported rhamnolipids peaks (Irorere et al., 2018; Mishra et al., 2021; Rooney et al., 2009; Scoma et al., 2017; Trudgeon et al., 2020).

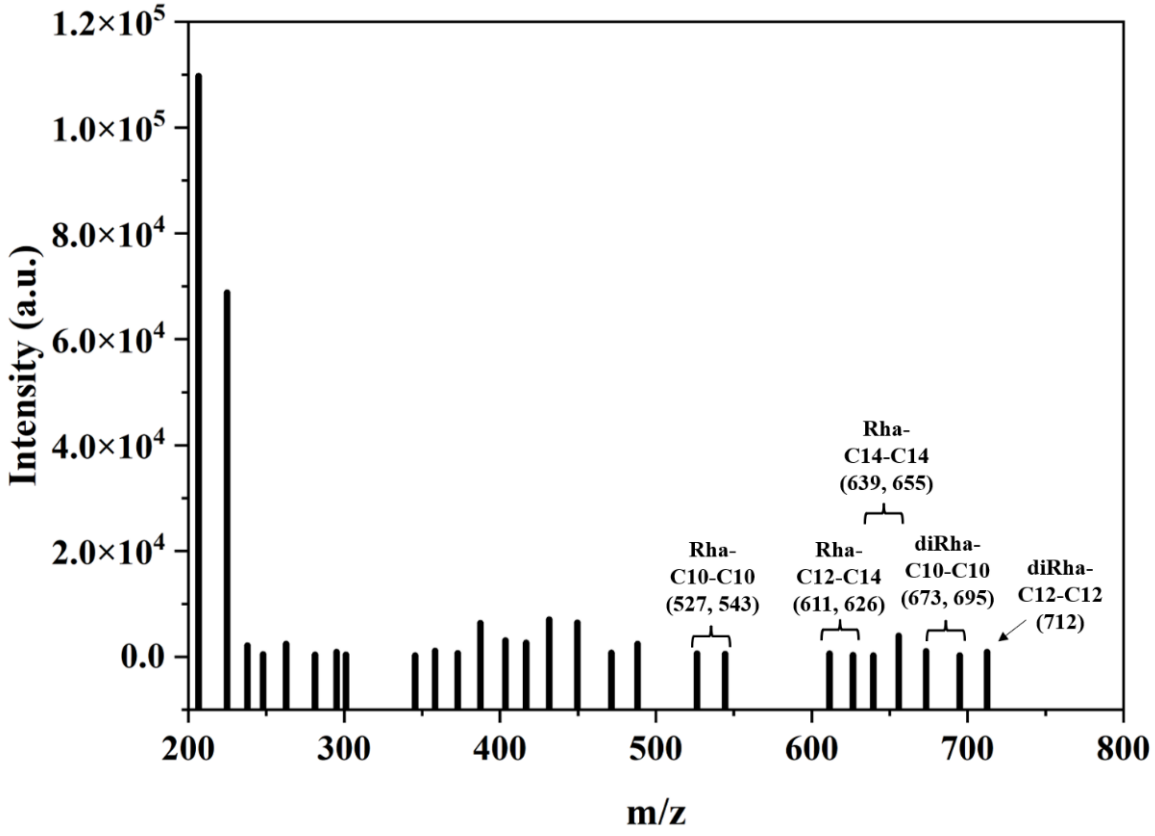

Figure 6.10. Mass spectroscopic analysis of crude biosurfactant using MALDI-TOF-MS

6.3.7.3. GC-FID analyses of residual oil

The GC-FID chromatograms at different time intervals in the cases of bagasse alone, microbe alone, and their conjugation on the overall oil degradation activity are shown in **Figure 6.11**. The

chromatograms presented the amount of residual oil at different time intervals, i.e., 0 h (raw crude oil), 8 h (after adsorption), and 32 h (after microbial biodegradation), during the integrated process in comparison to the control. It was observed that the crude oil used for the study was composed of long hydrocarbon chains varying from C_6 to C_{50} **(Figure 6.11 (A) and (B))**. Microbes were found to effectively biodegrade smaller carbon chains (C_7 to C_{20}) with retention time (RT, 5-15 min) within the initial 8 h **(Figure 6.11 (C))**. However, in the case of long hydrocarbon chains (C_{20} to C_{50}), the presence of peaks for RT > 20 min showed ineffective microbial remediation **(Figure 6.11 (D))**. In the case of the integrated strategy, it was observed that the maximum reduction in peak intensity occurred for hydrocarbon chains (C_7 to C_{50}) after bagasse biosorption within 8 h of incubation **(Figure 6.11 (E))**. Besides, such reduced concentrations of long-chained hydrocarbons were effectively utilized by microbes exhibiting even lower peak intensities after 32 h of incubation **(Figure 6.11 (F))**. Hence, almost complete elimination of oil in the case of the integrated strategy was observed, which agreed with the percentage of the overall oil degradation.

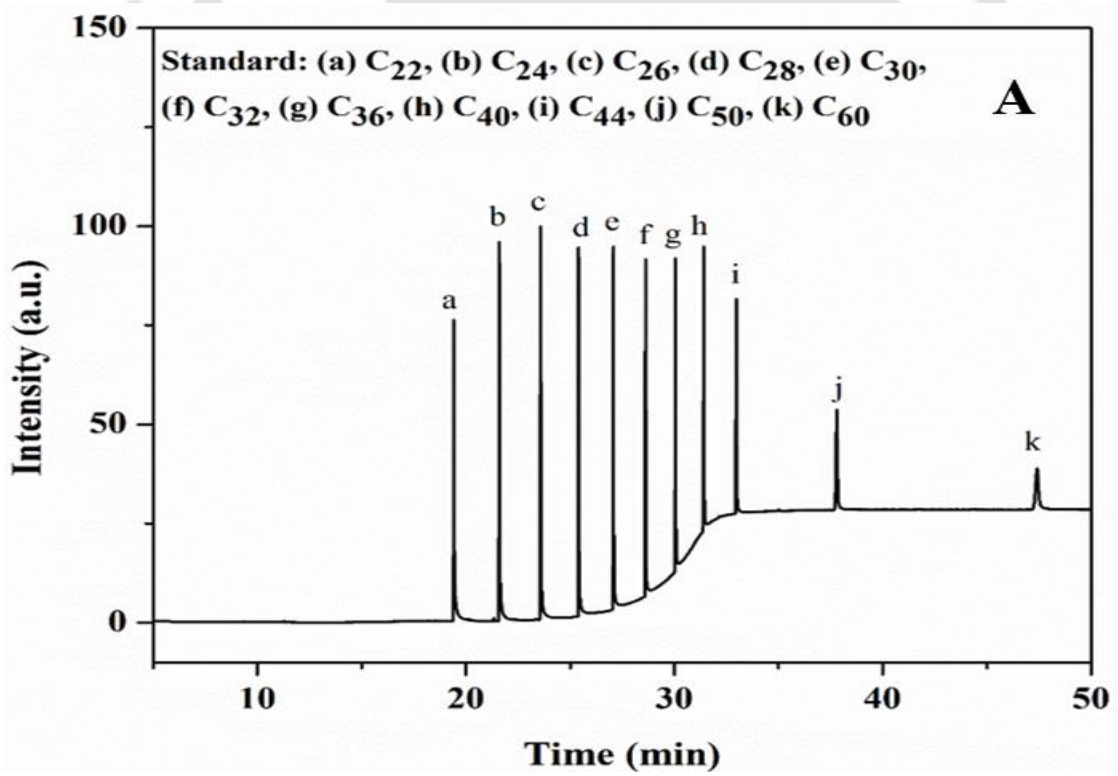

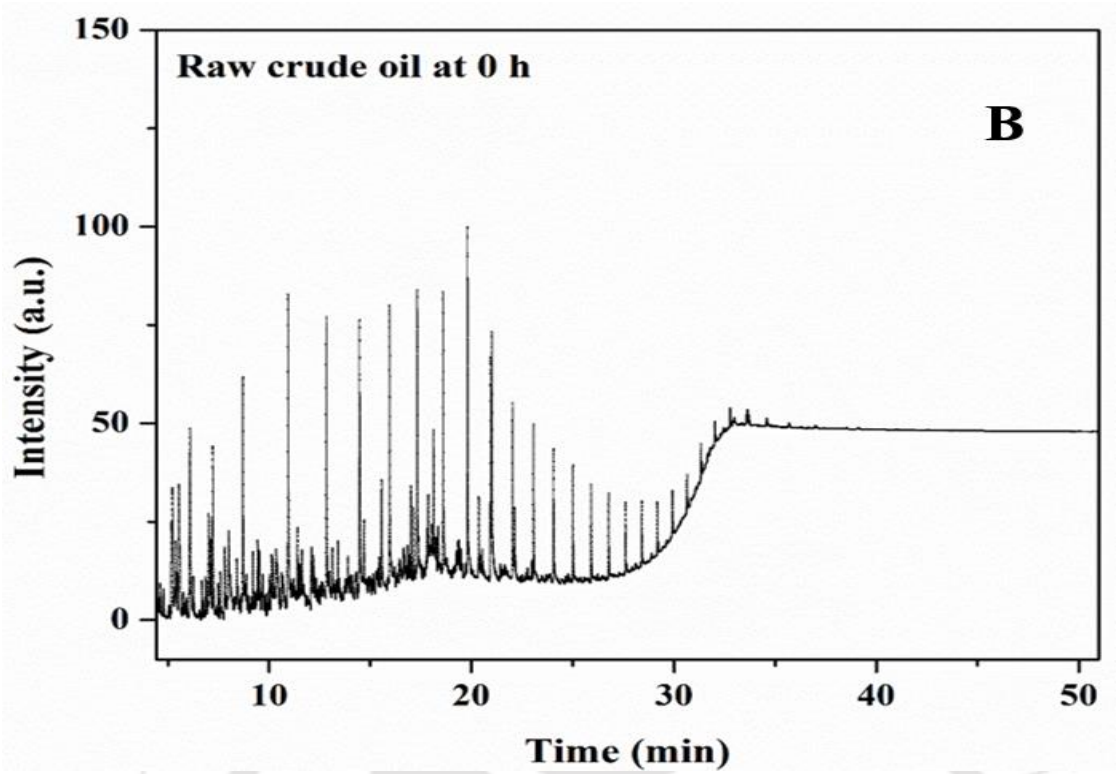

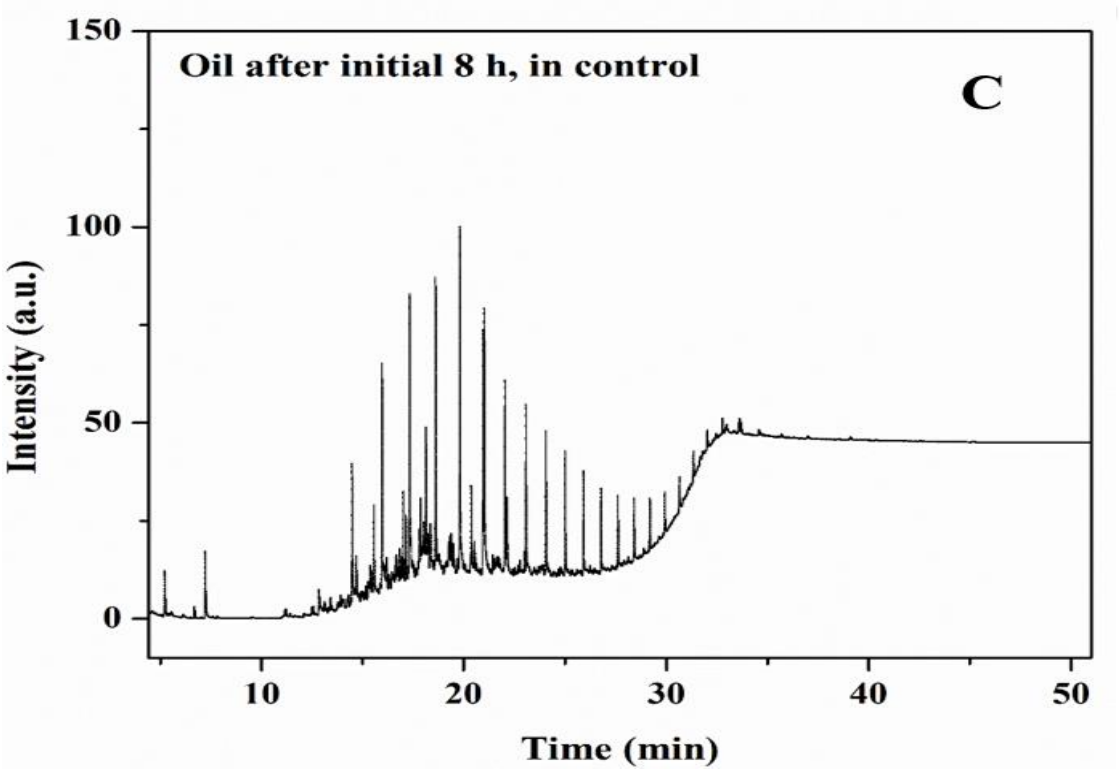

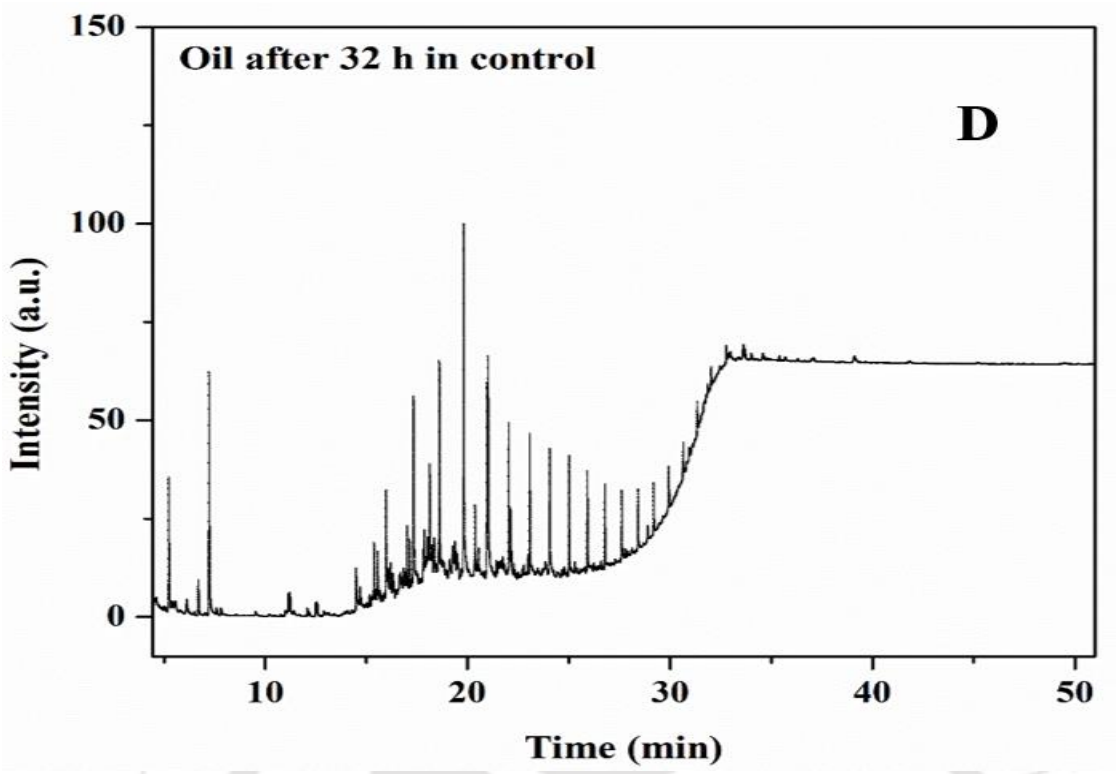

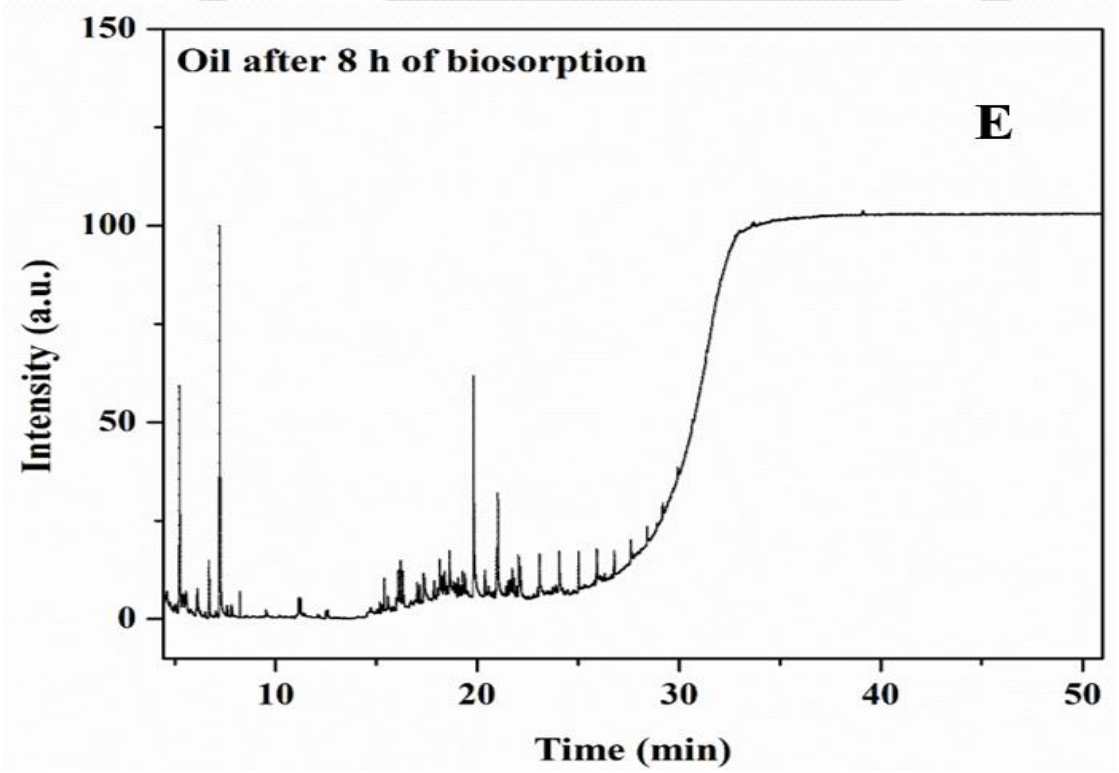

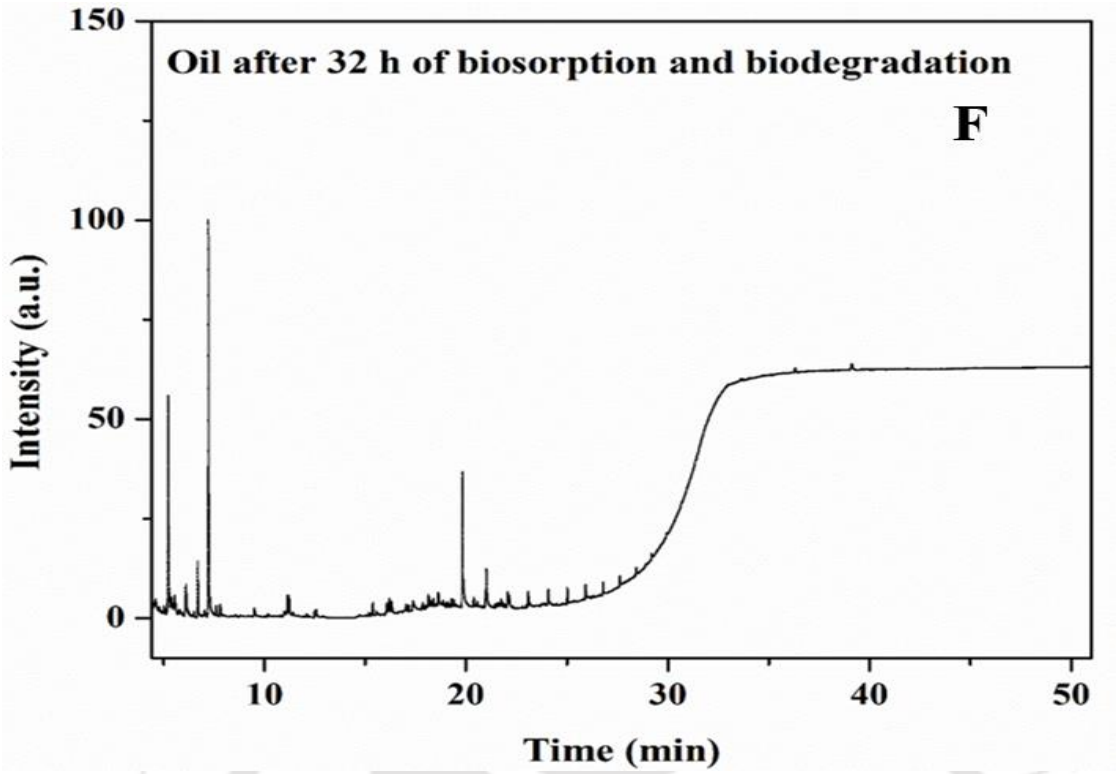

Figure 6.11. GC-FID chromatograms for integrated biosorption - biodegradation study. Standard (**A**); crude oil at t = 0 h (**B**); crude oil after microbial biodegradation t = 8 h (**C**), and t = 32 h (**D**), crude oil after bagasse biosorption at t = 8 h (**E**), and crude oil after biosorption assisted microbial biodegradation at t = 32 h (**F**)

6.3.8. Insights into the integrated strategy

The synergistic effect of biosorption and biodegradation is explained in the section 6.3.9 in terms of improved biomass, biosurfactant yield, and overall oil degradation ability of the residing microbes. This section examined the interactions between the microbes and bagasse based on FESEM and fluorescence images. Adhered bacterial cells were observed on the bagasse surface **(Figure 6.12 (A))**. FESEM image revealed the rod-shaped morphology of bacteria, and the average size of microbes was 1.03 ± 0.08 µm **(Figure 6.12 (B))**. It ascertained the presence of normal *P.aeruginosa* cells. The bacterial cells attached to the bagasse were blue in fluorescence images **Figures 6.12 (C and D)**. Oil was seen adsorbed on the bagasse surface (red color in **Figures 6.12 (C) and (D)**) in the vicinity of microbes. The bagasse surface was fully covered by oil. It revealed that oil was quickly adsorbed on the bagasse surface due to the

faster adsorption (6.1 h^{-1}) and later was slowly utilized (degraded) by the adhered microbes (0.01 h^{-1}). Hence, the bagasse-coupled microbes exhibited a commensalism relationship between biosorption and biodegradation. The oil pre-adsorbed bagasse encouraged adherence of bacterial cells due to the improved bioavailability of the oil. Various literature also has supported the improvement in cell growth and metabolism in the presence of the biocompatible carrier (Dashti et al., 2017; Dashti et al., 2019). An improved interfacial interaction is expected to affect the sub-cellular bacterial machinery. AH is one of the key enzymes of oil degradation produced by bacteria (extracellularly and intracellularly). The activity of extracellular AH is greatly influenced by substrate availability in the culture. In the case of crude oil pre-adsorbed bagasse, the formation of a substrate bed improved the oil availability for the microbes. Likewise, from **Figure 6.9 (A)**, it was observed that there were two-folds improved AH activity (0.69 mM/mL/min) than the control **(Figure 6.9 (B))**. It was due to the improved oil availability in the case of pre-adsorbed bagasse, which enhanced the activity of AH, as explained in the reported literature (Elumalai et al., 2017; Kochius et al., 2018).

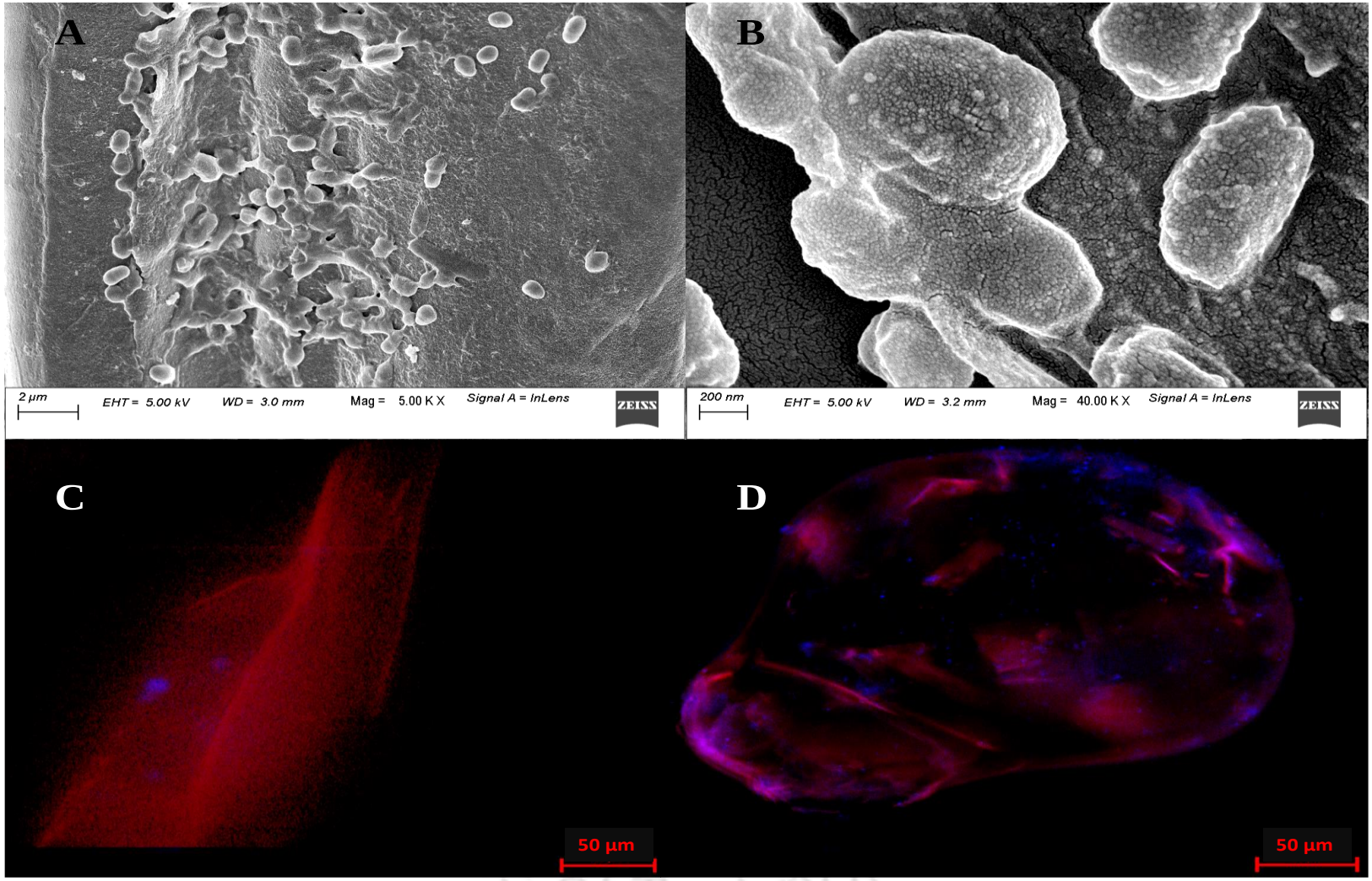

Figure 6.12. Microscopic studies of the interaction between oil pre-adsorbed bagasse and microbes (**A-B**) FESEM; and (**C-D**) Fluorescence imaging (Nile red for oil adhered bagasse and DAPI for bacteria)

6.3.9. Integrated fed-batch oil biodegradation study

Microbial degradation is considered to be one of the eco-friendly approaches for bioremediation. The microbes are equipped with well-organized machinery to survive in an extreme environment, utilize different substrates, and produce value-added metabolites. However, complex hydrocarbons like crude oil are poorly biodegradable and toxic to microbes. Thus, the remediation of oil-contaminated sites is still a challenge due to the slower degradation rate and susceptibility of microbes to a higher concentration of oil. Biodegradation of crude oil was performed in fed-batch mode using an oil-degrader *Pseudomonas aeruginosa* to address the issue of substrate toxicity.

Further, the slower biodegradation was integrated with a faster biosorption process for the effective remediation of crude oil. Highly fibrous and porous sugarcane bagasse was used as adsorbent and was further surface modified with hydrophobic octyl groups to improve the surface-oil interactions. The results are discussed in two parts: (i) Fed-batch biodegradation and (ii) Biosorption coupled fed-batch biodegradation.

A fed-batch study was opted to improve the biodegradation ability of the bacteria. The ability of bacteria to utilize crude oil as the sole carbon source was previously explored using a batch study wherein an initial crude oil concentration of 1.5 g/L was added to BH media with a 5 % (v/v) inoculum and allowed to incubate at 37°C and 180 rpm (Sharma and Pandey, 2021). The growth curve showed the bacteria exhibited a μ value of 0.052 h^{-1}. The biosurfactant yield ($Y_{P/S}$) and q_P values were found to be 1.47 and 0.011 g/g/h, respectively. The substrate utilization rate was estimated to be 0.02 g/L/h, i.e., 0.48 g/L/day The overall oil degradation in 24 h was 15 ± 2 % (Sharma and Pandey, 2021).

Based on batch data, a substrate concentration was fixed at 0.5 g/L/day in the fed-batch study. A regular oil feed was performed to maintain cells in the exponential phase. A typical microbial growth profile was observed in **Figure 6.13 (A)**, where ln X initially increased and remained constant after that with regular feeding of oil up to 26 days, reflecting the extended stationary phase. However, the specific growth rate, μ, started slightly declining after 2nd day, which presumably corresponded to the decrease in dilution factor **(Figure 6.13 (B))**. Thus, in this strategy, a total of 11 g/L of crude oil was remediated compared to 1.5 g/L in the batch study. Also, the overall oil degradation was 34.72 ± 2.8 %, enhanced by more than 2 folds. Summarily, in the fed-batch oil biodegradation strategy, the oil degradation ability

was enhanced due to adequate bioavailability of oil for uplifting the bacterial metabolism and oil degradation machinery. However, constant feeding for an extended duration results in excess bioavailability, which may cause an inhibitory effect on the bacterial metabolic activity (Sharma et al., 2020; Sharma et al., 2019).

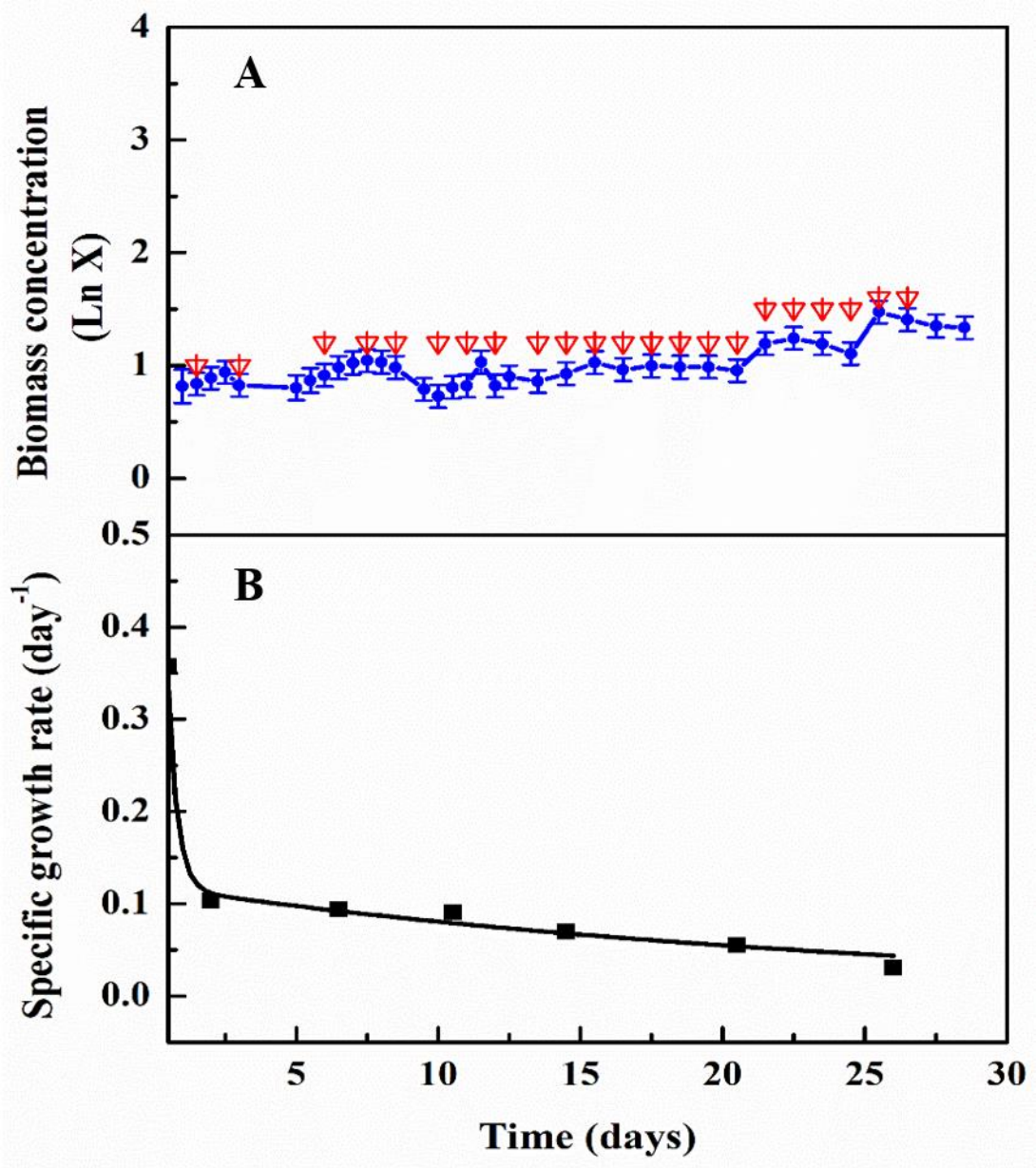

Figure 6.13. Effect of intermittent oil feeding on biodegradation ability of *P. aeruginosa* P7815 (A) Biomass growth curve (Red arrows represents oil feed time intervals), and (B) Specific growth rate (μ) with time

6.3.9.1. Biosorption coupled fed-batch biodegradation

The previous fed-batch strategy improvised biosorption coupled microbial oil degradation to diminish the inhibitory effect of high initial oil concentration on bacterial growth and biodegradation activity. Herein, the initial oil was preliminarily subjected to adsorption using octyl-modified hydrophobic bagasse for the first 8 h. Next, the bacteria were inoculated to this oil-adsorbed bagasse in BH media, and a regular oil feeding of 0.5 g/L was performed. Such a biosorption-assisted biodegradation approach kept the microbes metabolically more active, allowing them to grow ~ 1.5 folds higher than without a biosorbent fed-batch study **(Figure 6.14 (A))**. The specific growth rate μ followed a typical fed-batch pattern **(Figure 6.14 (B))**. A total of 11 g/L of crude oil was remediated, similar to that of fed-batch without biosorption. However, this integrated strategy enhanced the overall oil biodegradation to 54.87 ± 2.1 %. During constant oil feeding in the presence of biosorbent, the continuous adsorption accompanied sustained bioavailability of the oil. This approach thus improved biomass growth and resulted in better oil degradation.

In addition, the biosurfactant production profile of the bacteria was also investigated. Biosurfactants improve the oil surface area by mobilization, emulsification, or solubilization and thus enhance its bioavailability for microbial biodegradation. They are also known to improve the bacterial cell surface hydrophobicity, which increases its affinity towards oil for effective utilization (Sharma et al., 2020; Tahseen et al., 2016). An improvement in oil biodegradation with the increase in biosurfactant concentration was evidenced. While the biosurfactant concentration was obtained as 0.35 g/L in the batch study (Sharma and Pandey, 2021), an increment of ~3 folds (1.02 ± 0.08 g/L) was obtained during the fed-batch mode of operation. It was further improved by ~ 5 folds (1.7 ± 0.07 g/L) in the integrated fed-batch approach, establishing the positive role of biosurfactant in microbial oil degradation activity. **Table 6.3** summarizes the overall oil degradation and biosurfactant production in all three modes of operations.

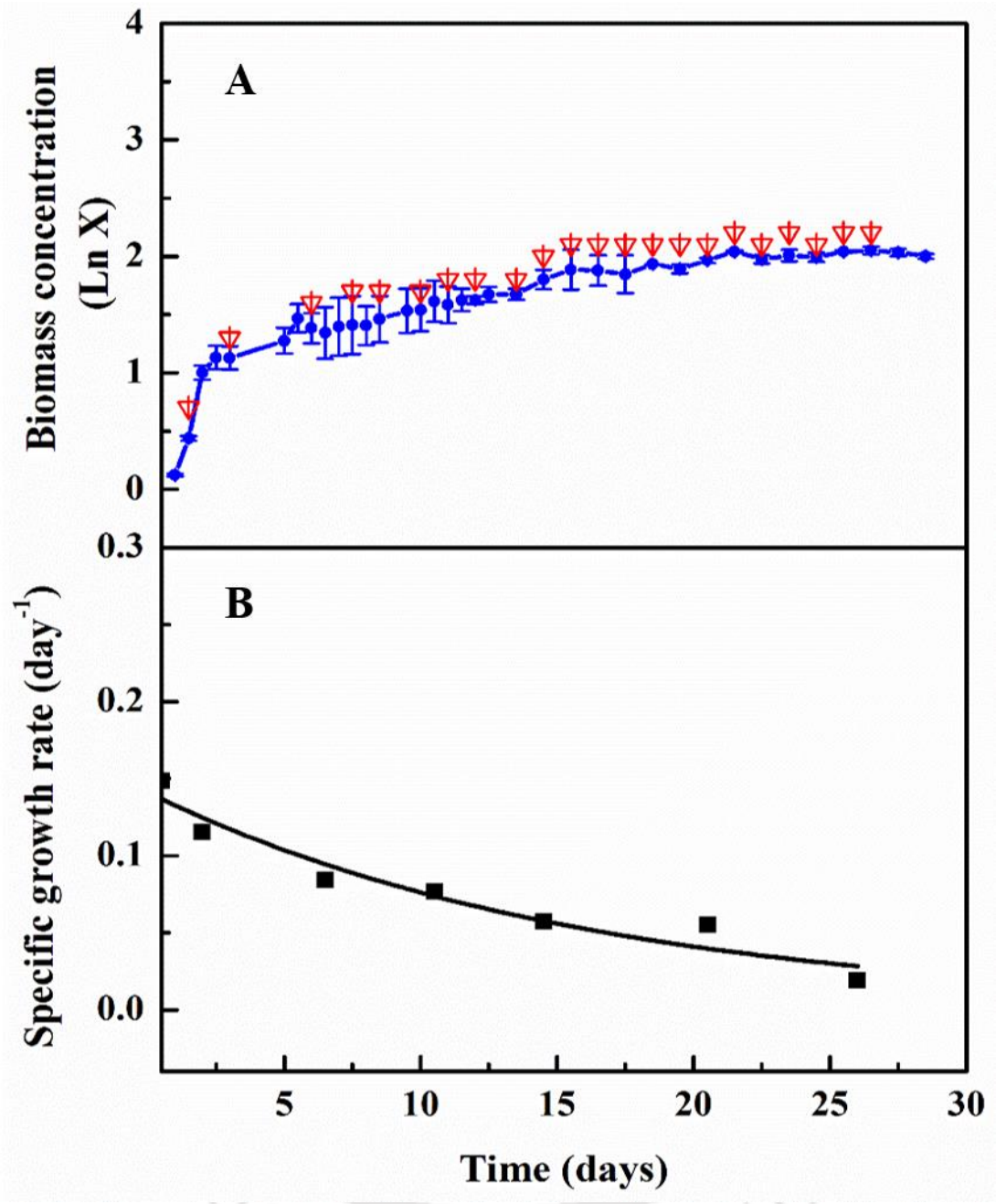

Figure 6.14. Effect of intermittent oil feeding on biosorption coupled biodegradation ability of *P. aeruginosa* P7815 (A) Biomass growth curve (Red arrow represents oil feed), and (B) Specific growth rate (μ) with time

Table 6.3. Overall oil degradation and biosurfactant production in the batch mode of oil feeding, after 30 days of incubation

Experimental setup	Oil Degradation		Biosurfactant production	
	Total oil feed (g/L)	Degradation (%)	$Y_{P/S}$ (g/g)	Concentration (g/L)
Batch	1.5	15 ± 2.5	1.47	0.35 ± 0.03
Fed-batch without biosorbent	11.0	34.72 ± 2.8	0.27	1.02 ± 0.08
Fed-batch with biosorbent	11.0	54.87 ± 1.1	0.28	1.7 ± 0.07

Hence, biosorption facilitated the better utilization of oil by microbes as the overall oil degradation rate was increased by 150 % compared to the fed-batch without biosorption. Various literature supports the aerobic exterior and anoxic interior of bagasse as the unique feature for microbial niche development and improved metabolic activities, yet, the studies are limited to heavy metals and single hydrocarbons (Mazzeo et al., 2020; Nie et al., 2018). However, the synergistic effect of bagasse on microbial biodegradation in crude oil, a complex mixture of long chains of hydrocarbons was examined in this chapter.

Similar biosorption coupled microbial biodegradation of crude oil has been reported using sawdust as an oil sorbent. The study reported the crude oil (0.25 %, w/v) biodegradation ability of inherent sawdust harboring bacteria such as *Actinobacterium* sp. SDB1, *Micrococcus luteus* SDB2, *Rhodococcus erythropolis* SDB3, and *Rhodococcus opacus* SDB4 as 35, 38, 37, and 48 %, respectively, after 10 days of incubation (Ali et al., 2011). Dashti et al. also reported crude oil (1 %, w/v) biodegradation activity by the inherent microbial consortium, ranging from 34 to 45 % in 8 months when incubated with moist sorbents such as wheat straw and corn cobs (Dashti et al., 2017).

6.4. Conclusions

The oil adsorption capacity of bagasse as a low-cost model biosorbent was improved by modifying its surface by forming octyl SAMs. The kinetics of surface modification was studied using FTIR, and successful modification was achieved in 8 h. The modified bagasse was characterized using FTIR, BET, and XRD analyses. The *qm* value of modified bagasse was enhanced by two folds (6.8 g/g) than raw bagasse. *Pseudomonas aeruginosa* effectively biodegrade crude oil up to 0.75 g/L (0.1 % v/v). An integrated biosorption coupled biodegradation approach was implemented for effective crude oil bioremediation. A kinetic model was proposed for oil degradation, confirming simultaneous biosorption and biodegradation. Hydrophobically modified bagasse supported the improved bacterial adhesion and enhanced the oil bioavailability as confirmed using the microscopic techniques. This biosorption coupled biodegradation strategy exhibited 17 folds higher oil degradation than microbial degradation. The biodegradation of crude oil was also confirmed by synthesizing biosurfactants and lowering surface tension. Greater biosurfactant production and extracellular alkane hydroxylase activity also correlated with the synergistic effect of biosorption and biodegradation.

A fed-batch strategy was opted to further improve the oil biodegradation ability. A 2-folds improved oil degradation and 3-folds increased biosurfactant production was achieved when bacteria were grown in fed-batch mode than batch. With the integrated strategy, enhanced oil degradation by 150 % with 5 folds improved biosurfactant production was obtained. Conclusively, the enhanced microbial growth, biosurfactant production, and oil degradability show the potential role of using sugarcane bagasse as a sorbent for oil remediation. Insights into the change in microbial growth, substrate (oil) utilization, and product formation are deciphered. Such setup shows potential suitability in the oil refinery effluent treatment, soil-washing amendments, tertiary water treatment, and other biosorption-assisted remediation applications. Conclusively, the octyl-modified bagasse is proven to be an economic, eco-friendly, and efficient biosorbent for crude oil bioremediation and other environmental applications. The surfaces of natural biosorbents being used for the remediation can be modified by forming hydrophobic SAMs to improve their performances for the treatments of oil spillage and contaminated soils.

Chapter 7

Overall Conclusions and Future Scopes of the Work

This chapter describes the key inclusive inferences of studies performed in the present dissertation. Furthermore, the chapter also prospects future research in this direction.

7.1. Overall conclusions

Remediation of petroleum and oil-contaminated sites using microbial biodegradation ability is the most sustainable and eco-friendly approach; however, studies are required to improve the biodegradation rate and amend the poor affinity of microbes to oil. Minimizing the bacterial exposure to excess contaminants using immobilization within carrier or oil sorbents can mitigate the biotoxicity challenges. Biosurfactants are surface-active molecules that are well reported for their surface-active property significant for oil emulsification, mobilization, and solubilization.

The present dissertation explored potential inherent oil-degrading bacterial strains for their hydrocarbon biodegradation ability by focussing on improving their biosurfactant production ability. Three major factors driving the bacterial biosurfactant production were optimized: pH, Temperature, C source, N source and their C/N ratio. Using OFAT based optimization tool, *Agrobacterium fabrum* SLAJ 731 exhibited a maximum biosurfactant production of 5.77 ± 0.3 g/L under optimal parameters: pH 6 and 30 °C using glucose and yeast extract as C and N sources in a mass ratio of 2:1. The crude oil biodegradation ability of A. fabrum under maximized biosurfactant production condition was further studied by supplementing bacteria with 1% crude oil. The study revealed an approximately 1.5 folds high crude oil biodegradation of 58 ± 5 % and simultaneous 1.5 folds increased biosurfactant production at a concentration of 4.15 ± 0.2 g/L within 6 days of incubation. The study hypothesized that the bacteria showed improved growth in the presence of Glucose, which led to improved biosurfactant production, revealing it to be growth associated product. Similarly, Glucose also enhanced AH enzyme activity by maintaining the redox potential, thus leading to improved crude oil degradation. Insights into crude oil biodegradation and biosurfactant production showed they are directly related under optimized growth

conditions. Chapter 3 concluded that bacterial biosurfactant production could be considered a critical factor in enhancing its biodegradation ability

Another inherent sludge bacterium, *Bacillus subtilis* RSL 2, was optimized for maximum biosurfactant production in the presence of sole crude oil as a C source and YE as N source. The pH, Temperature, and crude oil concentration optimization were performed using the RSM-CCD technique. The study revealed that a maximum biosurfactant production of 3.6 ± 0.3 g/L was obtained at optimized pH 4, 25°C and 1 g/L crude oil concentration. The obtained crude biosurfactant was used as a biostimulant for further biodegradation study. When used as a simultaneous inoculant with bacteria, the biosurfactant increased the CSH improving the oil and microbe interactions and bioavailability of the oil. The biosurfactant-mediated biodegradation under optimized conditions enhanced overall oil degradation and biosurfactant production by 1.6 folds. Chapter 4 concluded that bacterial biosurfactants could be used as a biostimulant to uplift the crude oil biodegradation efficiency above the optimal value.

To diversify the bacterial catabolic activities and thus improve overall oil biodegradation efficiency, a consortium was prepared using three potential inherent oil-degrading bacterial strains, *A. fabrum, P. aeruginosa and B. subtilis*, in Chapter 5 of the dissertation. The bacteria were studied for the biodegradation of sole aliphatic (HEX), aromatic (PHE), or their binary mixture (HEX+PHE) as axenic and consortium. The study revealed the consortium's mode of interaction and substrate utilization behaviours. An integrated model combining first-order exponential decay and Monod equation fitted well to the biodegradation data. Parallel assimilation of HEX and serial assimilation of PHE was experienced in the consortium. The study concluded that the designed microconsortium achieved a biodegradation efficiency for sole HEX at 92.4 %, PHE at 88.7 %, HEX = 97.2 %, and PHE = 91.9 % in the binary mixture. Increased biodegradation at a lower initial concentration highlighted the biotoxicity effect of hydrocarbon on biodegradation efficacy; thus, next chapter focussed on mitigating such limitations.

A biosorption-mediated biodegradation strategy was opted to decrease the toxicity of high oil concentration exposure to bacteria in Chapter 6. Sugarcane bagasse surface was hydrophobically modified using octyl SAMs improving its qm value of bagasse by two folds (6.8 g/g). The modified bagasse was used as a pre-treatment to adsorb the oil before bacterial biodegradation as an integrated

bioremediation approach. A kinetic model fitted well for the integrated process, stating the occurrence of simultaneous biosorption and biodegradation where modified bagasse improved bacterial-oil interactions, exhibiting a 17-fold higher oil degradation than sole microbial degradation. Higher biosurfactant production and AH enzyme activity confirmed biosorption and biodegradation synergistic effect. This strategy was further extended to the fed-batch mode of operation to increase the bacterial biosurfactant production ability while being exposed to increased oil concentration in the presence and absence of biosorbent. A 2-fold and 3-fold increased oil degradation and biosurfactant production, respectively, was obtained for fed-batch than the batch biodegradation study. Concludingly, the integrated fed-batch strategy achieved a 150 % increased oil degradation and 5 folds improved biosurfactant production.

To summarize, biosorbent aided biosurfactant producing bacterial biodegradation is a promising solution to in-situ bioremediation of oil spills and other hydrocarbons contaminated site bioremediation such as oil refinery effluent treatment, soil-washing amendments, tertiary water treatment, and other biosorption-assisted remediation applications.

7.2. Future Scopes

Presently, crude oil spilled sites take months to years to achieve a significant microbial load to accelerate biodegradation. While various expensive biostimulants and genetically engineered strains have shown promising results for in-situ bioremediation applications, exploration of inherent oil-degrading bacterial strains and optimizing their growth parameters and nutrient requirements could be a more economically sustainable solution. Design of synergistically growing microbial consortium will aid in achieving high microbial load in no time and simultaneously provide diverse catabolic enzymes that will also accelerate the biodegradation rates by many folds. To further improve the present research inferences, detailed studies are required.

7.2.1. Exploration of metabolic pathways involved in mixed hydrocarbon biodegradation

Understanding the metabolic pathways involved in bacteria while utilizing hydrocarbon as the sole C source will help prepare a consortium where by-products of one bacterium can act as co-substrate for

the other, thus preventing the accumulation of toxic by-products and starvation phenomenon that are often limiting factors in bacterial growth.

7.2.2. Exploring kinetic model predicting the effect of biosurfactant concentration on hydrocarbon biodegradation

Studies have revealed the synergistic effect of biosurfactant concentration on bacterial hydrocarbon biodegradation; however, deducing these findings as a kinetic model predicting the minimum biosurfactant concentration required to achieve maximum biodegradation will aid in strategizing feed dosage and recovering extra biosurfactant for other potential applications.

7.2.3. Exploring light-weight biosorbent and tunning its hydrophobicity using biosurfactant conjugation

Apart from chemically modified bagasse, few naturally occurring hydrophobic substrates such as Kapok fiber can also be further explored for oil remediation studies. The surface of these fibers can be tunned using amphiphilic biosurfactants, acting as a bridge for floating hydrophobic substrate and aqueous suspended bacteria. These fibers have a hollow lumen that imparts natural floatability, thus increasing the contact time and area to spilled oils. Studies revealed that these natural fibers harbor many microbes. Hence, designing a suitable oil-degrading consortium and immobilizing them into such low-cost natural carriers is a sustainable, low-cost, and eco-friendly approach towards oil bioremediation.

7.2.4. Scale-up of integrated biosurfactant-modified-biosorbent coupled microbial biodegradation of crude oil and enhanced biosurfactant production

The integrated biosorbent coupled biodegradation study can be further scaled up to increase tolerance of microbial consortium to high crude oil concentration and simultaneously increase biosurfactant production. The biosurfactant can be maintained within the bioreactor using a continuous fill and draw set up to recover the biosurfactant-rich froth. Biosurfactant is precipitated, whereas the residual nutrient-

rich broth is sent back to the bioreactor. The recovered biosurfactant can be used for antibacterial, soil washing, and other bioremediation and biomedical applications **(Figure 7.1)**.

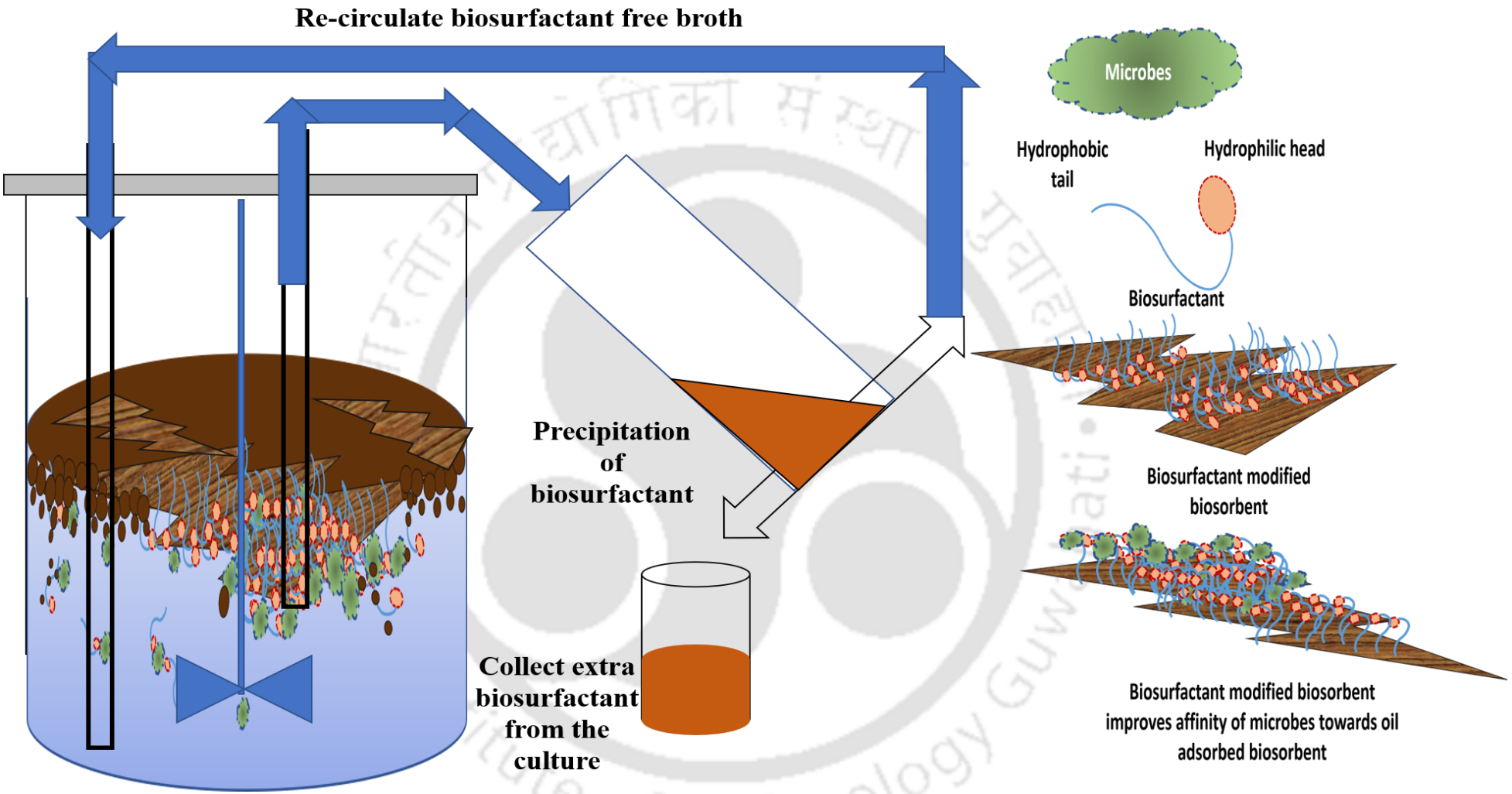

Figure 7.1. An integrated biosurfactant modified biosorbent coupled microbial biodegradation strategy to improve bacterial biosurfactant production as well tolerance to high crude oil concentration

Appendices

Appendix 4A

Production of biosurfactant by *Bacillus subtilis* RSL-2 isolated from sludge and biosurfactant mediated degradation of oil

S4-1. Results and discussion

S4-1.1. Estimation of residual crude oil using GC-FID

The GC-FID chromatograms for the recovered residual oil after biosurfactant-assisted biodegradation studies are represented in **Figure S4-1**. Complete degradation of small chains of hydrocarbons represented as RT= 0-15 min, in all the experimental cases. An almost 50 % reduction was obtained in peak intensities for long chains of hydrocarbons (RT = 15-51 min). In the case of simultaneous biosurfactant and oil feeding (B+C), the maximum decrease in peak intensities (degradation) was observed.

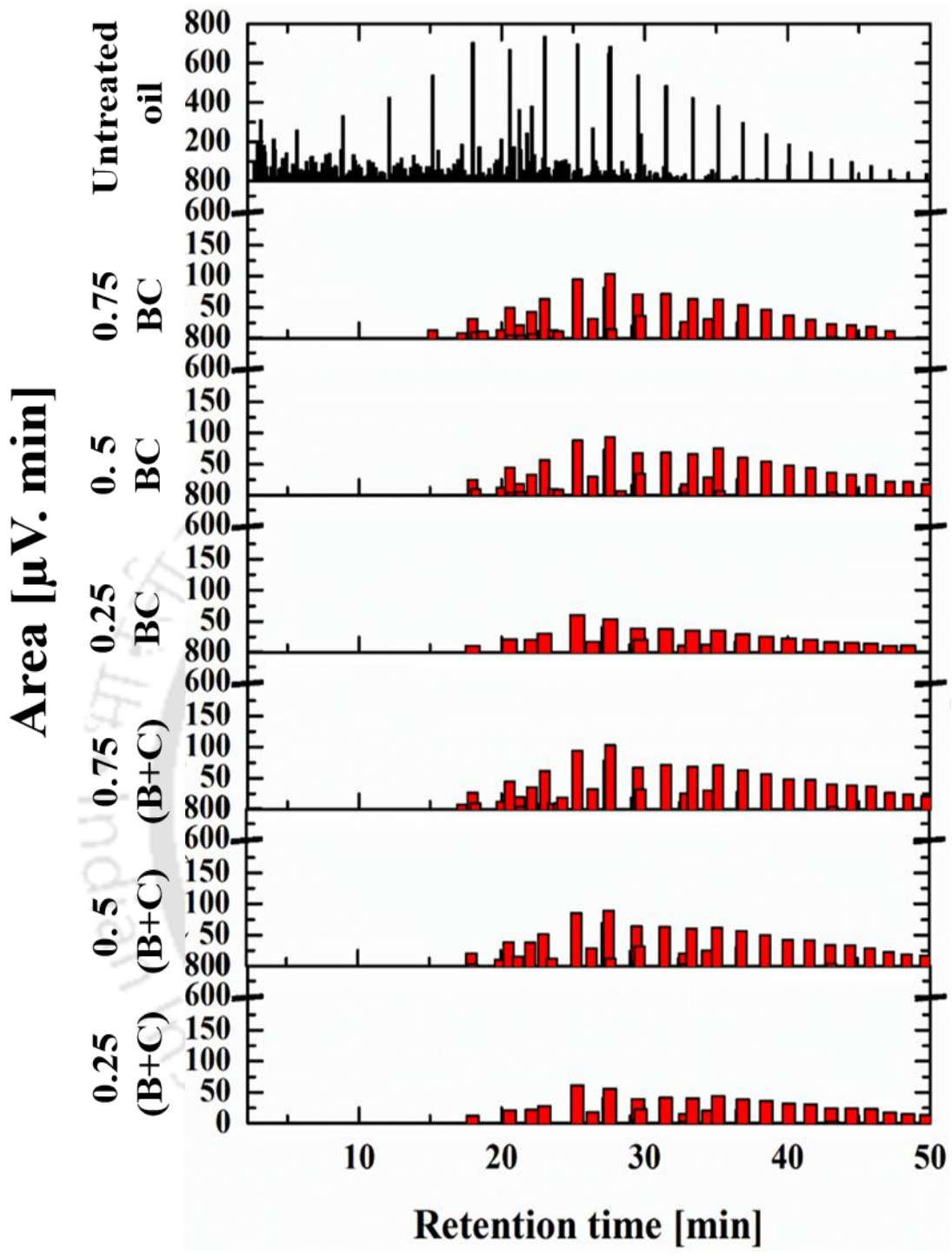

Figure S4-1. GC-FID analysis of crude oil degradation in different experimental setup

Appendix 5A

Biodegradation kinetics of binary mixture of hexadecane and phenanthrene by the bacterial microconsortium

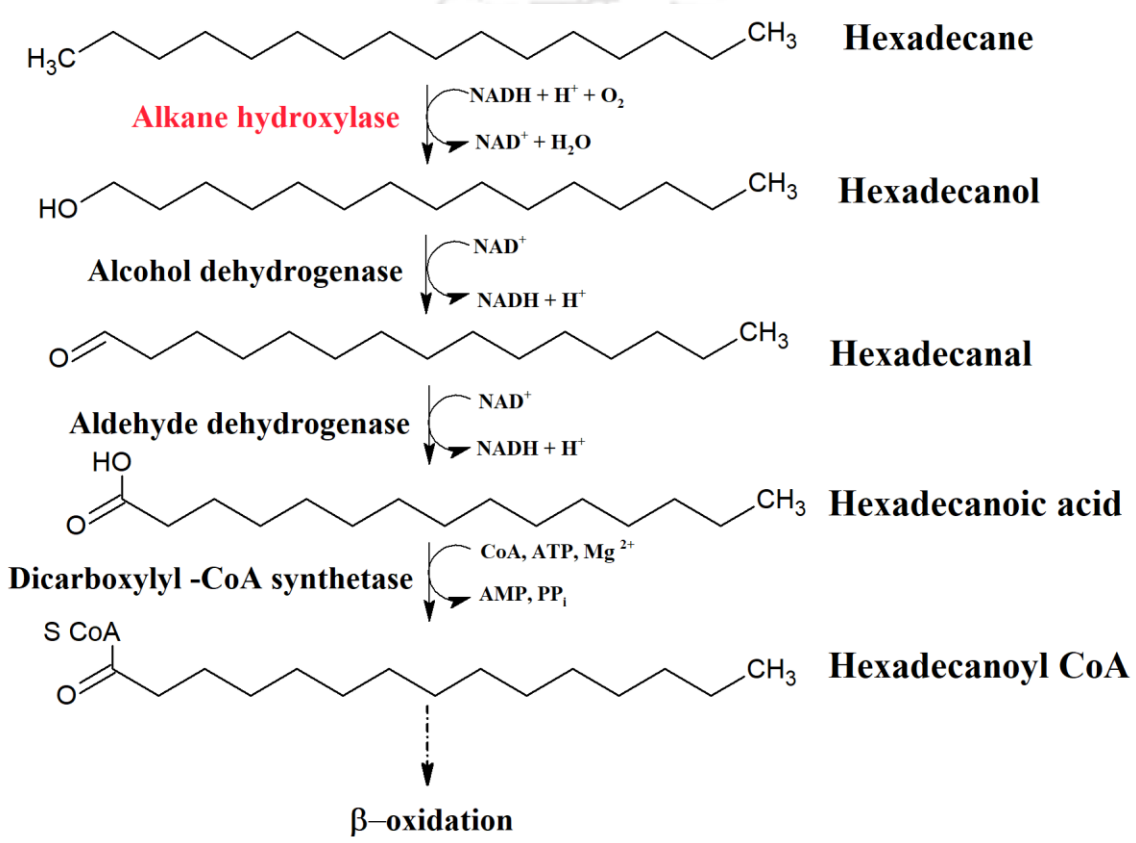

Figure S5-4. The proposed hexadecane biodegradation pathway by the selected bacteria

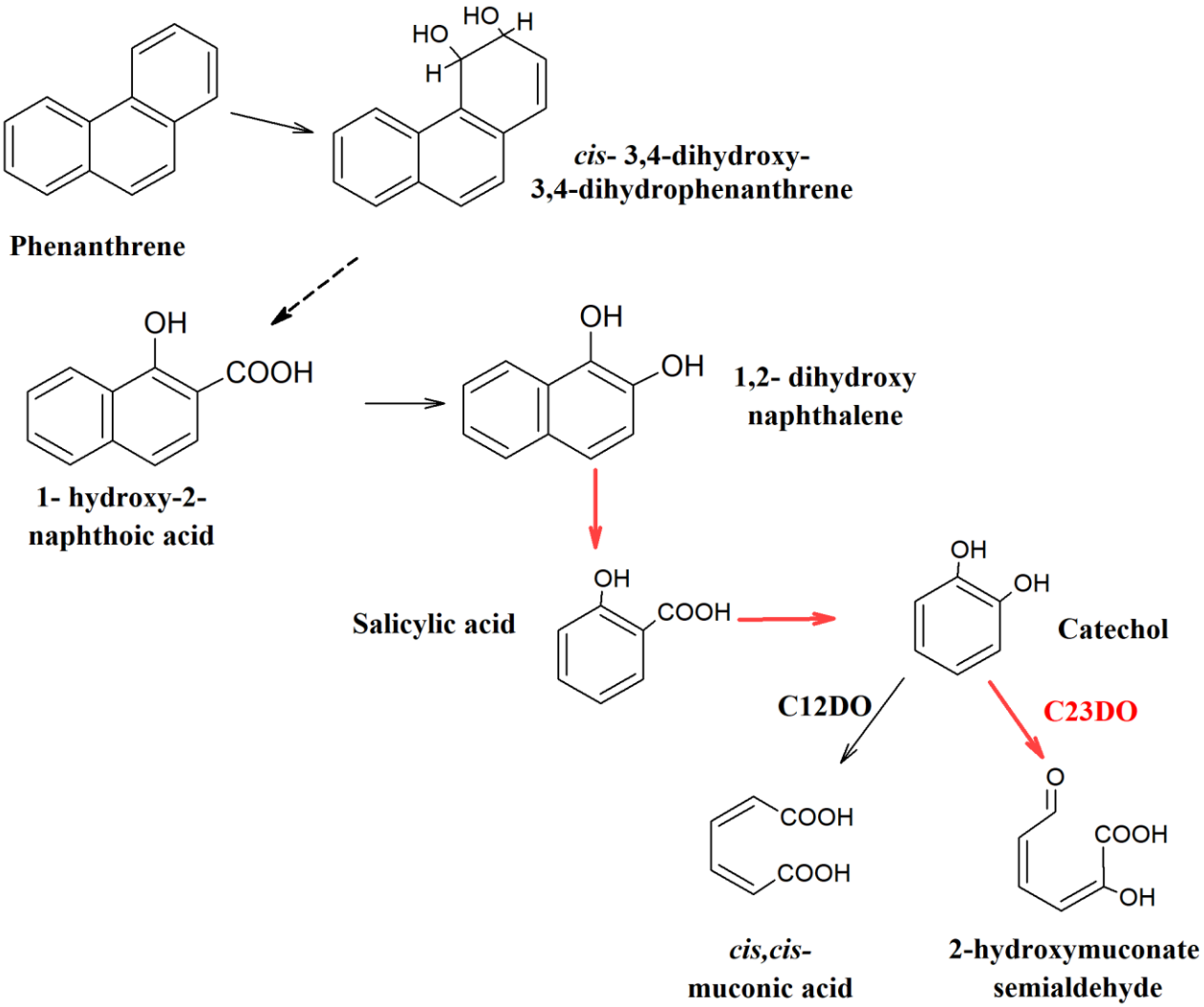

Figure S5-2. The proposed Phenanthrene biodegradation pathway by the selected bacteria

References

Abbas, S.Z., Whui, T.C., Hossain, K., Ahmad, A. and Rafatullah, M., 2018. Isolation and characterization of oil-degrading bacteria from marine sediment environment. Desalination and Water Treatment, 136: 282-289.

Abdel-Megeed, A., Al-Harbi, N. and Al-Deyab, S., 2010. Hexadecane degradation by bacterial strains isolated from contaminated soils. African Journal of Biotechnology, 9(44): 7487-7494.

Abdelwahab, N.A., Shukry, N. and El-Kalyoubi, S.F., 2017. Preparation and characterization of polymer coated partially esterified sugarcane bagasse for separation of oil from seawater. Environ Technol, 38(15): 1905-1914.

Abdelwahab, N.A., Shukry, N. and El-kalyoubi, S.F., 2021. Separation of emulsified oil from wastewater using polystyrene and surfactant modified sugarcane bagasse wastes blend. Clean Technologies and Environmental Policy, 23(1): 235-249.

Abdulsalam, O., Tijjani, M., Aliyu, M., Garba, I. and Wada-Kura, A., 2016. Comparative Studies on the Biosurfactant Production Capacity of Bacillus Subtilis and Pseudomonas Aeruginosa Using Engine Oil and Diesel Respectively as Substrate. Nigerian Journal of Basic and Applied Sciences, 24(2): 102-108.

Abouseoud, M., Yataghene, A., Amrane, A. and Maachi, R., 2010. Effect of pH and salinity on the emulsifying capacity and naphthalene solubility of a biosurfactant produced by Pseudomonas fluorescens. J Hazard Mater, 180(1-3): 131-6.

Agnello, A.C., Bagard, M., van Hullebusch, E.D., Esposito, G. and Huguenot, D., 2016. Comparative bioremediation of heavy metals and petroleum hydrocarbons co-contaminated soil by natural attenuation, phytoremediation, bioaugmentation and bioaugmentation-assisted phytoremediation. Sci Total Environ, 563-564: 693-703.

Aguilera, F., Mendez, J., Pasaro, E. and Laffon, B., 2010. Review on the effects of exposure to spilled oils on human health. J Appl Toxicol, 30(4): 291-301.

Ahmed, F. and Fakhruddin, A., 2018. A review on environmental contamination of petroleum hydrocarbons and its biodegradation. International Journal of Environmental Sciences Natural Resources, 11(3): 1-7.

Akbari, A., David, C., Rahim, A.A. and Ghoshal, S., 2021. Salt selected for hydrocarbon-degrading bacteria and enhanced hydrocarbon biodegradation in slurry bioreactors. Water Res, 202: 117424.

Akbari, E., Beheshti-Maal, K., Rasekh, B., Emami-Karvani, Z. and Omidi, M., 2020. Isolation and identification of current biosurfactant-producing microbacterium maritypicum ABR5 as a candidate for oily sludge recovery. Journal of Surfactants And Detergents, 23(1): 137-144.

Akbari, S., Abdurahman, N.H., Yunus, R.M., Fayaz, F. and Alara, O.R., 2018. Biosurfactants—a new frontier for social and environmental safety: a mini review. Biotechnology Research and Innovation, 2(1): 81-90.

Ali, N., Eliyas, M., Al-Sarawi, H. and Radwan, S.S., 2011. Hydrocarbon-utilizing microorganisms naturally associated with sawdust. Chemosphere, 83(9): 1268-72.

Almansoory, A.F., Abu Hasan, H., Idris, M., Abdullah, S.R.S., Anuar, N. and Tibin, E.M., 2017. Biosurfactant production by the hydrocarbon-degrading bacteria (HDB) Serratia marcescens: Optimization using central composite design (CCD). Journal of Industrial and Engineering Chemistry, 47: 272-280.

Alves, A.R., Sequeira, A.M. and Cunha, A., 2019. Increase in bacterial biosurfactant production by co-cultivation with biofilm-forming bacteria. Lett Appl Microbiol, 69(1): 79-86.

Amodu, O.S., Ojumu, T.V. and Ntwampe, K., 2016. Bioremediating silty soil contaminated by phenanthrene, pyrene, benz (a) anthracene, benzo (a) pyrene using Bacillus sp. and Pseudomonas sp.: Biosurfactant/Beta vulgaris agrowaste effects. African Journal of Biotechnology, 15(22): 1058-1068.

Arivalagan, P., Singaraj, D., Haridass, V. and Kaliannan, T., 2014. Removal of cadmium from aqueous solution by batch studies using Bacillus cereus. Ecological Engineering, 71: 728-735.

Arslan, M., Afzal, M., Amin, I., Iqbal, S. and Khan, Q.M., 2014. Nutrients Can Enhance the Abundance and Expression of Alkane Hydroxylase CYP153 Gene in the Rhizosphere of Ryegrass Planted in Hydrocarbon-Polluted Soil. Plos One, 9(10).

Bacosa, H.P., Erdner, D.L. and Liu, Z., 2015. Differentiating the roles of photooxidation and biodegradation in the weathering of Light Louisiana Sweet crude oil in surface water from the Deepwater Horizon site. Mar Pollut Bull, 95(1): 265-72.

Bai, N., Wang, S., Abuduaini, R., Zhang, M., Zhu, X. and Zhao, Y., 2017. Rhamnolipid-aided biodegradation of carbendazim by Rhodococcus sp. D-1: Characteristics, products, and phytotoxicity. Sci Total Environ, 590-591: 343-351.

Bajagain, R., Park, Y. and Jeong, S.W., 2018. Feasibility of oxidation-biodegradation serial foam spraying for total petroleum hydrocarbon removal without soil disturbance. Sci Total Environ, 626: 1236-1242.

Balan, S.S., Kumar, C.G. and Jayalakshmi, S., 2016. Pontifactin, a new lipopeptide biosurfactant produced by a marine Pontibacter korlensis strain SBK-47: Purification, characterization and its biological evaluation. Process Biochemistry, 51(12): 2198-2207.

Balzamo, G., Singh, N., Wang, N.J., Vladisavljevic, G.T., Bolognesi, G. and Mele, E., 2019. 3D Arrays of Super-Hydrophobic Microtubes from Polypore Mushrooms as Naturally-Derived Systems for Oil Absorption. Materials, 12(1): 132.

Bao, M., Pi, Y., Wang, L., Sun, P., Li, Y. and Cao, L., 2014. Lipopeptide biosurfactant production bacteria Acinetobacter sp. D3-2 and its biodegradation of crude oil. Environ Sci Process Impacts, 16(4): 897-903.

Behnood, R., Anvaripour, B., Jaafarzadeh, N. and Farasati, M., 2016. Oil spill sorption using raw and acetylated sugarcane bagasse. Journal of Central South University, 23(7): 1618-1625.

Bender, M.L., Giebichenstein, J., Teisrud, R.N., Laurent, J., Frantzen, M., Meador, J.P., Sorensen, L., Hansen, B.H., Reinardy, H.C., Laurel, B. and Nahrgang, J., 2021. Combined effects of crude oil exposure and warming on eggs and larvae of an arctic forage fish. Sci Rep, 11(1): 8410.

Bertrand, B., Martínez-Morales, F., Rosas-Galván, N.S., Morales-Guzmán, D. and Trejo-Hernández, M.R., 2018. Statistical Design, a Powerful Tool for Optimizing Biosurfactant Production: A Review. Colloids and Interfaces, 2(3): 36.

Bhardwaj, N. and Bhaskarwar, A.N., 2018. A review on sorbent devices for oil-spill control. Environ Pollut, 243(Pt B): 1758-1771.

Bhattacharya, M., Guchhait, S., Biswas, D. and Singh, R., 2019. Evaluation of a microbial consortium for crude oil spill bioremediation and its potential uses in enhanced oil recovery. Biocatalysis and Agricultural Biotechnology, 18: 101034.

Bianco, F., Race, M., Papirio, S. and Esposito, G., 2022. Phenanthrene biodegradation in a fed–batch reactor treating a spent sediment washing solution: Techno–economic implications for the recovery of ethanol as extracting agent. Chemosphere, 286: 131361.

Bidja Abena, M.T., Sodbaatar, N., Li, T., Damdinsuren, N., Choidash, B. and Zhong, W., 2019. Crude Oil Biodegradation by Newly Isolated Bacterial Strains and Their Consortium Under Soil Microcosm Experiment. Appl Biochem Biotechnol, 189(4): 1223-1244.

Biniarz, P., Coutte, F., Gancel, F. and Lukaszewicz, M., 2018. High-throughput optimization of medium components and culture conditions for the efficient production of a lipopeptide pseudofactin by Pseudomonas fluorescens BD5. Microb Cell Fact, 17(1): 121.

Birolli, W.G., da Silva, B.F. and Rodrigues-Filho, E., 2020. Biodegradation of the fungicide Pyraclostrobin by bacteria from orange cultivation plots. Sci Total Environ, 746: 140968.

Bisoli, E., Freire, T.V., Yoshida, N.C., Garcez, W.S., Queiroz, L.M.M., Matos, M.F.C., Perdomo, R.T. and Garcez, F.R., 2020. Cytotoxic Phenanthrene, Dihydrophenanthrene, and Dihydrostilbene Derivatives and Other Aromatic Compounds from Combretum laxum. Molecules, 25(14): 3154.

Bodour, A.A., Guerrero-Barajas, C., Jiorle, B.V., Malcomson, M.E., Paull, A.K., Somogyi, A., Trinh, L.N., Bates, R.B. and Maier, R.M., 2004. Structure and characterization of flavolipids, a novel class of biosurfactants produced by Flavobacterium sp. strain MTN11. Appl Environ Microbiol, 70(1): 114-20.

Bodour, A.A. and Miller-Maier, R.M., 1998. Application of a modified drop-collapse technique for surfactant quantitation and screening of biosurfactant-producing microorganisms. Journal of Microbiological Methods, 32(3): 273-280.

Boleydei, H., Mirghaffari, N. and Farhadian, O., 2018. Comparative study on adsorption of crude oil and spent engine oil from seawater and freshwater using algal biomass. Environ Sci Pollut Res 25(21): 21024-21035.

Borges, W.S., Moura, A.A.O., Coutinho, U., Cardoso, V.L. and Resende, M.M., 2015. Optimization of the Operating Conditions for Rhamnolipid Production Using Slaughterhouse-Generated Industrial Float as Substrate. Brazilian Journal of Chemical Engineering, 32(2): 357-365.

Brumano, L.P., Antunes, F.A.F., Souto, S.G., Dos Santos, J.C., Venus, J., Schneider, R. and da Silva, S.S., 2017. Biosurfactant production by Aureobasidium pullulans in stirred tank bioreactor: New approach to understand the influence of important variables in the process. Bioresour Technol, 243: 264-272.

Cai, Q., Zhang, B., Chen, B., Zhu, Z., Lin, W. and Cao, T., 2014. Screening of biosurfactant producers from petroleum hydrocarbon contaminated sources in cold marine environments. Marine pollution bulletin, 86(1-2): 402-410.

Câmara, J.M.D., Sousa, M.A.S. and Barros Neto, E.L., 2019. Optimization and characterization of biosurfactant rhamnolipid production by Pseudomonas aeruginosa isolated from an artificially contaminated soil. Journal of Surfactants and Detergents, 22(4): 711-719.

Carolin, C.F., Kumar, P.S., Joshiba, G.J., Madhesh, P. and Ramamurthy, R., 2021. Sustainable strategy for the enhancement of hazardous aromatic amine degradation using lipopeptide biosurfactant isolated from Brevibacterium casei. Journal of Hazardous Materials, 408: 124943.

Cavalca, L., Rao, M.A., Bernasconi, S., Colombo, M., Andreoni, V. and Gianfreda, L., 2008. Biodegradation of phenanthrene and analysis of degrading cultures in the presence of a model organo-mineral matrix and of a simulated NAPL phase. Biodegradation, 19(1): 1-13.

Cerqueira, V.S., Hollenbach, E.B., Maboni, F., Vainstein, M.H., Camargo, F.A., do Carmo, R.P.M. and Bento, F.M., 2011. Biodegradation potential of oily sludge by pure and mixed bacterial cultures. Bioresour Technol, 102(23): 11003-10.

Çevik, P., Eroğlu, A., Yildizli, G., Coşan, D., Kantar, Ç. and Coral, G., 2019. Isolation and characterization of diethyl phthalate degrading bacteria from crude oil contaminated soil. Journal of Environmental Biology, 40(3): 275-282.

Chakraborty, T., Sen, A. and Pal, R., 2012. Chemical characterization and the stress induced changes of the extracellular polysaccharide of the marine cyanobacterium, Phormidium tenue. J. Algal Biomass Utln, 3: 11-20.

Chandel, A.K., Antunes, F.A.F., Anjos, V., Bell, M.J.V., Rodrigues, L.N., Polikarpov, I., de Azevedo, E.R., Bernardinelli, O.D., Rosa, C.A., Pagnocca, F.C. and da Silva, S.S., 2014. Multi-scale structural and chemical analysis of sugarcane bagasse in the process of sequential acid-base pretreatment and ethanol production by Scheffersomyces shehatae and Saccharomyces cerevisiae. Biotechnology for Biofuels, 7(1): 63.

Chang, C.C., Chen, W.C., Ho, T.F., Wu, H.S. and Wei, Y.H., 2011. Development of natural anti-tumor drugs by microorganisms. J Biosci Bioeng, 111(5): 501-11.

Chang, J., Shi, Y., Si, G., Yang, Q., Dong, J. and Chen, J., 2020. The bioremediation potentials and mercury(II)-resistant mechanisms of a novel fungus Penicillium spp. DC-F11 isolated from contaminated soil. J Hazard Mater, 396: 122638.

Che, S. and Men, Y., 2019. Synthetic microbial consortia for biosynthesis and biodegradation: promises and challenges. J Ind Microbiol Biotechnol, 46(9-10): 1343-1358.

Chebbi, A., Hentati, D., Cheffi, M., Bouabdallah, R., Choura, C., Sayadi, S. and Chamkha, M., 2018. Promising abilities of mercapto-degrading Staphylococcus capitis strain SH6 in both crude oil and waste motor oil as sole carbon and energy sources: its biosurfactant production and preliminary characterization. Journal of Chemical Technology & Biotechnology, 93(5): 1401-1412.

Chen, B.C., Lin, C.X., Chen, N.P., Gao, C.X., Zhao, Y.J. and Qian, C.D., 2018. Phenanthrene Antibiotic Targets Bacterial Membranes and Kills Staphylococcus aureus With a Low Propensity for Resistance Development. Front Microbiol, 9: 1593.

Chen, C., Sun, N., Li, D., Long, S., Tang, X., Xiao, G. and Wang, L., 2018. Optimization and characterization of biosurfactant production from kitchen waste oil using Pseudomonas aeruginosa. Environmental Science and Pollution Research, 25(15): 14934-14943.

Chen, Y., Liu, S.A., Mou, H., Ma, Y., Li, M. and Hu, X., 2017. Characterization of lipopeptide biosurfactants produced by Bacillus licheniformis MB01 from marine sediments. Frontiers in microbiology, 8: 871.

Chettri, B. and Singh, A.K., 2019. Kinetics of hydrocarbon degradation by a newly isolated heavy metal tolerant bacterium Novosphingobium panipatense P5:ABC. Bioresour Technol, 294: 122190.

CHOOKLIN, C.S. and SAIMMAI, A., 2020. Production and Properties of Biosurfactant from Pectinatus cerevisiiphilus CT3 Isolated from Marine Sediments. Walailak Journal of Science Technology, 17(6): 543-558.

Christova, N., Tuleva, B., Kril, A., Georgieva, M., Konstantinov, S., Terziyski, I., Nikolova, B. and Stoineva, I., 2013. Chemical structure and in vitro antitumor activity of rhamnolipids from Pseudomonas aeruginosa BN10. Appl Biochem Biotechnol, 170(3): 676-89.

Clesceri, L.S., Greenberg, A.E. and Eaton, A.D., 1998. Standard methods for the examination of water and wastewater. American public health association, Washington, DC.

Colvin, K.A., Lewis, C. and Galloway, T.S., 2020. Current issues confounding the rapid toxicological assessment of oil spills. Chemosphere, 245: 125585.

Cornell, J.A. and Khuri, A.I., 1987. Response surfaces: designs and analyses. Marcel Dekker, Inc.

Coronel-León, J., de Grau, G., Grau-Campistany, A., Farfan, M., Rabanal, F., Manresa, A. and Marqués, A.M., 2015. Biosurfactant production by AL 1.1, a Bacillus licheniformis strain isolated from Antarctica: production, chemical characterization and properties. Annals of microbiology, 65(4): 2065-2078.

Council, N.R., 1993. In situ bioremediation: When does it work? National Academies Press.

Coutte, F., Lecouturier, D., Dimitrov, K., Guez, J.S., Delvigne, F., Dhulster, P. and Jacques, P., 2017. Microbial lipopeptide production and purification bioprocesses, current progress and future challenges. Biotechnol J, 12(7): 1600566.

Cubitto, M.A., Morán, A.C., Commendatore, M., Chiarello, M.N., Baldini, M.D. and Siñeriz, F., 2004. Effects of Bacillus subtilis O9 biosurfactant on the bioremediation of crude oil-polluted soils. Biodegradation, 15(5): 281-287.

D'Auria, M., Emanuele, L., Racioppi, R. and Velluzzi, V., 2009. Photochemical degradation of crude oil: Comparison between direct irradiation, photocatalysis, and photocatalysis on zeolite. Journal of hazardous materials, 164(1): 32-38.

Darvishi, P., Ayatollahi, S., Mowla, D. and Niazi, A., 2011. Biosurfactant production under extreme environmental conditions by an efficient microbial consortium, ERCPPI-2. Colloids and Surfaces B: Biointerfaces, 84(2): 292-300.

Daryasafar, A., Jamialahmadi, M., Moghaddam, M.B. and Moslemi, B., 2016. Using biosurfactant producing bacteria isolated from an Iranian oil field for application in microbial enhanced oil recovery. Petroleum Science and Technology, 34(8): 739-746.

Das, K. and Mukherjee, A.K., 2007. Differential utilization of pyrene as the sole source of carbon by Bacillus subtilis and Pseudomonas aeruginosa strains: role of biosurfactants in enhancing bioavailability. Journal of Applied Microbiology, 102(1): 195-203.

Das, S. and Dash, H.R., 2014. Microbial bioremediation: A potential tool for restoration of contaminated areas, Microbial biodegradation and bioremediation. Elsevier, pp. 1-21.

Dashti, N., Ali, N., Khanafer, M. and Radwan, S.S., 2017. Oil uptake by plant-based sorbents and its biodegradation by their naturally associated microorganisms. Environ Pollut, 227: 468-475.

Dashti, N., Ali, N., Khanafer, M. and Radwan, S.S., 2019. Plant-based oil-sorbents harbor native microbial communities effective in spilled oil-bioremediation under nitrogen starvation and heavy metal-stresses. Ecotoxicol Environ Saf, 181: 78-88.

Datta, P., Tiwari, P. and Pandey, L.M., 2018. Isolation and characterization of biosurfactant producing and oil degrading Bacillus subtilis MG495086 from formation water of Assam oil reservoir and its suitability for enhanced oil recovery. Bioresour Technol, 270: 439-448.

Datta, P., Tiwari, P. and Pandey, L.M., 2020. Oil washing proficiency of biosurfactant produced by isolated Bacillus tequilensis MK 729017 from Assam reservoir soil. Journal of Petroleum Science and Engineering: 107612.

Dave, D. and Ghaly, A.E., 2011. Remediation technologies for marine oil spills: A critical review and comparative analysis. American Journal of Environmental Sciences, 7(5): 423.

Davis, D., Lynch, H. and Varley, J., 1999. The production of surfactin in batch culture by Bacillus subtilis ATCC 21332 is strongly influenced by the conditions of nitrogen metabolism. Enzyme and Microbial Technology, 25(3-5): 322-329.

Davis, S. and Gibbs, C., 1975. The effect of weathering on a crude oil residue exposed at sea. Water Res, 9(3): 275-285.

de Andrade, C.J., de Andrade, L.M., Bution, M.L., Dolder, M.A.H., Barros, F.F.C. and Pastore, G.M., 2016. Optimizing alternative substrate for simultaneous production of surfactin and 2, 3-butanediol by Bacillus subtilis LB5a. Biocatalysis and agricultural biotechnology, 6: 209-218.

De Meester, N., Gingold, R., Rigaux, A., Derycke, S. and Moens, T., 2016. Cryptic diversity and ecosystem functioning: a complex tale of differential effects on decomposition. Oecologia, 182(2): 559-71.

Deepika, K.V., Kalam, S., Ramu Sridhar, P., Podile, A.R. and Bramhachari, P.V., 2016. Optimization of rhamnolipid biosurfactant production by mangrove sediment bacterium Pseudomonas aeruginosa KVD-HR42 using response surface methodology. Biocatalysis and Agricultural Biotechnology, 5: 38-47.

Dehghani, M., Taatizadeh, S.B., Samaei, M.R., Shamsedini, N., Shahsavani, S., Derakhshan, Z. and Conti, G.O., 2018. Impact of bioaugmentation of soil with n-hexadecane-degrading bacteria and phosphorus source on the rate of biodegradation in a soil-slurry system. Global Nest Journal, 20(3): 504-511.

Demirbas, A., Alidrisi, H. and Balubaid, M.A., 2015. API Gravity, Sulfur Content, and Desulfurization of Crude Oil. Petroleum Science and Technology, 33(1): 93-101.

Deng, Z., Jiang, Y., Chen, K., Li, J., Zheng, C., Gao, F. and Liu, X., 2020. One Biosurfactant-Producing Bacteria Achromobacter sp. A-8 and Its Potential Use in Microbial Enhanced Oil Recovery and Bioremediation. Frontiers in Microbiology, 11(247).

Devaraj, S., Sabapathy, P.C., Nehru, L. and Preethi, K., 2019. Bioprocess optimization and production of biosurfactant from an unexplored substrate: Parthenium hysterophorus. Biodegradation, 30(4): 325-334.

Dikit, P., Maneerat, S. and Saimmai, A., 2019. The Effective Emulsifying Property of Biosurfactant–Producing Marinobacter hydrocarbonoclasticus ST1 Obtained from Palm Oil Contaminated Sites. Applied Biochemistry and Microbiology, 55(6): 615-625.

Durier, G., Nadalini, J.B., Saint-Louis, R., Genard, B., Comeau, L.A. and Tremblay, R., 2021. Sensitivity to oil dispersants: Effects on the valve movements of the blue mussel Mytilus edulis and the giant scallop Placopecten magellanicus, in sub-arctic conditions. Aquat Toxicol, 234: 105797.

Durval, I.J.B., Resende, A.H.M., Figueiredo, M.A., Luna, J.M., Rufino, R.D. and Sarubbo, L.A., 2019. Studies on biosurfactants produced using Bacillus cereus isolated from seawater with biotechnological potential for marine oil-spill bioremediation. Journal of Surfactants and Detergents, 22(2): 349-363.

e Silva, N.M.P.R., Rufino, R.D., Luna, J.M., Santos, V.A. and Sarubbo, L.A., 2014. Screening of Pseudomonas species for biosurfactant production using low-cost substrates. Biocatalysis and Agricultural Biotechnology, 3(2): 132-139.

Ebadi, A., Khoshkholgh Sima, N.A., Olamaee, M., Hashemi, M. and Ghorbani Nasrabadi, R., 2017. Effective bioremediation of a petroleum-polluted saline soil by a surfactant-producing Pseudomonas aeruginosa consortium. J Adv Res, 8(6): 627-633.

Ejaz, M., Zhao, B., Wang, X., Bashir, S., Haider, F.U., Aslam, Z., Khan, M.I., Shabaan, M., Naveed, M. and Mustafa, A., 2021. Isolation and Characterization of Oil-Degrading Enterobacter sp. from Naturally Hydrocarbon-Contaminated Soils and Their Potential Use against the Bioremediation of Crude Oil. Applied Sciences, 11(8): 3504.

El-Housseiny, G.S., Aboshanab, K.M., Aboulwafa, M.M. and Hassouna, N.A., 2019. Rhamnolipid production by a gamma ray-induced Pseudomonas aeruginosa mutant under solid state fermentation. AMB Express, 9(1): 7.

Elazzazy, A.M., Abdelmoneim, T.S. and Almaghrabi, O.A., 2015. Isolation and characterization of biosurfactant production under extreme environmental conditions by alkali-halo-thermophilic bacteria from Saudi Arabia. Saudi J Biol Sci, 22(4): 466-75.

Elumalai, P., Parthipan, P., Huang, M., Muthukumar, B., Cheng, L., Govarthanan, M. and Rajasekar, A., 2021. Enhanced biodegradation of hydrophobic organic pollutants by the bacterial consortium: Impact of enzymes and biosurfactants. Environ Pollut, 289: 117956.

Elumalai, P., Parthipan, P., Karthikeyan, O.P. and Rajasekar, A., 2017. Enzyme-mediated biodegradation of long-chain n-alkanes (C32 and C40) by thermophilic bacteria. 3 Biotech, 7(2): 116.

Fai, A.E.C., Simiqueli, A.P.R., de Andrade, C.J., Ghiselli, G. and Pastore, G.M., 2015. Optimized production of biosurfactant from Pseudozyma tsukubaensis using cassava wastewater and consecutive production of galactooligosaccharides: an integrated process. Biocatalysis and Agricultural Biotechnology, 4(4): 535-542.

Fan, R.J., Guo, S.H., Li, T.T., Li, F.M., Yang, X.L. and Wu, B., 2015. Contributions of Electrokinetics and Bioremediation in the Treatment of Different Petroleum Components. Clean-Soil Air Water, 43(2): 251-259.

Fang, L., Xu, Y., Xu, L., Shi, T., Ma, X., Wu, X., Li, Q.X. and Hua, R., 2021. Enhanced biodegradation of organophosphorus insecticides in industrial wastewater via immobilized Cupriavidus nantongensis X1(T). Sci Total Environ, 755(Pt 1): 142505.

Farag, S., Soliman, N.A. and Abdel-Fattah, Y.R., 2018. Statistical optimization of crude oil bio-degradation by a local marine bacterium isolate Pseudomonas sp. sp48. J Genet Eng Biotechnol, 16(2): 409-420.

Femina Carolin, C., Kumar, P.S., Joshiba, G.J., Madhesh, P. and Ramamurthy, R., 2021. Sustainable strategy for the enhancement of hazardous aromatic amine degradation using lipopeptide biosurfactant isolated from Brevibacterium casei. J Hazard Mater, 408: 124943.

Feng, L., Jiang, X., Huang, Y., Wen, D., Fu, T. and Fu, R., 2021. Petroleum hydrocarbon-contaminated soil bioremediation assisted by isolated bacterial consortium and sophorolipid. Environ Pollut, 273: 116476.

Flaherty, L.M. and Jordan, J.M., 1989. Sorbent performance study for crude and refined petroleum products, International Oil Spill Conference. American Petroleum Institute, pp. 155-160.

Fonseca, R.R., Silva, A.J.R., De Franca, F.P., Cardoso, V.L. and Sérvulo, E.F.C., 2007. Optimizing Carbon/Nitrogen Ratio for Biosurfactant Production by a Bacillus subtilis Strain. In: J.R. Mielenz, K.T. Klasson, W.S. Adney and J.D. McMillan (Editors), Applied Biochemistry and Biotecnology: The Twenty-Eighth Symposium Proceedings of the Twenty-Eight Symposium on Biotechnology for Fuels and Chemicals Held April 30–May 3, 2006, in Nashville, Tennessee. Humana Press, Totowa, NJ, pp. 471-486.

Fooladi, T., Abdeshahian, P., Moazami, N., Soudi, M.R., Kadier, A., Yusoff, W.M.W. and Hamid, A.A., 2018. Enhanced Biosurfactant Production by Bacillus pumilus 2IR in Fed-Batch Fermentation Using 5-L Bioreactor. Iranian Journal of Science and Technology Transaction a-Science, 42(A3): 1111-1123.

Gadore, V. and Ahmaruzzaman, M., 2021. Tailored fly ash materials: A recent progress of their properties and applications for remediation of organic and inorganic contaminants from water. Journal of Water Process Engineering, 41: 101910.

Gao, H., Zhang, J., Lai, H. and Xue, Q., 2017. Degradation of asphaltenes by two Pseudomonas aeruginosa strains and their effects on physicochemical properties of crude oil. International biodeterioration biodegradation, 122: 12-22.

Gaur, V.K., Bajaj, A., Regar, R.K., Kamthan, M., Jha, R.R., Srivastava, J.K. and Manickam, N., 2019. Rhamnolipid from a Lysinibacillus sphaericus strain IITR51 and its potential application for dissolution of hydrophobic pesticides. Bioresour Technol, 272: 19-25.

Gaur, V.K., Gupta, S. and Pandey, A., 2021. Evolution in mitigation approaches for petroleum oil-polluted environment: recent advances and future directions. Environ Sci Pollut Res 1-17.

Gein, S.V., Kuyukina, M.S., Ivshina, I.B., Baeva, T.A. and Chereshnev, V.A., 2011. In vitro cytokine stimulation assay for glycolipid biosurfactant from Rhodococcusruber: role of monocyte adhesion. Cytotechnology, 63(6): 559-566.

George, S. and Jayachandran, K., 2013. Production and characterization of rhamnolipid biosurfactant from waste frying coconut oil using a novel P seudomonas aeruginosa D. Journal of Applied Microbiology, 114(2): 373-383.

Ghazala, I., Bouallegue, A., Haddar, A. and Ellouz-Chaabouni, S., 2019. Characterization and production optimization of biosurfactants by Bacillus mojavensis I4 with biotechnological potential for microbial enhanced oil recovery. Biodegradation, 30(4): 235-245.

Ghorbannezhad, H., Moghimi, H. and Dastgheib, S.M.M., 2021. Evaluation of pyrene and tetracosane degradation by mixed-cultures of fungi and bacteria. J Hazard Mater, 416: 126202.

Gontikaki, E., Potts, L.D., Anderson, J.A. and Witte, U., 2018. Hydrocarbon-degrading bacteria in deep-water subarctic sediments (Faroe-Shetland Channel). J Appl Microbiol, 125(4): 1040-1053.

Grimm, A.C. and Harwood, C.S., 1999. NahY, a catabolic plasmid-encoded receptor required for chemotaxis of Pseudomonas putida to the aromatic hydrocarbon naphthalene. J Bacteriol, 181(10): 3310-6.

Gudiña, E.J., Fernandes, E.C., Rodrigues, A.I., Teixeira, J.A. and Rodrigues, L.R., 2015. Biosurfactant production by Bacillus subtilis using corn steep liquor as culture medium. Front Microbiol, 6: 59.

Guilharduci, V.V., Martelli, P.B. and Gorgulho, H.F., 2017. Efficiency of sugarcane bagasse-based sorbents for oil removal from engine washing wastewater. Water Sci Technol, 75(1-2): 173-181.

Gupta, K., 2021. Increased bioavailability of hydrophobic polycyclic aromatic hydrocarbons (PAH) using biosurfactants. In: Inamuddin and C.O. Adetunji (Editors), Green Sustainable Process for Chemical and Environmental Engineering and Science. Elsevier, pp. 419-432.

Ha, S., Kim, H.M., Chun, H.H., Hwang, I.M., Lee, J.-H., Kim, J.-C., Kim, I.S. and Park, H.W., 2018. Effect of oxygen supply on surfactin production and sporulation in submerged culture of Bacillus subtilis Y9. Applied Sciences, 8(9): 1660.

Habib, S., Ahmad, S.A., Wan Johari, W.L., Abd Shukor, M.Y., Alias, S.A., Smykla, J., Saruni, N.H., Abdul Razak, N.S. and Yasid, N.A., 2020. Production of Lipopeptide Biosurfactant by a Hydrocarbon-Degrading Antarctic Rhodococcus. Int J Mol Sci, 21(17): 6138.

Habibi, N. and Pourjavadi, A., 2022. Magnetic, thermally stable, and superhydrophobic polyurethane sponge: A high efficient adsorbent for separation of the marine oil spill pollution. Chemosphere, 287(Pt 3): 132254.

Hajieghrari, M. and Hejazi, P., 2020. Enhanced biodegradation of n-Hexadecane in solid-phase of soil by employing immobilized Pseudomonas Aeruginosa on size-optimized coconut fibers. J Hazard Mater, 389: 122134.

Hakima, A. and Ian, S., 2017. Isolation of indigenous hydrocarbon transforming bacteria from oil contaminated soils in Libya: Selection for use as potential Inocula for soil bioremediation. International Journal of Environmental Bioremediation & Biodegradation, 5(1): 8-17.

Haleyur, N., Shahsavari, E., Taha, M., Khudur, L.S., Koshlaf, E., Osborn, A.M. and Ball, A.S., 2018. Assessing the degradation efficacy of native PAH-degrading bacteria from aged, weathered soils in an Australian former gasworks site. Geoderma, 321: 110-117.

Haloi, S. and Medhi, T., 2019. Optimization and characterization of a glycolipid produced by Achromobacter sp. to use in petroleum industries. Journal of basic microbiology, 59(3): 238-248.

Hannam, M.L., Bamber, S.D., Moody, A.J., Galloway, T.S. and Jones, M.B., 2010. Immunotoxicity and oxidative stress in the Arctic scallop Chlamys islandica: effects of acute oil exposure. Ecotoxicol Environ Saf, 73(6): 1440-8.

Hao, Z., Wang, Q., Yan, Z. and Jiang, H., 2021. Novel magnetic loofah sponge biochar enhancing microbial responses for the remediation of polycyclic aromatic hydrocarbons-contaminated sediment. J Hazard Mater, 401: 123859.

Harayama, S., Kishira, H., Kasai, Y. and Shutsubo, K., 1999. Petroleum biodegradation in marine environments. J Mol Microbiol Biotechnol, 1(1): 63-70.

Hasan, A. and Pandey, L.M., 2016. Kinetic studies of attachment and re-orientation of octyltriethoxysilane for formation of self-assembled monolayer on a silica substrate. Mater Sci Eng C Mater Biol Appl, 68: 423-429.

Hasan, A., Saxena, V. and Pandey, L.M., 2018. Surface Functionalization of Ti6Al4V via Self-assembled Monolayers for Improved Protein Adsorption and Fibroblast Adhesion. Langmuir, 34(11): 3494-3506.

Hasan, A., Waibhaw, G. and Pandey, L.M., 2018. Conformational and Organizational Insights into Serum Proteins during Competitive Adsorption on Self-Assembled Monolayers. Langmuir, 34(28): 8178-8194.

Hema, T., Kiran, G.S., Sajayyan, A., Ravendran, A., Raj, G.G. and Selvin, J., 2019. Response surface optimization of a glycolipid biosurfactant produced by a sponge associated marine bacterium Planococcus sp. MMD26. Biocatalysis and Agricultural Biotechnology, 18: 101071.

Hoefler, B.C., Gorzelnik, K.V., Yang, J.Y., Hendricks, N., Dorrestein, P.C. and Straight, P.D., 2012. Enzymatic resistance to the lipopeptide surfactin as identified through imaging mass spectrometry of bacterial competition. Proceedings of the National Academy of Sciences of the United States of America, 109(32): 13082-13087.

Hook, S.E. and Osborn, H.L., 2012. Comparison of toxicity and transcriptomic profiles in a diatom exposed to oil, dispersants, dispersed oil. Aquat Toxicol, 124-125: 139-51.

Hoshino, S., Onaka, H. and Abe, I., 2019. Activation of silent biosynthetic pathways and discovery of novel secondary metabolites in actinomycetes by co-culture with mycolic acid-containing bacteria. J Ind Microbiol Biotechnol, 46(3-4): 363-374.

Hou, C.T., 1982. Microbial transformation of important industrial hydrocarbons. Microbial transformations of bioactive compounds, 1: 81-107.

Hou, C.T., 2005. Handbook of industrial biocatalysis. CRC press.

Hou, C.T., 2006. Biotransformation of Aliphatic Hydrocarbons and Fatty Acids.

Hou, C.T., 2017. Microbiology and biochemistry of methylotrophic bacteria, Methylotrophs: Microbiology. Biochemistry and Genetics. CRC Press, pp. 1-53.

Hsia, K.F., Chen, C.C., Ou, J.H., Lo, K.H., Sheu, Y.T. and Kao, C.M., 2021. Treatment of petroleum hydrocarbon-polluted groundwater with innovative in situ sulfate-releasing biobarrier. Journal of Cleaner Production, 295: 126424.

Huang, Y., He, Z., Xu, L., Yang, B., Hou, Y., Lei, L. and Li, Z., 2021. Alternating current enhanced bioremediation of petroleum hydrocarbon-contaminated soils. Environ Sci Pollut Res 28(34): 47562-47573.

Hunt, J.M., 1990. Generation and Migration of Petroleum from Abnormally Pressured Fluid Compartments. Aapg Bulletin-American Association of Petroleum Geologists, 74(1): 1-12.

Ibrahim, U., Yahaya, S., Yusuf, I. and Kawo, A., 2020. Cadmium (Cd) and Lead (Pb) Uptake Potential and Surface Properties of Aeromonas spp. Isolated from Soil of Local Mining Site. Microbiology Research Journal International: 36-47.

Ibrar, M. and Zhang, H., 2020. Construction of a hydrocarbon-degrading consortium and characterization of two new lipopeptides biosurfactants. Sci Total Environ, 714: 136400.

Ifelebuegu, A.O., Ukpebor, J.E., Ahukannah, A.U., Nnadi, E.O. and Theophilus, S.C., 2017. Environmental effects of crude oil spill on the physicochemical and hydrobiological characteristics of the Nun River, Niger Delta. Environ Monit Assess, 189(4): 173.

Irorere, V.U., Smyth, T.J., Cobice, D., McClean, S., Marchant, R. and Banat, I.M., 2018. Fatty acid synthesis pathway provides lipid precursors for rhamnolipid biosynthesis in Burkholderia thailandensis E264. Appl Microbiol Biotechnol, 102(14): 6163-6174.

Iyer, B. and Rajkumar, S., 2019. Succinate irrepressible periplasmic glucose dehydrogenase of Rhizobium sp. Td3 and SN1 contributes to its phosphate solubilization ability. Arch Microbiol, 201(5): 649-659.

Jadhav, M., Kalme, S., Tamboli, D. and Govindwar, S., 2011. Rhamnolipid from Pseudomonas desmolyticum NCIM-2112 and its role in the degradation of Brown 3REL. J Basic Microbiol, 51(4): 385-96.

Jahan, R., Bodratti, A.M., Tsianou, M. and Alexandridis, P., 2020. Biosurfactants, natural alternatives to synthetic surfactants: Physicochemical properties and applications. Adv Colloid Interface Sci, 275: 102061.

Jannat, M.A.H., Lee, J., Shin, S.G. and Hwang, S., 2021. Long-term enrichment of anaerobic propionate-oxidizing consortia: Syntrophic culture development and growth optimization. J Hazard Mater, 401: 123230.

Jasperse, L., Levin, M., Tsantiris, K., Smolowitz, R., Perkins, C., Ward, J.E. and De Guise, S., 2018. Comparative toxicity of Corexit® 9500, oil, and a Corexit®/oil mixture on the eastern oyster, Crassostrea virginica (Gmelin). Aquat Toxicol, 203: 10-18.

Jauhari, N., Mishra, S., Kumari, B. and Singh, S.N., 2014. Bacteria-mediated aerobic degradation of hexacosane in vitro conditions. Bioresour Technol, 170: 62-68.

Jenny, K., Kappeli, O. and Fiechter, A., 1991. Biosurfactants from Bacillus licheniformis: structural analysis and characterization. Appl Microbiol Biotechnol, 36(1): 5-13.

Jeroh, E., Tonukari, N. and Anigboro, A., 2011. Glucose level and amylase activity in crude oil contaminated soil bioremediated with poultry manure and sawdust. Asian Journal of Biological Sciences, 4(4): 369-374.

Ji, Y., Mao, G., Wang, Y. and Bartlam, M., 2013. Structural insights into diversity and n-alkane biodegradation mechanisms of alkane hydroxylases. Front Microbiol, 4(58): 58.

Jiang, J., Cao, J.Z., Wang, W. and Xue, J., 2018. How silanization influences aggregation and moisture sorption behaviours of silanized silica: analysis of porosity and multilayer moisture adsorption. Royal Society Open Science, 5(6): 180206.

Jiao, S., Liu, Z.S., Lin, Y.B., Yang, J., Chen, W.M. and Wei, G.H., 2016. Bacterial communities in oil contaminated soils: Biogeography and co-occurrence patterns. Soil Biology & Biochemistry, 98: 64-73.

Jie, Z., Xue, R., Liu, S., Xu, N., Xin, F., Zhang, W., Jiang, M. and Dong, W., 2019. High di-rhamnolipid production using Pseudomonas aeruginosa KT1115, separation of mono/di-rhamnolipids, and evaluation of their properties. Frontiers in bioengineering and biotechnology, 7: 245.

Jimoh, A.A. and Lin, J., 2019. Enhancement of Paenibacillus sp. D9 lipopeptide biosurfactant production through the optimization of medium composition and its application for biodegradation of hydrophobic pollutants. Applied biochemistry and biotechnology, 187(3): 724-743.

Jimoh, A.A. and Lin, J., 2020. Bioremediation of contaminated diesel and motor oil through the optimization of biosurfactant produced by Paenibacillus sp. D9 on waste canola oil. Bioremediation Journal, 24(1): 21-40.

Jin, J., Wang, H., Jing, Y., Liu, M., Wang, D., Li, Y. and Bao, M., 2019. An efficient and environmental-friendly dispersant based on the synergy of amphiphilic surfactants for oil spill remediation. Chemosphere, 215: 241-247.

Johann, S., Goßen, M., Mueller, L., Selja, V., Gustavson, K., Fritt-Rasmussen, J., Wegeberg, S., Ciesielski, T.M., Jenssen, B.M., Hollert, H. and Seiler, T.-B., 2021. Comparative toxicity assessment of in situ burn residues to initial and dispersed heavy fuel oil using zebrafish embryos as test organisms. Environmental Science and Pollution Research, 28(13): 16198-16213.

Joy, S., Rahman, P.K., Khare, S.K. and Sharma, S., 2019. Production and characterization of glycolipid biosurfactant from Achromobacter sp.(PS1) isolate using one-factor-at-a-time (OFAT) approach with feasible utilization of ammonia-soaked lignocellulosic pretreated residues. Bioprocess and biosystems engineering, 42(8): 1301-1315.

Joy, S., Rahman, P.K., Khare, S.K., Soni, S. and Sharma, S., 2019. Statistical and sequential (fill-and-draw) approach to enhance rhamnolipid production using industrial lignocellulosic hydrolysate C6 stream from Achromobacter sp.(PS1). Bioresour Technol, 288: 121494.

Jurelevicius, D., Alvarez, V.M., Peixoto, R., Rosado, A.S. and Seldin, L., 2013. The use of a combination of alkB primers to better characterize the distribution of alkane-degrading bacteria. PloS one, 8(6): e66565.

Kaczorek, E. and Olszanowski, A., 2011. Uptake of Hydrocarbon by Pseudomonas fluorescens (P1) and Pseudomonas putida (K1) Strains in the Presence of Surfactants: A Cell Surface Modification. Water Air Soil Pollut, 214(1-4): 451-459.

Kaczorek, E., Pacholak, A., Zdarta, A. and Smułek, W., 2018. The impact of biosurfactants on microbial cell properties leading to hydrocarbon bioavailability increase. Colloids and Interfaces, 2(3): 35.

Kadri, T., Rouissi, T., Magdouli, S., Brar, S.K., Hegde, K., Khiari, Z., Daghrir, R. and Lauzon, J.M., 2018. Production and characterization of novel hydrocarbon degrading enzymes from Alcanivorax borkumensis. Int J Biol Macromol, 112: 230-240.

Kalaimurugan, D., Sivasankar, P., Durairaj, K., Lakshmanamoorthy, M., Ali Alharbi, S., Al Yousef, S.A., Chinnathambi, A. and Venkatesan, S., 2021. Novel strategy for biodegradation of 4-nitrophenol by the immobilized cells of Pseudomonas sp. YPS3 with Acacia gum. Saudi J Biol Sci, 28(1): 833-839.

Kanaly, R.A. and Harayama, S., 2010. Advances in the field of high-molecular-weight polycyclic aromatic hydrocarbon biodegradation by bacteria. Microb Biotechnol, 3(2): 136-64.

Kanaly, R.A., Harayama, S. and Watanabe, K., 2002. Rhodanobacter sp. strain BPC1 in a benzo[a]pyrene-mineralizing bacterial consortium. Appl Environ Microbiol, 68(12): 5826-33.

Kavanagh, R.J., Frank, R.A., Solomon, K.R. and Van Der Kraak, G., 2013. Reproductive and health assessment of fathead minnows (Pimephales promelas) inhabiting a pond containing oil sands process-affected water. Aquat Toxicol, 130-131: 201-9.

Khademolhosseini, R., Jafari, A., Mousavi, S.M., Hajfarajollah, H., Noghabi, K.A. and Manteghian, M., 2019. Physicochemical characterization and optimization of glycolipid biosurfactant production by a native strain of Pseudomonas aeruginosa HAK01 and its performance evaluation for the MEOR process. RSC Adv, 9(14): 7932-7947.

Khan, K., Naeem, M., Arshed, M.J. and Asif, M., 2006. Extraction and characterization of oil degrading bacteria. Journal of Applied Sciences, 6(10): 2302-6.

Khan, M.A.I., Biswas, B., Smith, E., Naidu, R. and Megharaj, M., 2018. Toxicity assessment of fresh and weathered petroleum hydrocarbons in contaminated soil- a review. Chemosphere, 212: 755-767.

Khopade, A., Ren, B., Liu, X.Y., Mahadik, K., Zhang, L. and Kokare, C., 2012. Production and characterization of biosurfactant from marine Streptomyces species B3. J Colloid Interface Sci, 367(1): 311-8.

Kim, Y.M., Ahn, C.K., Woo, S.H., Jung, G.Y. and Park, J.M., 2009. Synergic degradation of phenanthrene by consortia of newly isolated bacterial strains. J Biotechnol, 144(4): 293-8.

Kiran, G.S., Priyadharsini, S., Sajayan, A., Priyadharsini, G.B., Poulose, N. and Selvin, J., 2017. Production of Lipopeptide Biosurfactant by a Marine Nesterenkonia sp. and Its Application in Food Industry. Front Microbiol, 8: 1138.

Klekner, V. and Kosaric, N., 1993. Biosurfactants for cosmetics. Surfactant science series: 373-373.

Kochius, S., van Marwijk, J., Ebrecht, A.C., Opperman, D.J. and Smit, M.S., 2018. Deconstruction of the CYP153A6 Alkane Hydroxylase System: Limitations and Optimization of In Vitro Alkane Hydroxylation. Catalysts, 8(11): 531.

Koolivand, A., Abtahi, H., Parhamfar, M., Didehdar, M., Saeedi, R. and Fahimirad, S., 2019. Biodegradation of high concentrations of petroleum compounds by using indigenous bacteria isolated from petroleum hydrocarbons-rich sludge: Effective scale-up from liquid medium to composting process. Journal of Environmental Management, 248: 109228.

Koolivand, A., Saeedi, R., Coulon, F., Kumar, V., Villasenor, J., Asghari, F. and Hesampoor, F., 2020. Bioremediation of petroleum hydrocarbons by vermicomposting process bioaugmentated with indigenous bacterial consortium isolated from petroleum oily sludge. Ecotoxicol Environ Saf, 198: 110645.

Koutinas, M., Vasquez, M.I., Nicolaou, E., Pashali, P., Kyriakou, E., Loizou, E., Papadaki, A., Koutinas, A.A. and Vyrides, I., 2019. Biodegradation and toxicity of emerging contaminants: Isolation of an exopolysaccharide-producing Sphingomonas sp. for ionic liquids bioremediation. J Hazard Mater, 365: 88-96.

Krainara, S., Suraraksa, B., Prommeenate, P., Thayanukul, P. and Luepromchai, E., 2020. Enrichment and characterization of bacterial consortia for degrading 2-mercaptobenzothiazole in rubber industrial wastewater. J Hazard Mater, 400: 123291.

Kriipsalu, M., Marques, M. and Maastik, A., 2008. Characterization of oily sludge from a wastewater treatment plant flocculation-flotation unit in a petroleum refinery and its treatment implications. Journal of Material Cycles and Waste Management, 10(1): 79-86.

Kumar, A., Negi, Y.S., Choudhary, V. and Bhardwaj, N.K., 2014. Characterization of cellulose nanocrystals produced by acid-hydrolysis from sugarcane bagasse as agro-waste. Journal of Materials Physics and Chemistry, 2(1): 1-8.

Kumar, V., Chandra, R., Thakur, I.S., Saxena, G. and Shah, M.P., 2020. Recent advances in physicochemical and biological treatment approaches for distillery wastewater. Combined Application of Physico-Chemical Microbiological Processes for Industrial Effluent Treatment Plant: 79-118.

Kumari, S., Regar, R.K. and Manickam, N., 2018. Improved polycyclic aromatic hydrocarbon degradation in a crude oil by individual and a consortium of bacteria. Bioresour Technol, 254: 174-179.

KURNAZ, S.Ü. and BÜYÜKGÜNGÖR, H., 2016. Bioremediation of total petroleum hydrocarbons in crude oil contaminated soils obtained from southeast Anatolia. Acta Biologica Turcica, 29(2): 57-60.

Laczi, K., Erdeine Kis, A., Szilagyi, A., Bounedjoum, N., Bodor, A., Vincze, G.E., Kovacs, T., Rakhely, G. and Perei, K., 2020. New Frontiers of Anaerobic Hydrocarbon Biodegradation in the Multi-Omics Era. Front Microbiol, 11(2886): 590049.

Lan, G.H., Fan, Q., Liu, Y.Q., Chen, C., Li, G.X., Liu, Y. and Yin, X.B., 2015. Rhamnolipid production from waste cooking oil using Pseudomonas SWP-4. Biochemical Engineering Journal, 101: 44-54.

Laurel, B.J., Copeman, L.A., Iseri, P., Spencer, M.L., Hutchinson, G., Nordtug, T., Donald, C.E., Meier, S., Allan, S.E., Boyd, D.T., Ylitalo, G.M., Cameron, J.R., French, B.L., Linbo, T.L., Scholz, N.L. and Incardona, J.P., 2019. Embryonic Crude Oil Exposure Impairs Growth and Lipid Allocation in a Keystone Arctic Forage Fish. iScience, 19: 1101-1113.

Li, S., Pi, Y., Bao, M., Zhang, C., Zhao, D., Li, Y., Sun, P. and Lu, J., 2015. Effect of rhamnolipid biosurfactant on solubilization of polycyclic aromatic hydrocarbons. Mar Pollut Bull, 101(1): 219-225.

Liang, J., Cheng, T., Huang, Y. and Liu, J., 2018. Petroleum degradation by Pseudomonas sp. ZS1 is impeded in the presence of antagonist Alcaligenes sp. CT10. AMB Express, 8(1): 88.

Liang, M., Wang, D., Zhu, Y., Zhu, Z., Li, Y. and Huang, C.P., 2018. Nano-hematite bagasse composite (n -HBC) for the removal of Pb(II) from dilute aqueous solutions. Journal of Water Process Engineering, 21: 69-76.

Lima, F.A., Santos, O.S., Pomella, A.W.V., Ribeiro, E.J. and de Resende, M.M., 2020. Culture Medium Evaluation Using Low-Cost Substrate for Biosurfactants Lipopeptides Production by Bacillus amyloliquefaciens in Pilot Bioreactor. Journal of Surfactants and Detergents, 23(1): 91-98.

Lin, M., Hu, X.K., Chen, W.W., Wang, H. and Wang, C.Y., 2014. Biodegradation of phenanthrene by Pseudomonas sp BZ-3, isolated from crude oil contaminated soil. International Biodeterioration & Biodegradation, 94: 176-181.

Lin, S.C., Minton, M.A., Sharma, M.M. and Georgiou, G., 1994. Structural and immunological characterization of a biosurfactant produced by Bacillus licheniformis JF-2. Appl Environ Microbiol, 60(1): 31-8.

Lin, W.J., Liu, S.S., Tong, L., Zhang, Y.M., Yang, J., Liu, W.T., Guo, C.L., Xie, Y.Y., Lu, G.N. and Dang, Z., 2017. Effects of rhamnolipids on the cell surface characteristics of Sphingomonas sp GY2B and the biodegradation of phenanthrene. RSC Adv, 7(39): 24321-24330.

Liu, H., Yu, X., Liu, Z. and Sun, Y., 2018. Occurrence, characteristics and sources of polycyclic aromatic hydrocarbons in arable soils of Beijing, China. Ecotoxicol Environ Saf, 159: 120-126.

Liu, L., Wang, L., Song, W., Yang, L., Yin, L., Xia, S., Wang, H., Strong, P.J. and Song, Z., 2018. Crude oil removal from aqueous solution using raw and carbonized Xanthoceras sorbifolia shells. Environmental Science and Pollution Research, 25(29): 29325-29334.

Liu, S., 2017. How Cells Grow. In: S. Liu (Editor), Bioprocess Engineering. Elsevier, pp. 629-697.

Loureiro, D.B., Olivera, C., Tondo, M.L., Herrero, M.S., Salvatierra, L.M. and Perez, L.M., 2020. Microbial characterization of a facultative residual sludge obtained from a biogas plant with ability to degrade commercial B10 diesel oil. Ecological Engineering, 144: 105710.

Lv, N., Wang, X., Peng, S., Zhang, H. and Luo, L., 2018. Study of the Kinetics and Equilibrium of the Adsorption of Oils onto Hydrophobic Jute Fiber Modified via the Sol-Gel Method. Int J Environ Res Public Health, 15(5): 969.

Ma, Z., Liu, J., Dick, R.P., Li, H., Shen, D., Gao, Y., Waigi, M.G. and Ling, W., 2018. Rhamnolipid influences biosorption and biodegradation of phenanthrene by phenanthrene-degrading strain Pseudomonas sp. Ph6. Environ Pollut, 240: 359-367.

Madhuri, R.J., Saraswathi, M., Gowthami, K., Bhargavi, M., Divya, Y. and Deepika, V., 2019. Recent Approaches in the Production of Novel Enzymes From Environmental Samples by Enrichment Culture and Metagenomic Approach. In: V. Buddolla (Editor), Recent Developments in Applied Microbiology and Biochemistry. Academic Press, pp. 251-262.

Magnus, N., Weise, T. and Piechulla, B., 2017. Carbon Catabolite Repression Regulates the Production of the Unique Volatile Sodorifen of Serratia plymuthica 4Rx13. Frontiers in microbiology, 8: 2522-2522.

Mahesh, R., Naira, V.R. and Maiti, S.K., 2019. Concomitant production of fatty acid methyl ester (biodiesel) and exopolysaccharides using efficient harvesting technology in flat panel photobioreactor with special sparging system via Scenedesmus abundans. Bioresour Technol, 278: 231-241.

Malavenda, R., Rizzo, C., Michaud, L., Gerçe, B., Bruni, V., Syldatk, C., Hausmann, R. and Giudice, A.L., 2015. Biosurfactant production by Arctic and Antarctic bacteria growing on hydrocarbons. Polar biology, 38(10): 1565-1574.

Marchant, R., Sharkey, F.H., Banat, I.M., Rahman, T.J. and Perfumo, A., 2006. The degradation of n-hexadecane in soil by thermophilic geobacilli. FEMS Microbiol Ecol, 56(1): 44-54.

Martinez-Pascual, E., Grotenhuis, T., Solanas, A.M. and Vinas, M., 2015. Coupling chemical oxidation and biostimulation: Effects on the natural attenuation capacity and resilience of the native microbial community in alkylbenzene-polluted soil. J Hazard Mater, 300: 135-143.

Mazzeo, D.E.C., Misovic, A., Oliveira, F.A., Levy, C.E., Oehlmann, J. and de Marchi, M.R.R., 2020. Effects of biostimulation by sugarcane bagasse and coffee grounds on sewage sludges, focusing agricultural use: Microbial characterization, respirometric assessment and toxicity reduction. Waste Management, 118: 110-121.

Mehetre, G.T., Dastager, S.G. and Dharne, M.S., 2019. Biodegradation of mixed polycyclic aromatic hydrocarbons by pure and mixed cultures of biosurfactant producing thermophilic and thermo-tolerant bacteria. Sci Total Environ, 679: 52-60.

Meng, L., Li, H., Bao, M. and Sun, P., 2017. Metabolic pathway for a new strain Pseudomonas synxantha LSH-7': from chemotaxis to uptake of n-hexadecane. Sci Rep, 7: 39068.

Meng, L., Li, W., Bao, M. and Sun, P., 2019. Great correlation: Biodegradation and chemotactic adsorption of Pseudomonas synxantha LSH-7' for oil contaminated seawater bioremediation. Water Res, 153: 160-168.

Mikolasch, A., Donath, M., Reinhard, A., Herzer, C., Zayadan, B., Urich, T. and Schauer, F., 2019. Diversity and degradative capabilities of bacteria and fungi isolated from oil-contaminated and hydrocarbon-polluted soils in Kazakhstan. Appl Microbiol Biotechnol, 103(17): 7261-7274.

Mishra, N., Rana, K., Seelam, S.D., Kumar, R., Pandey, V., Salimath, B.P. and Agsar, D., 2021. Characterization and Cytotoxicity of Pseudomonas Mediated Rhamnolipids Against Breast Cancer MDA-MB-231 Cell Line. Front Bioeng Biotechnol, 9: 761266.

Miyazawa, D., Thanh, L.T.H., Tani, A., Shintani, M., Loc, N.H., Hatta, T. and Kimbara, K., 2020. Isolation and Characterization of Genes Responsible for Naphthalene Degradation from Thermophilic Naphthalene Degrader, Geobacillus sp. JF8. Microorganisms, 8(1): 44.

Mohsenzadeh, F. and Rad, A.C., 2015. Bioremediation of petroleum polluted soils using Amaranthus retroflexus L. and its rhizospheral funji, Phytoremediation for Green Energy. Springer, pp. 131-139.

Monzón, G.C., Nisenbaum, M., Seitz, M.K.H. and Murialdo, S.E., 2018. New findings on aromatic compounds' degradation and their metabolic pathways, the biosurfactant production and motility of the halophilic bacterium Halomonas sp. KHS3. Current microbiology, 75(8): 1108-1118.

Mora, V.C., Morelli, I.S. and Rosso, J.A., 2020. Co-treatment of an oily sludge and aged contaminated soil: permanganate oxidation followed by bioremediation. J Environ Manage, 261: 110169.

Morikawa, M., Daido, H., Takao, T., Murata, S., Shimonishi, Y. and Imanaka, T., 1993. A new lipopeptide biosurfactant produced by Arthrobacter sp. strain MIS38. J Bacteriol, 175(20): 6459-66.

Moshtagh, B., Hawboldt, K. and Zhang, B.Y., 2019. Optimization of biosurfactant production by Bacillus Subtilis N3-1P using the brewery waste as the carbon source. Environmental Technology, 40(25): 3371-3380.

Mouafi, F.E., Elsoud, M.M.A. and Moharam, M.E., 2016. Optimization of biosurfactant production by Bacillus brevis using response surface methodology. Biotechnology Reports, 9: 31-37.

Mulligan, C.N., Yong, R. and Gibbs, B., 2001. Surfactant-enhanced remediation of contaminated soil: a review. Engineering geology, 60(1-4): 371-380.

Mullin, J.V., Champ, M.A.J.S.S. and Bulletin, T., 2003. Introduction/overview to in situ burning of oil spills. Elsevier, pp. 323-330.

Murphy, S.M.C., Bautista, M.A., Cramm, M.A. and Hubert, C.R.J., 2021. Diesel and Crude Oil Biodegradation by Cold-Adapted Microbial Communities in the Labrador Sea. Appl Environ Microbiol, 87(20): e0080021.

Muthusamy, K., Gopalakrishnan, S., Ravi, T.K. and Sivachidambaram, P., 2008. Biosurfactants: properties, commercial production and application. Current science: 736-747.

Nalini, S., Parthasarathi, R. and Prabudoss, V., 2016. Production and characterization of lipopeptide from Bacillus cereus SNAU01 under solid state fermentation and its potential application as anti-biofilm agent. Biocatalysis and Agricultural Biotechnology, 5: 123-132.

Naloka, K., Polrit, D., Muangchinda, C., Thoetkiattikul, H. and Pinyakong, O., 2021. Bioballs carrying a syntrophic Rhodococcus and Mycolicibacterium consortium for simultaneous sorption and biodegradation of fuel oil in contaminated freshwater. Chemosphere, 282: 130973.

National Academies of Sciences, E., Medicine, 2016. Spills of diluted bitumen from pipelines: A comparative study of environmental fate, effects, and response. National Academies Press.

Nawong, C., Umsakul, K. and Sermwittayawong, N., 2018. Rubber gloves biodegradation by a consortium, mixed culture and pure culture isolated from soil samples. Braz J Microbiol, 49(3): 481-488.

Nganje, T., Edet, A. and Ekwere, S., 2007. Concentrations of heavy metals and hydrocarbons in groundwater near petrol stations and mechanic workshops in Calabar metropolis, southeastern Nigeria. Environmental Geosciences, 14(1): 15-29.

Nicolescu, T.O., 2017. Interpretation of Mass Spectra. Mass Spectrometry: 23.

Nie, C., Yang, X., Niazi, N.K., Xu, X., Wen, Y., Rinklebe, J., Ok, Y.S., Xu, S. and Wang, H., 2018. Impact of sugarcane bagasse-derived biochar on heavy metal availability and microbial activity: A field study. Chemosphere, 200: 274-282.

Niescher, S., Wray, V., Lang, S., Kaschabek, S.R. and Schlomann, M., 2006. Identification and structural characterisation of novel trehalose dinocardiomycolates from n-alkane-grown Rhodococcus opacus 1CP. Appl Microbiol Biotechnol, 70(5): 605-11.

Nogina, T., Fomina, M., Dumanskaya, T., Zelena, L., Khomenko, L., Mikhalovsky, S., Podgorskyi, V. and Gadd, G.M., 2020. A new Rhodococcus aetherivorans strain isolated from lubricant-contaminated soil as a prospective phenol-biodegrading agent. Applied microbiology biotechnology, 104(8): 3611-3625.

Nozari, M., Samaei, M.R., Dehghani, M. and Ebrahimi, A.A., 2018. Bioremediation of alkane hydrocarbons using bacterial consortium from soil. Health Scope, 7(3).

Nur Asshifa, M.N., Zambry, N.S., Salwa, M.S. and Yahya, A.R.M., 2017. The influence of agitation on oil substrate dispersion and oxygen transfer in Pseudomonas aeruginosa USM-AR2 fermentation producing rhamnolipid in a stirred tank bioreactor. 3 Biotech, 7(3): 189-189.

Nzila, A., Thukair, A., Sankara, S. and Abdur Razzak, S., 2017. Characterization of aerobic oil and grease-degrading bacteria in wastewater. Environ Technol, 38(6): 661-670.

Ohadi, M., Dehghannoudeh, G., Shakibaie, M., Banat, I.M., Pournamdari, M. and Forootanfar, H., 2017. Isolation, characterization, and optimization of biosurfactant production by an oil-degrading Acinetobacter junii B6 isolated from an Iranian oil excavation site. Biocatalysis and Agricultural Biotechnology, 12: 1-9.

Ojuederie, O.B. and Babalola, O.O., 2017. Microbial and Plant-Assisted Bioremediation of Heavy Metal Polluted Environments: A Review. Int J Environ Res Public Health, 14(12): 1504.

Oliveira, F.J.S., Vazquez, L., de Campos, N.P. and de Franca, F.P., 2009. Production of rhamnolipids by a Pseudomonas alcaligenes strain. Process Biochemistry, 44(4): 383-389.

Oren, A., 2008. Microbial life at high salt concentrations: phylogenetic and metabolic diversity. Saline systems, 4: 2-2.

Osborne, M.G., Geiger, C.J., Corzett, C.H., Kram, K.E. and Finkel, S.E., 2021. Removal of Toxic Volatile Compounds in Batch Culture Prolongs Stationary Phase and Delays Death of Escherichia coli. Appl Environ Microbiol, 87(24): e0186021.

Pachathu, A., Ponnusamy, K., Kizhakkuveettil, S.N. and Appusamy, A., 2016. Microwave-assisted preparation of bagasse and rice straw for the removal of emulsified oil from wastewater. Bioremediation Journal, 20(2): 153-163.

Pachathu, A., Ponnusamy, K. and Srinivasan, K.V.R., 2016. Packed bed column studies on the removal of emulsified oil from water using raw and modified bagasse and corn husk. Journal of Molecular Liquids, 223: 1256-1263.

Pacwa-Płociniczak, M., Płaza, G.A., Piotrowska-Seget, Z. and Cameotra, S.S., 2011. Environmental applications of biosurfactants: recent advances. International journal of molecular sciences, 12(1): 633-654.

Pal, S., Roy, A. and Kazy, S.K., 2019. Exploring Microbial Diversity and Function in Petroleum Hydrocarbon Associated Environments Through Omics Approaches, Microbial Diversity in the Genomic Era. Elsevier, pp. 171-194.

Paliukaite, M., Vaitkus, A. and Zofka, A., 2014. Evaluation of bitumen fractional composition depending on the crude oil type and production technology, Environmental engineering. Proceedings of the international conference on environmental engineering. ICEE. Vilnius Gediminas Technical University, Department of Construction Economics …, pp. 1.

Paliwal, V., Puranik, S. and Purohit, H.J., 2012. Integrated perspective for effective bioremediation. Appl Biochem Biotechnol, 166(4): 903-24.

Panda, S.K. and Maiti, S.K., 2019. An approach for simultaneous detoxification and increment of cellulase enzyme production by Trichoderma reesei using rice straw. Energy Sources Part a-Recovery Utilization and Environmental Effects, 41(22): 2691-2703.

Pandey, L.M., 2021. Surface engineering of nano-sorbents for the removal of heavy metals: Interfacial aspects. Journal of Environmental Chemical Engineering, 9(1): 104586.

Pandey, L.M., Le Denmat, S., Delabouglise, D., Bruckert, F., Pattanayek, S.K. and Weidenhaupt, M., 2012. Surface chemistry at the nanometer scale influences insulin aggregation. Colloids Surf B Biointerfaces, 100: 69-76.

Pandey, L.M. and Pattanayek, S.K., 2011. Hybrid surface from self-assembled layer and its effect on protein adsorption. Applied Surface Science, 257(10): 4731-4737.

Pandey, L.M. and Pattanayek, S.K., 2013. Properties of competitively adsorbed BSA and fibrinogen from their mixture on mixed and hybrid surfaces. Applied Surface Science, 264: 832-837.

Park, C. and Park, W., 2018. Survival and Energy Producing Strategies of Alkane Degraders Under Extreme Conditions and Their Biotechnological Potential. Front Microbiol, 9: 1081.

Park, H., Kim, H., Kim, G.-Y., Lee, M.-Y., Kim, Y. and Kang, S., 2021. Enhanced biodegradation of hydrocarbons by Pseudomonas aeruginosa-encapsulated alginate/gellan gum microbeads. Journal of Hazardous Materials, 406: 124752.

Parthipan, P., Preetham, E., Machuca, L.L., Rahman, P.K., Murugan, K. and Rajasekar, A., 2017. Biosurfactant and Degradative Enzymes Mediated Crude Oil Degradation by Bacterium Bacillus subtilis A1. Front Microbiol, 8: 193.

Patel, V., Patel, J. and Madamwar, D., 2013. Biodegradation of phenanthrene in bioaugmented microcosm by consortium ASP developed from coastal sediment of Alang-Sosiya ship breaking yard. Mar Pollut Bull, 74(1): 199-207.

Patowary, K., Patowary, R., Kalita, M.C. and Deka, S., 2017. Characterization of Biosurfactant Produced during Degradation of Hydrocarbons Using Crude Oil As Sole Source of Carbon. Front Microbiol, 8: 279.

Patowary, R., Patowary, K., Kalita, M.C. and Deka, S., 2018. Application of biosurfactant for enhancement of bioremediation process of crude oil contaminated soil. International Biodeterioration & Biodegradation, 129: 50-60.

Pavlova, A. and Papazova, D., 2003. Oil-spill identification by gas chromatography-mass spectrometry. J Chromatogr Sci, 41(5): 271-3.

Payne, J.R., Mcnabb, G.D. and Clayton, J.R., 1991. Oil-Weathering Behavior in Arctic Environments. Polar Research, 10(2): 631-662.

Peng, R.H., Xiong, A.S., Xue, Y., Fu, X.Y., Gao, F., Zhao, W., Tian, Y.S. and Yao, Q.H., 2008. Microbial biodegradation of polyaromatic hydrocarbons. FEMS Microbiol Rev, 32(6): 927-55.

Peng, Y.H., Chen, Y.J., Chang, Y.J. and Shih, Y.H., 2015. Biodegradation of bisphenol A with diverse microorganisms from river sediment. J Hazard Mater, 286: 285-90.

Persson, A. and Molin, G.r., 2004. Capacity for biosurfactant production of environmental Pseudomonas and Vibrionaceae growing on carbohydrates. Applied Microbiology Biotechnology, 26: 439-442.

Pinto, J., Athanassiou, A. and Fragouli, D., 2016. Effect of the porous structure of polymer foams on the remediation of oil spills. Journal of Physics D-Applied Physics, 49(14): 145601.

Poontawee, R. and Limtong, S., 2020. Feeding Strategies of Two-Stage Fed-Batch Cultivation Processes for Microbial Lipid Production from Sugarcane Top Hydrolysate and Crude Glycerol by the Oleaginous Red Yeast Rhodosporidiobolus fluvialis. Microorganisms, 8(2): 151.

Pourfadakari, S., Ahmadi, M., Jaafarzadeh, N., Takdastan, A., Neisi, A., Ghafari, S. and Jorfi, S., 2019. Remediation of PAHs contaminated soil using a sequence of soil washing with biosurfactant produced by Pseudomonas aeruginosa strain PF2 and electrokinetic oxidation of desorbed solution, effect of electrode modification with Fe3O4 nanoparticles. Journal of Hazardous Materials, 379: 120839.

Price, N.P., Rooney, A.P., Swezey, J.L., Perry, E. and Cohan, F.M., 2007. Mass spectrometric analysis of lipopeptides from Bacillus strains isolated from diverse geographical locations. FEMS Microbiol Lett, 271(1): 83-9.

Pugazhendhi, A., Boovaragamoorthy, G.M., Ranganathan, K., Naushad, M. and Kaliannan, T., 2018. New insight into effective biosorption of lead from aqueous solution using Ralstonia solanacearum: Characterization and mechanism studies. Journal of Cleaner Production, 174: 1234-1239.

Rabodonirina, S., Rasolomampianina, R., Krier, F., Drider, D., Merhaby, D., Net, S. and Ouddane, B., 2019. Degradation of fluorene and phenanthrene in PAHs-contaminated soil using Pseudomonas and Bacillus strains isolated from oil spill sites. J Environ Manage, 232: 1-7.

Rabus, R., Wohlbrand, L., Thies, D., Meyer, M., Reinhold-Hurek, B. and Kampfer, P., 2019. Aromatoleum gen. nov., a novel genus accommodating the phylogenetic lineage including Azoarcus evansii and related species, and proposal of Aromatoleum aromaticum sp. nov., Aromatoleum petrolei sp. nov., Aromatoleum bremense sp. nov., Aromatoleum toluolicum sp. nov. and Aromatoleum diolicum sp. nov. Int J Syst Evol Microbiol, 69(4): 982-997.

Rajendran, R.K., Lee, Y.-W., Chou, P.-H., Huang, S.-L., Kirschner, R. and Lin, C.-C., 2020. Biodegradation of the endocrine disrupter 4-t-octylphenol by the non-ligninolytic fungus Fusarium falciforme RRK20: Process optimization, estrogenicity assessment, metabolite identification and proposed pathways. Chemosphere, 240: 124876.

Ramachandran, S.D., Hodson, P.V., Khan, C.W. and Lee, K., 2004. Oil dispersant increases PAH uptake by fish exposed to crude oil. Ecotoxicol Environ Saf, 59(3): 300-8.

Ramadan, B.S., Sari, G.L., Rosmalina, R.T., Effendi, A.J. and Hadrah, 2018. An overview of electrokinetic soil flushing and its effect on bioremediation of hydrocarbon contaminated soil. J Environ Manage, 218: 309-321.

Ramesh, M. and Sakthishobana, K., 2021. Significance of biosurfactants in oil recovery and bioremediation of crude oil. In: Inamuddin and C.O. Adetunji (Editors), Green Sustainable Process for Chemical and Environmental Engineering and Science. Elsevier, pp. 211-226.

Ravi, L.M.P., 2019. Isolation, characterization, and optimization of biosurfactant production by inherent microbes and its applications Master Thesis Report 2019.

Rayeni, L.T. and Nezhad, S.S., 2018. Characterization of biosurfactant produced by probiotic bacteria isolated from human breast milk. International Journal of Basic Science in Medicine, 3(1): 18-24.

Raza, Z.A., Khalid, Z.M., Ahmad, N. and Tehseen, B., 2020. Statistical Optimisation of Rhamnolipid Production using a Pseudomonas putida Strain Cultivated on Renewable Carbon Sources of Waste Vegetable Oils. Tenside Surfactants Detergents, 57(1): 13-21.

Renfro, T.D., Xie, W., Yang, G. and Chen, G., 2014. Rhamnolipid surface thermodynamic properties and transport in agricultural soil. Colloids Surf B Biointerfaces, 115: 317-22.

Rita de Cássia, F., Almeida, D.G., Meira, H.M., Silva, E.J., Farias, C.B., Rufino, R.D., Luna, J.M. and Sarubbo, L.A., 2017. Production and characterization of a new biosurfactant from Pseudomonas cepacia grown in low-cost fermentative medium and its application in the oil industry. Biocatalysis and Agricultural Biotechnology, 12: 206-215.

Rizzo, C., Rappazzo, A.C., Michaud, L., De Domenico, E., Rochera, C., Camacho, A. and Lo Giudice, A., 2018. Efficiency in hydrocarbon degradation and biosurfactant production by Joostella sp A8 when grown in pure culture and consortia. Journal of Environmental Sciences, 67: 115-126.

Ron, E.Z. and Rosenberg, E., 2014. Enhanced bioremediation of oil spills in the sea. Current Opinion in biotechnology, 27: 191-194.

Rooney, A.P., Price, N.P., Ray, K.J. and Kuo, T.M., 2009. Isolation and characterization of rhamnolipid-producing bacterial strains from a biodiesel facility. FEMS Microbiol Lett, 295(1): 82-7.

Ruiz-Lara, A., Fierro, F., Carrasco, U., Oria, J. and Tomasini, A., 2020. Proteomic analysis of the response of Rhizopus oryzae ENHE to pentachlorophenol: Understanding the mechanisms for tolerance and degradation of this toxic compound. Process Biochemistry.

Saadoun, I.M., 2015. Impact of oil spills on marine life. Emerging pollutants in the environment-current further implications: 75-104.

Sabarinathan, D., Vanaraj, S., Sathiskumar, S., Poorna Chandrika, S., Sivarasan, G., Arumugam, S.S., Preethi, K., Li, H. and Chen, Q., 2021. Characterization and application of rhamnolipid from Pseudomonas plecoglossicida BP03. Letters in Applied Microbiology, 72(3): 251-262.

Safitri, R.M., Mangunwardoyo, W. and Ambarsari, H., 2018. Biodegradation of diesel oil hydrocarbons using Bacillus subtilis InaCC B289 and Pseudomonas aeruginosa InaCC B290 in single and mixed cultures, AIP Conference Proceedings. AIP Publishing LLC, pp. 030013.

Sahoo, P. and Barman, T.K., 2012. ANN modelling of fractal dimension in machining. In: J.P. Davim (Editor), Mechatronics and Manufacturing Engineering. Woodhead Publishing, pp. 159-226.

Saimmai, A., Kaewrueng, J. and Maneerat, S., 2012. Used lubricating oil degradation and biosurfactant production by SC-9 consortia obtained from oil-contaminated soil. Annals of Microbiology, 62(4): 1757-1767.

Saimmai, A., Onlamool, T., Sobhon, V. and Maneerat, S., 2013. An efficient biosurfactant-producing bacterium Selenomonas ruminantium CT2, isolated from mangrove sediment in south of Thailand. World Journal of Microbiology and Biotechnology, 29(1): 87-102.

Sajna, K.V., Sukumaran, R.K., Gottumukkala, L.D. and Pandey, A., 2015. Crude oil biodegradation aided by biosurfactants from Pseudozyma sp. NII 08165 or its culture broth. Bioresour Technol, 191: 133-9.

Salah, T.A., Mohammad, A.M., Hassan, M.A. and El-Anadouli, B.E., 2014. Development of nano-hydroxyapatite/chitosan composite for cadmium ions removal in wastewater treatment. Journal of the Taiwan Institute of Chemical Engineers, 45(4): 1571-1577.

Samaei, M.R., Jalili, M., Abbasi, F., Mortazavi, S.B., Jafari, A.J. and Bakhshi, B., 2020. Isolation and Kinetic Modeling of New Culture from Compost with High Capability of Degrading n-Hexadecane, Focused on Ochrobactrum Oryzae and Paenibacillus Lautus. Soil & Sediment Contamination, 29(4): 384-396.

Sanchez, M., Aranda, F.J., Teruel, J.A., Espuny, M.J., Marques, A., Manresa, A. and Ortiz, A., 2010. Permeabilization of biological and artificial membranes by a bacterial dirhamnolipid produced by Pseudomonas aeruginosa. J Colloid Interface Sci, 341(2): 240-7.

Santos, D.K., Rufino, R.D., Luna, J.M., Santos, V.A. and Sarubbo, L.A., 2016. Biosurfactants: Multifunctional Biomolecules of the 21st Century. Int J Mol Sci, 17(3): 401.

Santos, E.F., Teixeira, M.F.S., Converti, A., Porto, A.L.F. and Sarubbo, L.A., 2019. Production of a new lipoprotein biosurfactant by Streptomyces sp. DPUA1566 isolated from lichens collected in the Brazilian Amazon using agroindustry wastes. Biocatalysis and Agricultural Biotechnology, 17: 142-150.

Sar, P., Dutta, A., Bose, H., Mandal, S. and Kazy, S.K., 2019. Deep Biosphere: Microbiome of the Deep Terrestrial Subsurface, Microbial Diversity in Ecosystem Sustainability and Biotechnological Applications. Springer, pp. 225-265.

Saravanakumar, K. and Kathiresan, K., 2014. Bioremoval of the synthetic dye malachite green by marine Trichoderma sp. Springerplus, 3(1): 631.

Saravanan, A., Kumar, P.S., Vardhan, K.H., Jeevanantham, S., Karishma, S.B., Yaashikaa, P.R. and Vellaichamy, P., 2020. A review on systematic approach for microbial enhanced oil recovery technologies: Opportunities and challenges. Journal of Cleaner Production, 258: 120777.

Saxena, V., Hasan, A., Sharma, S. and Pandey, L.M., 2018. Edible oil nanoemulsion: An organic nanoantibiotic as a potential biomolecule delivery vehicle. International Journal of Polymeric Materials and Polymeric Biomaterials, 67(7): 410-419.

Sayed, K., Baloo, L., Kutty, S.R.B.M. and Makba, F., 2021. Potential biodegradation of Tapis Light Crude Petroleum Oil, using palm oil mill effluent final discharge as biostimulant for isolated halotolerant Bacillus strains. Mar Pollut Bull, 172: 112863.

Scarlett, A., Galloway, T.S., Canty, M., Smith, E.L., Nilsson, J. and Rowland, S.J., 2005. Comparative toxicity of two oil dispersants, superdispersant-25 and corexit 9527, to a range of coastal species. Environ Toxicol Chem, 24(5): 1219-27.

Scheller, S., Goenrich, M., Boecher, R., Thauer, R.K. and Jaun, B., 2010. The key nickel enzyme of methanogenesis catalyses the anaerobic oxidation of methane. Nature, 465(7298): 606-8.

Schlusselhuber, M., Godard, J., Sebban, M., Bernay, B., Garon, D., Seguin, V., Oulyadi, H. and Desmasures, N., 2018. Characterization of Milkisin, a Novel Lipopeptide With Antimicrobial Properties Produced By Pseudomonas sp. UCMA 17988 Isolated From Bovine Raw Milk. Front Microbiol, 9: 1030.

Scoma, A., Hernandez-Sanabria, E., Lacoere, T., Junca, H., Boon, N., Pieper, D.H. and Vilchez-Vargas, R., 2017. Primers: Bacterial Genes Encoding Enzymes for Aerobic Hydrocarbon Degradation. In: T.J. McGenity, K.N. Timmis and B. Nogales (Editors), Hydrocarbon and Lipid Microbiology Protocols: Primers. Springer Berlin Heidelberg, Berlin, Heidelberg, pp. 23-37.

Selesi, D., Jehmlich, N., von Bergen, M., Schmidt, F., Rattei, T., Tischler, P., Lueders, T. and Meckenstock, R.U., 2010. Combined genomic and proteomic approaches identify gene clusters involved in anaerobic 2-methylnaphthalene degradation in the sulfate-reducing enrichment culture N47. J Bacteriol, 192(1): 295-306.

Shahebrahimi, Y., Fazlali, A., Motamedi, H. and Kord, S., 2019. Experimental Insight into the Effects of Two Asphaltene-Degrading Bacterial Consortia on Crude Oil Properties. Energy & Fuels, 33(9): 8007-8013.

Shaligram, N.S. and Singhal, R.S., 2010. Surfactin–a review on biosynthesis, fermentation, purification and applications. Food technology and biotechnology, 48(2): 119-134.

Shao, Z. and Wang, W., 2013. Enzymes and genes involved in aerobic alkane degradation. Frontiers in microbiology, 4: 116.

Sharma, R., Singh, J. and Verma, N., 2018. Optimization of rhamnolipid production from Pseudomonas aeruginosa PBS towards application for microbial enhanced oil recovery. 3 Biotech, 8(1): 20-20.

Sharma, R., Singh, J. and Verma, N., 2020. Statistical optimization and comparative study of lipopeptides produced by Bacillus amyloliquefaciens SAS-1 and Bacillus subtilis BR-15. Biocatalysis and Agricultural Biotechnology: 101575.

Sharma, R., Singh, N.S., Dhingra, N. and Parween, T., 2020. Bioremediation of Oil-Spills from ShoreLine Environment, Modern Age Waste Water Problems. Springer, pp. 275-291.

Sharma, S., 2012. Bioremediation: features, strategies and applications. Asian Journal of Pharmacy Life Science, 2231: 4423.

Sharma, S., Datta, P., Kumar, B., Tiwari, P. and Pandey, L.M., 2019. Production of novel rhamnolipids via biodegradation of waste cooking oil using Pseudomonas aeruginosa MTCC7815. Biodegradation, 30(4): 301-312.

Sharma, S., Hasan, A., Kumar, N. and Pandey, L.M., 2018. Removal of methylene blue dye from aqueous solution using immobilized Agrobacterium fabrum biomass along with iron oxide nanoparticles as biosorbent. Environmental Science and Pollution Research, 25(22): 21605-21615.

Sharma, S. and Pandey, L.M., 2021. Hydrophobic Surface Induced Biosorption and Microbial Ex Situ Remediation of Oil-Contaminated Sites. Industrial & Engineering Chemistry Research, 60(26): 9378-9388.

Sharma, S. and Pandey, L.M., 2021. Integration of biosorption and biodegradation in a fed-batch mode for the enhanced crude oil remediation. Lett Appl Microbiol, 73(4): 471-476.

Sharma, S. and Pandey, L.M., 2022. Biodegradation kinetics of binary mixture of hexadecane and phenanthrene by the bacterial microconsortium. Bioresource Technology, 358: 127408.

Sharma, S., Tiwari, P. and Pandey, L., 2022. Identification of Various Metabolites like Gases, Biopolymers and Biosurfactants. In: L. Pandey and P. Tiwari (Editors), Microbial Enhanced Oil Recovery. Green Energy and Technology. Springer Singapore, Singapore, pp. 197-220.

Sharma, S., Verma, R. and Pandey, L.M., 2019. Crude oil degradation and biosurfactant production abilities of isolated Agrobacterium fabrum SLAJ731. Biocatalysis and Agricultural Biotechnology, 21: 101322.

Shekhar, S.K., Godheja, J. and Modi, D.R., 2020. Molecular Technologies for Assessment of Bioremediation and Characterization of Microbial Communities at Pollutant-Contaminated Sites. In: R.N. Bharagava and G. Saxena (Editors), Bioremediation of Industrial Waste for Environmental Safety. Springer Singapore, Singapore, pp. 437-474.

Sierra-Garcia, I.N. and de Oliveira, V.M., 2013. Microbial hydrocarbon degradation: efforts to understand biodegradation in petroleum reservoirs. Biodegradation-engineering and technology, 10: 55920.

Siggins, A., Abram, F. and Healy, M.G., 2020. Pyrolysed waste materials show potential for remediation of trichloroethylene-contaminated water. Journal of Hazardous Materials, 390: 121909.

Silva, E.J., Correa, P.F., Almeida, D.G., Luna, J.M., Rufino, R.D. and Sarubbo, L.A., 2018. Recovery of contaminated marine environments by biosurfactant-enhanced bioremediation. Colloids Surf B Biointerfaces, 172: 127-135.

Silveira, R.G., Kakizono, T., Takemoto, S., Nishio, N. and Nagai, S., 1991. Medium Optimization by an Orthogonal Array Design for the Growth of Methanosarcina-Barkeri. Journal of Fermentation and Bioengineering, 72(1): 20-25.

Simister, R., Antzis, E. and White, H., 2016. Examining the diversity of microbes in a deep-sea coral community impacted by the Deepwater Horizon oil spill. Deep Sea Research Part II: Topical Studies in Oceanography, 129: 157-166.

Singh, P. and Tiwary, B.N., 2017. Optimization of conditions for polycyclic aromatic hydrocarbons (PAHs) degradation by Pseudomonas stutzeri P2 isolated from Chirimiri coal mines. Biocatalysis and Agricultural Biotechnology, 10: 20-29.

Singh, V., Haque, S., Niwas, R., Srivastava, A., Pasupuleti, M. and Tripathi, C.K., 2016. Strategies for Fermentation Medium Optimization: An In-Depth Review. Front Microbiol, 7: 2087.

Singh, V., Tripathi, C.K.M. and Bihari, V., 2008. Production, optimization and purification of an antifungal compound from Streptomyces capoamus MTCC 8123. Medicinal Chemistry Research, 17(2-7): 94-102.

Siracusa, V., 2019. Microbial Degradation of Synthetic Biopolymers Waste. Polymers (Basel), 11(6): 1066.

Sofla, M.R.K., Brown, R.J., Tsuzuki, T. and Rainey, T.J., 2016. A comparison of cellulose nanocrystals and cellulose nanofibres extracted from bagasse using acid and ball milling methods. Advances in Natural Sciences: Nanoscience and Nanotechnology, 7(3): 035004.

Sokker, H.H., El-Sawy, N.M., Hassan, M.A. and El-Anadouli, B.E., 2011. Adsorption of crude oil from aqueous solution by hydrogel of chitosan based polyacrylamide prepared by radiation induced graft polymerization. J Hazard Mater, 190(1-3): 359-65.

Sorkhoh, N.A., Ghannoum, M.A., Ibrahim, A.S., Stretton, R.J. and Radwan, S.S., 1990. Crude oil and hydrocarbon-degrading strains of Rhodococcus rhodochrous isolated from soil and marine environments in Kuwait. Environmental Pollution, 65(1): 1-17.

Sotirova, A., Spasova, D., Vasileva-Tonkova, E. and Galabova, D., 2009. Effects of rhamnolipid-biosurfactant on cell surface of Pseudomonas aeruginosa. Microbiol Res, 164(3): 297-303.

Speight, J.G., 2018. Biological Transformations. In: J.G. Speight (Editor), Reaction Mechanisms in Environmental Engineering. Butterworth-Heinemann, pp. 269-306.

Suganthi, S.H., Murshid, S., Sriram, S. and Ramani, K., 2018. Enhanced biodegradation of hydrocarbons in petroleum tank bottom oil sludge and characterization of biocatalysts and biosurfactants. J Environ Manage, 220: 87-95.

Sumarsih, S., Nimatuzahroh, F., Puspitasari, M. and Rusdiana, M., 2017. Effect of aliphatic and aromatic hydrocarbons on the oxygenase production from hydrocarbonoclastic bacteria. J Chem Technol Biotechnol, 52: 1062-1069.

Sunkar, S., Nachiyar, C.V., Sethia, S., Ghosh, B., Prakash, P. and Devi, K.R., 2019. Biosurfactant from endophytic Bacillus cereus: Optimization, characterization and cytotoxicity study. Malaysian Journal of Microbiology

Szulc, A., Ambrozewicz, D., Sydow, M., Lawniczak, L., Piotrowska-Cyplik, A., Marecik, R. and Chrzanowski, L., 2014. The influence of bioaugmentation and biosurfactant addition on bioremediation efficiency of diesel-oil contaminated soil: feasibility during field studies. J Environ Manage, 132: 121-8.

Tahseen, R., Afzal, M., Iqbal, S., Shabir, G., Khan, Q.M., Khalid, Z.M. and Banat, I.M., 2016. Rhamnolipids and nutrients boost remediation of crude oil-contaminated soil by enhancing bacterial colonization and metabolic activities. International Biodeterioration & Biodegradation, 115: 192-198.

Tamai, K., Murakami, K., Hosokawa, S., Asakura, H., Teramura, K. and Tanaka, T., 2017. Visible-Light Selective Photooxidation of Aromatic Hydrocarbons via Ligand-to-Metal Charge Transfer Transition on Nb2O5. Journal of Physical Chemistry C, 121(41): 22854-22861.

Tang, J.-S., Zhao, F., Gao, H., Dai, Y., Yao, Z.-H., Hong, K., Li, J., Ye, W.-C. and Yao, X.-S., 2010. Characterization and online detection of surfactin isomers based on HPLC-MSn analyses and their inhibitory effects on the overproduction of nitric oxide and the release of TNF-α and IL-6 in LPS-induced macrophages. Marine drugs, 8(10): 2605-2618.

Tao, W., Lin, J., Wang, W., Huang, H. and Li, S., 2020. Biodegradation of aliphatic and polycyclic aromatic hydrocarbons by the thermophilic bioemulsifier-producing Aeribacillus pallidus strain SL-1. Ecotoxicol Environ Saf, 189: 109994.

Tavakoli, A. and Hamzah, A., 2017. Characterization and evaluation of catechol oxygenases by twelve bacteria, isolated from oil contaminated soils in Malaysia. Biological Journal of Microorganism, 5(20): 71-80.

Tavares, L.F., Silva, P.M., Junqueira, M., Mariano, D.C., Nogueira, F.C., Domont, G.B., Freire, D.M. and Neves, B.C., 2013. Characterization of rhamnolipids produced by wild-type and engineered Burkholderia kururiensis. Appl Microbiol Biotechnol, 97(5): 1909-21.

Tavassoli, T., Mousavi, S.M., Shojaosadati, S.A. and Salehizadeh, H., 2012. Asphaltene biodegradation using microorganisms isolated from oil samples. Fuel, 93(1): 142-148.

Techtmann, S.M., Zhuang, M., Campo, P., Holder, E., Elk, M., Hazen, T.C., Conmy, R. and Santo Domingo, J.W., 2017. Corexit 9500 Enhances Oil Biodegradation and Changes Active Bacterial Community Structure of Oil-Enriched Microcosms. Appl Environ Microbiol, 83(10): e03462-16.

Thavasi, R., Jayalakshmi, S. and Banat, I.M., 2011. Application of biosurfactant produced from peanut oil cake by Lactobacillus delbrueckii in biodegradation of crude oil. Bioresour Technol, 102(3): 3366-72.

Thavasi, R., Jayalakshmi, S. and Banat, I.M., 2011. Effect of biosurfactant and fertilizer on biodegradation of crude oil by marine isolates of Bacillus megaterium, Corynebacterium kutscheri and Pseudomonas aeruginosa. Bioresour Technol, 102(2): 772-8.

Thulasinathan, B., Nainamohamed, S., Samuel, J.O.E., Soorangkattan, S., Muthuramalingam, J., Kulanthaisamy, M., Balasubramani, R., Nguyen, D.D., Chang, S.W., Bolan, N., Tsang, Y.F., Amabilis-Sosa, L.E. and Alagarsamy, A., 2019. Comparative study on Cronobacter sakazakii and Pseudomonas otitidis isolated from septic tank wastewater in microbial fuel cell for bioelectricity generation. Fuel, 248: 47-55.

Tian, X., Wang, X., Peng, S., Wang, Z., Zhou, R. and Tian, H., 2018. Isolation, screening, and crude oil degradation characteristics of hydrocarbons-degrading bacteria for treatment of oily wastewater. Water Sci Technol, 78(12): 2626-2638.

Tiwari, S., Hasan, A. and Pandey, L.M., 2017. A novel bio-sorbent comprising encapsulated Agrobacterium fabrum (SLAJ731) and iron oxide nanoparticles for removal of crude oil co-contaminant, lead Pb(II). Journal of Environmental Chemical Engineering, 5(1): 442-452.

Trudgeon, B., Dieser, M., Balasubramanian, N., Messmer, M. and Foreman, C.M., 2020. Low-Temperature Biosurfactants from Polar Microbes. Microorganisms, 8(8): 1183.

Tu, Y.T., Liu, J.K., Lin, W.C., Lin, J.L. and Kao, C.M., 2014. Enhanced anaerobic biodegradation of OCDD-contaminated soils by Pseudomonas mendocina NSYSU: microcosm, pilot-scale, and gene studies. J Hazard Mater, 278: 433-43.

Tuleva, B., Christova, N., Cohen, R., Antonova, D., Todorov, T. and Stoineva, I., 2009. Isolation and characterization of trehalose tetraester biosurfactants from a soil strain Micrococcus luteus BN56. Process Biochemistry, 44(2): 135-141.

Ubogu, M., Odokuma, L.O. and Akponah, E., 2019. Enhanced rhizoremediation of crude oil–contaminated mangrove swamp soil using two wetland plants (Phragmites australis and Eichhornia crassipes). Brazilian Journal of Microbiology, 50(3): 715-728.

Ummalyma, S.B., Pandey, A., Sukumaran, R.K. and Sahoo, D., 2018. Bioremediation by microalgae: current and emerging trends for effluents treatments for value addition of waste streams, Biosynthetic Technology and Environmental Challenges. Springer, pp. 355-375.

Unás, J.H., de Alexandria Santos, D., Azevedo, E.B. and Nitschke, M., 2018. Brevibacterium luteolum biosurfactant: Production and structural characterization. Biocatalysis and Agricultural Biotechnology, 13: 160-167.

Varjani, S., Pandey, A. and Upasani, V.N., 2021. Petroleum sludge polluted soil remediation: Integrated approach involving novel bacterial consortium and nutrient application. Sci Total Environ, 763: 142934.

Varjani, S. and Upasani, V.N., 2019. Evaluation of rhamnolipid production by a halotolerant novel strain of Pseudomonas aeruginosa. Bioresour Technol, 288: 121577.

Vasilyeva, G., Kondrashina, V., Strijakova, E. and Ortega-Calvo, J.J., 2020. Adsorptive bioremediation of soil highly contaminated with crude oil. Sci Total Environ, 706: 135739.

Vecino Bello, X., Devesa-Rey, R., Cruz, J.M. and Moldes, A.B.n., 2012. Study of the synergistic effects of salinity, pH, and temperature on the surface-active properties of biosurfactants produced by Lactobacillus pentosus. Journal of agricultural and food chemistry, 60(5): 1258-1265.

Velioğlu, Z. and ÜREK, R.Ö., 2015. Biosurfactant production by Pleurotus ostreatus in submerged and solid-state fermentation systems. Turkish Journal of Biology, 39(1): 160-166.

Vera, E.C.S., de Azevedo, P.O.D., Dominguez, J.M. and Oliveira, R.P.D., 2018. Optimization of biosurfactant and bacteriocin-like inhibitory substance (BLIS) production by Lactococcus lactis CECT-4434 from agroindustrial waste. Biochemical Engineering Journal, 133: 168-178.

Vergeynst, L., Greer, C.W., Mosbech, A., Gustavson, K., Meire, L., Poulsen, K.G. and Christensen, J.H., 2019. Biodegradation, Photo-oxidation, and Dissolution of Petroleum Compounds in an Arctic Fjord during Summer. Environ Sci Technol, 53(21): 12197-12206.

Verma, R., Sharma, S., Kundu, L.M. and Pandey, L.M., 2020. Experimental investigation of molasses as a sole nutrient for the production of an alternative metabolite biosurfactant. Journal of Water Process Engineering, 38: 101632.

Veshareh, M.J., Azad, E.G., Deihimi, T., Niazi, A. and Ayatollahi, S., 2019. Isolation and screening of Bacillus subtilis MJ01 for MEOR application: biosurfactant characterization, production optimization and wetting effect on carbonate surfaces. Journal of Petroleum Exploration and Production Technology, 9(1): 233-245.

Vidal, R.R.L., Desbrières, J., Borsali, R. and Guibal, E., 2019. Oil removal from crude oil-in-saline water emulsions using chitosan as biosorbent. Separation Science and Technology: 1-13.

Vidali, M., 2001. Bioremediation. an overview. Pure applied chemistry, 73(7): 1163-1172.

Vigneshwaran, C., Sivasubramanian, V., Vasantharaj, K., Krishnanand, N. and Jerold, M., 2018. Potential of Brevibacillus sp. AVN 13 isolated from crude oil contaminated soil for biosurfactant production and its optimization studies. Journal of Environmental Chemical Engineering, 6(4): 4347-4356.

Vigneshwaran, C., Vasantharaj, K., Krishnanand, N. and Sivasubramanian, V., 2021. Production optimization, purification and characterization of lipopeptide biosurfactant obtained from Brevibacillus sp. AVN13. Journal of Environmental Chemical Engineering, 9(1): 104867.

Villegas-Méndez, M.Á., Papadaki, A., Pateraki, C., Balagurusamy, N., Montañez, J., Koutinas, A.A. and Morales-Oyervides, L., 2021. Fed-batch bioprocess development for astaxanthin production by Xanthophyllomyces dendrorhous based on the utilization of Prosopis sp. pods extract. Biochemical Engineering Journal, 166: 107844.

Wanapaisan, P., Laothamteep, N., Vejarano, F., Chakraborty, J., Shintani, M., Muangchinda, C., Morita, T., Suzuki-Minakuchi, C., Inoue, K., Nojiri, H. and Pinyakong, O., 2018. Synergistic degradation of pyrene by five culturable bacteria in a mangrove sediment-derived bacterial consortium. J Hazard Mater, 342: 561-570.

Wang, C., Li, Y.Z., Tan, H., Zhang, A.K., Xie, Y.L., Wu, B. and Xu, H., 2019. A novel microbe consortium, nano-visible light photocatalyst and microcapsule system to degrade PAHs. Chemical Engineering Journal, 359: 1065-1074.

Wang, G., Zhou, Y., Wang, X., Chai, X., Huang, L. and Deng, N., 2010. Simultaneous removal of phenanthrene and lead from artificially contaminated soils with glycine-beta-cyclodextrin. J Hazard Mater, 184(1-3): 690-695.

Wang, J., Xu, H.K., An, M.Q. and Yan, G.W., 2008. Kinetics and characteristics of phenanthrene degradation by a microbial consortium. Petroleum Science, 5(1): 73-78.

Wang, J., Xu, H.K. and Guo, S.H., 2007. Isolation and characteristics of a microbial consortium for effectively degrading phenanthrene. Petroleum Science, 4(3): 68-75.

Wang, P., Zhang, Y., Jin, J., Wang, T., Wang, J. and Jiang, B., 2020. A high-efficiency phenanthrene-degrading Diaphorobacter sp. isolated from PAH-contaminated river sediment. Sci Total Environ, 746: 140455.

Wang, T., Su, D., Wang, X. and He, Z., 2020. Adsorption-Degradation of Polycyclic Aromatic Hydrocarbons in Soil by Immobilized Mixed Bacteria and Its Effect on Microbial Communities. J Agric Food Chem, 68(50): 14907-14916.

Wang, Y., Zhou, L.H., Luo, X.S., Zhang, Y.P., Sun, J., Ning, X.N. and Yuan, Y., 2019. Solar-heated graphene sponge for high-efficiency clean-up of viscous crude oil spill. Journal of Cleaner Production, 230: 995-1002.

Wei, Z., Wang, J.J., Gaston, L.A., Li, J., Fultz, L.M., DeLaune, R.D. and Dodla, S.K., 2020. Remediation of crude oil-contaminated coastal marsh soil: Integrated effect of biochar, rhamnolipid biosurfactant and nitrogen application. J Hazard Mater, 396: 122595.

Whang, L.M., Liu, P.W., Ma, C.C. and Cheng, S.S., 2008. Application of biosurfactants, rhamnolipid, and surfactin, for enhanced biodegradation of diesel-contaminated water and soil. J Hazard Mater, 151(1): 155-63.

White, D.A., Hird, L.C. and Ali, S.T., 2013. Production and characterization of a trehalolipid biosurfactant produced by the novel marine bacterium Rhodococcus sp., strain PML026. J Appl Microbiol, 115(3): 744-55.

Wise, J. and Wise, J.P., Sr., 2011. A review of the toxicity of chemical dispersants. Rev Environ Health, 26(4): 281-300.

Wolf, D., Cryder, Z., Khoury, R., Carlan, C. and Gan, J., 2020. Bioremediation of PAH-contaminated shooting range soil using integrated approaches. Science of The Total Environment: 138440.

Wu, J., Zhang, J., Zhang, H., Gao, M., Liu, L. and Zhan, X., 2019. Recycling of cooking oil fume condensate for the production of rhamnolipids by Pseudomonas aeruginosa WB505. Bioprocess Biosyst Eng, 42(5): 777-784.

Xu, X., Liu, W., Wang, W., Tian, S., Jiang, P., Qi, Q., Li, F., Li, H., Wang, Q., Li, H. and Yu, H., 2019. Potential biodegradation of phenanthrene by isolated halotolerant bacterial strains from petroleum oil polluted soil in Yellow River Delta. Sci Total Environ, 664: 1030-1038.

Yang, H., Li, X., Li, X., Yu, H. and Shen, Z., 2015. Identification of lipopeptide isoforms by MALDI-TOF-MS/MS based on the simultaneous purification of iturin, fengycin, and surfactin by RP-HPLC. Anal Bioanal Chem, 407(9): 2529-42.

Yap, C.L., Gan, S. and Ng, H.K., 2011. Fenton based remediation of polycyclic aromatic hydrocarbons-contaminated soils. Chemosphere, 83(11): 1414-30.

Yaraguppi, D.A., Bagewadi, Z.K., Muddapur, U.M. and Mulla, S.I., 2020. Response surface methodology-based optimization of biosurfactant production from isolated Bacillus aryabhattai strain ZDY2. Journal of Petroleum Exploration and Production Technology: 1-16.

Yuan, X., Zhang, X., Chen, X., Kong, D., Liu, X. and Shen, S., 2018. Synergistic degradation of crude oil by indigenous bacterial consortium and exogenous fungus Scedosporium boydii. Bioresour Technol, 264: 190-197.

Zahed, M.A., Aziz, H.A., Isa, M.H., Mohajeri, L., Mohajeri, S. and Kutty, S.R., 2011. Kinetic modeling and half life study on bioremediation of crude oil dispersed by Corexit 9500. J Hazard Mater, 185(2-3): 1027-31.

Zaragoza, A., Teruel, J.A., Aranda, F.J. and Ortiz, A., 2013. Interaction of a trehalose lipid biosurfactant produced by Rhodococcus erythropolis 51T7 with a secretory phospholipase A2. J Colloid Interface Sci, 408: 132-7.

Zegzouti, Y., Boutafda, A., Ezzariai, A., El Fels, L., El Hadek, M., Hassani, L.A.I. and Hafidi, M., 2020. Bioremediation of landfill leachate by Aspergillus flavus in submerged culture: Evaluation of the process efficiency by physicochemical methods and 3D fluorescence spectroscopy. J Environ Manage, 255: 109821.

Zeng, J., Zhu, Q., Li, Y., Dai, Y., Wu, Y., Sun, Y., Miu, L., Chen, H. and Lin, X., 2019. Isolation of diverse pyrene-degrading bacteria via introducing readily utilized phenanthrene. Chemosphere, 222: 534-540.

Zhang, B.W., Guo, Y., Huo, J.Y., Xie, H.J., Xu, C.H. and Liang, S., 2020. Combining chemical oxidation and bioremediation for petroleum polluted soil remediation by BC-nZVI activated persulfate. Chemical Engineering Journal, 382: 123055.

Zhang, C., Xu, L.-h., Zhou, H., Tan, Z., Xie, Q. and Xu, Y., 2018. BIODEGRADATION OF-HEXADECANE BY ENTERIC BACTERIA ISOLATED FROM AN OIL-FIELD WASTEWATER TREATMENT PLANT. FRESENIUS ENVIRONMENTAL BULLETIN: 4942.

Zhang, L., Li, P., Gong, Z. and Li, X., 2008. Photocatalytic degradation of polycyclic aromatic hydrocarbons on soil surfaces using TiO(2) under UV light. J Hazard Mater, 158(2-3): 478-84.

Zhang, Q., Zhang, P.F., Pei, Z.J. and Wang, D.H., 2017. Investigation on characteristics of corn stover and sorghum stalk processed by ultrasonic vibration-assisted pelleting. Renewable Energy, 101: 1075-1086.

Zhao, Z., Xia, L., Qin, Z., Cao, J., Omer Mohammed, A.A. and Toland, H., 2021. The environmental fate of phenanthrene in paddy field system and microbial responses in rhizosphere interface: Effect of water-saving patterns. Chemosphere, 269: 128774.

Zhen, L., Hu, T., Lv, R., Wu, Y., Chang, F., Jia, F. and Gu, J., 2021. Succession of microbial communities and synergetic effects during bioremediation of petroleum hydrocarbon-contaminated soil enhanced by chemical oxidation. J Hazard Mater, 410: 124869.

Zhen, M., Tang, J., Li, C. and Sun, H., 2021. Rhamnolipid-modified biochar-enhanced bioremediation of crude oil-contaminated soil and mediated regulation of greenhouse gas emission in soil. Journal of Soils and Sediments, 21(1): 123-133.

Zhong, H., Jiang, Y., Zeng, G., Liu, Z., Liu, L., Liu, Y., Yang, X., Lai, M. and He, Y., 2015. Effect of low-concentration rhamnolipid on adsorption of Pseudomonas aeruginosa ATCC 9027 on hydrophilic and hydrophobic surfaces. J Hazard Mater, 285: 383-8.

Zhou, J.F., Gao, P.K., Dai, X.H., Cui, X.Y., Tian, H.M., Xie, J.J., Li, G.Q. and Ma, T., 2018. Heavy hydrocarbon degradation of crude oil by a novel thermophilic Geobacillus stearothermophilus strain A-2. International Biodeterioration & Biodegradation, 126: 224-230.

Zhu, L., Yang, X., Xue, C., Chen, Y., Qu, L. and Lu, W., 2012. Enhanced rhamnolipids production by Pseudomonas aeruginosa based on a pH stage-controlled fed-batch fermentation process. Bioresour Technol, 117: 208-13.

Zhu, Z., Zhang, B., Cai, Q., Ling, J., Lee, K. and Chen, B., 2020. Fish Waste Based Lipopeptide Production and the Potential Application as a Bio-Dispersant for Oil Spill Control. Front Bioeng Biotechnol, 8: 734.

Zou, C.J., Wang, M., Xing, Y., Lan, G.H., Ge, T.T., Yan, X.L. and Gu, T., 2014. Characterization and optimization of biosurfactants produced by Acinetobacter baylyi ZJ2 isolated from crude oil-contaminated soil sample toward microbial enhanced oil recovery applications. Biochemical Engineering Journal, 90: 49-58.

Research Outputs

(A) Journal Publications from Thesis:

1. **Swati Sharma**, Rahul Verma, and L.M. Pandey (2019). Crude oil degradation and biosurfactant production abilities of isolated *Agrobacterium fabrum* SLAJ731. Biocatalysis and Agricultural Biotechnology, 21, p.101322.
2. **Swati Sharma,** and L.M. Pandey (2020). Production of biosurfactant by *Bacillus subtilis* RSL-2 isolated from sludge and biosurfactant mediated degradation of oil. Bioresource Technology, p.123261.
3. **Swati Sharma**, L.M. Pandey (2021). Hydrophobic Surface Induced Biosorption and Microbial Ex Situ Remediation of Oil-Contaminated Sites. Industrial & Engineering Chemistry Research 60 (26), 9378-9388.
4. **Swati Sharma**, and L.M. Pandey (2021). Integration of biosorption and biodegradation in a fed-batch mode for the enhanced crude oil remediation. Letters in Applied Microbiology.
5. **Swati Sharma,** and L.M. Pandey (2022). Biodegradation kinetics of binary mixture of hexadecane and phenanthrene by the bacterial microconsortium. Bioresource Technology, p.127408.

(B) Journal Publications from Miscellaneous Work

1. N Mahanta, **Swati Sharma**, LG Sharma, LM Pandey, US Dixit (2022). Unfolding of the SARS-CoV-2 spike protein through infrared and ultraviolet-C radiation-based disinfection. International Journal of Biological Macromolecules (10.1016/j.ijbiomac.2022.08.197)
2. **Swati Sharma** and Lalit M. Pandey (2021). Prospective of fungal pathogen-based bioherbicides for the control of water hyacinth: A review. Journal of Basic Microbiology.
3. **Swati Sharma**, Rahul Verma, Sahil Dhull, Soumen K. Maiti, and Lalit M. Pandey (2021). Biodegradation of waste cooking oil and simultaneous production of rhamnolipid biosurfactant by *Pseudomonas aeruginosa* P7815 in batch and fed-batch bioreactor. Bioprocess and Biosystems Engineering.1-11.
4. **Swati Sharma**, V Saxena, A Baranwal, P Chandra, L.M. Pandey (2018). Engineered nanoporous materials mediated heterogeneous catalysts and their implications in biodiesel production. Materials Science for Energy Technologies 1 (1), 11-21

5. **Swati Sharma**, P Datta, B Kumar, P Tiwari, L.M. Pandey (2019). Production of novel rhamnolipids via biodegradation of waste cooking oil using *Pseudomonas aeruginosa* MTCC7815. Biodegradation 30 (4), 301-312.
6. **Swati Sharma**, CS Rashmitha, L.M. Pandey (2020). Synthesis and characterization of methyl acrylamide cellulose nanowhiskers for environmental applications. Lett. Appl. NanoBioScience 9, 880-884.
7. **Swati Sharma,** A Hasan, N Kumar, L.M. Pandey (2018). Removal of methylene blue dye from aqueous solution using immobilized Agrobacterium fabrum biomass along with iron oxide nanoparticles as biosorbent. Environmental Science and Pollution Research 25 (22), 21605-21615.
8. **Swati Sharma**, S Tiwari, A Hasan, V Saxena, L.M. Pandey (2018). Recent advances in conventional and contemporary methods for remediation of heavy metal-contaminated soils. 3 Biotech 8 (4), 1-18.
9. V Saxena, **Swati Sharma**, L.M. Pandey (2019). Fe (III) doped ZnO nano-assembly as a potential heterogeneous nano-catalyst for the production of biodiesel. Materials Letters 237, 232-235
10. A Kumar**, Swati Sharma**, L.M. Pandey, P Chandra (2018). Nanoengineered material based biosensing electrodes for enzymatic biofuel cells applications. Materials Science for Energy Technologies 1 (1), 38-48.
11. S Sevda, **Swati Sharma,** C Joshi, L Pandey, N Tyagi, I Abu-Reesh, TR Sreekrishnan. Biofilm formation and electron transfer in bioelectrochemical systems (2018). Environmental Technology Reviews 7 (1), 220-234.
12. R Verma, **Swati Sharma**, LM Kundu, L.M. Pandey (2020). Experimental investigation of molasses as a sole nutrient for the production of an alternative metabolite biosurfactant. Journal of Water Process Engineering 38, 101632.
13. A Kumar, **Swati Sharma**, L.M. Pandey, P Chandra (2018). Advance engineered materials in fabrication of biosensing electrodes of enzymatic biofuel cells. Materials Science for Energy Technologies 1 (1), 38-48.

14. V Saxena, A Hasan, **Swati Sharma**, L.M. Pandey (2018). Edible oil nanoemulsion: An organic nanoantibiotic as a potential biomolecule delivery vehicle. International Journal of Polymeric Materials and Polymeric Biomaterials 67 (7), 410-419.
15. R Fopase, SR Pathode**, Swati Sharma**, P Datta, L.M. Pandey (2020). Lipopeptide and essential oil based nanoemulsion for controlled drug delivery. Polymer-Plastics Technology and Materials 59 (18), 2076-2086.
16. Mizanur Rahman, Trinayan Sarmah, Pubali Dihingia, Rahul Verma, **Swati Sharma**, Divesh N Srivastava, Lalit M Pandey, Mayur Kakati. (2022) Bulk synthesis of tungsten-oxide nanomaterials by a novel, plasma chemical reactor configuration, studies on their performance for waste-water treatment and hydrogen evolution reactions. Chemical Engineering Journal 428, 131111.
17. Gopikishan Sabavath, Mizanur Rahman, Trinayan Sarmah, Pubali Dihingia, Divesh N Srivastava, **Swati Sharma**, L.M. Pandey, M Kakati (2020). Single-step, DC thermal plasma-assisted synthesis of Ag-C nanocomposites with less than 10 nm sizes for antibacterial applications. Journal of Physics D: Applied Physics 53 (36), 365201.

Manuscript submitted:

1. R Verma, **Swati Sharma,** LM Kundu, L.M. Pandey (2022). Enhanced production of biosurfactant by Bacillus subtilis RSL2 in semicontinuous bioreactor utilizing molasses as a sole substrate. Journal of Biotechnology.

Chapters published:

1. **Swati Sharma**, and L.M. Pandey (2020). Nano-sorbents-assisted microbial bioremediation of hazardous petroleum hydrocarbons. In Removal of Toxic Pollutants Through Microbiological and Tertiary Treatment (pp. 233-247). Elsevier.
2. **Swati Sharma**, Pankaj Tiwari, and Lalit Pandey (2022). Optimization of Culture Conditions for the Production of Biosurfactants. Microbial Enhanced Oil Recovery, pp. 149-178. Springer, Singapore.

3. **Swati Sharma**, Pankaj Tiwari, and Lalit Pandey (2022). Design of Consortium for the Production of Desired Metabolites. Microbial Enhanced Oil Recovery, pp. 179-195. Springer, Singapore.
4. **Swati Sharma**, Pankaj Tiwari, and Lalit Pandey (2022). Identification of Various Metabolites like Gases, Biopolymers and Biosurfactants. Microbial Enhanced Oil Recovery, pp. 197-220. Springer, Singapore.
5. R Fopase, **Swati Sharma**, L.M. Pandey. Nano (Bio) Catalysts: An Effective Tool to Utilize Waste Cooking Oil for the Biodiesel Production (2021). Nano-and Biocatalysts for Biodiesel Production. John Wiley & Sons.
6. A Jawed, **Swati Sharma**, AK Golder, L.M. Pandey (2021). Plant-polyphenol-mediated synthesis of iron oxide nanomaterials for heavy metal removal: a review. New Trends in Removal of Heavy Metals from Industrial Wastewater, 115-129.
7. S Sevda, S Singh, VK Garlapati, **Swati Sharma**, L Pandey, TR Sreekrishnan, Anoop Singh (2019). Sustainability Assessment of Microbial Fuel Cells, Waste to Sustainable Energy, 313-330.

Conferences and seminars attended:

1. **Swati Sharma**, Poulami Datta and Lalit M. Pandey, Utilization of waste cooking oil for Rhamnolipid production using Pseudomonas aeruginosa strain, BIOPROCESSING INDIA 2017 BEYOND CONVENTIONS at Indian Institute of Technology Guwahati, December 09-11, 2017.
2. **Swati Sharma,** and Lalit M. Pandey, Production of biosurfactant and degradation of crude oil by Agrobacterium fabrum SLAJ731, International conference on waste management RECYCLE-2018 at Indian Institute of Technology Guwahati, February 22-24, 2018.
3. **Swati Sharma,** and Lalit M. Pandey, Bio-stimulation of biosurfactant on the biodegradation of crude oil by Bacillus subtilis RSL-2, International Conference on Bioprocess for Sustainable Environment and Energy, ICBSEE-INDIA-2020, March 5-7, 2020, NIT Rourkela, Odisha
4. **Swati Sharma,** Lalit M. Pandey, Biosorption of methylene blue dye and lead removal from wastewater immobilized Agrobacterium fabrum SLAJ731, Workshop cum Symposium on Bioinspired Nanomaterials for Environmental Applications, February 12-13, 2020, Centre for the Environment, Indian Institute of Technology Guwahati, Assam

5. **Swati Sharma,** Lalit M. Pandey, Synthesis and characterization of methyl acryl functionalized amido-cellulose nanowhiskers, Workshop cum Symposium on Bioinspired Nanomaterials for Environmental Applications, February 12-13, 2020, Centre for the Environment, Indian Institute of Technology Guwahati, Assam
6. Mizanur Rahman, Gopikishan Sabavath, Trinayan Sarmah, Pubali Dihingia, **Swati Sharma**, Lalit M. Pandey, and M. Kakati, Plasma assisted, single-step synthesis of Ag-C nanocomposites with less than ten nano-meter average sizes for antibacterial applications, Workshop cum Symposium on Bioinspired Nanomaterials for Environmental Applications; February 12-13, 2020, Centre for the Environment, Indian Institute of Technology Guwahati, Assam.
7. **Swati Sharma**, Lipopeptide modified iron oxide nanoparticles as anodic coating in microbial fuel cells: waste to sustainable energy, Mapping the Changemakers of North East Region 2020 (PhD/ Post-Doctoral category) BIRAC Regional Techno-Entrepreneurship Promotion Centre (BRTC) January 6, 2021, at KIIT-TBI BioNEST supported by BIRAC, DBT, Govt. of India.
8. **Swati Sharma**, Particle Size & Zeta Potential Measurement by Dynamic Light Scattering (DLS) & Electrophoretic Light Scattering (ELS) Techniques, webinar dated March 15, 2021, Indian Institute of Technology Guwahati, Assam